TECHNISCHE UNIVERSITÄT MÜNCHEN

Lehrstuhl für Pharmazeutische Radiochemie

Innovative Complexation Strategies for the Introduction of Short-lived PET Isotopes into Radiopharmaceuticals

Jakub Šimeček

Vollständiger Abdruck der von der Fakultät für Chemie der Technischen Universität zur Erlangung des akademischen Grades eines Doktors der Naturwissenschaften genehmigten Dissertation.

Vorsitzender: Univ.-Prof. Dr. Klaus Köhler

Prüfer der Dissertation:

1. Univ.-Prof. Dr. Hans-Jürgen Wester
2. Univ.-Prof. Dr. Dr. h.c. Horst Kessler (i.R.)
3. Univ.-Prof. Dr. Markus Schwaiger

Die Dissertation wurde am 04.06.2013 bei der Technischen Universität München eingereicht und durch die Fakultät für Chemie am 18.12.2013 angenommen.

I would like to thank especially to Prof. Dr. Hans-Jürgen Wester for giving me the opportunity to work independently on an interesting topic and for necessary support during the whole project. His expertise helped to give the work a meaningful direction resulting in sound data for further research on Ga-68 radiopharmaceuticals.

Many thanks belong to Dr. Johannes Notni not only for inviting me to work on my dissertation at TU München but mainly for endless support and critical and constructive comments to my project.

I would also like to thank to Prof. Dr. Petr Hermann, Ondřej Zemek and Miroslav Pniok from Charles University in Prague for keeping in touch and a very fruitful cooperation.

All my colleagues from TU München are gratefully acknowledged for a friendly working atmosphere and help whenever asked.

Work on presented PhD. thesis resulted in following publications:

J. Notni, **J. Šimeček**, P. Hermann, H.-J. Wester. TRAP, a powerful and versatile framework for Gallium-68 radiopharmaceuticals. *Chem. Eur. J.* **2011**, *17*, 14718–14722.

J. Šimeček, M. Schulz, J. Notni, J. Plutnar, V. Kubíček, J. Havlíčková, P. Hermann. Complexation of metal ions with TRAP (1,4,7-triazacyclononane phosphinic acid) ligands and 1,4,7-triazacyclononane-1,4,7-triacetic acid: phosphinate-containing ligands as unique chelators for trivalent gallium. *Inorg.Chem.* **2012**, *51*, 577–590.

J. Šimeček, O. Zemek, P. Hermann, H.-J. Wester, J. Notni. A monoreactive bifunctional triazacyclononane-phosphinate chelator with high selectivity for Gallium-68. *ChemMedChem* **2012**, *7*, 1375–1378.

J. Šimeček, H.-J. Wester, J. Notni. Copper-64 labelling of triazacyclononane-triphosphinate chelators. *Dalton Trans.* **2012**, *41*, 13803–13806.

J. Šimeček, P. Hermann, H.-J. Wester, J. Notni. How is ^{68}Ga-labelling of macrocyclic chelators influenced by metal ion contaminants in ^{68}Ge/^{68}Ga generator eluates? *ChemMedChem* **2013**, *8*, 95–103.

Work on presented PhD thesis resulted in following conference oral presentations:

J. Šimeček, J. Notni, H.-J. Wester. Compared to DOTA and NOTA only TRAP chelators show superior selectivity for gallium-68 in presence of metal ion contaminants; 15–17th September **2011**, 19th Meeting of Radiochemistry and Radiopharmacy Work Groups (AGRR), Ochsenfurt, Germany.

J. Šimeček, J. Notni, H.-J. Wester. NOPO: A new asymmetrical TRAP chelator for Gallium-68; 25–28th April **2012**, 50th Symposium of German Society of Nuclear Medicine (DGN), Bremen, Germany.

J. Šimeček, J. Notni, H.-J. Wester. NOPO as a chelator for preparation of ^{68}Ga-labeled monoconjugates; 9–13th June **2012**, SNM Annual Meeting, Miami, FL, USA.

J. Šimeček, J. Notni, H.-J. Wester. ^{64}Cu-labelled triazacyclononane triphosphinates; 4–6th October **2012**, 20th Meeting of Radiochemistry and Radiopharmacy Work Groups (AGRR), Bad Honnef, Germany.

J. Šimeček, J. Notni, O. Zemek, P. Hermann, H.-J. Wester. NOPO, a novel bifunctional and highly selective chelator for Gallium-68; 27–31st October **2012**, Annual Congress of the European Association of Nuclear Medicine, Milan, Italy.

J. Šimeček, H.-J. Wester, J. Notni. Chelators highly selective for Ga-68 and practical consequences thereof; 28th February – 2nd March **2013**, 2nd World Congress on Ga-68, Chandigarh, India.

J. Šimeček, J. Notni, T. Kapp, H. Kessler and H.-J. Wester. Ga-68 and Cu-64 labelled c(RGDfK) monoconjugates with exceptionally high affinity for $\alpha_v\beta_3$ integrins; 17–20th April **2013**, 51st Symposium of German Society of Nuclear Medicine (DGN), Bremen, Germany.

J. Šimeček, J. Notni, P. Hermann, H.-J. Wester. Chelators tailored for preparation of ^{68}Ga-labelled mono-, di- and trimeric bioconjugates; 12–17th May **2013**, 20th International Symposium on Radiopharmaceutical Sciences, Jeju, South Korea.

Work on presented PhD thesis resulted in following invited lecture:

J. Šimeček. Gallium-68: From basic coordination chemistry to highly efficient radiolabelling; 13th September **2012**, Symposium on Ga-68 in PET diagnostics, Debrecen, Hungary.

Work on presented PhD thesis resulted in following conference poster presentations:

J. Šimeček, J. Notni, P. Hermann, H.-J. Wester. Towards optimized ligand design for Ga-68 and its application in PET; 28th August – 2nd September **2011**, 19th International Symposium on Radiopharmaceutical Sciences, Amsterdam, The Netherlands.

J. Šimeček, O. Zemek, H.-J. Wester, J. Notni. ^{68}Ga-labeling via metal-induced de-esterification of NOPO-peptides; 12–17th May **2013**, 20th International Symposium on Radiopharmaceutical Sciences, Jeju, South Korea.

Table of contents

List of abbreviations

AAZTA	1,4-bis(hydroxycarbonylmethyl)-6-[bis(hydroxycarbonylmethyl)] amino-6-methylperhydro-1,4-diazepine
AZAPA	*N*,*N*'-[1-Benzyl-1,2,3-triazole-4-yl]methyl-*N*,*N*'-[6-(carboxy)-pyridin-2-yl]-1,2-diaminoethane
BFC	Bifunctional chelator
BPAMD	(4-{[(bis(phosphonomethyl)) carbamoyl]methyl}-7,10-bis(carboxymethyl)-1,4,7,10-tetraazacyclododec-1-yl)acetic acid
CT	Computed tomography
DEDPA, BCPE	*N*,*N*'-[6-(carboxy)-pyridin-2-yl]-1,2-diaminoethane
DFO	Desferrioxamine
DFT	Density functional theory
DOTA	1,4,7,10-tetraazacyclododecane-1,4,7,10-tetraacetic acid
DTPA	Diethylenetriaminepentaacetic acid
EDTA	Ethylenediaminetetraacetic acid
FDG	2-deoxy-2-fluoro-D-glucose
FEC	Fluoroethyl-dimethyl-2-hydroxyethylammonium; Fluoroethylcholine
FET	*O*-(2-Fluoroethyl)-L-tyrosine; Fluoroethyltyrosine
FLT	3'-fluoro-3'-deoxy-L-thymidine
FMISO	1-(2-Nitro-imidazolyl)-3-fluoro-2-propanol
GMP	Good manufacturing practice
HBED	*N*,*N*'-bis(2-hydroxybenzyl)-1,2-ethylenediamine-*N*,*N*'-diacetic acid
HBED-CC	*N*,*N*'-bis[2-hydroxy-5-(carboxyethyl)benzyl]ethylenediamine-*N*,*N*'-diacetic acid
HEPES	2-[4-(2-hydroxyethyl)-1-piperazinyl]-ethanesulfonic acid
HPLC	High-pressure liquid chromatography
ICP-AES	Inductively coupled plasma atomic emission spectroscopy
ID/g	Injected dose per gram
MIP	Maximum intensity projection
MRI	Magnetic resonance imaging
MS	Mass spectrometry
NMR	Nuclear magnetic resonance
NOC	NaI^{3}-Octreotide
NODAGA	1,4,7-triazacyclononane-1-glutaric acid-4,7-diacetic acid

NODAPA-NCS	1,4,7-triazacyclononane-1,4-diacetic acid-7-*p*-isothio-cyanatophenyl-acetic acid
NODAPA-OH	1,4,7-triazacyclononane-1,4-diacetic acid-7-*p*-hydroxyphenyl-acetic acid
NODASA	1,4,7-triazacyclononane-1-succinic acid-4,7-diacetic acid
NOKA	1,4,7-triazacyclononane-tris(6-methylene-5-hydroxy-2-hydroxymethyl-3Hpyran-4-one)
NOPO	1,4,7-triazacyclononane-1,4-bis[methylene(hydroxymethyl)phosphinic acid]-7-[methylene(2-carboxyethyl)phosphinic acid]
NOTA	1,4,7-triazacyclononane-1,4,7-triacetic acid
NOTEP	1,4,7-triazacyclononane-1,4,7-tris[methylene(ethyl)phosphinic acid]
NOTGA	1,4,7-triazacyclononane-1,4,7-triglutaric acid
NOTMP	1,4,7-triazacyclononane-1,4,7-tris[methylene(methyl)phosphinic acid]
OCTAPA	*N*,*N*´-bis(6-carboxy-2-pyridylmethyl)ethylenediamine-*N*,*N*´-diacetic acid
p.i.	Post injection
PET	Positron emission tomography
PiB	Pittsburgh compound B
PSMA	Prostate-specific membrane antigen
RGD	Arginine-Glycine-Aspartic acid
SA	Specific activity
SAX	Strong anionic exchanger
SCI	Scientific citation index
SCX	Strong cationic exchanger
SPECT	Single photon emission computed tomography
sst	Somatostatin
TACN	1,4,7-triazacyclononane
TATE	Tyr^3-Octreotate
TLC	Thin layer chromatography
TOC	Tyr^3-Octreotide
TRAP	Triazacyclononane-triphosphinate

1. Introduction

1.1. Insight in molecular imaging with focus on PET

"Molecular imaging" originally understood as visualisation of targeted structures in living organisms has further developed in modalities allowing for tracking the biochemical processes in vivo on a molecular level. The administered radiolabelled probe follows in an ideal case a biological pathway very similar to its endogenous analogue. Indirectly, the biological counterparts (receptors, enzymes, and transporters) of such a substance can be visualised after binding of a radiolabel.[1]

Today, clinicians have remarkable range of medical imaging techniques. Diagnosis with sonography (ultrasound), radiography (X-ray) or computed tomography (CT) provides the information concerning tissue morphology. Magnetic resonance imaging (MRI) with its high spatial resolution (< 1 mm) is mostly employed also for obtaining the anatomical information. Nevertheless, measuring of the brain activity associated with changes in blood flow (degree of oxygenation), or determination of metabolites (*e.g. N*-acetyl aspartate, choline, creatine, lactate) in body tissues broaden the application of MRI also to functional imaging. Single photon emission tomography (SPECT) and positron emission tomography (PET) are associated with radiolabelled contrast agents, and provide the purely functional information.[2] The latest advanced technologies combine the acquisition of functional and anatomical imaging in one device (PET/CT, PET/MRI).[3]

Both SPECT and PET have had high impact on medicine, particularly on oncology,[4] cardiology[5] and neurology.[6] The unique sensitivity of PET and SPECT providing information complementary to the anatomical images produced by other modalities makes these techniques ideal for imaging with biomarker- and microenvironment-targeted tracers. Both modalities have become extremely important in the clinic; however, PET undoubtedly possesses a number of significant advantages over its single-photon cousin. PET provides higher sensitivity (required tracer concentration $\approx 10^{-8}$ to 10^{-10} M; concentration for SPECT approaches 10^{-6} M), higher resolution (2–3 mm or lower, 6 – 8 mm for SPECT) and mainly the ability to quantify the absolute radioactivity uptake in the tissue of interest.[7] On the other hand, SPECT is competing PET with its generally lower prize and estimated at least 10-times higher number of installed devices worldwide.[8]

What comes before we may construct the actual PET image? Briefly, the tracer usually administered as a bolus injection follows its biological pathway (ideally, accumulates in the region of interest and the residual fraction is excreted) upon simultaneous decay of its radioactive label. A positron released from the atomic nucleus by β^+-decay travels in the ambient tissue until it loses its kinetic energy. At this stage, it encounters its antiparticle (an electron) and these two mutually annihilate. Their mass is converted into two almost antiparallel 511 keV γ-rays. These γ-rays leave the tissue and strike the coincidence detectors in a ring of a PET camera. Importantly, the output is generated only when signals from two coincidence detectors simultaneously trigger the circuit. Thus, the main advantages of PET lie in physics: the short distance reached by a positron prior to annihilation results in high spatial resolution, the coincidence detection allows for tremendous sensitivity.[9]

1.2. PET nuclides and tracers

For years after the introduction of the first positron-emission transaxial tomograph by Michael Ter-Pogossian *et al.* in mid-'70s,[10] the portfolio of PET radiopharmaceuticals was dominated by small tracers with short biological half-life. Accordingly, the choice of a radiolabel was in favour of non-metallic radionuclides with correspondingly short half-lives. This holds true in many respects till today as the most used PET radiopharmaceuticals contain ^{18}F, ^{11}C, ^{13}N and ^{15}O (Table 1).

Table 1: Common non-metallic PET nuclides, their physical properties and production route.[11]

Nuclide	β^+ decay (%)	$t_{1/2}$ (min)	E_{max} (MeV)	Production
^{11}C	99.8	20.38	0.96	$^{14}N(p,\alpha)^{11}C$
^{13}N	99.8	9.96	1.19	$^{16}O(p,\alpha)^{13}N$
^{15}O	99.9	2.04	1.72	$^{14}N(d,n)^{15}O$
^{18}F	96.9	109.70	0.63	$^{18}O(p,n)^{18}F$

In small organic molecules, the radiolabels are attached via a covalent bond as for example in ^{11}C-choline[12] and ^{18}F-FEC[13] (prostate cancer), ^{11}C-PiB[14] and ^{18}F-Florbetapir[15] (Alzheimer´s disease, targeting of the β-amyloid), ^{18}F-FDG[16] (enhanced glucose uptake), ^{18}F-FMISO[17] (imaging of hypoxic tissues), ^{18}F-FLT[18] (proliferation), ^{11}C-methionine[19] and ^{18}F-FET[20] (brain tumours). Somewhat simpler are ^{13}N-ammonia[21] and ^{15}O-water[22] (myocardial perfusion) or ^{18}F-fluoride[23] (bone imaging).

Larger molecules (peptides, proteins, antibodies), whose pharmacokinetics and receptor affinity are not influenced to a considerable extent by addition of a chelating moiety and optionally a linker, can be easily and efficiently labelled with radiometals (Figure 1).[24]

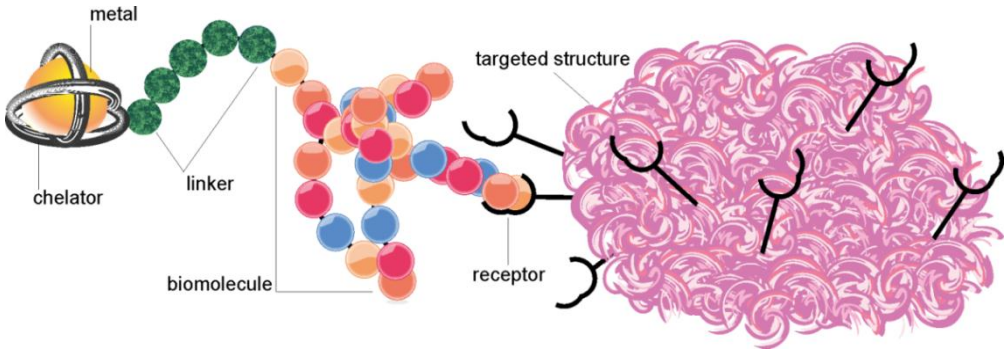

Figure 1: A schematic structure of a radiometallated bioconjugate binding to the receptor of the targeted structure.

Although there were attempts to introduce non-metallic radiolabels via a covalent bond to a peptide, those strategies have met certain limitations. A prime example might be ^{18}F-Galacto-RGD labelled via ^{18}F-fluoroacylation of glycosylated c(RGDfK).[25] This tracer for targeting $\alpha_v\beta_3$ integrins showed to be very promising imaging agent in clinical studies with patients suffering from malignant melanomas, sarcomas, glioblastomas, breast cancer and head and neck cancer.[26] Unfortunately, despite being the most extensively studied integrin $\alpha_v\beta_3$-specific PET tracer in the clinical setting, rather complicated synthetic protocol is hardly transferrable to a GMP-compliant production.[27]

Contrary to that, a NODAGA-coupled c(RGDyK) showed improved in vivo performance in preclinical studies and could be sufficiently labelled with ^{68}Ga.[28] Recently, unprecedently robust labelling strategy, higher tumour uptake and promising pharmacokinetics were achieved with a novel trimeric c(RGDfK) tracer ^{68}Ga-TRAP(RGD)$_3$ (Figure 2).[29,30]

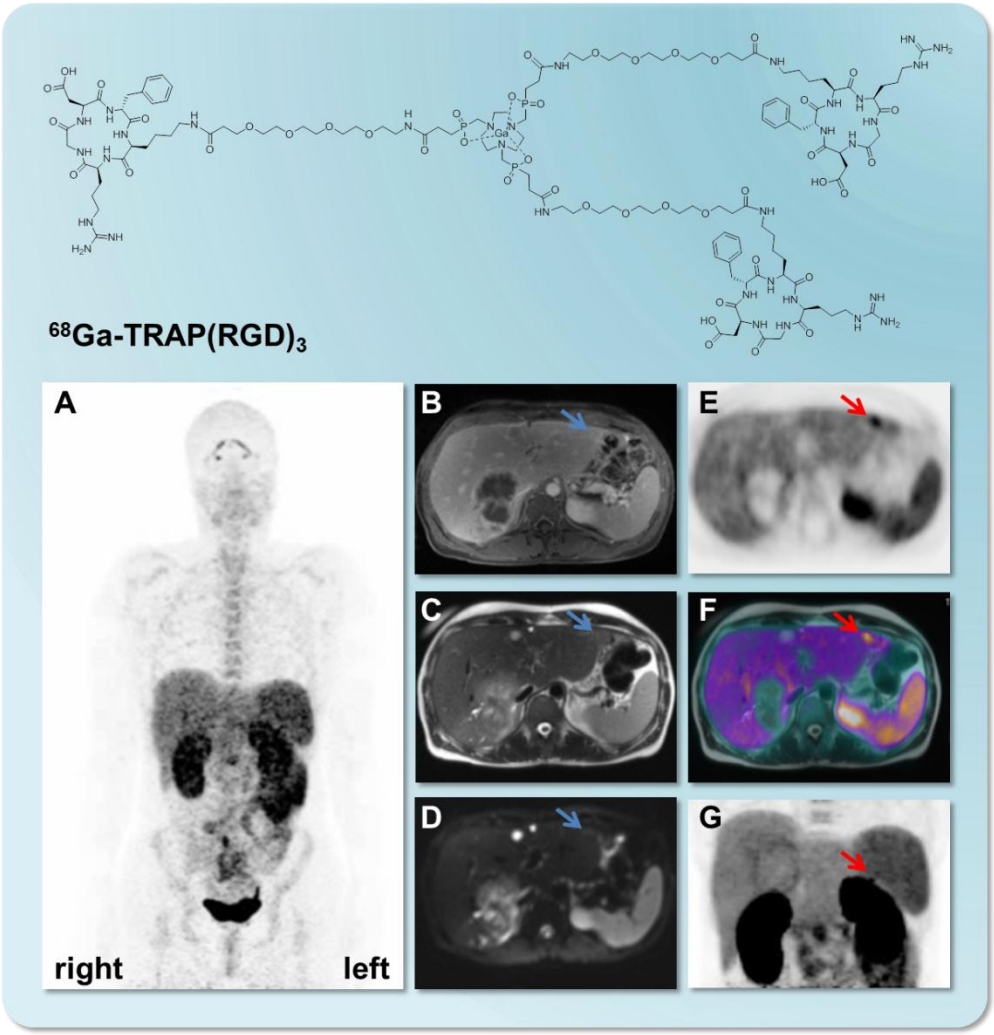

Figure 2: A schematic structure of ^{68}Ga-TRAP(RGD)$_3$ and an example of its whole-body biodistribution (A) followed by PET (MIP, 90 min p.i.). Transaxial slice in abdomen of a patient suffering from pancreatic adenocarcinoma: Gd-contrast-based T_1-weighted (B), T_2-weighted (C) and diffusion-weighted (D) MRI images showing no malignancy (blue arrow); the liver metastasis in left lobe detected by PET 60 min p.i. (E) and the PET/MRI fusion (F). Detail of PET image of abdominal, 60 min p.i. (G). PET/MRI, recorded on Siemens Biograph mMR, Klinikum rechs der Isar, TU München - unpublished data, with courtesy of Dr. J. Notni, Dr. med. A. Beer and Prof. M. Schwaiger.

An elegant approach for labelling of small peptides with ^{18}F was developed by McBride *et al.* who introduced the radiolabel via an aluminium complex. ^{18}F-$[AlF]^{2+}$ is prepared in aqueous solution and further complexed by NOTA-like conjugates.[31] Interestingly, shortly after the introduction of a new method, the first kit for ^{18}F-$[AlF]^{2+}$ labelling was reported.[32] The method seems to need further optimisation to reach its full potential since elevated temperatures have been inevitable and reached specific activities are relatively low.[33] However, the first human study with ^{18}F-Alfatide, a c(RGDyK) NOTA-linked dimer labelled via Al^{III} complex, in lung cancer patients showed very promising results.[34]

Nowadays, a variety of available metallic radionuclides allows for a precise selection of a radiolabel fitting to a desired application. Among them, ^{64}Cu, ^{68}Ga and recently also ^{89}Zr (Table 2) have been in focus for development of new PET radiopharmaceuticals.[24,35] Utilisation of ^{82}Rb has been limited to myocardial perfusion PET using ^{82}Rb-RbCl.[36]

Table 2: Selected metallic PET nuclides, their physical properties and production route.[11]

Nuclide	β^+ decay (%)	$t_{1/2}$	E_{max} (MeV)	Production
^{64}Cu	17.6	12.7 h	0.66	$^{64}Ni(p,n)^{64}Cu$
^{68}Ga	89.1	67.7 min	1.89	$^{68}Ge/^{68}Ga$
^{82}Rb	95.5	1.3 min	3.15	$^{82}Sr/^{82}Rb$
^{89}Zr	22.7	78.5 h	0.90	$^{89}Y(p,n)^{89}Zr$

Short-lived ^{68}Ga suits to pharmacokinetics of small peptidic tracers. ^{64}Cu with β^+ energy similar to that of ^{18}F allows for better spatial resolution of μ-PET images in preclinical research.[37] In the clinical context, differences in β^+ energy between ^{18}F and ^{68}Ga were shown as a minor issue, since the spatial resolution is in this case determined rather by the technical parameters of current PET devices.[38] Considering the half-life of a radionuclide, ^{68}Ga allows for acquisition of the PET images in the range of several hours p.i., ^{64}Cu serves for experiments in the frame of hours to days and recently popular ^{89}Zr is a label of choice for antibodies whose destiny in vivo can be observed in the range of days to approximately one week.[39]

Lately, development of novel ^{68}Ga-PET tracers has attracted large scientific community, especially because of the radionuclide availability from the ^{68}Ge/^{68}Ga generator (see Chapter 2).[40] Chemists have been on the search for ^{68}Ga-based alternatives for SPECT with ^{99m}Tc and have been trying to improve the current radiolabelling strategies.[41,62,76b] Physicians have investigated the potential of ^{68}Ga-peptides along with well-established and approved "gold standard PET tracer" ^{18}F-FDG.[42] Novel ^{68}Ga-based probes, *e.g.* ^{68}Ga-DOTA-CPCR4-2 (imaging of chemokine receptor CXCR4, metastatic processes),[43] ^{68}Ga-DOTA-BASS (sst2 and sst3 receptor antagonist),[44] ^{68}Ga-DOTA-BPAMD (bone imaging),[45] ^{68}Ga-NODAGA-5,8-dideazafolic acid (folate receptor imaging)[46] or ^{68}Ga-PSMA (prostate cancer)[47] have been evaluated. At the same time, the industry reacts to increasing demand for ^{68}Ga by providing sophisticated automated systems for GMP-compliant[48] preparation of ^{68}Ga-labelled tracers.

2. Background of the studies

2.1. Renaissance of Gallium-68

Gallium-68 was introduced as a non-invasive molecular imaging agent for brain scanning already in early '50s. It was investigated along with ^{64}Cu, ^{74}As and ^{203}Hg.[49] One of the reasons for including ^{68}Ga in the studies was already published report on ^{72}Ga as a potential therapeutic agent for bone tumours.[50] The original Gleason´s "Positron cow", how the first liquid ^{68}Ge/^{68}Ga generator was called,[51] was further optimised and followed by Greene and Tucker´s attempts to immobilise the parent ^{68}Ge on an inorganic resin (Al_2O_3).[52] This idea gave a sound base for development of the generators as we know them today.[53]

The early column-based generators provided ^{68}Ga in a complex with EDTA.[54] [^{68}Ga(EDTA)]$^-$ became a popular brain-imaging tracer which allowed for measurement of increased blood-flow of brain tumours.[55] Nevertheless, stability of [Ga(EDTA)]$^-$ ($\log K = 21.0$)[56] prevented the direct use of ^{68}Ga for labelling procedures and therefore limited the wider use of this otherwise very interesting nuclide.

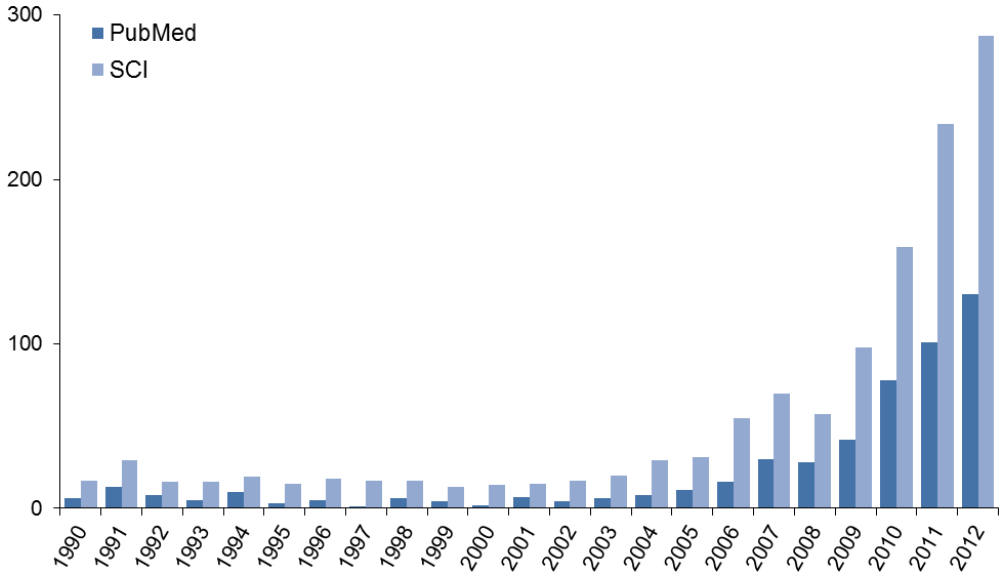

Figure 3: Number of publications on ^{68}Ga registered in Science Citation Index (SCI) and PubMed per year. Search: "Gallium-68" or "Ga-68" or "68Ga".

After the first reported column-based generators, a number of generators providing $^{68}Ga^{3+}$ in its ionic form had been developed but, generally, their use stayed restricted to the inventors or close collaborators. A number of pioneering studies with ^{68}Ga-labelled peptides in Europe was done with so called "Heidelberg generator" with pyrogallol-based resin.[57] Limited supplies of ^{68}Ga became history in the year 1996, when the first commercially available generator was introduced to the market by Cyclotron Ltd. (Obninsk, Russian Federation).[58] Other producers entering the market in 2008 (Eckert & Ziegler, IDB Holland distributing the generator by iThemba LABS, or lately Isotope Technologies Garching) made the ^{68}Ga widely accessible.[59,60] The availability of the generators is reflected by increasing number of published studies (Figure 3).

The commercially available $^{68}Ge/^{68}Ga$ generators (Figure 4) are portable, led-shielded chromatographic columns filled with a matrix material for adsorption of the mother radionuclide ^{68}Ge. The matrix consists of inorganic materials as TiO_2, SnO_2 or a suitable organic polymer. Long half-life of ^{68}Ge (271 d) and the matrix stability allow for the use of a single generator up to a period of approximately two years. $^{68}Ga^{3+}$ for labelling purposes is then eluted with 0.05–1.0 M hydrochloric acid.[53,61]

Figure 4: Commercially available $^{68}Ge/^{68}Ga$ generators according to manufacturers and the year of introduction to the market.

2.2. Handling the $^{68}Ge/^{68}Ga$ generator eluate

Gallium-68 can be eluted several times a day, depending on the overall generator activity and/or the activity needed for a preparation of a radiopharmaceutical. Contrary to typical PET nuclides, ^{18}F and ^{11}C, there is no need for an on-site cyclotron and the $^{68}Ga^{3+}$ labelling strategies are in principle one-step reactions where the metal cation becomes coordinated into a chelate. However, taking a more detailed look at the practical conditions, we find a set of factors hindering the smooth $^{68}Ga^{3+}$ labelling chemistry. Among them, the limitations caused by high volume of the eluate and/or its acidity, labelling at elevated temperatures or upon use of the microwaves, and selection of the appropriate chelating systems have been reported more frequently.[62,66,76b]

Passionate discussions have been dedicated to the influence of metal contaminants in the $^{68}Ge/^{68}Ga$ generator eluate, water, buffers and hydrochloric acid that are typical components of a labelling procedure.[62] Besides the inevitable and constantly formed contaminant Zn^{2+}, the $^{68}Ga^{3+}$ decay product, the metals from matrix materials (Sn^{IV}, Ti^{IV}), Fe^{3+}, Al^{3+} and Cu^{2+} have been found in the eluate. Each of the listed metal cations is a potential competitor for $^{68}Ga^{3+}$ in binding to a chelator. In this respect, Fe^{3+} with chemical and physical properties similar to Ga^{3+} is to be considered. Recently published data revealed high influence of Cu^{2+} and Zn^{2+} on labelling of carboxylic derivatives of 9- and 12-membered polyazacycloalkanes. Since the abundance of Cu^{2+} in the eluate is negligible and reported only occasionally, content of Zn^{2+} stays as one of the crucial parameters for the efficient labelling.[63]

To eliminate the content of metal contaminants, three methods of eluate processing have been developed. A “cationic” purification is mostly applied for the TiO_2-based generators eluted with HCl of low concentration. It employs the column filled with a strong cationic exchanger (SCX) to adsorb the eluted $^{68}Ga^{3+}$, Fe^{3+}, Zn^{2+} and Ti^{IV} whereas $^{68}Ge^{IV}$ from the generator breakthrough passes through the column. A purification step using 80% acetone / 0.15 M HCl allows for wash-out of Fe^{3+}, Zn^{2+} and Ti^{IV} and ^{68}Ge from the dead volume of a SCX cartridge. $^{68}Ga^{3+}$ is then quantitatively eluted with 98% acetone / 0.05 M HCl. Acetone is classified as a solution with negligible intravenous toxicity of 5.5 g/kg (rat) and most of its content is evaporated during labelling procedure.[64] Alternatively, a method using 5 M NaCl solution for elution of ^{68}Ga from a SCX cartridge has been reported recently.[65]

An “anionic” purification demands mixing the generator eluate with highly concentrated HCl to form $[^{68}GaCl_4]^-$ complex that can be adsorbed on a strong anionic exchanger (SAX) whereas $^{68}Ge^{IV}$ is separated. The SAX is then washed with 5.5 M HCl and purged with nitrogen; $^{68}Ga^{3+}$ is eluted with a small amount of water.[66] Despite claiming the eluate purification, the authors of publications related to this method do not provide the metal contents proved by ICP-AES analysis before and after the purification step. With respect to the “cationic” method, this one is more oriented towards the eluate processing and activity concentration. It is aimed at achievement of lower labelling volumes and therefore higher precursor concentration resulting in higher achieved specific activity (SA) of the labelled conjugates.

A high activity concentration can be achieved very elegantly using the “fractionation”. Only a small fraction, typically 1.0–1.5 mL, of the eluate is separated, mixed with a buffer solution and directly used for labelling. Also the ratio $^{68}Ga^{3+}:M^{n+}$ (where M is a metal contaminant) is herewith maximised.[53c] This method is usually of choice for SnO_2-based generators eluted with 1 M HCl as they are characterised by very low ^{68}Ge breakthrough.

2.3. Gallium-68 chelating agents

Once the $^{68}Ga^{3+}$ containing solution is ready to use for labelling, the chemistry of Ga^{3+} and the chelator as a part of a bioconjugate play the decisive role. The optimal bifunctional chelator (BFC) should be compatible with the nature of a radiometal,[67] as well it ought to fulfil following requirements:[68]

- ✓ Stability/Kinetic inertness: The BFC should form highly stable complexes to prevent hydrolysis and transmetallation/transchelation in vivo resulting in unspecific biodistribution of a radiolabel.
- ✓ Fast complexation kinetics: The metal–chelate complex should be formed rapidly and quantitatively at low chelate concentration, ideally at room temperature and pH suitable for biologically active targeting vectors.
- ✓ Selectivity: The radiometal of interest should be bound preferably over other metal cations, *e.g.* its decay product(s) or contaminants from production of the radionuclide.
- ✓ Versatile conjugation chemistry: The BFC should be amenable to conjugation or modification with activating groups and/or linkers.
- ✓ Accessibility: The synthesis of a BFC should be straightforward, reproducible and generally as simple as possible. Cost-effective, scalable synthesis in at least gram amount is a key factor for making the new optimal BFC available for widespread utilisation.

However, fulfilment of the above listed parameters does not have to necessarily mean a success of a BFC since the nature of a formed metal–chelate complex can dramatically change the pharmacokinetics of the conjugated targeting group. On the other hand, not fulfilling the almost ideal features can be to some extent tolerated upon excellent in vivo performance of a tracer. An prime example of the latter is employment of 1,4,7,11-tetrazacyclododecane-1,4,7,11-tetraacetic acid (DOTA, Figure 5)[69] as a chelator for ^{68}Ga. Despite exhibiting a few notable drawbacks in labelling with $^{68}Ga^{3+}$, the great clinical success of ^{68}Ga-DOTA-TOC, ^{68}Ga-DOTA-NOC and ^{68}Ga-DOTA-TATE for the imaging of somatostatin receptor subtypes in patients with neuroendocrine tumours made DOTA the so far mostly employed chelator for ^{68}Ga.[70]

Nevertheless, optimisation of the $^{68}Ga^{3+}$ labelling properties of a chelate was challenging a couple of research groups over past years. To a coordination chemist,

the following features of DOTA with respect to $^{68}Ga^{3+}$ could appear as a springboard for ligand-design optimisation:

a) The size of DOTA cavity and 8 donor atoms are more suitable for binding rather large cations (trivalent lanthanides, Bi^{3+}, Y^{3+}, Sc^{3+}) than small Ga^{3+} preferring octahedral geometry.[71] That is also why the complexation of Ga^{3+} by DOTA shows relatively slow kinetics and demands elevated temperatures.[72]

b) The protonation constants of two opposite carboxylic pendant arms of DOTA exhibit relatively weak acidity (pK_a 4.68, 4.11).[73] Thus, DOTA is not fully deprotonated and "pre-prepared" for the complexation at low pH of the eluates. Correspondingly, the optimal pH for labelling of DOTA lies between 3 and 4.[74] In this region, formation of colloidal gallium (oxides/hydroxides phases) even at nanomolar concentration is favoured (Figure 10) and therefore hinders the smooth labelling process.

c) DOTA forms thermodynamically stable complexes also with other metal cations present in the $^{68}Ge/^{68}Ga$ eluates and therefore high chelator amounts are needed to eliminate the competitive coordination reactions.[75]

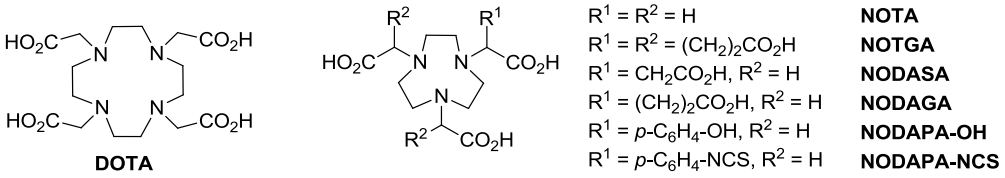

Figure 5: Schematic structures of DOTA and NOTA-like bifunctional chelators.

A certain improvement in labelling was achieved by employing somewhat smaller triazacyclononane derivatives. 1,4,7-triazacyclononane-1,4,7-triacetic acid (NOTA)[76] and its derived bifunctional chelators (Figure 5) NOTGA,[77] NODASA,[78] NODAGA,[79] NODAPA-OH[80] and NODAPA-NCS[80] also form stable Ga^{III} complexes. They can be labelled at their lower concentration at elevated temperatures or at higher concentration already at 25 °C.[74]

In early '90s Parker *et al.* reported on synthesis of several phosphinic acid analogues of NOTA (Figure 6) and suggested them as chelators for a γ-emitter ^{67}Ga.[81] Later on, they synthesised also bifunctional phosphinic chelators, where the coupling moiety (linked primary amine) was attached to one of the TACN nitrogen atoms or to a backbone.[82] Despite related compounds were synthesised and further studied,[83] to the author´s best knowledge, none of the compounds found their practical application over the years.

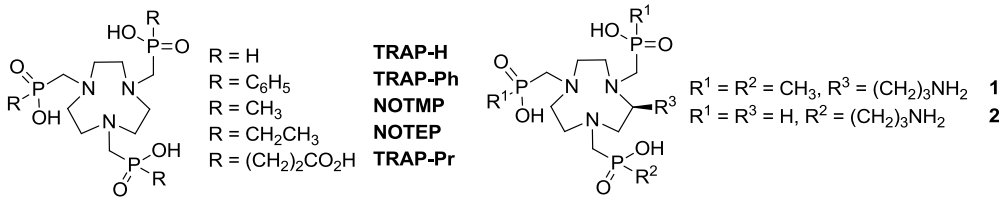

Figure 6: Discussed TACN-based phosphinic acid chelators.

A truly simple synthetic approach starting from cheap chemicals and resulting in good yields of TRAP-Pr[84] has made this bifunctional chelator (with three carboxylic groups amenable to coupling to primary amines) very attractive for ^{68}Ga. So far, TRAP-Pr has been successfully applied for preparation of number of trimeric[85,29] and bimodal[74] bioconjugates that could be labelled with ^{68}Ga in reproducible synthetic protocols providing high yields of radiochemically pure PET tracers.[30]

With respect to kinetic stability of ^{68}Ga-complexes in vivo, the use of open-chain chelators (Figure 7) like DFO or DTPA for Ga^{III} is disputable, even though the labelling is easily achievable already at room temperature.[86] Labelling at room temperature leading to formation of kinetically stable ^{68}Ga-complexes is extremely challenging since it allows for introduction of ^{68}Ga to sensitive biomolecules. Among the reported open-chain chelators for ^{68}Ga, HBED[87] in its modified form HBED-CC[88] seems to form relatively stable complexes with ^{68}Ga already at 25 °C.[89] Its conjugate with glutamate-urea-lysine motive linked via 6-aminohexanoic acid was labelled with $^{68}Ga^{3+}$ and has already entered the clinical studies with patients suffering from prostate cancer.[47] The Orvig group has recently reported on a number of ethylenediamine derivatives of DEDPA[90] (initially called BCPE)[91] forming stable complexes with ^{68}Ga, however the stability dramatically changes upon further functionalization and conjugation of small peptides.[92]

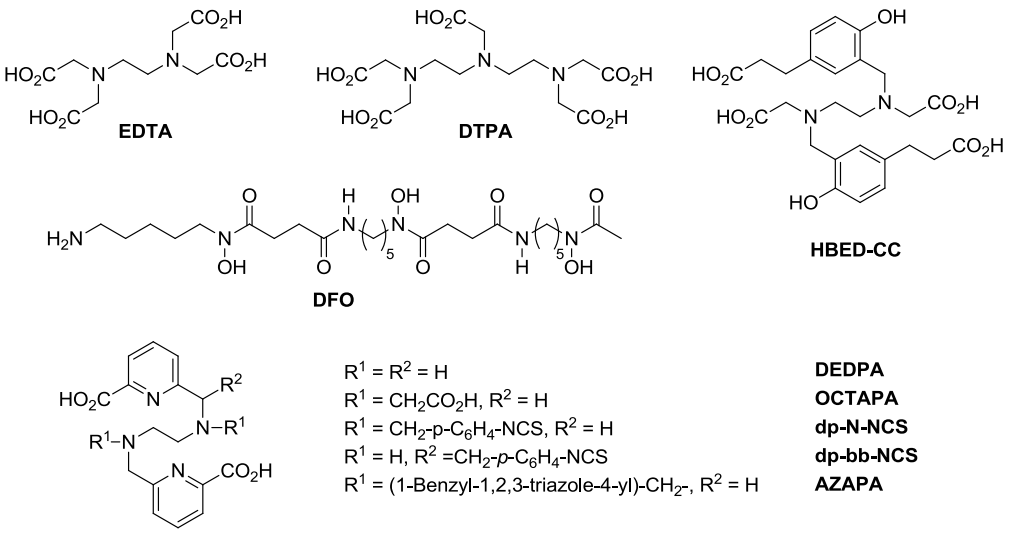

Figure 7: Open-chain chelators for ^{68}Ga recently or more often mentioned in literature.

Recently, also AAZTA ligand (Figure 8) introduced initially for binding Gd^{3+} as a potential MRI contrast agent[93] was investigated with Ga^{3+}, nevertheless with contradictory results published by different groups so far.[94] Based on the similarity with Fe^{3+}, a few siderophores with hydroxypyridinone (YM103)[95] and hydroxypyrone (NOKA)[96] motive were investigated for binding Ga^{3+} but too little has been known to judge their suitability.

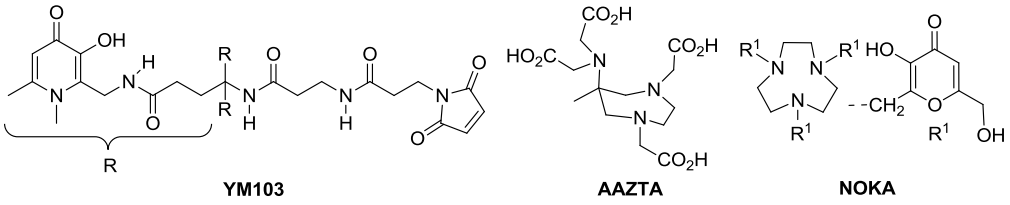

Figure 8: Recently introduced chelators suggested for ^{68}Ga.

2.4. Acidobasic and coordination behaviour of gallium, α-aminocarboxylic and α-aminophosphinic acids

Gallium is predominantly abundant in oxidation state +3 and prefers coordination number 6 in close to octahedral geometry, less often coordination to four ligands in the tetrahedron. Figure 9 shows structural similarity of [Ga(NOTA)][97] and [Ga(H_3TRAP-Pr)][84]. Ga^{III} is "sandwiched" between N_3 and O_3 planes (with dihedral angle 47.6° and 52.2° for NOTA and TRAP-Pr, respectively) in trigonal antiprismatic coordination sphere with Ga^{III} somewhat closer to the N_3 plane. Also comparison of average N–Ga–O "diagonal" angles (167.4° and 169.9° for NOTA and TRAP-Pr complexes, respectively) reveal the geometry of [Ga(H_3TRAP-Pr)] closer to octahedron (180°). Similar parameters were observed for [Ga(TRAP-Ph)][81] and [Ga(H-NODASA)][78] complexes.

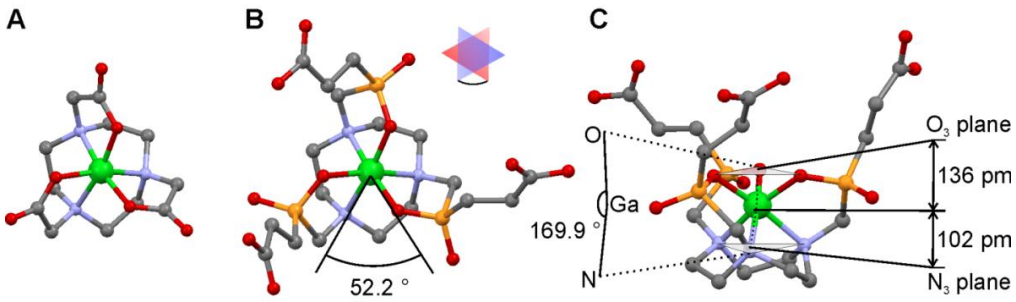

Figure 9: Structural similarity of [Ga(NOTA)] (A) and [Ga(H_3TRAP-Pr)] depicted as a top view (B) with highlighted torsion angle between N_3 and O_3 plane, and a side view (C) with detail on "diagonal angle" and distances between Ga^{III} and the barycentres of N_3 and O_3 planes. Atoms coloured as: Ga - green, P - orange, N - blue, O - red, C - grey, H atoms are omitted for simplicity.

The ionic radius of Ga^{3+} (62 pm in hexaaqua complex) is very similar to that of high-spin Fe^{3+} (65 pm).[98] The similarity of complexes was shown also by comparing [Ga(H_3TRAP-Pr)] and [Fe(H_3TRAP-Pr)]. The Fe^{III} complex adopted more distorted coordination geometry.[84] Both trivalent cations exhibit high affinity to transferrin and behave accordingly in vivo.[99]

From distribution of Ga^{III} species in aqueous solution along pH scale (Figure 10) might be noted the strong tendency for formation of colloidal polynuclear hydroxo species.[100] Gallium in its ionic form, respectively $[Ga(H_2O)_6]^{3+}$, is present predominantly only in very acidic pH (≤ 2.5). At pH 3, 50% is already presented as $Ga_6(OH)_{15}$ in equilibrium at 37 °C. At pH 7, soluble gallate starts to be formed and becomes a dominant species above pH 9.

The formation of colloidal gallium is dependent on concentration and temperature. Gallium at nanomolar concentration readily precipitates already at room temperature at pH ≈ 3 and the process is accelerated at elevated temperatures.[101] Therefore, chemically optimal conditions for complexation of Ga^{3+} are 25 °C and pH ≤ 2.5. Ideally, similar conditions ought to be applied for no-carrier-added ^{68}Ga.[102]

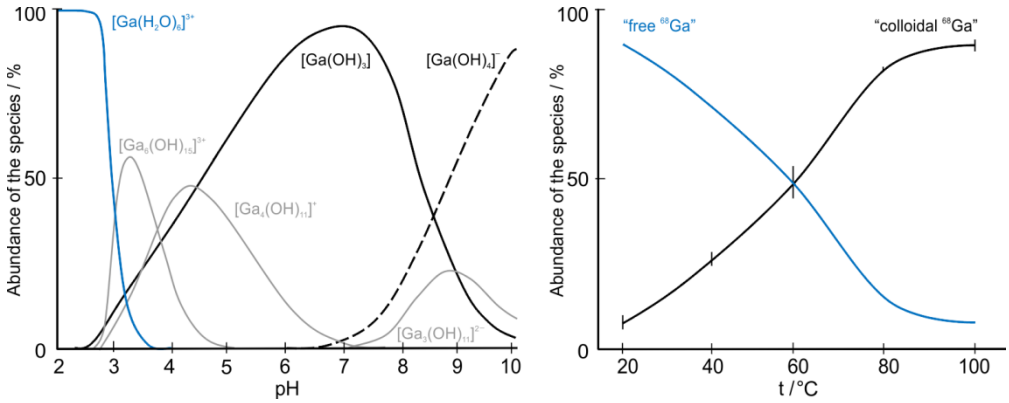

Figure 10: Left - distribution of Ga^{III} species (c_{Ga} = 2 mM in 0.15 M NaCl, 37 °C) as a function of pH; graphics adopted from ref. [100]. Right - formation of "colloidal ^{68}Ga" in a HEPES-buffered eluate (pH 3.3, 5 min, N = 3) as a function of temperature, determined by radio-TLC (0.1 M Na_3Citrate), blue line depicts the availability of "free ^{68}Ga" (calculated); author´s unpublished data.

According to the Pearson´s hard-soft acid-base theory, the Ga^{3+} ion is classified as a hard Lewis acid and forms the most stable complexes with hard Lewis donor atoms such as oxygen or nitrogen, *e.g.* carboxylates, phenols, phosphonates, phosphinates, hydroxamates, and amines.[103] The listed donor groups can be found in motifs of the mostly employed as well as novel chelators for Gallium-68 (Figures 5–8).

Carboxylate-functionalised macrocyclic amines have dominated the chelate design for Ga^{III}. Also the phosphinic acid derivatives (Figure 6) were shown a good alternative for ^{nat}Ga and later ^{67}Ga. Both phosphinic and carboxylic acids bear afterdeprotonation of acidic moiety a single negative charge. The sp^2-hybridised carbon atom gives the carboxylic acids a planar geometry whereas the phosphorus-containing acids are tetrahedral and generally bulkier. α-aminocarboxylic acids show higher basicity of the amino group ($\log K$ ≈ 9.5–11.0 compared to 8.0–9.0 for phosphinic analogues) whereas α-aminophosphinic acids show higher acidity ($\log K$ ≈ 0.5–1.5 compared to 2.0–3.0 for carboxylic analogues).[73b,104]

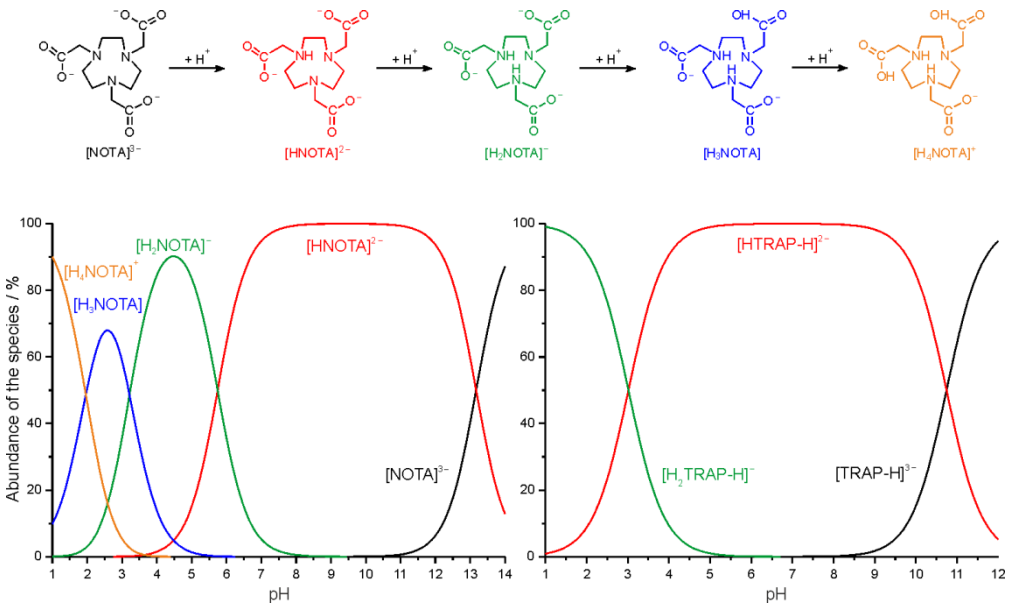

Figure 11: Protonation scheme of NOTA (top). Distribution diagram shows that NOTA (left) is fully deprotonated at highly basic pH, at pH < 5 one or more carboxylates are protonated. For comparison, phosphinic acid pendant arms of TRAP-H (right) are fully deprotonated even at strongly acidic pH. Protonation scheme and species notation for TRAP-H is analogous to NOTA.[105,106]

Different acidity of carboxylate-type NOTA and its phosphinate analogue TRAP-H results in notably different distribution of protonated species depending on pH (Figure 11). Descending pH from basic to acidic region, the protonation of first carboxylic pendant of NOTA occurs already at pH 5 (H_3NOTA) and reaches 50% abundance at pH ≈ 3.5 where the protonation of the second carboxylate begins. At pH 2.5 almost exclusively species with one and two protonated pendant arms were found. Looking back at the distribution of Ga^{III} in aqueous solution (Figure 10), at the same pH only 40% of Ga^{III} is present in ionic form amenable for complexation. Contrary, phosphinate-type TRAP-H with all three deprotonated acidic groups is the only present species at pH 1. The acidobasic behaviour of TACN-based phosphinates is therefore compatible with aqueous chemistry of gallium. At the same pH where $[Ga(H_2O)_6]^{3+}$ is present, the phosphinic acids are deprotonated and thus "pre-prepared" for the complexation as in this case, protonation is the process competing the complex formation.

2.5. Aim of the study

The goal of presented thesis was to develop a bifunctional chelator tailored for $^{68}Ga^{3+}$ and employ it further in preparation of novel ^{68}Ga-PET radiopharmaceuticals.

The search for the right chelate design was based on comparison of the model polyazamacrocyclic compounds (known as well as newly designed) as the potential chelators for $^{68}Ga^{3+}$. Such a comparison should have revealed the trends in coordination chemistry of Ga^{3+} with different carboxylic and phosphinic acid derivatives, and ought to help to suggest structural motives of new bifunctional chelates.

Not only Ga^{III} chemistry but also practical aspects given by the parameters of commercially available $^{68}Ge/^{68}Ga$ generators had to be taken in account. The desired chelator for application in ^{68}Ga-PET was expected to bind $^{68}Ga^{3+}$ quickly and into a stable complex. The labelling should have proceeded using the non-purified generator eluate, at low ligand concentration, over broad pH range and ideally also at room temperature. The complexation reaction had to provide only one product assuring the radiochemical purity of ^{68}Ga PET tracers.

Preferably, the chelator for preparation of monoconjugates was in our focus since we needed an additional building block together with TRAP-Pr meant for multimers and bimodal probes. The labelling properties should have been kept identical or in ideal case better. Certainly, the labelling strategy had to be transferrable to a fully automated, GMP-compliant procedure.

Upon availability of such a novel chelate, bioconjugation to already established small peptides and initial proof-of-concept preclinical studies were planned. In the case of positive results, the new chelate should have been further employed as a sound base for development of novel ^{68}Ga radiopharmaceuticals for diagnosis with PET.

3. General section - introduction to selected methods

Most of the methods described in the publications that resulted from the work on presented dissertation are well-known to a skilled artisan. Therefore only selected topics as the synthetic approach, NMR spectroscopy and labelling methods are pinpointed in this chapter.

3.1. The synthesis of TRAP chelators

The Mannich synthesis is a multicomponent condensation reaction. Non-enolisable aldehyde (*e.g.* formaldehyde) forms an imine or iminium salt with a primary or secondary amine that further accepts the free electron pair of an enolisable carbonyl compound (Scheme 1).[107]

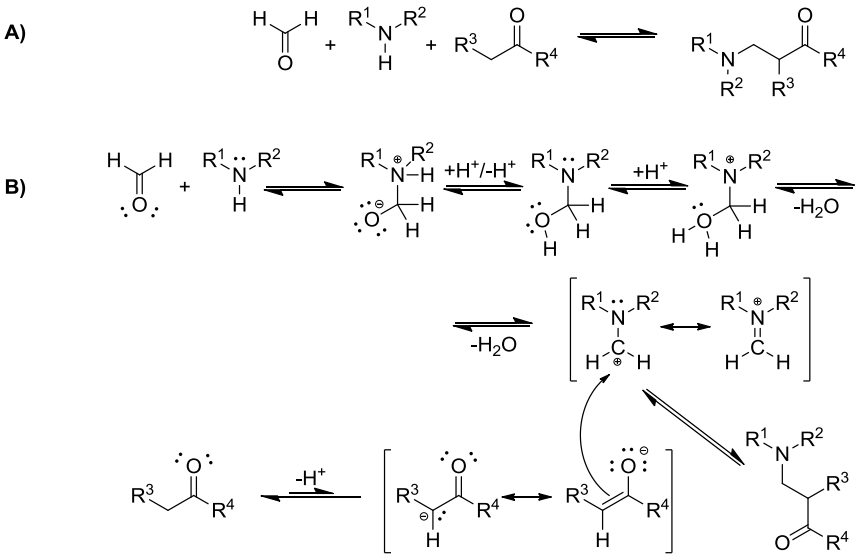

Scheme 1: The Mannich reaction (A) and its mechanism (B).

Kurt Moedritzer and Riyard Irani have shown that a hydrogen atom bound directly to the phosphonic and phosphinic acids exhibits also acidic behaviour, similarly to the acidic proton of enolisable ketones. The Mannich reaction was then easily adopted for preparation of the aminomethylphoshonic/-phosphinic acids (Scheme 2).[108]

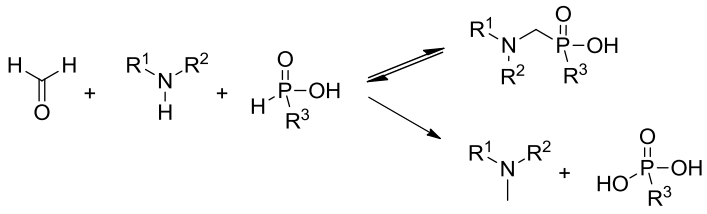

Scheme 2: Mannich-type reaction for phosphinic acids according to Moedritzer and Irani.

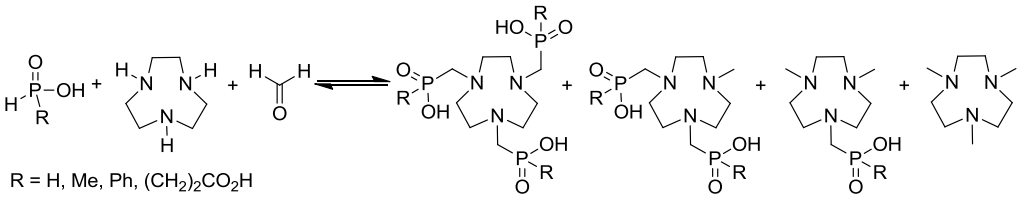

Scheme 3: Moedritzer-Irani reaction yielding TRAP and typical by-products.

Nevertheless, the synthesis of TRAP chelators (Scheme 3) as well as other aminomethylphosphinic acid derivatives via Moedritzer-Irani reaction is accompanied by a formation of methylated amines.[109] The reductive methylation upon oxidation of phosphinic acids to phosphonic ones is complicating the otherwise simple synthetic approach, mainly because of problematic separation of by-products. Generally, the methylation is supressed by enhancing the concentration of the reactants, lowering the reaction temperature and optimised the acidity of a solvent.[110] The mentioned parameters can be tuned according to reactivity of different phosphinic acids. The reaction with hypophosphorous acid bearing two phosphorus-bound hydrogen atoms is feasible already at 25 °C whereas alkylphosphinic acids generally demand elevated temperatures (60–95 °C). Statistically, the formation of methylated by-products correlates with the number of reactive sites on nitrogen atoms of primary and/or secondary amines in a polyamine or a macrocycle.[111]

3.2. ^{31}P and ^{71}Ga NMR spectroscopy

The nuclear magnetic resonance spectroscopy (NMR) is an indispensable analytical tool for characterisation of organic compounds. Typically, the chemical shifts in ^{1}H and ^{13}C spectrum as well as the interaction constants allow for assignment of the signals to a chemical structure.

From 23 know isotopes of phosphorus, only ^{31}P is stable and therefore present at 100% abundance. Moreover, ^{31}P is has a NMR active nucleus with ½ spin and gyromagnetic ratio (γ_n) 10.841×10^7 rad·T^{-1}·s^{-1} (42.5% of that for ^{1}H) which makes it suitable for evaluation of phosphorus-containing molecules. The typical chemical shifts span a relatively large range ($\Delta\delta \approx 2000$ ppm) and are referenced to the shift of 85% aq. H_3PO_4 ($\delta = 0$ ppm). Interaction constants $^{1}J_{PH}$ are generally large (400–1000 Hz) and increase with decreasing bulk of the substituent on a phosphorus atom, $^{3}J_{PX} > {}^{2}J_{PX}$, $^{4}J_{PH}$ are hardly observable, J_{PP} in –P–E–P– (where element E is C or O) ranges approximately from 20 to 80 Hz.[112]

Besides the characterisation of the products, fast acquisition of ^{31}P NMR spectra allows for following the reaction mixtures and efficient optimisation of the reaction steps and conditions accordingly. Therefore, we can observe the formation of –C–P–H or –C–P–C– bonds on phosphinic acids or oxidation of phosphinic to phosphonic acids (Figure 12). Further, in the case of formation of metal complexes accompanied by the change of ^{31}P chemical shifts we can derive the complexation kinetics. ^{31}P shifts and interaction constants can also help to determine the structure of a complex in solution.

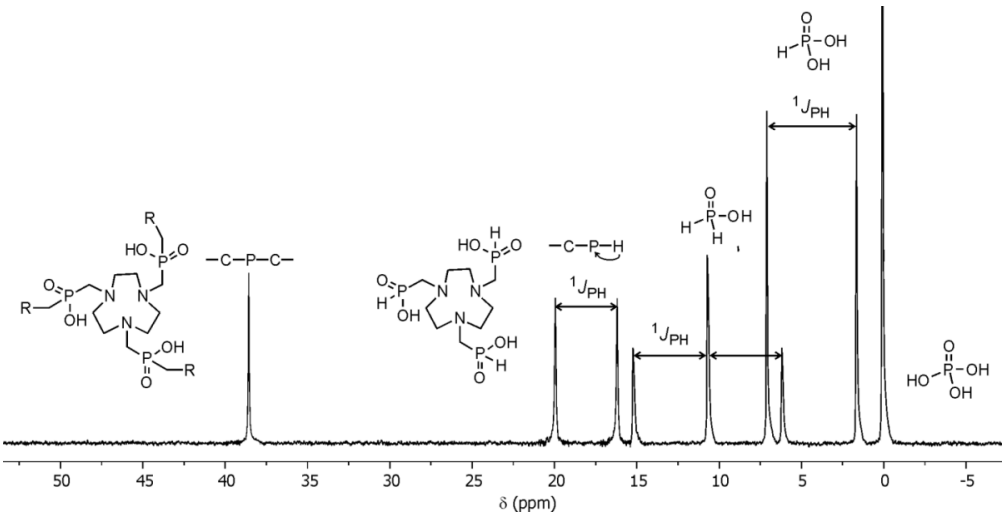

Figure 12: The typical ^{31}P NMR chemical shifts and coupling patterns of phosphinic and phosphonic acids and their derivatives.[113]

Accordingly, the Ga^{III} complex formation/decomposition kinetics can be also evaluated by ^{71}Ga NMR spectroscopy, which is highly valuable especially in the case of carboxylic chelators.[114] Although both naturally abundant Ga isotopes ^{69}Ga (60%) and ^{71}Ga (40%) have quadrupole NMR active nuclei with spin 3/2, ^{71}Ga is the nucleus of choice for NMR studies. ^{71}Ga ($\gamma_n = 8.1731 \times 10^7$ rad·T^{-1}·s^{-1}) is more sensitive and provides more narrow signals compared to ^{69}Ga ($\gamma_n = 6.4323 \times 10^7$ rad·T^{-1}·s^{-1}). ^{71}Ga signals are referenced to $[Ga(H_2O)_6]^{3+}$ (δ = 0 ppm) or $[Ga(OH)_4]^-$ (δ = 220 ppm). The broadening of ^{71}Ga NMR signals generally complicates the spectra interpretation especially for Ga^{III} complexes with lower symmetry. Therefore, no ^{71}Ga NMR signal can be detected for *e.g.* Ga^{III} citrate or acetate complexes.[115] The same holds true for less symmetrical [Ga(TRAP)] complexes. However, highly symmetrical [Ga(TRAP-Pr)] complexes with N_3O_3 coordination planes provide relatively sharp ^{71}Ga singlets at $\delta \approx 100–150$ ppm whereas "out-of-cage" complexes with O_6 coordination are detected at about $\delta \approx -10$ to -50 ppm.[84]

The complex formation can be observed as the integral intensity difference between ^{71}Ga NMR signal of $[Ga(H_2O)_6]^{3+}$ being changed to Ga^{III}-chelate. Accordingly, the acid- or base-promoted hydrolysis can be followed by integral intensity changes between signals for Ga^{III}-chelate and $[Ga(H_2O)_6]^{3+}$ or $[Ga(OH)_4]^-$, respectively.[84,114,116]

3.3. Approaches to labelling with Gallium-68

Since the $^{68}Ge/^{68}Ga$ generators with SnO_2 matrix (iTHEMBA Labs, South Africa) used in reported studies showed low ^{68}Ge breakthrough and generally low content of metal contaminants, labelling with the fractionated eluate was of our choice. Fractionation is the simplest and fastest from the so far reported methods and in our case provided also reproducible results. Three types of labelling setup were described in attached publications (Appendix 2–4): manual labelling, automated labelling and manual labelling with addition of metal salts.

Manual labelling procedure allows for relatively fast evaluation of a chelator by means of labelling yields depending on precursor concentration, temperature, pH and time. Typically, about 20 samples could be evaluated within 1 hour, which is approximately the time needed for obtaining only one value from automated procedure. Moreover, changing the parameters is fast and simple without necessity to adjust the operating software. Therefore, manual labelling is recommended for fast evaluation of optimal labelling conditions for a certain chelating system or comparison of more chelators. Each data point should be obtained using different batches of the eluate and at least as a triplicate to assure the statistically reliable data.[74]

Obtaining the labelling data using automated procedure is generally more time-consuming but since it eliminates variations possibly caused by a human factor, it allows for more precise and better reproducible results. It is generally recommended for labelling of final bioconjugates meant for preclinical studies. GMP-compliant, fully automated synthesis is mandatory for transfer of novel tracers from preclinical research to clinical trials. The same holds true for routine production of ^{68}Ga PET radiopharmaceuticals.[117,30]

The chemoselectivity of chelators for $^{68}Ga^{3+}$ was evaluated upon artificial contamination of the eluate with ascending concentration of Zn^{2+}, Cu^{2+}, Fe^{3+}, Al^{3+}, Sn^{IV} and Ti^{IV} salts dissolved in 1 M HCl in prior to labelling. The experiments were conducted in a similar manner as manual labelling, here with the constant chelator concentration. Decrease of radioactivity incorporation upon enhanced contaminant concentration was compared to blank labelling solution (no contaminant added). To answer the concerns of potential contamination with long-lived parent $^{68}Ge^{IV}$, the investigated chelators were labelled also with $^{68}Ge^{IV}$ at identical labelling conditions.[63]

The labelling in presence of metal contaminants is answering the academic question of chemoselectivity under radiochemical conditions and describing the effect of competing metal cations. Therefore, and from practical point of view, manual labelling procedure is of choice here.

The technique using artificial contamination of the labelling solution can be further utilised also for evaluation of chelators tailored for different radiometals. Accordingly, the chelators for $^{64}Cu^{2+}$ would be among other parameters characterised by resistance to presence of Ni^{2+}, and the chelators for $^{89}Zr^{4+}$ would be efficiently binding Zr^{4+} even in the presence of Y^{3+}. Recently, a related study investigating the influence of different cations on labelling of DOTA-TATE with ^{90}Y and ^{177}Lu was reported.[118]

4. Results and discussion

This chapter primarily outlines the reported project and logical order of the development of tailored chelators for preparation of ^{68}Ga-radiopharmaceuticals for PET. Rather than the scientific details available in attached original peer-reviewed publications (Appendix 1–5), the overall idea and achieved success should be apparent to a reader in brief.

Complexation of metal ions with TRAP (1,4,7-triazacyclononane phosphinic acid) ligands and 1,4,7-triazacyclononane-1,4,7-triacetic acid: phosphinate-containing ligands as unique chelators for trivalent gallium

J. Šimeček, M. Schulz, J. Notni, J. Plutnar, V. Kubíček, J. Havlíčková, P. Hermann,

Inorg. Chem. **2012**, *51*, 577–590.

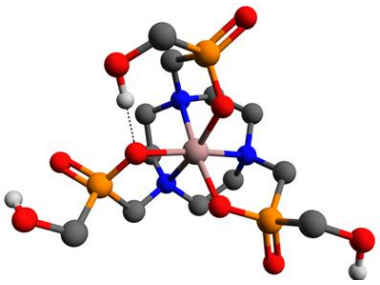

The publication is focused on comparison of acidobasic and coordination properties of TACN-based phosphinic acid chelators and NOTA. Two already described TRAP chelators, TRAP-H and TRAP-Ph, were prepared with improved yields in optimised synthetic strategy. The synthetic part describes also further modification of TRAP-H into a novel chelator TRAP-OH. Since TRAP-Pr, published by Notni *et al.* in 2010, showed very promising coordination properties towards Ga^{III}, it was also included into the comparison. We wanted to find out, what makes TRAP-Pr a better chelator for Ga^{3+} compared to NOTA. Knowing the role of different phosphinic acid derivatives should help us in designing new bifunctional chelators for ^{68}Ga.

Thermodynamic stabilities ($\log K$) of Ga^{III} and Zn^{II}, Ca^{II}, Mg^{II}, Cu^{II}, Lu^{III} or Gd^{III} TRAP complexes were determined by potentiometry. Comparison of $\log K$ values showed that Ga^{3+} is preferred by TRAP over other investigated bivalent and trivalent metals. The phosphinic acid chelators TRAP-OH and TRAP-Pr formed Ga^{III} complexes much faster than the other compared ligands (followed by ^{31}P and/or ^{71}Ga NMR). The phosphinic acid complexes were fully resistant to the acid-promoted hydrolysis. Generally, it seemed that the phosphinic acid has to be further modified with a hydrophilic or oxygen-bearing moiety to bind Ga^{3+} quickly into a stable complex.

For the first time, the direct observation of stable “out-of-cage” Ga^{III} complex was reported for TRAP-OH at slightly basic pH. The most probable structure corresponding to observation with multinuclear NMR spectroscopy and potentiometry was suggested according to the DFT calculations.

TRAP, a powerful and versatile framework for Gallium-68 radiopharmaceuticals

J. Notni, J. Šimeček, P. Hermann, H.-J. Wester, *Chem. Eur. J.* **2011**, *17*, 14718–22.

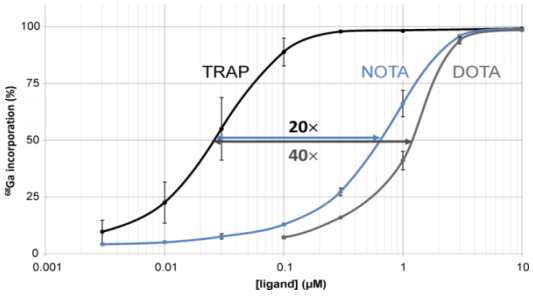

To prove the suitability of previously described TRAP chelators (*Inorg. Chem.* **2012**) for preparation of ^{68}Ga-radiopharmaceuticals, they had to be compared under radiochemical conditions. All aforementioned TRAP chelators, NOTA and DOTA were labelled with $^{68}Ga^{3+}$ obtained from a commercially available ^{68}Ge/^{68}Ga generator.

Based on the previous results from comparison at millimolar concentrations, we expected certain improvements with TRAP as for example the possibility of labelling at lower temperatures or in more acidic region because of the presence of phosphinic acids. Surprisingly, the differences between NOTA, DOTA and TRAP chelators were dramatic. TRAP could be labelled at 20 and 40 times lower concentration (and molar amount) compared to NOTA and DOTA, respectively. TRAP-Pr and TRAP-OH were labelled quantitatively even at pH 0.5. Phosphinates were efficiently labelled at lower precursor amounts already at 25 °C, meanwhile DOTA needed elevated temperatures and NOTA had to be used in higher excess in order to achieve quantitative labelling at room temperature.

Further, this publication describes preparation of trimeric conjugates of TRAP-Pr and the first automated labelling of TRAP(RGD)$_3$ followed by preclinical evaluation. The first data showed not only superior labelling properties but also excellent affinity of TRAP(RGD)$_3$ to the $\alpha_v\beta_3$ integrin, both in vitro and in vivo using mice models xenografted with M21/M21L (high/low $\alpha_v\beta_3$ expression) human melanoma. Preparation of TRAP(RGD)$_2$(Rhodamine) is mentioned as an example of achievable bimodal probes.

A monoreactive bifunctional triazacyclononane-phosphinate chelator with high selectivity for Gallium-68

J. Šimeček, O. Zemek, P. Hermann, H.-J. Wester, J. Notni, *ChemMedChem* **2012**, *7*, 1375–1378.

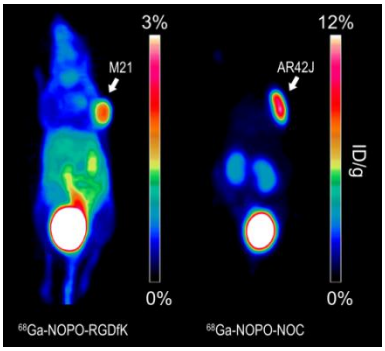

This study is focused on development of a bifunctional chelator NOPO and the results from preclinical studies with ^{68}Ga-NOPO-peptides. According to the results from previous publications, chelate design of NOPO comprises TACN substituted with one methylene(2-carboxyethyl)-phosphinic acid pendant arm and two methylene-(hydroxymethyl)phosphinates. Compared to TRAP-Pr (three conjugation sites) and TRAP-OH (no conjugation site), NOPO bears one carboxylic moiety for coupling to primary amines. Even this asymmetrically substituted derivative showed excellent labelling properties previously found with the symmetrical TACN-based chelators.

Moreover, NOPO showed high chemoselectivity for $^{68}Ga^{3+}$ even in the presence of chemically similar Fe^{3+} and ^{68}Ga decay product, Zn^{2+}. Tolerance for those critical metal ions resulted in highly reproducible radiochemical yields and high specific activities of investigated bioconjugates.

Proof-of-concept preclinical imaging was done with conjugates of two well established peptides. NaI^3-Octreotide (NOC) for targeting the sst2 receptors overexpressed in neuroendocrine tumours was employed for preparation of ^{68}Ga-NOPO-NOC. The in vivo experiments using nude mice bearing AR42J (rat pancreas carcinoma) tumour xenografts proved high and specific uptake of ^{68}Ga-NOPO-NOC and fast renal clearance of the tracer. ^{68}Ga-NOPO-c(RGDfK) was used for mapping of $\alpha_v\beta_3$ integrin expression in a nude mouse bearing human melanoma xenografts.

After the initial evaluation, NOPO was found an attractive framework for development of new ^{68}Ga-labelled tracers and/or transfer of current vectors from research to clinics.

How is ^{68}Ga-labelling of macrocyclic chelators influenced by metal ion contaminants in ^{68}Ge/^{68}Ga generator eluates?

J. Šimeček, P. Hermann, H.-J. Wester, J. Notni, *ChemMedChem* **2013**, *8*, 95–103.

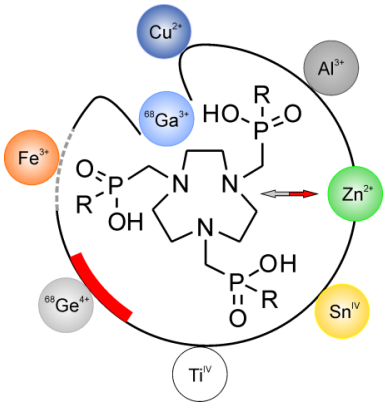

The results from previous publication (ChemMedChem **2012**) opened the discussion about the chemoselectivity of the phosphinic acids ligands for $^{68}Ga^{3+}$. The macrocyclic chelators are known for selectivity for certain metal ions according to the ligand´s size, number of coordination sites and their type. Since Zn^{2+}, Fe^{3+}, Al^{3+}, Cu^{2+}, Sn^{IV}, Ti^{IV} and $^{68}Ge^{IV}$ are the most frequently detected trace contaminants in the ^{68}Ge/^{68}Ga generator eluate, we artificially contaminated the $^{68}Ga^{3+}$ eluate with them. Labelling efficiency in ascending concentrations of the metal salts (from “no metal added” to thousand-fold excess of a contaminant over the chelator) was compared for DOTA, NOTA, TRAP chelators, NOPO and corresponding c(RGDfK) conjugates.

The investigated chelators were not significantly influenced by presence of Fe^{3+}, Al^{3+}, Cu^{2+}, Sn^{IV} and Ti^{IV} at concentrations typically abundant in ^{68}Ge/^{68}Ga generator eluate. Zn^{2+} as the product of parent $^{68}Ga^{3+}$ decay can reach a critical concentration influencing the labelling of NOTA and DOTA-like bioconjugates. At the same time, NOPO and TRAP showed exceptional tolerance to high excess of Zn^{2+} over the chelator.

This observation was further clarified as transmetallation of Zn^{II} complexes to $^{68}Ga^{III}$ by direct labelling of Zn^{II} complexes of investigated ligands. The transmetallation of Zn^{II} complexes was studied also by ^{31}P and ^{71}Ga NMR and MS.

The reported observations helped to explain common limitations for labelling of NOTA and DOTA with $^{68}Ga^{3+}$ and showed a completely new feature of phosphinic acid chelators, their chemoselectivity for $^{68}Ga^{3+}$. The experimental setup reported in this study could be also used as a new method for evaluation of chelators for the use in nuclear medicine.

Copper-64 labelling of triazacyclononane-triphosphinate chelators

J. Šimeček, H.-J. Wester, J. Notni, *Dalton Trans.* **2012**, *41*, 13803–13806.

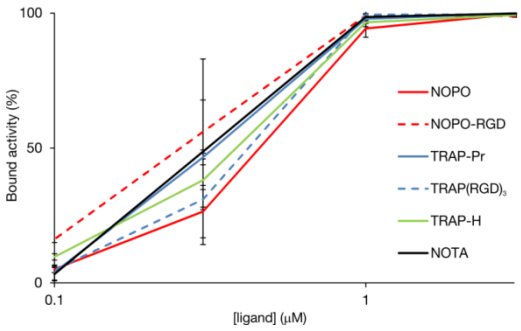

In the study "How is ^{68}Ga-labelling of macrocyclic chelators influenced by metal ion contaminants in ^{68}Ge/^{68}Ga generator eluates?" we found that the presence of Cu^{2+} reduced labelling efficiency with NOTA. Also TRAP-like chelators were influenced by Cu^{2+} more significantly than by Zn^{2+}. As a couple of recent publications reported on feasible preparation of ^{64}Cu-labelled NOTA-like conjugates and high in vivo stability of the formed ^{64}Cu-chelates, we were interested if the same holds true also for the phosphinic acid chelators.

We carried out standard set of labelling experiments using NOTA, DOTA and TRAP-like chelators, this time with $^{64}Cu^{2+}$. The comparable performance of triazacyclononane-based chelators independently on *N*-substituents was observed. All TACN-based chelators performed better than DOTA. The absolute molar amount of the chelator showed to be the critical parameter for efficient and reproducible labelling. Generally, the labelling was quantitative when the molar amount of a chelator exceeded the total content of metal contaminants in $^{64}Cu^{2+}$ solution.

We also labelled a number of TRAP-like conjugates and briefly investigated the in vivo properties of ^{64}Cu-TRAP(RGD)$_3$. Both ^{64}Cu- and ^{68}Ga-TRAP(RGD)$_3$ showed similar biodistribution and tracer accumulation in M21 tumour xenografts. The in vivo stability of ^{64}Cu-labelled TRAP-like conjugates remained an opened issue.

However, we concluded that in the case of TRAP-like conjugates, $^{68}Ga^{III}$ can be exchanged by $^{64}Cu^{II}$ in order to achieve higher spatial resolution of μ-PET imaging in rodent species at early time point after the tracer administration.

5. Summary

The presented dissertation describes the process of tailoring the design of macrocyclic chelators for $^{68}Ga^{3+}$. We prepared and evaluated a number of phosphinic acid derivatives of triazacyclononane with symmetrical *N*,*N*´,*N*´´-substitution pattern to see the influence of different pendant arms. So called TRAP chelators were compared with the carboxylic triazacyclononane derivative NOTA with respect to formation kinetics, selectivity and stability of Ga^{III} chelates.

After chemical ($^{69,71}Ga^{III}$) and radiochemical ($^{68}Ga^{III}$) evaluation of NOTA, TRAP-H, TRAP-Ph, TRAP-Pr and TRAP-OH, we selected the most promising chelators TRAP-Pr (with three conjugation sites) and TRAP-OH (no conjugation via amide bond possible). These two chelators could be efficiently labelled already at 0.03 μM concentration, pH 0.2, at 25 °C or within 1 min, which made them far more suitable for $^{68}Ga^{3+}$ in comparison to the other investigated ligands.

Their substitution patterns were combined in the design of NOPO, a ligand for direct monoconjugation to primary amines of small biomolecules. After the first set of radiochemical evaluation, NOPO became the focused chelator in our further research with $^{68}Ga^{3+}$.

NOPO suits to the critically selected features that a bifunctional chelator designed for binding $^{68}Ga^{3+}$ should fulfil. The synthetic protocol was simplified and optimised to good isolated yields (45% in multistep synthesis). NOPO has a long shelf-life and does not demand any special handling. Its Ga^{III} complex is thermodynamically stable ($\log K = 25.01$) and kinetically inert (stable in 6 M $HClO_4$ over months). Direct monoconjugation to small peptides is easily achievable in 10 minutes and followed by standard purification procedures.

NOPO showed high chemoselectivity for $^{68}Ga^{3+}$ even in presence of other metal cations in huge excess, namely Zn^{2+}, the daughter product of ^{68}Ga decay. This feature of a chelator for $^{68}Ga^{3+}$allows for convenient labelling strategies using non-purified eluate, independently on the content of other metallic impurities. Radiolabelling of the conjugates is comparable with the free chelator within the error margins. An excellent reproducibility of the labelling yields is one of the strongest features of NOPO with respect to translation of new PET tracers to the clinics.

Besides chemical and radiochemical evaluation, we proved the clinical potential of ^{68}Ga-NOPO-peptides using two conjugates of well-established vectors, Nal^{3}-Octreotide and c(RGDfK).

^{68}Ga-NOPO-c(RGDfK) was used for mapping the $\alpha_v\beta_3$ integrin expression in nude mice bearing human melanoma xenografts with high (M21) and low (M21L) $\alpha_v\beta_3$ expression. The radiotracer accumulated specifically in tissues expressing $\alpha_v\beta_3$ integrins. The uptake in M21 tumour was 2.02% ID/g at 60 min p.i.

PET imaging of mice bearing rat pancreatic carcinoma AR42J xenografts with ^{68}Ga-NOPO-NOC resulted in images with low background, biodistribution studies showed high and specific tumour uptake (13.87% ID/g at 120 min p.i.) and high tumour to background ratio.

Both investigated radiotracers were fully stable against transchelation to EDTA, in human plasma and PBS at 37 °C, and in vivo in small animal models. The complete preclinical evaluation of ^{68}Ga-NOPO-NOC and ^{68}Ga-NOPO-c(RGDfK) proved NOPO a good platform for preparation of ^{68}Ga-radiopharmaceuticals. Additionally, the straightforward labelling procedure and repeatedly achievable quantitative yields made NOPO preferable over DOTA- and NOTA-like chelators for development of the monoconjugates with diagnostic potential.

From the preclinical point of view, ^{68}Ga-labelled NOPO-monoconjugates are important because of exceptionally high achievable SA (up to 7 TBq/µmol). Extremely low precursor amounts (≈ 0.1 µg compared to ≈ 20.0 µg for DOTA-like conjugates) necessary for quantitative labelling yields are valuable for targeting the receptors with low density in rodents. At the same time, no pharmacological effects of unlabelled conjugate might be expected. Moreover, once reaching the maximally achievable SA, it can be exactly tuned by addition of corresponding amount of a ^{nat}Ga-NOPO-peptide. It allows for very precise dosing of a ^{68}Ga-radio-pharmaceutical and the studies of influence of the SA on the tracer´s biodistribution.

In order to obtain the µ-PET images with higher spatial resolution or the images at the late time point p.i., NOPO-conjugates can be alternatively labelled with $^{64}Cu^{2+}$.

The so far reported features of NOPO make it the cutting edge ligand for $^{68}Ga^{3+}$. Our novel approach to labelling with $^{68}Ga^{3+}$ was quickly recognised within the scientific community dealing with the similar problematic. The latest results have been extensively presented at a number of international meetings (see the list of conference contributions) and the cooperating network has started being developed. The significance of our results is reflected by interest coming also from the industry.

6. References

[1] a) R. Weissleder, M. J. Pittet, *Nature* **2008**, *452*, 580–589; b) H.-J. Wester, *Clin. Cancer Res.* **2007**, *13*, 3470–3481.

[2] a) T. Gupta, S. Beriwal, *Indian J. Cancer* **2010**, *47*, 126–133; b) A. Bockisch, L. S. Freudenberg, D. Schmidt, T. Kuwert, *Semin. Nucl. Med.* **2009**, *39*, 276–289; c) B. J. Pichler, A. Kolb, T. Nägele, H. P. Schlemmer, *J. Nucl. Med.* **2010**, *51*, 333–336; d) A. W. Sauter, H. F. Wehrl, A. Kolb, M. S. Judenhofer, B. J. Pichler, *Trends Mol. Med.* **2010**, *16*, 508–515; e) A. Boss, L. Stegger, S. Bisdas, A. Kolb, N. Schwenzer, M. Pfister, C. D. Claussen. B. J. Pichler, C. Pfannenberg, *Eur. Radiol*. **2011**, *21*, 1439–1446.

[3] F. C. Gaertner, S. Fürst, M. Schwaiger, *Cancer Imaging* **2013**, *13*, 36–52.

[4] a) R. J. Hicks, M. S. Hofman, *Nat. Rev. Clin. Oncol.* **2012**, *12*, 712–720; b) J. P. Holland, P. Cumming, N. Vasdev, *J. Nucl. Med.* **2012**, *53*, 1333–1336.

[5] a) C. Rischpler, S. Nekolla, M. Schwaiger, *Curr. Cardiol. Rep.* **2013**, *15*, 337–348; b) E. E. van der Wall, *Neth. Heart J.* **2012**, *20*, 297–298; c) B. A. McArdle, T. D. Dowsley, R. A. de Kemp, G. A. Wells, R. S. Beanlands, *J. Am. Coll. Cardiol.* **2012**, *60*, 1828–1837.

[6] a) N. Torosyan, D. H. Silverman, *Semin. Nucl. Med.* **2012**, *42*, 415–422; b) E. M. Reiman, W. J. Jagust, *Neuroimage* **2012**, *61*, 505–516; c) A. D. Murray, *Am. J. Neuroradiol.* **2012**, *33*, 1836–1844.

[7] S. V. Smith, *J. Inorg. Biochem.* **2004**, *98*, 1874–1901.

[8] R. G. Zimmermann, *Nucl. Med. Biol.* **2013**, *40*, 155–166.

[9] M. E. Phelps, E. J. Hoffman, S. C. Huang, D. E. Kuhl, *J. Nucl. Med.* **1978**, *19*, 635–647.

[10] M. M. Ter-Pogossian, M. E. Phelps, E. J. Hoffman, N. A. Mullani, *Radiology* **1975**, *114*, 89–98.

[11] a) Brookhaven National Laboratory: National Nuclear Decay Center, *http://www.nndc.bnl.gov*, Accessed May **2013**; b) M. J. Welch, C. S. Redvanly, *Handbook of Radiopharmaceuticals: Radiochemistry and Applications*, Wiley, New York, **2003**.

[12] a) T. Hara, N. Kosaka, H. Kishi, *J. Nucl. Med.* **1998**, *39*, 90–99; b) S. N. Reske, S. Moritz, T. Kull, *Q. J. Nucl. Med. Mol. Imaging* **2012**, *56*, 430–439.

[13] a) T. R. DeGrado, S. W. Baldwin, S. Wang, M. D. Orr, R. P. Liao, H. S. Friedmann, R. Reiman, D. T. Price, R. E. Coleman, *J. Nucl. Med.* **2001**, *12*, 1805–1814; b) F. Würschmid, C. Petersen, A. Wahl, J. Dahle, M. Kretschmer, *Radiat. Oncol.* **2011**, *6*, 44.

[14] a) C. A. Mathis, Y. Wang, D. P. Holt, G.-F. Huang, M. L. Debnath, W. E. Klunk, *J. Med. Chem.* **2003**, *46*, 2740–2754; b) S. Hatashita, H. Yamasaki, *J. Alzheimers Dis.* **2010**, *21*, 995–1003.

[15] a) S. R. Choi, G. Golding, Z. Zhuang, W. Zhang, N. Lim, F. Hefti, T. Benedum, M. R. Kilbourn, D. Skovronsky, H. F. Kung, *J. Nucl. Med.* **2009**, *50*, 1887–1894; b) M. Romano, E. Buratti, *Drugs Today **2013***, *49*, 181–193.

[16] a) J. Pacák, Z. Točík, M. Černý, *J. Chem. Soc.* **1969**, 77; b) T. Ido, C. N. Wan, V. Casella, J. S. Fowler, A. P. Wolf, M. Reivich, D. E. Kuhl, *J. Labelled Compd. Radiopharm.* **1978**, *24*, 174–183; c) D. A. Mankov, J. F. Deary, J. M. Link, M. Muzi, J. G. Rajendran, A. M. Spence, K. A. Krohn, *Clin. Cancer Res.* **2007**, *13*, 3660–3669.

[17] a) P. A. Jerabek, T. B. Patrick, M. R. Kilbourn, D. D. Dischino, M. J. Welch, *Int. J. Rad. Appl. Instrum.* **1986**, *37*, 599–605; b) J. L. Lim, M. S. Berridge, *Appl. Radiat. Isot.* **1993**, *44*, 1085–1091; c) S. T. Lee, A. M. Scott, *Semin. Nucl. Med.* **2007**, *37*, 451–461.

[18] a) A. F. Shields, J. R. Grierson, B. M. Dohmen, H. J. Machulla, J. C. Styanoff, J. M. Lawhorn-Crews, J. E. Obradovich, O. Muzik, T. J. Mangner, *Nat. Med.* **1998**, *4*, 1334–1336; b) T. Barwick, B. Bencherif, J. M. Mountz, N. Avril, *Nucl. Med. Commun.* **2009**, *30*, 908–917.

[19] a) D. Comar, J. Cartron, M. Maziere, C. Marazano, *Eur. J. Nucl. Med.* **1976**, 11–14; b) T. Singhal, T. K. Narayan, V. Jain, J. Mukherjee, J. Mantil, *Mol. Imaging Biol.* **2008**, *10*, 1–18.

[20] a) H.-J. Wester, M. Herz, W. Weber, P. Heiss, R. Senekowitsch-Schmidtke, M. Schwaiger, G. Stöcklin, *J. Nucl. Med.* **1999**, *40*, 205–212; b) P. Heiss, S. Mayer, M. Herz, H.-J. Wester, M. Schwaiger, R. Senekowitsch-Schmidtke, *J. Nucl. Med.* **1999**, *40*, 1367–1373; c) V. Dunet, C. Rossier, A. Buck, R. Stupp, J. O. Prior, *J. Nucl. Med.* **2012**, *53*, 207–214.

[21] G. H. Hutchins, *Cardiology* **1997**, *88*, 106–115.

[22] M. Schwaiger, O. Muzik, *Am. J. Cardiol.* **1991**, *67*, 35D–43D.

[23] a) F. D. Grant, F. H. Fahey, A. B. Packard, R. T. Davis, A. Alavi, S. T. Treves, *J. Nucl. Med.* **2008**, *49*, 68–78; b) K. K. Wong, M. Piert, *J. Nucl. Med.* **2013**, *54*, 590–599.

[24] a) M. Fani, H. Mäcke, *Eur. J. Nucl. Med. Mol. Imaging* **2012**, *39*, S11–S30; b) P. Lavermann, J. K. Sosabowski, O. C. Boermann, W. J. G. Oyen, *Eur. J. Nucl. Med. Mol. Imaging* **2012**, *39*, S78–S92; c) M. Naji, A. Al-Nahnas, *Eur. J. Nucl. Med. Mol. Imaging* **2012**, *39*, S61–S67.

[25] a) R. Haubner, H.-J. Wester, W. A. Weber, C. Mang, S. Ziegler, S. L. Goodman, R. Senekowitsch-Schmidtke, H. Kessler, M. Schwaiger, *Cancer Res.* **2001**, *61*, 1781–1785; b) R. Haubner, B. Kuhnast, C. Mang, W. A. Weber, H. Kessler, H.-J. Wester, M. Schwaiger, *Bioconjugate Chem.* **2004**, *15*, 61–69.

[26] a) A. J. Beer, R. Haubner, M. Goebel, S. Luderschmidt, M. E. Spilker, H.-J. Wester, *J. Nucl. Med.* **2005**, *46*, 1333–1341; b) A. J. Beer, A. L. Grosu, J. Carlsen, A. Kolk, M. Sarbia, I. Stangier, P. Watzlowik, H.-J. Wester, R. Haubner, M. Schwaiger, *Clin. Cancer Res.* **2007**, *13*, 6610–6616; c) A. J. Beer, M. Niemeyer, J. Carlsen, M. Sarbia, J. Nährig, P. Watzlowik, H.-J. Wester, N. Harbeck, M. Schwaiger, *J. Nucl. Med.* **2008**, *49*, 255–259.

[27] a) F. C. Gaertner, H. Kessler, H.-J. Wester, M. Schwaiger, A. J. Beer, *Eur. J. Nucl. Med. Mol. Imaging* **2012**, *39*, S126–S138; b) A. J. Beer, H. Kessler, H.-J. Wester, M. Schwaiger, *Theranostics* **2011**, *1*, 48–57.

[28] K. Pohle, J. Notni, J. Bussemer, H. Kessler, M. Schwaiger, A. J. Beer, *Nucl. Med. Biol.* **2012**, *39*, 777–784.

[29] J. Notni, K. Pohle, H.-J. Wester, *Nucl. Med. Biol.* **2013**, *40*, 33–41.

[30] J. Notni, K. Pohle, H.-J. Wester, *EJNMMI Res.* **2013**, *2*, 28.

[31] a) W. J. McBride, R. M. Sharkey, H. Karacay, C. A. D´Souza, E. A. Rossi, P. Laverman, C.-H. Chang, O. C. Boermann, D. M. Goldenberg, *J. Nucl. Med.* **2009**, *50*, 991–998; b) P. Laverman, W. J. McBride, R. M. Sharkey, A. Eek, L. Joosten, W. J. G. Oyen, D. M. Goldenberg, O. C. Boermann, *J. Nucl. Med.* **2010**, *51*, 454–4612.

[32] a) W. J. McBride, C. A. D´Souza, H. Karacay, R. M. Sharkey, D. M. Goldenberg, *Bioconjugate Chem.* **2012**, 23, 538–547; b) N. Guo, L. Lang, W. Li, D. O. Kiesewetter, H. Gao, G. Niu, Q. Xie, X. Chen, *PLoS One* **2012**, *7*, e37506.

[33] a) W. J. McBride, C. A. D´Souza, R. M. Sharkey, H. Karacay, E. A. Rossi, C.-H. Chang, D. M. Goldenberg, *Bioconjugate Chem.* **2010**, 21, 1331–1340; b) C. A. D´Souza, W. J. McBride, R. M. Sharkey, L. J. Todaro, D. M. Goldenberg, *Bioconjugate Chem.* **2011**, 22, 1793–1803; c) P. Laverman, C. A. D´Souza, A. Eek, W. J. McBride, R. M. Sharkey, W. J. G. Oyen, D. M. Goldenberg, O. C. Boermann, *Tumor Biol.* **2012**, *33*, 427–434.

[34] W. Wan, N. Guo, D. Pan, Ch. Yu, Y. Weng, S. Luo, H. Ding, Y. Xu, L. Wang, L. Lang, Q. Xie, M. Yang, X. Chen, *J. Nucl. Med.* **2013**, *in press*, doi:10.2967/jnumed.112.113563.

[35] O. F. Ikotun, S. E. Lapi, *Future Med. Chem.* **2011**, *3*, 599–621.

[36] A. M. Groves, M. E. Speechly-Dick, J. C. Dickson, I. Kavani, R. Endozo, P. Blanchard, M. Shastry, E. Prvulovich, W. A. Waddington, S. Ben-Haim, J. B. Bomanii, J. R. McEwan, P. J. Ell, *Eur. J. Nucl. Med. Mol. Imaging* **2007**, *34*, 1965–1972.

[37] a) A. Sanchez-Crespo, P. Andreo, S. A. Larsson, *Eur. J. Nucl. Med. Mol. Imaging* **2004**, *31*, 44–51; b) A. Sanchez-Crespo, *Appl. Radiat. Isot.* **2013**, *76*, 55–62.

[38] M. Fellner, R. P. Baum, V. Kubíček, P. Hermann, I. Lukeš, V. Prasad, F. Rösch, *Eur. J. Nucl. Med. Mol. Imaging* **2010**, *37*, 834.

[39] M. A. Deri, B. M. Zeglis, L. C. Francesconi, J. S. Lewis, *Nucl. Med. Biol.* **2013**, *40*, 3–14.

[40] J. Notni, Nachr. Chem. **2012**, *60*, 645–649.

[41] I. Velikyan, *Recent Results Cancer. Res.* **2013**, *194*, 101–131.

[42] a) G. Treglia, P. Castaldi, M. F. Villani, G. Perotti, C. de Waure, A. Filice, V. Ambrosini, N. Cremonini, M. Santimaria, A. Versari, S. Fanti, A. Giordano, V. Rufini, *Eur. J. Nucl. Med. Mol. Imaging* **2012**, *39*, 569–580; b) S. Koukouraki, L. G. Strauss, V. Georgoulias, M. Eisenhut, U. Haberkorn, A. Dimitrakopoulou-Strauss, *Eur. J. Nucl. Med. Mol. Imaging* **2006**, *33*, 1115–1122; c) A. Dimitrakopoulou-Strauss, M. Seiz, J. Tuettenberg, K. Schmieder, M. Eisenhut, U. Haberkorn, L. G. Strauss, *Clin. Nucl. Med.* **2011**, *36*, 101–108.

[43] a) E. Gourni, O. Demmer, M. Schottelius, C. D´Alessandia, S. Schulz, I. Dijkgraaf, U. Schumacher, M. Schwaiger, H. Kessler, H.-J. Wester, *J. Nucl. Med.* **2011**, *52*, 1803–1810; b) U. Hennrich, L. Seyler, M. Schäfer,

U. Bauder-Wüst, M. Eisenhut, W. Semmler, T. Bäuerle, *Bioorg. Med. Chem.* **2012**, 1502–1510.

[44] a) M. Fani, M. Braun, B. Waser, K. Beetschen, R. Cescato, J. Erchegyi, J. E. Rivier, W. A. Weber, H. R. Mäcke, J. C. Reubi, *J. Nucl. Med.* **2012**, *53*, 1481–1489; b) M. Fani, L. Del Pozzo, K. Abiraj, R. Mansi, M. L. Tamma, R. Cescato, B. Wasser, W. A. Weber, J. C. Reubi, H. R. Mäcke, *J. Nucl. Med.* **2011**, *52*, 1110–1118.

[45] M. Fellner, B. Biesalski, N. Bausbacher, V. Kubíček, P. Hermann, F. Rösch, O. Thews, *Nucl. Med. Biol.* **2012**, *39*, 993–999.

[46] M. Fani, M.-L. Tamma, G. P. Nicolas, L. Lasri, Ch. Medina, I, Raynal, M. Port, W. A. Weber, H. R. Mäcke, *Mol. Pharmaceutics* **2012**, *9*, 1136–1145.

[47] a) M. Eder. M. Schäfer, U. Bauder-Wüst, W. E. Hull, C. Wängler, U. Haberkorn, M. Eisenhut, *Bioconjugate Chem.* **2012**, *23*, 688–697; b) A. Afshar-Oromieh, U. Haberkorn, M. Eder, M. Eisenhut, C. M. Zechmann, *Eur. J. Nucl. Med. Mol. Imaging* **2012**, *39*, 1085–1086.

[48] H.-J. Wester, Nuklearmedizin **2012**, *51*, N1–N4.

[49] a) G. L. Bronwell, W. H. Sweet, *Nucleonics* **1953**, *11*, 40–45; b) W. B. Seeman, M. M. Ter-Pogossian, H. G. Schwartz, *Radiology* **1954**, *62*, 30–36.

[50] M. Brucer, G. A. Andrews, H. D. Brunner, *Radiology* **1953**, *61*, 534–613.

[51] G. I. Gleason, *Int. J. Appl. Radiat. Isot.* **1960**, *8*, 90–94.

[52] M. W. Greene, W. D. Tucker, *Int. J. Appl. Radiat. Isot.* **1961**, *12*, 62–63.

[53] a) C. Loc'h, B. Mazi'ere, D. Comar, *J. Nucl. Med.* **1980**, *21*, 171–173; b) M. Lin, D. Ranganathan, T. Mori, A. Hagooly, R. Rossin, M. J. Welch, S. E. Lapi, *Appl. Radiat. Isot.* **2012**, *70*, 2539–2544; c) E. de Blois, H. S. Chan, C. Naidoo, D. Prince, E. P. Krenning, W. A. P. Breeman, *Appl. Radiat. Isot.* **2011**, *69*, 308– 315.

[54] Y. Yano, H. O. Anger, *J. Nucl. Med.* **1964**, *5*, 484–487.

[55] a) C. N. Shealy, S. Aronow, G. L. Brownell, *J. Nucl. Med.* **1964**, *5*, 161–167; b) H. O. Anger, A. Gottschalk, *J. Nucl. Med.* **1963**, *4*, 326–330; c) A. Gottschalk, H. O. Anger, *Am. J. Roentgenol. Radium Ther. Nucl. Med.* **1964**, *92*, 174–176; d) A. Gottschalk, K. R. McCormack, J. E. Adams, *Radiology* **1965**, *84*, 502–506.

[56] R. M. Smith, A. E. Martell, *Critical Stability Constants*; Plenum Press: New York, **1989**.

[57] J. Schuhmacher, W. Maier-Borst, *Int. J. Appl. Radiat. Isot.* **1981**, *32,* 31–36.

[58] From correspondence with A. Razbash, Cyclotron Co. Ltd., Obninsk, Russia, **4.2.2013**.

[59] a) K. Zhernosekov, M. Harfensteller, J. Moreno, O. Leib, O. Buck, A. Tuerler, R. Henkelmann, T. Nikula, *Eur. J. Nucl. Med. Mol. Imaging* **2010**, *37*, S251; b) A. A. Razbash, *Eur. J. Nucl. Med. Mol. Imaging* **2003**, *30*, S318.

[60] C. Decristoforo, R. D. Pickett, A. Verbruggen, *Eur. J. Nucl. Med. Mol. Imaging* **2012**, *39*, S31–S40.

[61] a) F. Rösch, P. J. Riss, *Curr. Top. Med. Chem.* **2010**, *10*, 1633–1648; b) F. Rösch, *Appl. Radiat. Isot.* **2013**, *76*, 24–30.

[62] a) I. Velikyan, G. J. Beyer, E. Bergström-Pettermann, P. Johannsen, M. Bergstöm, B. Långström, *Nucl. Med. Biol.* **2008**, *35*, 529–536; b) M. Asti, G. D. Pietri, A. Fraternali, E. Grassi, R. Sghedoni, F. Fioroni, F. Rösch, A. Versari, D. Salvo, *Nucl. Med. Biol.* **2008**, *35*, 721–724; c) I. Velikyan, G. J. Beyer, B. Långström, *Bioconjugate Chem.* **2004**, *15*, 554–560.

[63] J. Šimecek, P. Hermann, H.-J. Wester, J. Notni, *ChemMedChem* **2013**, *8*, 95–103.

[64] a) K. P. Zhernosekov, D. V. Filosofov, R. P. Baum, P. Aschoff, H. Bihl, A. A. Razbash, M. Jahn, M. Jennewein, F. Rösch, *J. Nucl. Med.* **2007**, *48*, 1741–1748; b) F. Zoller, P. J. Riss, F. P. Montforts, F. Rösch, Radiochim. Acta **2010**, *98*, 157–160; c) N. S. Loktionova, A. N. Belozub, D. V. Filosofov, K. P. Zhernosekov, T. Wagner, A. Tuerler, F. Rösch, *Appl. Radiat. Isot.* **2011**, *69*, 942–946.

[65] a) D. Mueller, I. Klette, R. P. Baum, M. Gottschaldt, M. K. Schultz, W. A. P. Breeman, *Bioconjugate Chem.* **2012**, *23*, 1712–1717; b) M. K. Schulz, D. Mueller, R. P. Baum, G. L. Watkins, W. Breeman, *Appl. Radiat. Isot.* **2013**, *in press*, doi:10.1016/j.apradiso.2012.08.011.

[66] G. J. Meyer, H. Mäcke, J. Schuhmacher, W. H. Knapp, M. Hofmann, *Eur. J. Nucl. Med. Mol. Imaging* **2004**, *31*, 1097–1104.

[67] a) B. M. Zeglis, J. S. Lewis, *Dalton Trans*. **2011**, *40*, 6168–6195; b) T. Wadas, E. H. Wong, G. R. Weisman, C. J. Anderson, *Chem. Rev.* **2010**, *110*, 2858–2902.

[68] M. D. Bartholomä, *Inorg. Chim. Acta.* **2012**, *389*, 36–51.

[69] J. F. Desreux, *Inorg. Chem.* **1980**, *19*, 1319–1324.

[70] a) W. A. P. Breeman, E. de Blois, H. S. Chan, M. Konijnenberg, D. J. Kwekkeboom, E. P. Krenning, *Semin. Nucl. Med.* **2011**, *41*, 314–321; b) M. Fani, J. P. Andre, H. R. Mäcke, *Contrast Media Mol. Imaging* **2008**, *3*, 67–77; c) M. Hoffmann, H. Mäcke, A. R. Boerner, E. Weckesser, P. Schoeffski, M. L. Oei, J. Schuhmacher, M. Henze, A. Heppeler, G. J. Meyer, W. H. Knapp, *Eur. J. Nucl. Med.* **2001**, *28*, 1751–1757; d) L. Kabasakal, E. Demirici, M. Ocak, C. Decristoforo, A. Araman, Y. Ozsoy, I. Uslu, B. Kanmaz, *Eur. J. Nucl. Med. Mol. Imaging* **2012**, *39*, 1271–1277.

[71] a) G. Bandoli, A. Dolmella, F. Tisato, M. Porchia, F. Refosco, *Coord. Chem. Rev.* **2009**, *253*, 56–57; b) N. A. Cola, R. S. Rarig, W. Ouellette, R. P. Doyle, *Polyhedron* **2006**, *25*, 3457–3462.

[72] V. Kubíček, J. Havlíčková, J. Kotek, G. Tircsó, P. Hermann, É. Tóth, I. Lukeš, *Inorg. Chem.* **2010**, *49*, 10960–10969.

[73] a) A. Bianchi, L. Calabi, C. Giorgi, P. Losi, P. Mariani, P. Paoli, P. Rossi, B. Valtancoli, M. Virtuani, *J. Chem. Soc. Dalton Trans.* **2000**, 697–705; b) I. Lukeš, J. Kotek, P. Vojtíšek, P. Hermann, *Coord. Chem. Rev.* **2001**, *216–217*, 287–312.

[74] J. Notni, J. Šimeček, P. Hermann, H.-J. Wester, *Chem. Eur. J.* **2011**, *17*, 14718–14722.

[75] N. Viola-Villegas, R. P. Doyle, *Coord. Chem. Rev.* **2009**, *253*, 1906–1925.

[76] a) S. Grös, H. Elias, *Inorg. Chim. Acta* **1996**, *251*, 347–354; b) I. Velikyan, H. Mäcke, B. Långström, *Bioconjugate Chem.* **2008**, *19*, 569–573; c) C. J. Broan, J. P. Cox, A. S. Craig, R. Kataky, D. Parker, A. Harrison, A. Randall, G. J. Ferguson, *J. Chem. Soc., Perkin Trans.* **1991**, *1*, 87–99.

[77] a) A. N. Singh, W. Liu, G. Hao, A. Kumar, A. Gupta, O. K. Oz, J.-T. Hsieh, X. Sun, *Bioconjugate Chem.* **2011**, *22*, 1650–1662; b) F. L. Guerra Gomez, T. Uehara, T. Rokugawa, Y. Higaki, H. Suzuki, H. Hanaoka, H. Akizawa, Y. Arano, *Bioconjugate Chem.* **2012**, *23*, 2229–2238.

[78] J. P. Andre, H. R. Mäcke, M. Zehnder, L. Macko, G. K. Akyel, *Chem. Commun.* **1998**, 1301–1302.

[79] K.-P. Eisenwiener, M. I. M. Prata, I. Buschmann, H.-W. Zhang, A. C. Santos, S. Wenger, J. C. Reubi, H. R. Mäcke, *Bioconjugate Chem.* **2002**, *13*, 530–541.

[80] P. J. Riss, C. Kroll, V. Nagel, F. Rösch, *Bioorg. Med. Chem. Lett.* **2008**, *18*, 5364–5367.

[81] a) E. Cole, D. Parker, G. Ferguson, J. F. Gallagher, B. Kaitner, *J. Chem. Soc. Chem. Commun.* **1991**, 1473–1475; b) E. Cole, R. C. B. Copley, J. A. K. Howard, D. Parker, G. Ferguson, J. F. Gallagher, B. Kaitner, A. Harrison, L. Royle, *J. Chem. Soc., Dalton Trans.* **1994**, 1619–1625.

[82] a) C. J. Broan, K. J. Jankowski, R. Kataky, D. Parker, *J. Chem. Soc., Chem. Commun.* **1990**, *23*, 1738–1739; b) C. J. Broan, E. Cole, K. J. Jankowski, D. Parker, K. Pulukkody, B. A. Boyce, N. R. A. Beeley, K. Millar, A. T. Millican, *Synthesis* **1992**, 63–68.

[83] a) K. Bazakas, I. Lukeš, *J. Chem. Soc., Dalton Trans.* **1995**, 1133–1137; b) M. I. M. Prata, A. C. Santos, C. F. G. C. Geraldes, J. J. P. de Lima, *Nucl. Med. Biol.* **1999**, *26*, 707–710; c) J. van Haveren, L. DeLeon, R. Ramasamy, J. van Westrenen, A. D. Sherry, *NMR Biomed.* **1995**, *8*, 197–205; d) J. Huskens, A. D. Sherry, *J. Am. Chem. Soc.* **1996**, *118*, 4396–4404.

[84] J. Notni, P. Hermann, J. Havlíčková, J. Kotek, V. Kubíček, J. Plutnar, N. Loktionova, P. J. Riss, F. Rösch, I. Lukeš, *Chem. Eur. J.* **2010**, *16*, 7174–7185.

[85] J. Notni, J. Plutnar, H.-J. Wester, *EJNMMI Res.* **2013**, *2*, 13.

[86] P. M. Smith-Jones, B. Stolz, C. Bruns, R. Albert, H. W. Reist, R. Fridrich, H. R. Mäcke, **1994**, *35*, 317–325.

[87] C. J. Mathias, Y. Z. Sun, M. J. Welch, J. M. Connet, G. W. Phillpott, A. E. Martell, *Bioconjugate Chem.* **1990**, *1*, 204–211.

[88] a) J. Schuhmacher, G. Klivény, W. E. Hull, R. Matys, H. Hauser, H. Kalthoff, W. H. Schmiegel, W. Maier-Borst, S. Matzku, *Nucl. Med. Biol.* **1992**, *19*, 809–824; b) M. Zöller, J. Schuhmacher, J. Reed, W. Maier-Borst, S. Matzku, *J. Nucl. Med.* **1992**, *33*, 1366–1372.

[89] M. Eder, B. Wängler, S. Knackmuss, F. LeGall, M. Little, U. Haberkorn, W. Mier, M. Eisenhut, *Eur. J. Nucl. Med. Mol. Imaging* **2008**, *35*, 1878–1886.

[90] a) E. Boros, C. L. Ferreira, J. F. Cawthray, E. W. Price, B. O. Patrick, D. W. Wester, M. J. Adam, C. Orvig, *J. Am. Chem. Soc.* **2010**, *132*, 15726–15733; b) E. W. Price, J. F. Cawtray, G. A. Bailey, C. L. Ferreira, E. Boros, M. J. Adam, C. Orvig, *J. Am. Chem. Soc.* **2012**, *134*, 8670−8683; c) G. A. Bailey, E. W. Price, B. M. Zeglis, C. L. Ferreira, E. Boros, M. J. Lacasse, B. O. Patrick, J. S. Lewis, M. J. Adam, C. Orvig, *Inorg. Chem.* **2012**, *51*, 12575–12589.

[91] a) C. Platas-Iglesias, M. Marto-Iglesias, K. Dhjanashvili, R. N. Muller, L. Vander Elst, J. A. Peters, A. de Blas, T. Rodrígues-Blas, *Chem. Eur. J.* **2004**, *10*, 3579–3590; b) R. Ferreirós-Martínez, D. Esteban-Gómez, C. Platas-Iglesias, A. de Blas, T. Rodríguez-Blas, *Dalton Trans.* **2008**, 5754–5765.

[92] E. Boros, C. L. Ferreira, D. T. T. Yapp, R. K. Gill, E. W. Price, M. J. Adam, C. Orvig, *Nucl. Med. Biol.* **2012**, *29*, 785–794.

[93] G. Gugliotta, M. Botta, L. Tei, *Org. Biomol. Chem.* **2010**, *8*, 4569–4574.

[94] a) B. P. Waldron, D. Parker, C. Burchardt, D. S. Yufit, M. Zimny, F. Rösch, *Chem. Commun.* **2013**, *49*, 579–581; b) Z. Baranyai, F. Uggeri, A. Maiocchi, G. B. Giovenzana, C. Cavallotti, A. Takács, I. Tóth, I. Bányai, A. Bényei, E. Brücher, S. Aime, *Eur. J. Inorg. Chem.* **2013**, 147–162.

[95] D. J. Berry, Y. Ma, J. R. Ballinger, R. Tavaré, A. Koers, K. Sunassee, T. Zhou, S. Nawaz, G. E. D. Mullen, R. C. Hider, P. J. Blower, *Chem. Commun.* **2011**, *47*, 7068–7070.

[96] C. T. Yang, S. G. Sreerama, W. Y. Hsieh, S. Liu, *Inorg. Chem.* **2008**, *47*, 2719–2727.

[97] a) A. Jyo, T. Kohno, Y. Terazono, S. Kawano, *Anal. Sci.* **1990**, *6*, 323–324; b) A. S. Craig, D. Parker, H. Adams, N. A. Bailey, *J. Chem. Soc., Chem. Commun.* **1989**, 1793–1794.

[98] R. D. Shannon, *Acta Crystallogr. Sect. A* **1976**, *32*, 751–767.

[99] a) W. R. Harris, V. L. Pecoraro, *Biochemistry* **1983**, *22*, 292–299; b) M. A. Green, M. J. Welch, *Nucl. Med. Biol.* **1989**, *16*, 435–448.

[100] B. Hacht, *Bull. Korean. Chem. Soc.* **2008**, *29*, 372–376.

[101] a) M. Uchida, A. Okuwaki, *J. Sol. Chem.* **1998**, *27*, 965–975; b) M. Uchida, A. Okuwaki, *J. Sol. Chem.* **1997**, *26*, 699–708; c) H. Gamsjäger, P. Schindler, *Helv. Chim. Acta* **1967**, *50*, 2053–2057; d) B. Das, R. N. Roy, K. S. Pitzer, D. R. Gregory, S. A. Kiefer, *J. Sol. Chem.* **2000**, *29*, 289–297.

[102] K. Sen, W. A. P. Breeman, H. T. Wolterbeek, *J. Radioanal. Nucl. Chem.* **2012**, *292*, 683–687.

[103] a) R. G. Pearson, *J. Am. Chem. Soc.* **1963**, *85*, 3533–3539. b) R. G. Pearson, *Inorg. Chim. Acta* **1995**, *240*, 93–98.

[104] I. Lukeš, K. Bazakas, P. Hermann, P. Vojtíšek, *J. Chem. Soc., Dalton Trans.* **1992**, 939–944.

[105] Unpublished diagrams, courtesy of J. Havlíčková, Charles University in Prague.

[106] a) W. Clegg, P. B. Iveson, J. C. Lockhart, *J. Chem. Soc. Dalton Trans.* **1992**, 3291–3298; b) C. F. C. G. Geraldes, A. D. Sherry, M. P. M. Marques, M. C. Alpoim, S. J. Cortes, *J. Chem. Soc., Perkin Trans. 2* **1991**, 137−146.

[107] C. Mannich, W. Krösche, *Arch. Pharm. Pharm. Med. Chem.* **1912,** *250*, 647–667.

[108] K. Moedritzer, R. R. Irani, *J. Org. Chem.* **1966**, *31*, 1603–1607.

[109] a) D. Remore, *J. Org. Chem.* **1978**, *43*, 992–996; b) I. Lázár, A. D. Sherry, *Synthesis* **1995**, 453–457.

[110] J. Šimeček, M. Schulz, J. Notni, J. Plutnar, V. Kubíček, J. Havlíčková, P. Hermann, *Inorg. Chem.* **2012**, *51*, 577–590.

[111] J. Šimeček, P. Hermann, J. Havlíčková, E. Herdtweck, T. G. Kapp, N. Engelbogen, H. Kessler, H.-J. Wester, J. Notni, *Chem. Eur. J.* **2013**, *in press*, doi:10.1002/chem.201300338.

[112] O. Kühl, *Phosphoros-31 NMR Spectroscopy*, Springer, **2008**.

[113] J. Šimeček, unpublished results.

[114] J.-F. Morfin, É. Tóth, *Inorg. Chem.* **2011**, *50*, 10371–10378.

[115] M. I. M. Prata, A. C. Santos, C. F. G. C. Geraldes, J. J. P. De Lima, *J. Inorg. Biochem.* **2000**, *79*, 359–363.

[116] J. Šimeček, M. Schulz, J. Notni, J. Plutnar, V. Kubíček, J. Havlíčková, P. Hermann, *Inorg. Chem.* **2012**, *51*, 577–590.

[117] J. Šimeček, O. Zemek, P. Hermann, H.-J. Wester, J. Notni, *ChemMedChem* **2012**, *7*, 1375–1378.

[118] M. Asti, M. Tegoni, D. Farioli, M. Lori, C. Guidotti, C. S. Cutler, P. Mayer, A. Versari, D. Salvo, *Nucl. Med. Biol.* **2012**, *39*, 509–517.

7. Appendix

Appendix 1: J. Šimeček, M. Schulz, J. Notni, J. Plutnar, V. Kubíček, J. Havlíčková, P. Hermann. Complexation of metal ions with TRAP (1,4,7-triazacyclononane phosphinic acid) ligands and 1,4,7-triazacyclononane-1,4,7-triacetic acid: phosphinate-containing ligands as unique chelators for trivalent gallium. *Inorg.Chem.* **2012**, *51*, 577–590.

Reprinted with permission from "Complexation of metal ions with TRAP (1,4,7-triazacyclononane phosphinic acid) ligands and 1,4,7-triazacyclononane-1,4,7-triacetic acid: phosphinate-containing ligands as unique chelators for trivalent gallium". Copyright (2012) American Chemical Society.

Appendix 2: J. Notni, J. Šimeček, P. Hermann, H.-J. Wester. TRAP, a powerful and versatile framework for Gallium-68 radiopharmaceuticals. *Chem. Eur. J.* **2011**, *17*, 14718–14722.

Reproduced with permission of John Wiley & Sons, Inc.

Available at http://onlinelibrary.wiley.com/doi/10.1002/chem.201103503/abstract

Appendix 3: J. Šimeček, O. Zemek, P. Hermann, H.-J. Wester, J. Notni. A monoreactive bifunctional triazacyclononane-phosphinate chelator with high selectivity for Gallium-68. *ChemMedChem* **2012**, *7*, 1375–1378.

Reproduced with permission of John Wiley & Sons, Inc.

Available at: http://onlinelibrary.wiley.com/doi/10.1002/cmdc.201200261/abstract

Appendix 4: J. Šimeček, P. Hermann, H.-J. Wester, J. Notni. How is ^{68}Ga-labelling of macrocyclic chelators influenced by metal ion contaminants in ^{68}Ge/^{68}Ga generator eluates? *ChemMedChem* **2013**, *8*, 95–103.

Reproduced with permission of John Wiley & Sons, Inc.

Available at: http://onlinelibrary.wiley.com/doi/10.1002/cmdc.201200471/abstract

Appendix 5: J. Šimeček, H.-J. Wester, J. Notni. Copper-64 labelling of triazacyclononane-triphosphinate chelators. *Dalton Trans.* **2012**, *41*, 13803–13806.

Reproduced by permission of The Royal Society of Chemistry.

Available at: http://pubs.rsc.org/en/Content/ArticleLanding/2012/DT/c2dt31880f

APPENDIX 1

Inorganic Chemistry

Article

pubs.acs.org/IC

Complexation of Metal Ions with TRAP (1,4,7-Triazacyclononane Phosphinic Acid) Ligands and 1,4,7-Triazacyclononane-1,4,7-triacetic Acid: Phosphinate-Containing Ligands as Unique Chelators for Trivalent Gallium

Jakub Šimeček,[†,‡] Martin Schulz,[§] Johannes Notni,[†,‡] Jan Plutnar,[†] Vojtěch Kubíček,[†] Jana Havlíčková,[†] and Petr Hermann*[,†]

[†]Department of Inorganic Chemistry, Univerzita Karlova (Charles University), Hlavova 2030, 12843 Prague 2, Czech Republic

[§]School of Chemical Sciences, Dublin City University, Glasnevin, Dublin 9, Ireland

Supporting Information

ABSTRACT: Three phosphinic acid 1,4,7-triazacyclononane (TACN) derivatives bearing methylphosphinic (TRAP-H), methyl(phenyl)phosphinic (TRAP-Ph), or methyl-(hydroxymethyl)phosphinic acid (TRAP-OH) pendant arms were investigated as members of a new family of efficient Ga^{3+} chelators, TRAP ligands (triazacyclononane phosphinic acids). Stepwise protonation constants of ligands and stability constants of their complexes with Ga^{3+}, selected divalent metal, and Ln^{3+} ions were determined by potentiometry. For comparison, equilibrium data for the metal ion−NOTA (1,4,7-triazacyclononane-1,4,7-triacetic acid) systems were redetermined. These ligands exhibit high thermodynamic selectivity for Ga^{3+} over the other metal ions (log K_{GaL} − log K_{ML} = 7−9) and a selective complexation of smaller Mg^{2+} over Ca^{2+}. Stabilities of the Ga^{3+} complexes are dependent on the basicity of the donor atoms: [Ga(NOTA)] (log K_{GaL} = 29.6) > [Ga(TRAP-OH)] (log K_{GaL} = 23.3) > [Ga(TRAP-H)] (log K_{GaL} = 21.9). The [Ga(TRAP-OH)] complex exhibits unusual reversible rearrangement of the "in-cage" N_3O_3 complex to the "out-of-cage" O_6 complex. The in-cage complex is present in acidic solutions, and at neutral pH, Ga^{3+} ion binds hydroxide anion, induces deprotonation and coordination of the *P*-hydroxymethyl group(s), and moves out of the macrocyclic cavity; the hypothesis is supported by a combination of results from potentiometry, multinuclear nuclear magnetic resonance spectrometry, and density functional theory calculations. Isomerism of the phosphinate Ga^{3+} complexes caused by a combination of the chelate ring conformation, the helicity of coordinated pendant arms, and the chirality of the coordinated phosphinate groups was observed. All Ga^{3+} complexes are kinetically inert in both acidic and alkaline solutions. Complex formation studies in acidic solutions indicate that Ga^{3+} complexes of the phosphinate ligands are formed quickly (minutes) and quantitatively even at pH <2. Compared to common Ga^{3+} chelators (e.g., 1,4,7,10-tetraazacyclododecane-1,4,7,10-tetraacetic acid (DOTA) derivatives), these novel ligands show fast complexation of Ga^{3+} over a broad pH range. The discussed TRAP ligands are suitable alternatives for the development of ^{68}Ga radiopharmaceuticals.

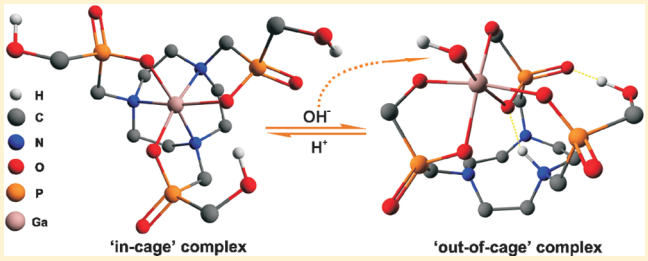

INTRODUCTION

Positron emission tomography (PET) is a noninvasive highly sensitive imaging modality providing a unique window for quantifying physiological functions and biochemical processes in living organisms. PET has become widely used over the past decade mainly in oncology and cardiology. The majority of PET examinations are conducted using [^{18}F]-fluorodeoxyglucose ([^{18}F]FDG), an agent for imaging of enhanced metabolic activity. Recent trends tend to combine PET with other imaging modalities as PET/CT[1] or PET/MRI.[2] Chemistry needed for progress in probe design should be developed to reach the full potential of the emerging scanners. In addition, new PET isotopes (mostly those of metallic elements) have been suggested for utilization in human medicine. Among the β^+-emitting radiometals, generator-produced[3] isotope ^{68}Ga [89% β^+; $\tau_{1/2}$ = 67.7 min; $E_{av}(\beta^+)$ = 740 keV] is the most promising, and its production, chemistry, and clinical use have been reviewed recently.[4−7] The metal radioisotopes cannot be used directly but must be bound by suitable ligands into thermodynamically stable and kinetically inert complexes. Also, other parameters, such as fast complexation kinetics, a pH suitable for quantitative complex formation, the solubility of the ligand and the complex, hydrophilicity and lipophilicity, an ability to attach the ligand and/or complex to a biomolecule, etc., have to be considered in designing radiometal-binding ligands.

Received: September 27, 2011
Published: December 20, 2011

   dx.doi.org/10.1021/ic202103v | *Inorg. Chem.* 2012, 51, 577−590

Chart 1. Ligands Discussed Herein

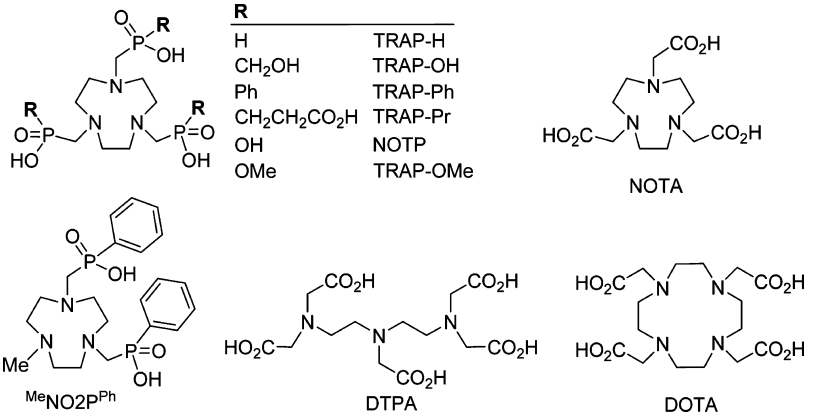

Scheme 1. Synthesis of TRAP-R Ligands[a]

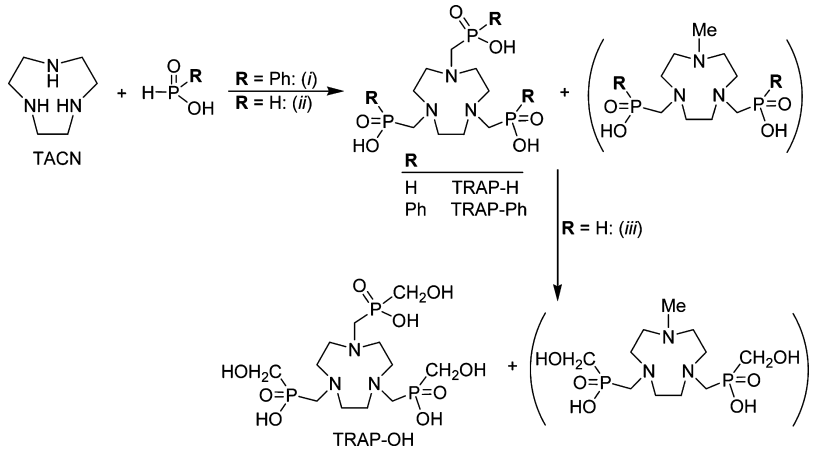

[a]Conditions: (i) $(CH_2O)_n$, 6 M aqueous HCl, 90 °C, 24 h; (ii) $(CH_2O)_n$, H_2O, room temperature, 24 h; (iii) $(CH_2O)_n$, 6 M aqueous HCl, reflux, 24 h.

Generally, hydrated Ga^{3+} ion, $[Ga(H_2O)_6]^{3+}$, is stable only in highly acidic solutions. Between pH 3.5 and 7, an insoluble precipitate of colloidal $Ga(OH)_3$ is formed. At pH ~7.5 and above, the hydroxide solubilizes due to formation of $[Ga(OH)_4]^-$ anion. The Ga^{3+} ion is classified as a hard Lewis acid and prefers octahedral coordination geometry. It forms the most stable complexes with ligands containing groups with hard Lewis donor atoms such as oxygen or nitrogen, e.g., carboxylates, phenols, phosphonates, phosphinates, hydroxyamates, and amines.

Among applicable chelators, those derived from macrocyclic ligands 1,4,7,10-tetraazacyclododecane-1,4,7,10-tetraacetic acid derivatives and 1,4,7-triazacyclononane-1,4,7-triacetic acid (DOTA and NOTA, respectively) (Chart 1) are preferred because of the increased thermodynamic stability as well as kinetic inertness of their gallium(III) complexes[8−10] compared with their open-chain analogues as DTPA derivatives.[11] Several DOTA-based ligands,[12] mainly in combination with small peptides, have shown their clinical potential in nuclear medicine. Among the ^{68}Ga PET tracers, ^{68}Ga-labeled somatostatin analogues (e.g., the golden standard ^{68}Ga-[DOTA^0,D-Phe^1,Tyr^3]-octreotide, ^{68}Ga-DOTATOC) are extensively studied because of their superior results in neuroendocrine tumor imaging.[13−15] Despite an extensive use of DOTA-like ligands for complexation of trivalent lanthanides, they cannot be considered as ideally suited for coordination of Ga^{3+} ion; it should be mentioned that Ga^{3+} complexes of the DOTA conjugates are the most commonly used because some bifunctional DOTA-like ligands are commercially available and their chemistry is well-established. The DOTA cavity geometry on one hand and the preference of Ga^{3+} ion for the regular octahedral coordination on the other hand result in bad fitting of the metal ion into the ligand cavity.[5,16,17] In contrast, NOTA-like ligands present a cavity that is almost ideal for small octahedral metal ions such as Ga^{3+};[16,18−20] thus, a number of NOTA-like ligands have been synthesized for gallium(III) complexation.[20−25]

It has been shown that complexation properties of 1,4,7-triazacyclononane derivatives as well as other macrocyclic chelators with respect to metal ions can be altered by replacement of carboxylate group(s) with phosphinates.[26] Early examples of such ligands showed good fitting of Ga^{3+} ion into the ligand cage.[27] A phosphinic acid derivative of TACN tailored for very efficient ^{68}Ga complexation is TRAP-Pr (Chart 1).[28] Using TRAP-Pr, radiolabeling could be performed even at room temperature and at pH <1 with a radiochemical yield of >90% within just a few minutes.

However, the reasons for the almost ideal properties of TRAP-Pr in complexation of carrier-free ^{68}Ga are not fully understood. Thus, we decided to study a set of macrocyclic phosphinate-containing ligands and to reinvestigate the complexation properties of NOTA, as data for the latter ligand

dx.doi.org/10.1021/ic202103v | Inorg. Chem. 2012, 51, 577−590

Table 1. Stepwise Protonation Constants of the Title Ligands and Comparison with the Values for Other TACN-Based Ligands

constant	TRAP-H[a]	TRAP-Ph[a]	TRAP-OH[a]	TRAP-Pr[28]	TRAP-OMe[41]	NOTP[42]	NOTA
log K_1	**10.48**,[a] 10.16[b]	**12.08**	**11.47**	11.48	11.8	12.1	11.98,[c] 13.0,[d] 13.17[e]
log K_2	**3.28**,[a] 3.13[b]	**3.24**	**3.85**	5.44	3.65	9.4	5.65,[c] 5.6,[d] 5.74[e]
log K_3	1.11[b]	**1.44**	**1.30**	4.84	1.4	7.5	3.18,[c] 2.5,[d] 3.22[e]
log K_4				4.23		5.9	1.9,[d] 1.96[e]
log K_5				3.45		2.9	
log K_6				1.66			

[a]From this work (bold), at 25 °C, I = 0.1 M $(NMe_4)Cl$. [b]From ref 35 (0.1 M KNO_3). [c]From ref 8 (0.1 M KCl). [d]From ref 40. [e]From ref 43 [0.1 M $(NMe_4)Cl$]; this set of constants was used for the metal ion stability constant determinations.

Table 2. Complex Stability and Stepwise Protonation Constants for Gallium(III) Complexes of the Studied Ligands and Some Others[a]

	log K_{LGa} or log K_A					
equilibrium[b]	TRAP-H	TRAP-OH	TRAP-Pr[28]	NOTA		DOTA[10]
L + Ga ⇄ LGa	21.91	23.3	26.24	29.60	31.0[8]	26.05
LGa + H^+ ⇄ HLGa		1.6	0.7[d]	0.9		1.57[e]
$H_{-1}LGa + H^+ ⇄ LGa + H_2O$	7.97	6.96[c]	9.8	9.83	9.70[8]	
$H_{-2}LGa + H^+ ⇄ H_{-1}LGa + H_2O$		9.0[c]				

[a]At 25 °C and I = 0.1 $(NMe_4)Cl$; for ligand structures, see Chart 1. [b]Charges of ligand and complex species have been omitted for the sake of simplicity. [c]For specification of the protonation sites and for structures of the corresponding deprotonated species, see the text. [d]Value corresponding to the protonation of the coordinated phosphinate groups and, so, to the $H_4LGa ⇄ H_3LGa + H^+$ equilibrium.[28] [e]Value corresponding to the protonation of the coordinated acetates and, so, to the $H_3LGa ⇄ H_2LGa + H^+$ equilibrium.[10]

are not fully consistent in the literature.[8,29,30] These ligands bearing acetate or phosphinic acid moieties with different substituents on the phosphorus atoms are used to study the influence of the TACN pendant arms on coordination behavior. TRAP-Pr and this series represent differences in coordinating groups [CO_2H vs $P(R)O_2H$], hydrophilicity and lipophilicity, and the ability to form weak complexes employing donor atoms only from the pendant arms (CH_2OH and $CH_2CH_2CO_2H$ phosphorus atoms substituents).

RESULTS AND DISCUSSION

Throughout this Article, the abbreviations, e.g., TRAP-H, will be used regardless of ligand protonation state, except in cases in which the distinction is necessary for comprehension or used in formulae of distinct complex species; then, the abbreviations will be used according to IUPAC nomenclature, e.g., H_3trap-H.

Ligand Synthesis. The title TRAP ligands were synthesized via Mannich-type Moedritzer–Irani reaction (Scheme 1).[31] However, the syntheses were complicated by problems commonly connected with Mannich-type reaction of organophosphorus compounds in aqueous media. The main side reaction is formation of *N*-methylated species;[32] it led to problematic purification of the reaction mixtures and decreased yields of the isolated products. The presence of the *N*-methylated compounds was proven by isolation of the corresponding byproduct in the case of TRAP-Ph synthesis. The reductive methylation of a nitrogen atom(s) can be suppressed by conducting the reaction at the high overall concentration of the reactants and lowering the reaction temperature with the optimal acidity of the solvent.[32,33] The synthesis of TRAP-Ph was complicated by low reactivity of phenylphosphinic acid requiring a high acidity of the reaction medium (6 M HCl) and a high temperature (90 °C).[34] As the reaction conditions support N-methylation, the spectroscopic reaction yield of TRAP-Ph never exceeded 70% [^{31}P nuclear magnetic resonance (NMR) of the reaction mixture] and was further decreased during purification.

To prepare TRAP-H, the reaction could be conducted even at 20 °C with hypophosphorus acid as the only acidifying agent. Under these mild conditions, the reaction resulted in a high spectroscopic yield (90%; ^{31}P NMR of the reaction mixture). However, in this case, small amounts of other common byproducts, *P*-hydroxymethylated compounds, were present. Further lowering the temperature led only to a prolonged reaction time with no further suppression of the methylation. Unfortunately, because of a very inefficient separation of these byproducts, the isolated yield was significantly lowered (33%). Regardless, TRAP-H was prepared with a slightly higher yield compared to that with the procedure described previously.[35]

The preparation of TRAP-OH proceeded in two steps. The first one was identical with the synthesis of TRAP-H. In the second step, nonpurified TRAP-H was converted directly to TRAP-OH by the reaction with an excess of newly added paraformaldehyde. Upon complete *P*-hydroxymethylation, the purification from any *N*-methylated species was much more efficient and TRAP-OH was then obtained in 70% yield.

Equilibrium Studies. Stepwise protonation constants (Table 1; the full set of experimental data is presented in Table S1.1 of the Supporting Information) were determined by potentiometry in the presence of tetramethylammonium cation to prevent the undesirable formation of the alkali metal ion complexes that occurs for various polyaminopolycarboxylates and similar ligands. In the case of NOTA, its weak interaction with alkali metal ions has been confirmed in solution by NMR measurements.[36] The first protonation constant can be assigned to protonation of a ring nitrogen atom and is the most important for the overall basicity of the ligands. As expected, the phosphinate ligands exhibit lower log K_1 values than the carboxylate (NOTA) or phosphonate (NOTP) analogues. For aminoalkylphosphinic acids,[26] the value depends on the electronic properties of the phosphorus-bound substituents. The hydrogen atom can be considered as the most electron-withdrawing substituent in this series, leading to the least basic nitrogen atoms; surprisingly, the electron-withdrawing phenyl

dx.doi.org/10.1021/ic202103v | Inorg. Chem. 2012, 51, 577–590

Table 3. Stability Constants (log K_{ML}) of Selected Metal Ions with the Title Ligands and Chosen NOTA Analogues[a]

metal ion	TRAP-H	TRAP-OH	TRAP-Ph	TRAP-Pr[28]	NOTA	
Ga^{3+}	21.91	23.3	*c*	26.24	29.63	31.0[d]
Mg^{2+}	5.32[b]	6.59	5.38	7.84	10.97	9.69[e]
Ca^{2+}	4.29[b]	4.87	3.77	6.04	10.32	8.92[e]
Cu^{2+}	13.43[b]	15.53	15.18	16.85	21.99	21.63[e]
Zn^{2+}	13.04[b]	16.12	*c*	16.88	21.58	
La^{3+}	7.42	8.56	*c*	11.26		13.5[f]
Gd^{3+}	8.75	10.10	*c*	13.46		14.4[f]
Y^{3+}	8.69	9.96	*c*			

[a]A full set of the determined stability constants is given in the Supporting Information; for ligand structures, see Chart 1. [b]From ref 35. [c]Not determined because of the precipitation of the complex. [d]From ref 8. [e]From ref 29. [f]From ref 47.

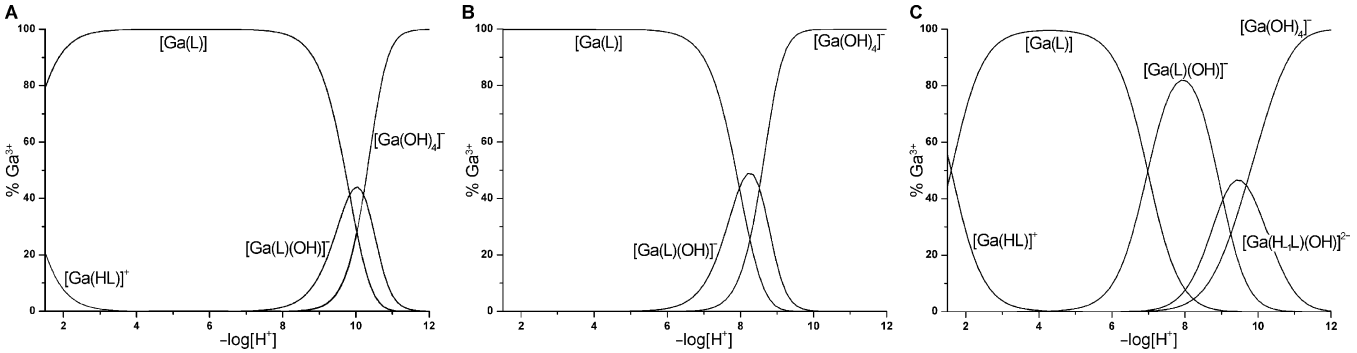

Figure 1. Distribution diagrams for Ga^{3+}–NOTA (A), Ga^{3+}–TRAP-H (B), and Ga^{3+}–TRAP-OH (C) systems ($c_{Ga} = c_L = 0.004$ M).

substituent exhibits the highest basicity. This effect can be caused by a shielding of the last *N*-bound proton by hydrophobic benzene rings from an interaction with surrounding water; a similar order of constant values has been observed for phosphinic acid derivatives of other polyaza macrocycles.[34,37,38] In general, the ligand basicity trends are similar to those observed for other amino acids: phosphonates > carboxylates > phosphinates ∼ phosphonic monoesters.[26]

The log K_2 value could be assigned to the protonation of the second ring nitrogen atom. Next, protonation (corresponding to K_3) should take place on acetate or phosphinate/phosphonate pendant arms;[39,42] the next constant, K_4, was determined only for NOTA (acetate arm protonation).[40] The three remaining possible protonation constants for the phosphinate ligands could not be determined as the protonations occur only in strongly acidic media; this has been directly proven by NMR titration of phosphinic acid derivatives of 1-oxa-4,7-diazacyclononane.[34] This observation agrees with the general knowledge that phosphinic acids exhibit higher acidity than carboxylic ones; in the title ligands, even at pH ∼1, some of the pendant arms are deprotonated and, thus, "pre-prepared" for the binding of metal cations.

The stability constants for complexes of NOTA and the title phosphinate ligands with gallium(III) as well as with some other cations were determined by potentiometric titrations (Tables 2 and 3; the full set of the experimental data is given in Table S1.2 of the Supporting Information). In the case of TRAP-Ph, determination of stability constants was possible only for Mg^{2+}, Ca^{2+}, and Cu^{2+} ions because of the insolubility of the other complexes.

In an acidic solution, some of the in-cage Ga^{3+} complexes are formed too slowly (see below) for a conventional potentiometric titration. Similarly in an alkaline solution, the rearrangement of the in-cage complexes and their full decomposition is also slow processes. Therefore, the titrations had to be performed using the out-of-cell technique with an equilibration time of 4 weeks at room temperature. As one can see from distribution diagrams (Figure 1), full complexation is reached even at pH 1.5, that is, in the beginning of the titrations. Therefore, the stability constants had to be determined from the equilibrium in the alkaline region where the macrocyclic ligands compete with hydroxide anions {$[Ga(OH)_4]^-$ formation}. Full hydroxide-induced dissociation occurs for the TRAP-H and NOTA complexes at slightly alkaline pH values, and the dissociation proceeds through formation of simple hydroxido species, $[Ga(L)(OH)]^-$; a similar chemical model was found for the Ga^{3+}–TRAP-Pr system.[28] A more complicated situation was observed in the case of the Ga^{3+}–TRAP-OH system where species with formal $[H_{-1}GaL]^-$ and $[H_{-2}GaL]^{2-}$ stoichiometries had to be included in the chemical model. The species start to form even in slightly acidic solutions (Figure 1) and could correspond either to the hydroxido complexes or to the complexes with deprotonated *P*-hydroxymethyl group(s). The site of deprotonation cannot be distinguished by potentiometry, because this method can observe only the amount of protons in the titrated solution. The presence of these species was surprising and led to a more thorough investigation as discussed below. The correctness of the potentiometric models was confirmed by NMR measurements; the determined concentrations of the species agreed with the abundances determined from the distribution diagram (Figure 1). The deprotonation of an alcohol group induced by its coordination to Ga^{3+} ion is not very common in aqueous solutions, and it was observed in only a few cases. The deprotonated alcoholate group is coordinated in the $[Ga(Hcitrate)_2]^{3-}$ anion,[44] and the only alcoholate groups are bound in the gallium(III) complex of an inositol derivative.[45] The data presented here extend this phenomenon to a new structural motif, the *P*-hydroxymethyl group.

dx.doi.org/10.1021/ic202103v | *Inorg. Chem.* 2012, 51, 577–590

In the monoprotonated $[Ga(HL)]^+$ species present in acidic solutions, Ga^{3+} cation is located inside the cavity of the phosphinate ligands and the proton is bound to an oxygen atom of a coordinated phosphinate group as suggested by NMR data (no free ligand was detected after the full equilibration at these pH values); the same phenomenon has been observed in the $[Ga(trap\text{-}Pr)]^{3-}$ complex[28] and in metal ion complexes of some polyaza macrocyclic polyphosphonate ligands[46] or for the $[Ga(dota)]^-$ complex.[10]

The stability constant of the [Ga(NOTA)] complex was redetermined in this work, but a comparison with the previous value is problematic as the original work[8] does not provide enough data on the equilibration time. The stability constants for gallium(III) complexes of the macrocyclic phosphinate ligands are lower than that for the [Ga(NOTA)] complex as a result of the lower basicity of the phosphinate ligands. It is clearly documented by the linear dependence of log K(GaL) on the sum of the protonation constants corresponding to ring nitrogen protonations, log K_1 + log K_2 (Figure S1.1 of the Supporting Information). Regardless, the thermodynamic stability of the complexes is high enough for possible in vivo utilizations. Comparison of log K_{GaL} values of the studied complexes with those of divalent metal ion complexes (Table 3) indicates an excellent thermodynamic selectivity of the studied ligands for Ga^{3+} ion. At least hexadentate macrocyclic ligands are required for the formation of thermodynamically stable complexes as stabilities of gallium(III) complexes with series of pentadentate 1-oxa-4,7-diazacyclononane derivatives with the same pendant arms are much lower [log K(GaL) = 8.9−14.9].[34]

To determine the selectivity of the ligands for gallium(III) complexation and to accumulate and/or redetermine data for more metal ions, we ran potentiometric titrations with the ligands and selected metal ions. The stability constants, K_{ML}, of complexes of the title ligands and similar TACN derivatives are listed in Table 3, and the full set of stability constants together with selected distribution diagrams and more comparisons of data for different systems are given in the Supporting Information (Tables S2 and S3 and Figures S1.2−S1.5). The stability constant values (Table 3) show high selectivity of all ligands for complexation of small metal ions, and this property is even more pronounced for the phosphinate ligands. The binding selectivities of the TRAP ligands for Ga^{3+} are 1−3 orders of magnitude greater than that of NOTA, and it might be a source of the efficient binding of carrier-free $^{68}Ga^{3+}$ (e.g., in the presence of the decay product, Zn^{2+}) observed previously.[28] This can be explained by a combination of the small internal ligand cavity, the difference in pendant arm donor atom hardness, and/or the coordination requirements of the metal cations. The data suggest that (i) log K_{ML} values are similar for copper(II) and zinc(II) complexes as in TACN-like ligands, one nitrogen atom has to be bound axially to Cu^{2+} ion leading to a lower thermodynamic stability of the complexes; (ii) complex stabilities are higher for the smaller and harder Mg^{2+} ion when compared with those of the Ca^{2+} ion and are more pronounced for hard phosphinate-containing ligands; (iii) there is a pronounced difference between La^{3+} and Gd^{3+} complex stability constants as the smaller Gd^{3+} ion fits the small ligand cavity better; and (iv) we noticed a high selectivity for the small and hard Ga^{3+} ion as mentioned above. In general, the values of stability constants depend on the overall basicity of the ligands and, therefore, are ordered as follows: phosphonate > carboxylate > phosphinate.

To obtain more data for trivalent metal ions relevant for biomedical applications and to test the correctness of the chemical model for the Ga^{3+}−TRAP-OH systems, we determined the stability constants of selected rare earth metal ions. The values of stability constants of phosphinate ligands are very low. However, potentiometric chemical models for these ions (requiring higher coordination numbers, mostly 8 or 9) and TRAP-OH (theoretically, a nonadentate ligand) were analogous to that for the Ga^{3+}−TRAP-OH system. Therefore, we can speculate that the hard Ln^{3+} or Y^{3+} ions can also induce a deprotonation of the *P*-hydroxymethyl group(s) with their simultaneous coordination to the central ions. Such a hypothesis is supported by facts that more deprotonated species ($H_{-1}LM$ and $H_{-2}ML$, or even $H_{-3}ML$ for Y^{3+}) had to be involved in the chemical model (Table S1.2 of the Supporting Information); their formation starts at neutral pH, and they have unusually high abundances and may contain coordinated hydroxide and/or alcoholate anion(s) (Figure S1.4 of the Supporting Information). As the analogous species were also suggested in the Ga^{3+}−TRAP-OH system (vide infra), the metal ion-induced deprotonation and simultaneous coordination of the hydroxymethyl group(s) seem to be a general case for this particular ligand. The phenomenon observed here is the first example of the formation of a chelate with an α-hydroxymethylphosphonic/phosphinic acid group involving alcoholate coordination.

DFT Calculations for Ga^{3+}−TRAP-OH Complexes. As one can see from Figure 1B, the [Ga(L)] species (H_3L = TRAP-OH) is dominant in acidic solutions; Ga^{3+} ion is bound in the in-cage complex having an octahedral N_3O_3 arrangement as found in other complexes of phosphinate[27,28] or phosphonate[48] TACN derivatives. With an increase in pH, the deprotonated species $[H_{-1}LGa]^-$ and $[H_{-2}LGa]^{2-}$ appear, followed by complex decomposition and formation of the free ligand and the $[Ga(OH)_4]^-$ anion. Because these species appear at higher pH values, the hydroxide anion seems to play a role in the processes. It can act as a Brönsted base deprotonating one or more *P*-hydroxymethyl moieties of the in-cage complex and/or coordinate to the Ga^{3+} ion that is still inside the ligand cage with replacement of a bound pendant arm(s). The other possibility is deprotonation of the *P*-hydroxymethyl moieties to furnish nucleophilic alcoholate anions that could coordinate Ga^{3+} ion; it induces the movement of the central ion out of the ligand cage with formation of an out-of-cage complex where Ga^{3+} ion is bound to the phosphinate side arms but not to the ring nitrogen atoms. In addition, this out-of-cage complex can bind water molecules or hydroxide anions if not all coordination sites are occupied by ligand oxygen atoms. These processes lead to an O_6 coordination arrangement. With these considerations in mind, a set of possible structures for the $[H_{-1}LGa]^-$ and $[H_{-2}LGa]^{2-}$ species was suggested. These structures cannot be distinguished by potentiometry, because this method can reveal only a number of protons in the titrated solution. However, from the comparison with the other complexes investigated here (see above), coordination of only hydroxide anion that would start at pH 5 seems to be rather improbable.

Once the equilibrium was reached, the unusual deprotonated species have high abundances. Unfortunately, any attempts to determine their structure by multinuclear NMR failed because of extremely broad and/or complicated spectra. NMR measurements of the purified [Ga(L)] complex prepared in an acidic solution showed the expected[27,28,48] spectra [Figure

dx.doi.org/10.1021/ic202103v | *Inorg. Chem.* 2012, 51, 577−590

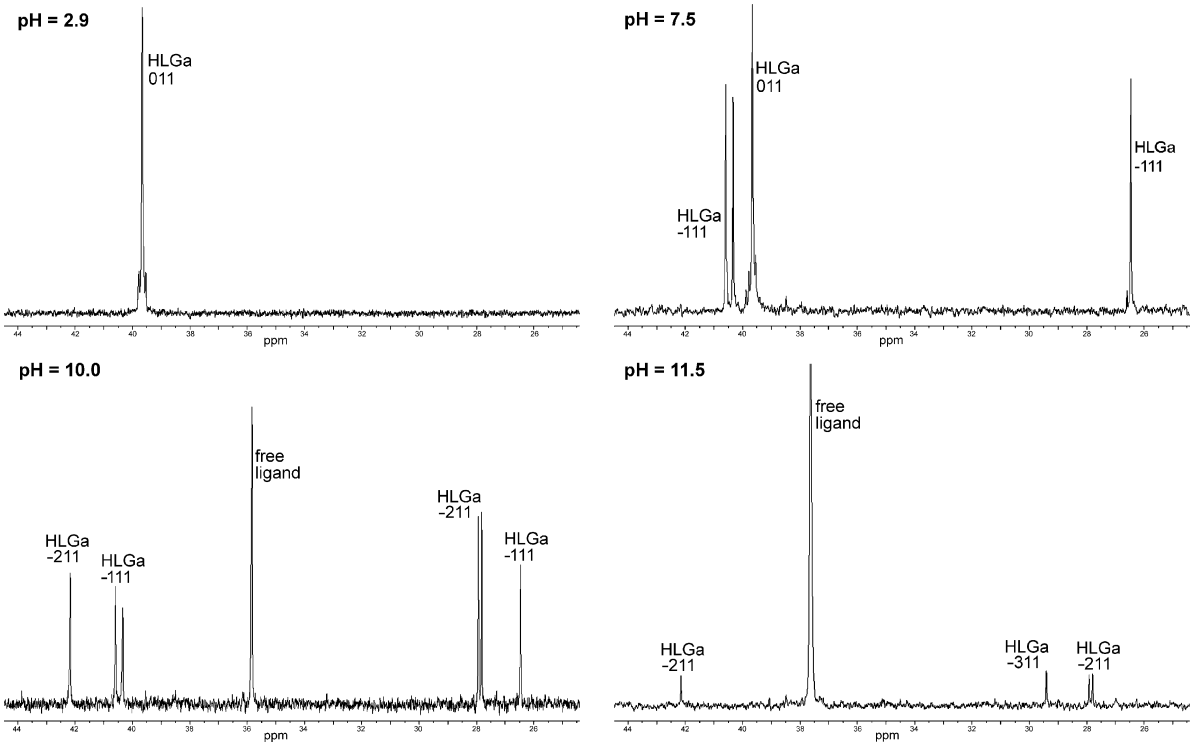

Figure 2. $^{31}P\{^{1}H\}$ NMR spectra of fully equilibrated solutions prepared by mixing Ga^{3+} ion and TRAP-OH ($c_{Ga} = c_L = 0.005$ M). The given pH values are those for the equilibrated solutions.

Scheme 2. The Most Suitable Species in the Ga^{3+}–TRAP-OH System As Suggested by the DFT Calculations[a]

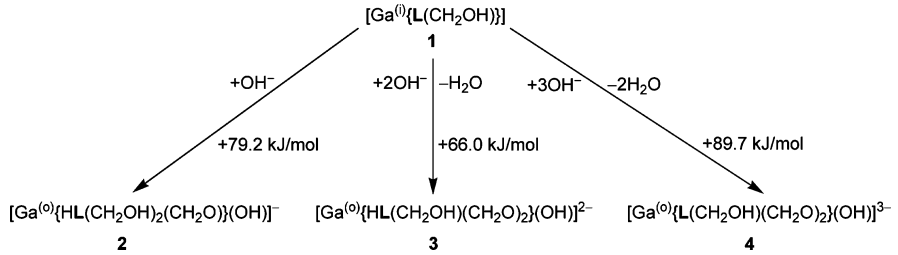

[a]Relative free energies, ΔG_{calc}, are referenced to a $\Delta G_{calc}(\mathbf{1})$ of 0 kJ/mol.

S3.1 of the Supporting Information; δ_P 37.3, δ_{Ga} 135.2 ($\omega_{1/2}$ = 305 Hz)] and the corresponding ^{1}H NMR spectrum with the presence of a single diastereoisomer (see below) of the complex. It is consistent with the structure of other gallium(III) in-cage complexes with NOTA-like ligands.[16] However, among the NMR spectra recorded for different nuclei on the complex solutions at higher pH values, only the $^{31}P\{^{1}H\}$ NMR spectra were reasonably resolved to be interpretable (Figure 2). The ^{71}Ga NMR signals of any deprotonated species were not detected. This points to rather unsymmetrical structures of the $[H_{-1}LGa]^{-}$ and $[H_{-2}LGa]^{2-}$ species. These species were not exchanging with each other or with the free ligand on the NMR time scale.

Thus, DFT calculations were employed to suggest structures of the species that can be present in the Ga^{3+}–TRAP-OH system. Because of a larger number of degrees of freedom in these molecules, the energies presented below must be considered only as estimates, and some considerations were taken into account prior to the calculations. At pH >6, the main ligand species present in solution is the $(Htrap\text{-}OH)^{2-}$ anion (Figure S2.1 of the Supporting Information) in which the proton is bound to the ring nitrogen atoms; in the considered out-of-cage complex species, the ring nitrogen atoms may also bind a proton as the pK_a for such deprotonation in the free ligand is as high as 11.5 (Table 1). It is well-known that phosphorus acid oxygen atoms are able to form strong hydrogen bonds. The most probable coordination environment of Ga^{3+} ion in such complexes should be close to the octahedron. During the calculations, a modeling of the solvent influence was conducted with conditions as close as possible to the experimental conditions. Stoichiometries, binding modes, and relative energies of selected species considered during DFT calculations are shown in Scheme 2. More details about the calculations and a full set of the species considered in the calculations together with figures of their structures can be found in the Supporting Information (Figures S2.2–S2.5). In the following text, the protonated ligand sites will be distinguished according to the following examples (charges will be omitted for the sake of simplicity). For ligand monoprotonated on a ring nitrogen atom and having all *P*-hydroxymethyl groups protonated, the notation will be $\{HL(CH_2OH)_3\}$ (with a charge of −2). For a ligand with

dx.doi.org/10.1021/ic202103v | *Inorg. Chem.* 2012, 51, 577–590

deprotonated ring nitrogen atoms and with two deprotonated *P*-hydroxymethyl groups, the notation will be $\{L(CH_2OH)(CH_2O)_2\}$ (having a charge of −5). Gallium(III) in the in-cage complex will be labeled as $Ga^{(i)}$ and in the out-of-cage complex as $Ga^{(o)}$.

In-Cage Complexes. The neutral in-cage complex $[Ga^{(i)}\{L(CH_2OH)_3\}]$ (**1**) was taken as a reference with a relative Gibbs free energy (ΔG) of 0.0 kJ/mol (Figure 3). To test the correctness of our calculations, the calculated geometric parameters were compared with the experimental X-ray diffraction data {for the $[Ga(H_3trap\text{-}Pr)]$ complex},[28] and the agreement was found to be very good (Table S2.1 of the Supporting Information). Although hydrogen bonds should be generally considered with great care within the presented calculations, a strong hydrogen bond between the PCH_2OH group and a coordinated phosphinate oxygen atom of the adjacent pendant arm [O_C−H···O_P, 2.819 Å; ∠O_C−H···O_P, 162° (Figure 3)] can be noted. Analogous hydrogen bonds were found in structures of most species discussed in this section. The structure of **1** corresponds to the measured NMR spectra. Sequential deprotonation of the external *P*-hydroxymethyl group(s) leading to $[Ga^{(i)}\{L(CH_2OH)_2(CH_2O)\}]^-$ (**1a**) and $[Ga^{(i)}\{L(CH_2OH)(CH_2O)_2\}]^{2-}$ (**1b**) species (Figures S2.2 of the Supporting Information) was considered, as well. However, the pK_a for deprotonation of the *P*-hydroxymethyl group in aqueous solution calculated from the Gibbs free energy difference using equations from ref 49 equals 15.1. This value is too high to be accessible in an aqueous solution under common conditions; therefore, these structures can be excluded as those corresponding to the $[H_{-1}LGa]^-$ and $[H_{-2}LGa]^{2-}$ species.

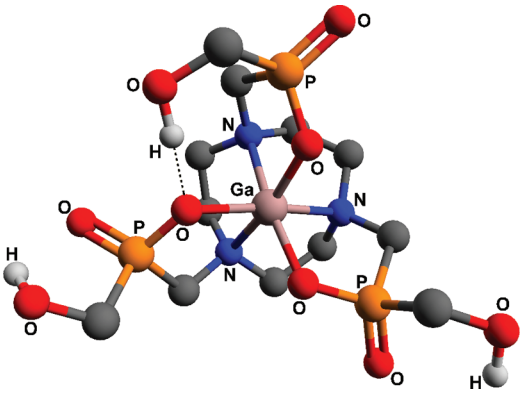

Figure 3. Calculated structure of the in-cage $[Ga^{(i)}\{L(CH_2OH)_3\}]$ (**1**) complex (H_3L = H_3trap-OH) taken as the lowest-energy complex. Hydrogen atoms except those in OH groups have been omitted for the sake of clarity, and the hydrogen bond is shown as a dashed line.

Out-of-Cage Complexes. As a first attempt, species having Ga^{3+} coordinated in an octahedral fashion by three phosphinate oxygen atoms and three oxygen atoms coming from the *P*-hydroxymethyl groups (1-, 2-, or 3-fold deprotonated) were tested. For the input structures, the Ga^{3+} ion was moved off the cage with a simultaneous transfer of a proton into the cage. In the output structure, the proton was found to be bound to a ring nitrogen atom with a rather strong hydrogen bond contact to a coordinated phosphinate oxygen atom (N−H···O, 2.6−2.9 Å; ∠N−H···O, 150−155°) and also exhibits a weak interaction with the other ring nitrogen atoms. However, the calculations for any simple isomerization or deprotonation did not lead to an octahedral Ga^{3+} coordination and always resulted in distorted pentacoordinate environments. All structures of the species [**A**−**C** (Figure S2.3 of the Supporting Information)] formed by sequential removal of the proton(s) from the reference in-cage $[Ga^{(i)}\{L(CH_2OH)_3\}]$ (**1**) complex have high relative energies (see the Supporting Information). The inaccessibility of the octahedral coordination sphere in these complexes can be explained by high sterical strain induced by the simultaneous presence of various Ga(−O−P−CH_2O−) chelate rings. In addition, the number and type of structurally clearly distinguishable phosphorus atoms in species **A**−**C** do not fit the peak pattern in experimentally observed $^{31}P\{^1H\}$ NMR spectra (Figure 2). Thus, the simple flip from the in-cage coordination sphere to an out-of-cage sphere with all three side arms coordinating in the same way can be ruled out.

This might be overcome by the introduction of a coligand, such as water or hydroxide anion; trivalent gallium has a high affinity for these ligands, and species with coordinated hydroxide anions had to be involved in the best chemical models for the gallium(III) systems with other NOTA analogues. As mentioned above, most of the structures were calculated with a protonated ring nitrogen atom (the proton is probably shared among all nitrogen atoms). The proton is bound inside the $(Htrap\text{-}OH)^{2-}$ anion in an analogous manner (Figure S2.1 of the Supporting Information), and a similar sharing of the last proton inside the ligand cavity was suggested for the 2-thioethyl TACN derivative.[50]

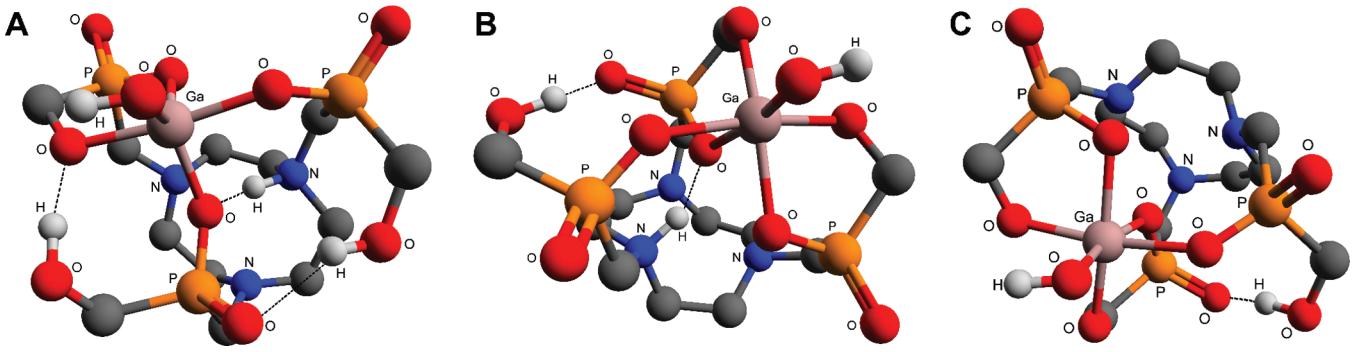

Figure 4. Structures of the out-of-cage species as suggested by calculations: (**A**) $[H_{-1}LGa]^-$ = $[Ga^{(o)}\{HL(CH_2OH)_2(CH_2O)\}(OH)]^-$ (**2**), (**B**) $[H_{-2}LGa]^{2-}$ = $[Ga^{(o)}\{HL(CH_2OH)(CH_2O)_2\}(OH)]^{2-}$ (**3**), and (**C**) $[H_{-3}LGa]^{3-}$ = $[Ga^{(o)}\{L(CH_2OH)(CH_2O)_2\}(OH)]^{3-}$ (**4**), where H_3L = TRAP-OH. Hydrogen atoms except those in OH or NH groups have been omitted for the sake of clarity, and the hydrogen bonds are shown as dashed lines.

dx.doi.org/10.1021/ic202103v | *Inorg. Chem.* 2012, 51, 577−590

Filling one coordination site with a water molecule furnished energetically disfavored (from 100 to 185 kJ/mol) and highly distorted pentacoordinated complexes [species **D** and **E** (Figures S2.4 of the Supporting Information)]. It was found that the water molecule is bound only loosely ($Ga-O_w$, 2.12−2.43 Å). As trivalent gallium has a high affinity for the hydroxide anion, the anion should be the most suitable coligand. In addition, deprotonated species found in other Ga^{3+}−ligand systems and experimentally studied in this Article contain a coordinated hydroxide anion. There are several possibilities for how to arrange various numbers of deprotonated *P*-hydroxymethyl moieties and the OH^- coligand. The structures are shown in Figure 4 and Figure S2.5 of the Supporting Information. Most of the calculated structures exhibit a distorted octahedral coordination arrangement expected for trivalent gallium and can be stabilized by intramolecular hydrogen bonds.

Among the species having a potentiometric $[H_{-1}LGa]^{1-}$ stoichiometry, the $[Ga^{(o)}\{HL(CH_2OH)_2(CH_2O)\}(OH)]^-$ (**2**) complex (Scheme 2 and Figure 4) is the most energetically favored species, although the coordination polyhedron of this species, a trigonal bipyramid, is not very common in gallium(III) complexes. Bond distances point to a strong coordination of the central ion ($Ga-O_P$, 1.96−1.99 Å; $Ga-O_C$, 2.01 Å; $Ga-O_H$, 1.88 Å). The in-cage proton is bound to a ring nitrogen atom and is kept inside the ligand cavity by a system of hydrogen bonds between nitrogen and oxygen atoms, as shown above and in Figure 4. Other species, **2a** and **2b**, were also considered (Figure S2.5 of the Supporting Information). Although they exhibit octahedral structures that are more common for the gallium(III) ion, their relative energies are very high in comparison (175 and 251 kJ/mol, respectively) with that of **2**.

The experimentally observed 2-fold deprotonated species, $[H_{-2}LGa]^{2-}$, should have one protonated ring nitrogen atom and only one *P*-hydroxymethyl group, as in the calculated $[Ga^{(o)}\{HL(CH_2OH)(CH_2O)_2\}(OH)]^{2-}$ (**3**) anion (Figure 4 and Scheme 2). This species has the lowest energy (66 kJ/mol) among all out-of-cage species and exhibits a distorted octahedral environment around the Ga^{3+} ion [$Ga-O_P$, 2.05−2.13 Å; $Ga-O_C$, 2.01 Å; $Ga-O_H$, 1.93 Å; ∠O−Ga−O, 80−98° (for adjacent oxygen atoms)]. The other considered species with such a stoichiometry was $[Ga^{(o)}\{HL(CH_2OH)_3\}(OH)_3]^{2-}$ (**3a**) (Figure S2.5 of the Supporting Information), but it exhibited a much higher relative energy (228 kJ/mol).

The fully deprotonated complex $[H_{-3}LGa]^{3-}$ might be the species present in alkaline solutions; however, $[Ga(OH)_4]^-$ anion formation should be more favorable under such conditions. Thus, in solution, this species is probably present (if ever) only with low abundance and could not be involved in the potentiometric chemical model. Regardless, the small singlet peak at 29.4 ppm was observed in the $^{31}P\{^1H\}$ NMR spectrum of the solution at high pH (Figure 2). Hence, this stoichiometry was also heeded during calculations. At high pH values, the nitrogen atom(s) should be deprotonated [ligand log K_1 = 11.47 (Table 1)] and the $[Ga^{(o)}\{L(CH_2OH)(CH_2O)_2\}(OH)]^{3-}$ (**4**) species (Figure 4 and Scheme 2), possessing a structure analogous to that of **3** but without the in-cage proton, is the most likely for the $[H_{-3}LGa]^{3-}$ stoichiometry. The coordination polyhedron around the Ga^{3+} ion [$Ga-O_P$, 1.98−2.14 Å; $Ga-O_C$, 2.03 Å; $Ga-O_H$, 1.94 Å; ∠O−Ga−O, 82−101° (for adjacent oxygen atoms)] is still distorted. Although the $[Ga^{(o)}\{HL(CH_2O)_3\}(OH)]^{3-}$ [**4a** (Figure S2.5 of the Supporting Information)] species has an only slightly higher energy (93 kJ/mol), there is a protonated ring nitrogen atom; thus, this structure was excluded. All three low-energy structures might be further stabilized by another intramolecular hydrogen bond between the phosphinate and the neighboring hydroxymethyl group ($O_C-H\cdots O_P$, 2.6−2.9 Å; $\angle O_C-H\cdots O_P$, 146−168°), as shown in Figure 4.

Structures **2**−**4** are in accordance with $^{31}P\{^1H\}$ NMR spectra (Figure 2). As stated above, these solution species are not fluxional and do not convert into each other on the NMR time scale, probably because of the rigidifying role of the proton inside the ligand cavity. Thus, the phosphorus atom environment in species **2** ($[H_{-1}LGa]^-$ stoichiometry) should exhibit two signals like reference in-cage complex **1** (the *P*-hydroxymethyl groups are protonated) and one signal with a much smaller δ_P (with a more electronegative P substituent, i.e., the deprotonated alcoholate). Analogously, species **3** ($[H_{-2}LGa]^{2-}$ stoichiometry) should exhibit one signal close to reference complex **1** and two peaks in the 22−28 ppm region. The small singlet at 29.4 ppm observed at high pH might be attributed to species **4** ($[H_{-3}LGa]^{3-}$ stoichiometry), where phosphorus atoms are averaged on the NMR time scale because of fast proton exchange between *P*-hydroxymethyl groups.

Information from the calculations can be summarized as follows. (i) Reference in-cage complex **1** has the most stable structure of all species investigated. (ii) As expected, a simple deprotonation of the *P*-hydroxymethyl moiety in in-cage complex **1** is difficult to achieve in an aqueous solution. (iii) A simple flip from the in-cage arrangement to the octahedral out-of-cage coordination sphere with three fully coordinated side arms only (chelate rings formed by the $^-OPCH_2O^-$ or $^-OPCH_2OH$ moieties only) will not occur because of the steric strain. (iv) The out-of-cage species possessing an O_6 coordination environment can be obtained only by addition of the hydroxide anion as a coligand. (v) Structures with reasonably low relative energies can comprise both penta- and hexacoordinated Ga^{3+} ion. (vi) The structures might be stabilized by intramolecular hydrogen bonds.

Isomerism of Gallium(III) Complexes in Solution. As mentioned above, the most stable in-cage gallium(III) complexes of the NOTA-like ligands exhibit distorted octahedral coordination arrangements. From another point of view, the Ga^{3+} ion is "sandwiched" between twisted trigonal O_3 and N_3 planes. Such an arrangement leads to chiral complexes in which the chirality is caused by a combination of the conformation of macrocycle-containing chelate rings ($\delta\delta\delta/\lambda\lambda\lambda$) and the helicity of the coordinated pendant arms (Δ/Λ). It leads to two diastereomeric pairs, $\Delta\delta\delta\delta/\Lambda\lambda\lambda\lambda$ and $\Lambda\delta\delta\delta/\Delta\lambda\lambda\lambda$. The phenomenon is fully analogous to the isomerism well-documented in lanthanide(III) complexes of DOTA-like ligands[51] and has been observed for NOTA complexes with different metal ions.[36,52] In the phosphinic acid NOTA analogues, the phosphorus atoms become chiral (*R*/*S*) after coordination to a central metal ion; again, the same chirality originating from the metal ion coordination of the phosphinate group is commonly observed in lanthanide(III) complexes of phosphinic acid analogues of DOTA.[51] Hence, combination of all the chiralities in complexes of TACN bearing three phosphinate pendant arms results in four possible diastereomeric pairs, $\Lambda\delta\delta\delta$-*RRR*/$\Delta\lambda\lambda\lambda$-*SSS*, $\Lambda\delta\delta\delta$-*RRS*/$\Delta\lambda\lambda\lambda$-*SSR*, $\Lambda\delta\delta\delta$-*RSS*/$\Delta\lambda\lambda\lambda$-*SRR*, and $\Lambda\delta\delta\delta$-*SSS*/$\Delta\lambda\lambda\lambda$-*RRR* (Figure S2.7 of the Supporting Information). In the solid state, only one of

dx.doi.org/10.1021/ic202103v | *Inorg. Chem.* 2012, 51, 577−590

the diastereomers, Λ*δδδ-RRR*/Δ*λλλ-SSS*, was observed for the [Ga(trap-Ph)] and [Ga(H_3trap-Pr)] complexes.[27,28] In solution, isomerism was investigated only for the $[Ga(trap\text{-}Pr)]^{3-}$ complex; the isomer present in solution was shown to be identical to that in the solid state.[28]

It is known that the [Ga(NOTA)] complex is present as a single diastereomer in the solid state but is fluxional in solution at room temperature as its ^{1}H NMR spectrum exhibits average signals.[18] On the other hand, phosphonate or phosphinate complexes are more rigid and the diastereomers of their complexes do not convert into each other.[27,28,42] As described above, the NMR spectrum of the in-cage [Ga(trap-OH)] complex and DFT calculations indicate that, in solution, the complex is present as a rigid Λ*δδδ-RRR*/Δ*λλλ-SSS* isomer, like the $[Ga(trap\text{-}Pr)]^{3-}$ complex.[28]

A different situation was observed for the [Ga(trap-H)] complex as unusual NMR spectra were obtained. Despite the common quadrupole broadening of ^{71}Ga NMR spectra, four very narrow NMR signals in a 1:3:4:2 intensity ratio (δ_{Ga} values of 132.00, 134.96, 137.80, and 140.45 ppm and $\omega_{1/2}$ values of 154, 200, 186, and 162 Hz, respectively) were observed (Figure 5). The signals probably correspond to the presence of all four diastereomers of the complex (Figure S2.7 of the Supporting Information). The doublet in the ^{31}P NMR spectrum centered at 22.0 ppm ($^1J_{PH}$ = 599 Hz) shows inconspicuous shouldering of the 20.1 ppm signal (Figure 5); the doublet is in agreement with the ^{1}H NMR spectrum that shows two overlapping H−P doublets centered at 7.20 and 7.25 ppm with $^1J_{PH}$ values of 607 and 561 Hz, respectively. Unfortunately, one-dimensional and two-dimensional ^{1}H and/or ^{13}C NMR spectra (or correlations with ^{31}P NMR spectra) of the isomeric mixture were too complicated or had signals that were overly broad to be useful for assignment of the structures of the individual isomers (Figure S3.2 of the Supporting Information).

The extraordinarily narrow ^{71}Ga NMR resonances (compared with those of complexes of other TACN-based ligands)[18,24,25,27,28,48] point to the high symmetry of the donor atom arrangements in the [Ga(trap-H)] diastereomers. The ratio of the four ^{71}Ga NMR signals is independent of the conditions used for preparation of the complex [different temperatures ranging from 25 to 80 °C, different rates of reactant mixing, the source of the Ga^{3+} cation, $Ga(NO_3)_3$ or $GaCl_3$, and dilution of the reacting solutions]. In addition, the ratio of ^{71}Ga signals remained constant under all conditions applied during the preparation of the complex, such as heating. Evidently, the isomers are not fluxional, and an energetic barrier for their mutual transformation has to be relatively high. This hypothesis was examined by DFT calculations.

The relative Gibbs energies were calculated for these four diastereoisomers and were found to be very close to each other (Table S2.4 of the Supporting Information). This supports the assumption, made above, that four signals in the ^{71}Ga NMR spectrum originate from four different diastereomers. The obtained relative energies of particular isomers are 0.00, −3.68, −7.25, and −6.25 kJ/mol for Λ*δδδ-RRR*, Λ*δδδ-RRS*, Λ*δδδ-RSS*, and Λ*δδδ-SSS*, respectively. However, the conversion from one diastereomer to another is accomplished by rotation of the N−CH_2−PO_2 moiety or inversion of the ethylene chain in the ethylenediamine chelate ring; activation barriers of the processes should be substantially high. We calculated the barrier height for the conversion from Λ*δδδ-SSS* to Λ*δδδ-RSS* ($\Delta G^{\#}$) to be 130 kJ/mol relative to the Λ*δδδ-SSS* isomer.

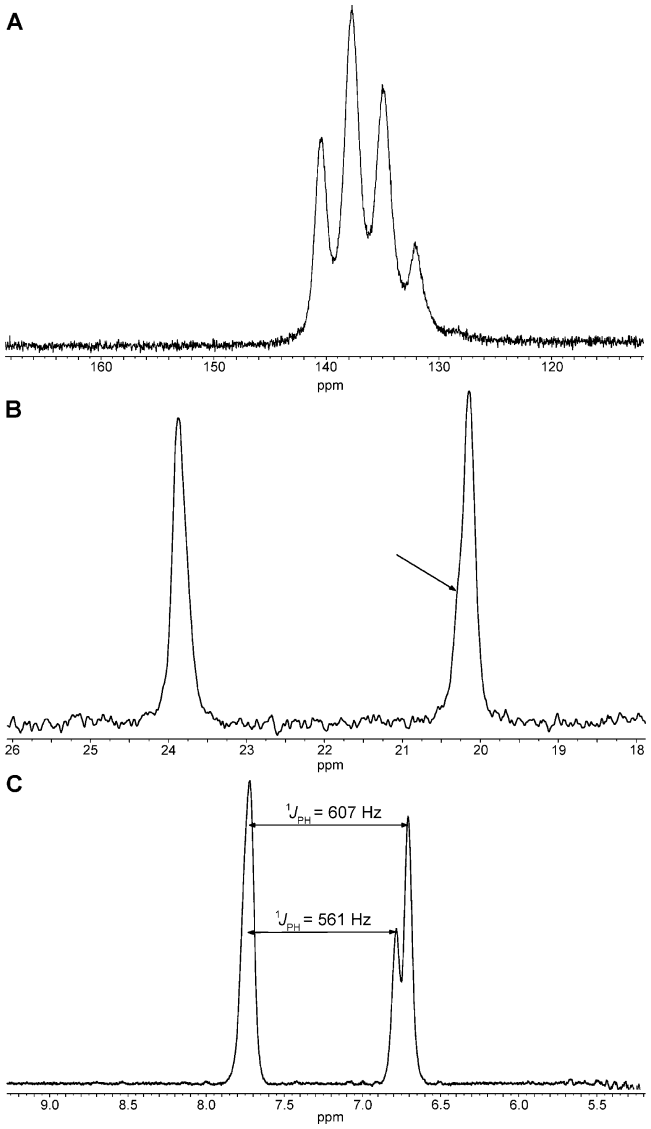

Figure 5. ^{71}Ga (A), ^{31}P (B), and a low-field part of ^{1}H (C) NMR spectra of the [Ga(trap-H)] complex (the shoulder in the ^{31}P NMR spectrum is marked with an arrow).

Interconversions among the other isomers should have similar energetic barriers.

The Ga^{3+}−TRAP-Ph system cannot be experimentally investigated in a similar manner because of the precipitation of a white solid (presumably the previously investigated complex, its Λ*δδδ-RRR*/Δ*λλλ-SSS* isomer[27]). However, the diluted supernatant solution taken before complete precipitation exhibits several ^{31}P{^{1}H} NMR signals in the region expected for the gallium(III) complex.

The differences in abundance of the complex diastereoisomers with varied substituents on phosphorus atoms show an interesting analogy with the lanthanide(III) complexes of the tetraphosphorus acid derivatives of DOTA.[38] In these complexes (with a square antiprismatic coordination geometry), only one major diastereoisomer was present in solution if the phosphorus atom substituents were alkyls such as Me, CH_2OH, Et, and Bn. For more electronegative phosphorus atom substituents such as H, Ph, and OR′, a full set of all possible diastereomers was observed in solution. The same phenomenon was observed here for gallium(III) complexes of

dx.doi.org/10.1021/ic202103v | *Inorg. Chem.* 2012, 51, 577−590

tris(phosphinic acid) derivatives, TRAP-R. The ligands with alkyl substituents ($CH_2CH_2CO_2H$ in TRAP-Pr or CH_2OH in TRAP-OH) give rise to only one diastereoisomer of the complexes, while those with more electron-withdrawing substituents (H in TRAP-H or probably also Ph in TRAP-Ph) form a mixture of diastereoisomers during complexation. However, such a hypothesis needs more data to be confirmed.

Formation and Decomposition of the Gallium(III) Complexes. To study the formation and decomplexation of the gallium(III) complexes, we used ^{31}P and ^{71}Ga NMR spectroscopy. Formation of the complexes at room temperature was monitored by ^{71}Ga NMR spectroscopy and quantified by comparison to the intensity of the $[Ga(OH)_4]^-$ signal as a standard; monitoring of the reaction progress by ^{71}Ga NMR spectroscopy has been recently used for the quantitative kinetic evaluations of complex formation and decomplexation in the Ga^{3+}–DOTA[10] and Ga^{3+}–NOTA–citrate[53] systems. The ^{31}P NMR spectra were used to show more detailed changes in the abundance of the free ligands, intermediates, and final gallium(III) complexes.

The rate of formation of the complex is strongly influenced by the substituent on the phosphorus atom, showing the important role of the substituents in the design of the TRAP ligands for trivalent gallium complexation (Table 4). At pH 2.8, all examined ligands except TRAP-H showed very fast complexation; gallium(III) was quantitatively bound in less than 5 min, which is the shortest possible time needed between preparation of a sample and measurement of the NMR spectra. At pH 1, TRAP-OH and TRAP-Pr showed much faster complexation than NOTA; however, the Ga^{3+}–TRAP-H complex needed approximately 15 days to be fully formed. At pH 0, all the phosphinate ligands were still able to form complexes with Ga^{3+} ion, albeit slowly (weeks); meanwhile, NOTA showed no signs of complex formation even after 40 days. Such measurements were not possible for TRAP-Ph; however, the fast precipitation even in acidic solutions points to rather fast complexation. The results emphasize the importance of careful pH control during the complexation with NOTA as described previously.[4] The higher acidity of the phosphinic acid groups and the lower basicity of the ring nitrogen atoms of the phosphinic acid TACN derivatives are responsible for complexation even at pH 0, where the more basic NOTA exhibits no gallium(III) binding. The results also show that ligands with electron rich side-chain substituents are able to interact with Ga^{3+} ion (TRAP-OH, TRAP-Pr, and probably TRAP-Ph) and thereby significantly accelerate the formation of the final in-cage complexes. The comparison of TRAP-OH and TRAP-H complexation can serve as an example; the Ga^{3+} ion is bound by the ligand with P–CH_2OH groups much faster than by the ligand with P–H groups, although both ligands do not have dramatically different basicities and the primary donor atoms are the same. Weakly interacting pendant arms move the metal ion closer to the macrocyclic cavity as seen Figure S3.3 of the Supporting Information. The deprotonated phosphinate group accelerates the transfer of the metal ion into the ligand cavity and helps to simultaneously remove nitrogen-bound protons from the cavity. The data for complexation at low pH are in accord with the recent observation that mixed acetate–phosphonate derivatives of TACN are more efficient chelators for carrier-free $^{68}Ga^{3+}$ than NOTA.[23]

Table 4. Half-Times ($t_{1/2}$) and Times of the Quantitative Formation ($t_{100\%}$) of the [Ga(L)] Complexes[a]

ligand	pH	$t_{1/2}$	$t_{100\%}$
TRAP-H	2.8	30 min	220 min
	1	21 h	15 days
	0	36 days	240 days
TRAP-OH	2.8	*c*	<5 min
	1	14 min	60 min
	0	3.8 days	31 days
TRAP-Pr[b]	2.8	*c*	<5 min
	1	3 min	12 min
	0.8	20 min	100 min
	0		12 days
NOTA	2.8	*c*	<5 min
	1	270 min	6 days
	0	*d*	*d*

[a]At 25 °C, 1:1 L:Ga molar ratio, c_{Ga} = 0.01 M. [b]From ref 28. [c]Not measurable because of a fast reaction. [d]No reaction observed.

We point out that Ga^{3+} complexation at pH values as low as 1 is of outstanding practical importance, as 0.1 M aqueous HCl is used for elution of some popular commercially available $^{68}Ge/^{68}Ga$ generators. Our study shows that, in contrast to NOTA, particularly TRAP-Pr is able to form a complex with Ga^{3+} rapidly under these conditions. In full accordance with this finding, our recently published results for the ^{68}Ga radiochemistry of the TRAP chelators[54] showed that these can indeed be readily labeled with ^{68}Ga at pH <1 and, therefore, also using the neat $^{68}Ge/^{68}Ga$ generator eluate. Despite not being applicable for all purposes, this method is compatible with many targeting moieties, such as most of the oligopeptides used for peptide receptor imaging. We therefore hold the view that TRAP ligands represent a big step forward in the development of kit production of ^{68}Ga radiopharmaceuticals in a "shake-and-shoot" synthetic approach, which is known from ^{99m}Tc radiotracers. Moreover, the highly selective and efficient Ga^{3+} complexation by TRAP ligands, as shown in this study, readily corresponds to the finding that much lower chelator concentrations are required for ^{68}Ga labeling.[54] TRAP-based ^{68}Ga radiopharmaceuticals can therefore be produced with hitherto unknown specific activitites, thereby allowing the smallest molar amounts of tracers to be administered for PET imaging. As an "ideal tracer" should be applied in the smallest possible amounts, to minimize interference with the biochemical equilibria governing the biosystem or organism under investigation, TRAP ligands can be considered of fundamental importance for future ^{68}Ga radiopharmaceutical research.

The kinetic inertness of the [Ga(trap-H)] and [Ga(trap-OH)] complexes was tested in 6 M $HClO_4$ at room temperature. No sign of decomposition was observed over 6 weeks, confirming the high kinetic inertness of these complexes against proton-assisted decomposition. The same complete inertness to proton-assisted decomplexation has been observed for the [Ga(NOTA)] and $[Ga(trap\text{-}Pr)]^{3-}$ complexes.[18,28]

Decomplexation in alkaline solutions proceeds for weeks for NOTA and TRAP-Pr complexes.[18,28] However, the situation was different for the [Ga(trap-OH)] complex. This in-cage complex is transformed to the out-of-cage complexes as discussed above. The reaction was followed only by $^{31}P\{^1H\}$ NMR spectroscopy as the out-of-cage complexes exhibit no ^{71}Ga NMR signal. The in-cage complex is fully stable up to pH ~5. At higher pH values, the transformation proceeds progressively faster. Equilibrium was reached after ~3 weeks

dx.doi.org/10.1021/ic202103v | Inorg. Chem. 2012, 51, 577–590

at pH 7.2, after ~6.5 days at pH 8.1, and after ~1.5 days at pH 9.5, and no signals or species other than those shown in the fully equilibrated samples (Figure 2) were observed during the course of the reaction. The rearrangement of the in-cage to the out-of-cage complex at physiological pH over hours to days does not interfere with the suitability of the TRAP-OH-based ligands for practical application as the decomposition is still slow in comparison with the half-life of the ^{68}Ga isotope and/or the labeled tracer pharmacokinetics (minutes to hours). Similar considerations concerning a relation of ^{68}Ga half-life and the rate of decomplexation of the Ga^{3+} complexes of DOTA and its monoamide in the slightly alkaline region have been pointed out recently.[10]

CONCLUSION

The properties of TRAP ligands, phosphinic acid derivatives of 1,4,7-triazacyclononane bearing different phosphorus substituents (H, Ph, CH_2OH, or $CH_2CH_2CO_2H$), were compared with those of the carboxylic acid analogue, NOTA. Thermodynamic studies showed that the phosphinic acid ligands are more acidic than NOTA and their acidity or basicity depends on the substituent on the phosphorus atom. The stability constants were determined for their complexes with Ga^{3+} and other metal ions; in addition, this parameter was redetermined for the [Ga(NOTA)] complex by applying the improved method. The thermodynamic stability of the gallium(III) complexes strongly depends on the ligand basicity, in the following order: [Ga(NOTA)] > [Ga(trap-Pr)] > [Ga(trap-OH)] > [Ga(trap-H)]. Although selectivity for Ga^{3+} complexation is very high for all TACN-based ligands, phosphinate ligands exhibit higher selectivity than NOTA for binding small metal ions. All investigated phosphinate ligands are able to bind trivalent gallium efficiently even at pH 0 and are, generally, more efficient than NOTA. The binding is very fast for TRAP-Pr and TRAP-OH, possessing coordinating substituents on the phosphorus atoms that increase the local metal ion concentration close to the macrocyclic cavity. Thus, the presence of phosphinic acid pendant arms improves the coordination ability of the ligands in acidic media, which represents one of the most important properties for the practical application in nuclear medicine. All complexes are fully inert against proton-assisted decomplexation. Our data suggest an importance of weakly coordinating side chains for the acceleration of the transfer of the metal ion into the macrocyclic cavity. Altogether, we found that the methylenephosphinic acid group is a potent alternative to the commonly used acetic acid pendant arm in macrocyclic ligands, and the phosphinic acid analogues of NOTA are excellent gallium(III) chelators, with ideal properties for ^{68}Ga-based PET imaging agent elaboration.

The in-cage [Ga(trap-OH)] complex exhibited unexpected behavior in solutions at pH >5. It slowly reacts with hydroxide anions to form out-of-cage complexes where an oxygen-only coordination environment is present. The possible structures of these species were suggested by DFT calculations, the study being only the second[55] in-depth computational treatment of gallium(III) complexes of macrocyclic ligands. The calculations showed some unexpected results. To form the out-of-cage complexes, hydroxide anion must be coordinated together with at least one deprotonated *P*-hydroxymethyl group. This deprotonation is facilitated by a polarization effect of a small and charged Ga^{3+} ion once it moves out; subsequently, a deprotonated hydroxymethyl group will coordinate. Simultaneously, a proton has to be moved into the ligand cavity where it is bound to a nitrogen atom and held in-cage by a network of intramolecular hydrogen bonds. Such reactivity is caused by the affinity of the hard Ga^{3+} ion for the hard oxygen atoms. This is the first direct observation of thermodynamically stable out-of-cage gallium(III) complexes in aqueous solution that are commonly assumed as kinetic intermediates during formation and decomplexation of the complexes of macrocyclic ligands.

EXPERIMENTAL SECTION

Materials and Methods. All reactants and solvents were commercially available analytical grade chemicals. The 1,4,7-triazacyclononane as a free base was purchased from CheMatech and as a trihydrochloride was prepared via modified Richman–Atkins cyclization.[56] Characteristic NMR spectra were recorded using Varian UNITY Inova (400 MHz) or VNMRS (300 MHz) spectrometers. ^{1}H and ^{13}C NMR shifts are referenced to the *t*-BuOH signal, and ^{31}P NMR shifts are referenced to 85% aqueous H_3PO_4. Elemental analyses were performed using the HERAEUS Varian EL III system. Mass spectra were recorded on a Bruker Esquire 3000 spectrometer with ESI as an ion source and ion trap as a detector in positive or negative mode.

1,4,7-Triazacyclononane-1,4,7-tris[methylene(phenyl)-phosphinic acid] (TRAP-Ph) and 1,4,7-Triazacyclononane-7-methyl-1,4-bis[methylene(phenyl)phosphinic acid] (^{Me}NO2P^{Ph}). 1,4,7-Triazacyclononane trihydrochloride (1.50 g, 6.29 mmol), paraformaldehyde (0.74 g, 24.67 mmol), and phenylphosphinic acid (13.40 g, 94.37 mmol) were mixed with 6 M aqueous HCl (15 mL). The solution was stirred at 90 °C for 24 h and, then, evaporated in vacuo. The crude product was purified on Dowex 50 resin (H^+ form, elution with water followed by 5% aqueous ammonia). The ammonia fractions were combined and evaporated in vacuo. The resulting mixture of TRAP-Ph and ^{Me}NO2P^{Ph} was purified on silica gel [elution with a 1:1 aqueous ammonia/EtOH mixture; R_f 0.85 (TRAP-Ph), 0.34 (^{Me}NO2P^{Ph})]. The fractions containing pure ^{Me}NO2P^{Ph} were evaporated in vacuo, yielding ^{Me}NO2P^{Ph}·2NH_3·8.5H_2O as a dark-brown oil (1.2 g, 32%). The fractions containing pure TRAP-Ph were combined and evaporated in vacuo. The target product was further purified on Dowex 1 resin (OH^- form, elution with water followed by 6 M aqueous HCl) to remove the traces of ammonia. After evaporation of HCl fractions containing the ligand in vacuo, the remaining oil was dissolved in a minimal amount of water and freeze-dried to give TRAP-Ph·2.4HCl·3.5H_2O (1.60 g, 35%).

TRAP-Ph. ^{1}H NMR (300 MHz, D_2O/NaOD, 25 °C): δ 2.72 (d, $^2J_{PH}$ = 6.9 Hz, N-C$\underline{H}_2$-P, 6H), 2.78 (s, ring C$\underline{H}_2$, 12H), 7.42–7.45 (m, $\underline{H}_{ar}$, 9H), 7.59–7.63 (m, $\underline{H}_{ar}$, 6H). ^{13}C{^{1}H} NMR (75.4 MHz, D_2O/NaOD): δ 50.2 (s, ring $\underline{C}H_2$, 6C), 54.7 (d, $^1J_{PC}$ = 100.1 Hz, $\underline{C}H_2$-P), 129.4 (s, $\underline{C}_{ar}$), 131.73 (s, $\underline{C}_{ar}$), 132.3 (s, $\underline{C}_{ar}$), 136.8 (d, $^1J_{PC}$ = 121.5 Hz, $\underline{C}_{ar}$-P). ^{31}P{^{1}H} NMR (121.4 MHz, D_2O/NaOD, 25 °C): δ 26.3 (s). MS (ESI, negative mode): *m*/*z* 612 [TRAP-Ph + Na^+ − 2H^+]. Anal. Calcd (%) for $C_{27}H_{36}N_3O_6P_3$·3.5H_2O·2.4HCl: C, 43.70; H, 6.17; N, 5.66; Cl, 11.47. Found: C, 43.76; H, 5.43; N, 5.63; Cl, 11.28.

^{Me}NO2P^{Ph}. ^{1}H NMR (300 MHz, D_2O/NaOD, 25 °C): δ 2.52 (s, N-C$\underline{H}_3$, 3H), 2.68 (s, ring C$\underline{H}_2$, 4H), 2.86–3.11 (m, ring C$\underline{H}_2$, 8H, and N-C$\underline{H}_2$-P, 4H), 7.50–7.57 (m, $\underline{H}_{ar}$, 5H), 7.68–7.74 (m, $\underline{H}_{ar}$, 5H). ^{13}C{^{1}H} NMR (75.4 MHz, NaOD, 25 °C): δ 41.8 (s, ring $\underline{C}H_2$), 47.1 (s, ring $\underline{C}H_2$), 51.2 (s, ring $\underline{C}H_2$), 53.5 (s, $\underline{C}H_3$), 56.1 (d, $^1J_{PC}$ = 105.1 Hz, $\underline{C}H_2$-P), 128.5 (d, $^2J_{PC}$ = 11.6 Hz, $\underline{C}_{ar}$), 130.8 (d, $^3J_{PC}$ = 9.4 Hz, $\underline{C}_{ar}$), 131.2 (s, $\underline{C}_{ar}$), 136.6 (d, $^1J_{PC}$ = 120.0 Hz, $\underline{C}_{ar}$-P). ^{31}P{^{1}H} NMR (121.4 MHz, D_2O/NaOD, 25 °C): δ 29.5 (s). MS (ESI, negative mode): *m*/*z* 450 [^{Me}NO2P^{Ph} − H^+]. Anal. Calcd (%) for $C_{21}H_{31}N_3O_4P_2$·8.5H_2O·2NH_3: C, 39.49; H, 8.52; N, 10.97. Found: C, 39.92; H, 8.43; N, 10.71; Cl, 11.28.

1,4,7-Triazacyclononane-1,4,7-tris(methylenephosphinic acid) (TRAP-H). Triazacyclononane (1.0 g, 7.75 mmol), paraformaldehyde (0.74 g, 24.67 mmol), and hypophosphorous acid (2.30 g, 34.8 mmol) were dissolved in water (20 mL) and stirred at room temperature for 48 h. The reaction mixture was evaporated in vacuo (bath temperature of <40 °C). The resulting oil was purified on a weak

dx.doi.org/10.1021/ic202103v | *Inorg. Chem.* 2012, 51, 577–590

cationic exchanger, Amberlite 50, with water elution. Fractions containing the pure ligand (by ^{31}P NMR) were combined, evaporated in vacuo as described above, and freeze-dried to give TRAP-H·H_2O (0.93 g, 33%). ^{1}H NMR (300 MHz, D_2O, 25 °C): δ 3.22 (d, $^2J_{PH}$ = 9.0 Hz, N-C$\underline{H}_2$-P, 6H), 3.45 (s, ring C$\underline{H}_2$, 12H), 7.14 (d, $^1J_{PH}$ = 543.9 Hz, P-$\underline{H}$, 3H). ^{13}C{^{1}H} NMR (150.9 MHz, D_2O, 25 °C): δ 52.20 (s, ring $\underline{C}H_2$), 56.21 (d, $^1J_{PC}$ = 90.5 Hz, N-$\underline{C}H_2$-P). ^{31}P{^{1}H} NMR (121.4 MHz, D_2O, 25 °C): δ 16.1 (s). ^{31}P NMR (121.4 MHz, D_2O, 25 °C): δ 16.2 (d, $^1J_{PH}$ = 543.9 Hz). MS (ESI, negative): m/z 362 [TRAP-H$^+$]. Anal. Calcd (%) for $C_9H_{24}N_3O_6P_3$·H_2O: C, 28.35; H, 6.87; N, 11.02. Found: C, 28.28; H, 6.70; N, 11.13.

1,4,7-Triazacyclononane-1,4,7-tris[methylene-(hydroxymethyl)phosphinic acid] (TRAP-OH). Triazacyclononane trihydrochloride (1.50 g, 6.23 mmol), paraformaldehyde (0.74 g, 24.67 mmol), and solid hypophosphorous acid (2.80 g, 42.42 mmol) were dissolved in water (20 mL) and stirred at room temperature for 48 h. The reaction mixture was evaporated in vacuo (bath temperature of <40 °C). The resulting oil was dissolved in 6 M HCl (50 mL). Paraformaldehyde (0.74 g, 24.67 mmol) was added, and the solution was heated at 105 °C in a bath for 24 h. The reaction mixture was evaporated in vacuo and purified on Dowex 50 resin (H^+ form, elution with water). The fractions containing product were combined, evaporated in vacuo, and freeze-dried to give TRAP-OH·0.3HCl·1.5-H_2O (2.16 g, 70%). ^{1}H NMR (300 MHz, D_2O, 25 °C): δ 3.47 (d, $^2J_{PH}$ = 6.8 Hz, N-C$\underline{H}_2$-P, 6H), 3.62 (s, ring C$\underline{H}_2$, 12H), 3.82 (d, $^2J_{PH}$ = 6.0 Hz, P-C$\underline{H}_2$-OH, 6H). ^{13}C{^{1}H} NMR (100.6 MHz, D_2O, 25 °C): δ 52.46 (s, ring $\underline{C}H_2$), 54.14 (d, $^1J_{PC}$ = 87.42 Hz, N-$\underline{C}H_2$-P), 60.36 (d, $^1J_{PC}$ = 113.8 Hz, O-$\underline{C}H_2$-P). ^{31}P{^{1}H} NMR (121.4 MHz, D_2O, 25 °C): δ 34.58 (s). MS (ESI, negative): m/z 474 [TRAP-OH + Na^+ − 2H^+]. Anal. Calcd (%) for $C_{12}H_{30}N_3O_9P_3$·1.5H_2O·0.3HCl: C, 29.34; H, 6.83; N, 8.55. Found: C, 29.30; H, 6.58; N, 8.28.

Potentiometric Measurements. Potentiometry was conducted according to the previously published procedures; for the preparation of stock solutions and chemicals, the equipment, electrode system calibration, titration procedures, and data treatment, see refs 10, 46b, and 57. The $Ga(NO_3)_3$ stock solution was acidified with aqueous HNO_3, and the excess of acids in the stock solution was determined independently by acid−base titration. Throughout the paper, pH means −log[H^+]. Protonation and stability constants were determined in 0.1 M (NMe_4)Cl at 25.0 °C with a pK_w of 13.81. Protonation constants and stability constants for the complexes with metal ions except Ga^{3+} were determined by in-cell titrations from data obtained in the pH range of 1.6−12 (or until precipitation of metal hydroxides) with ~40 points per full titration and four parallel titrations (c_L = 0.004 M; c_M = 0.004 or 0.002 M). The stability constants of the gallium(III) complexes were obtained by the out-of-cell method as described previously [starting pH of 1.5, 15−25 points per titration, points with precipitated $Ga(OH)_3$ excluded].[10,28] The full sets of determined constants (with their standard deviations given directly by the program) are given in the Supporting Information (Tables S1.1 and S1.2). The titration data were treated with OPIUM,[58] and the presented chemical models were chosen to have a chemical sense and to exhibit the best fitting statistics. Stability constants of metal hydroxy complexes were taken from ref 59.

Complexation−Decomplexation NMR Measurements. Formation of the Ga^{3+}−TRAP-R (R = H, Ph, or CH_2OH) complexes was followed by ^{31}P and ^{71}Ga NMR spectroscopy (25 °C, c_L = c_{Ga} = 10 mM). The experiments were conducted at pH 2.8 (1 M sodium chloroacetate buffer), pH 1.0 (0.1 M HCl), and pH 0 (1.0 M HCl); the solution pH was checked at the end of the complexation. The ^{71}Ga and ^{31}P{^{1}H} NMR signals were referenced to a 0.2 M aqueous $[Ga(OH)_4]^-$ solution and 85% aqueous H_3PO_4, respectively, in the insert tube. We preformed the complexes for other NMR measurements in solution by mixing of the ligand and Ga^{3+} salt stock solutions in a 1:1 Ga:L molar ratio and increasing the pH to 2.5 with a hydroxide solution (with heating if necessary for quantitative formation). Proton-assisted decomplexation of the complexes (c_{GaL} = 10 mM) in 6 M $HClO_4$ was followed by ^{31}P{^{1}H} NMR over a period of 6 weeks.

Computational Method. If not stated otherwise, all calculations were performed with the Gaussian 03 suite.[60] The geometries were optimized using a pure DFT functional with Ahlrichs' triple-ξ basis set (BP86/TZVP/auto).[61−63] The basis was automatically fitted to improve performance. Stationary points were confirmed as local minima by a frequency calculation (absence of imaginary frequencies). Transition states were also confirmed by a frequency calculation by the occurrence of one imaginary frequency. The conductor-like polarizable continuum model (C-PCM) was applied to model the influence of water (ε = 78.39) with the following nonstandard input.[64,65] Atomic radii were modeled with the United Force Field (UFF) model that uses individual spheres for all hydrogen atoms. The *nosymmcav* keyword was applied to break the symmetry of the cavity. The number of added spheres was decreased by setting O_{fac} equal to 0.8 and R_{min} equal to 0.5. In cases where the optimization did not converge, the GDIIS algorithm was applied to arrive at a stationary point.[66−68] Energies for the hydroxide anion and water molecule were taken from ref 49. Values reported therein were obtained at the BP/TZVP level of theory and with application of COMSO-RS, which combines the electrostatic advantages and computational efficiency of the dielectric continuum solvation model COSMO with a statistical thermodynamics method for the local interaction of surfaces. It also takes into account local deviations from dielectric behavior as well as hydrogen bonding (see ref 49 and references cited therein).

To obtain more accurate energies for the four TRAP-H diastereoisomers and the transition state of the isomerization, we optimized their geometries at the BP86/TZVP level of theory using the C-PCM solvent model with the alterations given above followed by a frequency calculation with the Gaussian 03 suite. With the obtained geometry, a single-point calculation was conducted with Gaussian 09 using Truhlar and Zhao's M06 functional and Ahlrichs' def2-TZVPP basis set.[69−72] The influence of the solvent water (water ε = 78.3553) was modeled with C-PCM and the alterations given above. Because the values for the thermal correction to the Gibbs free energy change only slightly with a different basis, they were taken from the TZVP calculation and added to the SCF energy obtained from the single-point calculation to yield more accurate Gibbs free energies.

■ ASSOCIATED CONTENT

Ⓢ Supporting Information

Additional experimental details of potentiometric titrations, experimentally determined protonation and stability constants, comparison of stability constants of more ligands, distribution diagrams, dependence of gallium(III) complexes on the basicity of the ligands, reactions considered in DFT calculations together with the complex species, summary of relative energies of all species, atomic coordinates of all species, diastereoisomers of the [Ga(trap-H)] complex, NMR spectra of [Ga(trap-R)] complexes, and time course of complexation of Ga^{3+} with TRAP-OH. This material is available free of charge via the Internet at http://pubs.acs.org.

■ AUTHOR INFORMATION

Corresponding Author

*Department of Inorganic Chemistry, Universita Karlova, Hlavova 2030, 12843 Prague 2, Czech Republic. Telephone: +420-22195-1263. Fax: +420-22195-1253. E-mail: petrh@natur.cuni.cz.

Present Address

‡Department of Pharmaceutical Radiochemistry, Technische Universität München, Walther-Meissner Strasse 3, 85748 Garching, Germany.

■ ACKNOWLEDGMENTS

Support from the Grant Agency of the Czech Republic (203/09/1056) and the Long-Term Research Plan of the Ministry of

Education of the Czech Republic (MSM0021620857) is acknowledged. The work was conducted under the framework of COST D38, CM0807, and BM607 Actions. J.Š. is thankful for support by the Grant Agency of Charles University (19310), and V.K. is thankful for support from RP MSMT 14/63. We are grateful to M. Pniok (Charles University, Prague, Czech Republic) for help with a large-scale synthesis of TRAP-Ph and MS measurements. J.N. and M.S. thank S. Schenk (BASF) for fruitful discussion. All the calculations were performed at the Universitätsrechenzentrum of the Friedrich-Schiller-Universität (Jena, Germany).

DEDICATION

Dedicated to Prof. Ernst Anders on the occasion of his 70th birthday.

REFERENCES

(1) (a) Gupta, T.; Beriwal, S. *Indian J. Cancer* **2010**, *47*, 126−133. (b) Bockisch, A.; Freudenberg, L. S.; Schmidt, D.; Kuwert, T. *Semin. Nucl. Med.* **2009**, *39*, 276−289.

(2) (a) Pichler, B. J.; Kolb, A.; Nägele, T.; Schlemmer, P. H. *J. Nucl. Med.* **2010**, *51*, 333−336. (b) Sauter, A. W.; Wehrl, H. F.; Kolb, A.; Judenhofer, M. S.; Pichler, B. J. *Trends Mol. Med.* **2010**, *16*, 508−515. (c) Boss, A.; Stegger, L.; Bisdas, L. S.; Kolb, A.; Schwenzer, N.; Pfister, M.; Claussen., C. D.; Pichler, B. J.; Pfannenberg, C. *Eur. Radiol.* **2011**, *21*, 1439−1446.

(3) (a) Zhernosekov, K. P.; Filosofov, D. V.; Baum, R. P.; Aschoff, P.; Bihl, H.; Razbash, A. A.; Jahn, M.; Jennewein, M.; Rösch, F. *J. Nucl. Med.* **2007**, *48*, 1741−1748. (b) Ocak, M.; Antretter, M.; Knopp, R.; Kunkel, F.; Petrik, M.; Bergisadi, N.; Decristoforo, C. *Appl. Radiat. Isot.* **2010**, *68*, 297−302.

(4) Fani, M.; André, J. P.; Mäcke, H. R. *Contrast Media Mol. Imaging* **2008**, *3*, 67−77.

(5) Wadas, T. J.; Wong, E. H.; Weisman, G. R.; Anderson, C. J. *Chem. Rev.* **2010**, *110*, 2858−2902.

(6) Rösch, F.; Riss, J. P. *Curr. Top. Med. Chem.* **2010**, *10*, 1633−1668.

(7) Rösch, F.; Baum, R. P. *Dalton Trans.* **2011**, *40*, 6104−6111.

(8) Clarke, E. T.; Martell, A. E. *Inorg. Chim. Acta* **1991**, *181*, 273−280.

(9) Clarke, E. T.; Martell, A. E. *Inorg. Chim. Acta* **1991**, *190*, 37−46.

(10) Kubíček, H.; Havlíčková, J.; Kotek, J.; Tircsó, G.; Hermann, P.; Tóth, É.; Lukeš, I. *Inorg. Chem.* **2010**, *49*, 10960−10969.

(11) (a) Wei, L.; Zhang, X.; Gallazzi, F.; Miao, Y.; Jin, X.; Brechbiel, M. W.; Xu, H.; Clifford, T.; Welch, M. J.; Lewis, J. S.; Quinn, T. P. *Nucl. Med. Biol.* **2009**, *36*, 345−354. (b) Li, J.; Vanbilloen, H.; Vermaelen, P.; Devos, E.; Mortelmans, L.; Bormans, G.; Ni, Y.; Verbruggen, A. *Bioorg. Med. Chem.* **2010**, *18*, 5274−5281.

(12) (a) Liu, S. *Adv. Drug Delivery Rev.* **2008**, *60*, 1347−1370. (b) Lattuada, L.; Barge, A.; Cravotto, G.; Giovenzana, G. B.; Tei, L. *Chem. Soc. Rev.* **2011**, *40*, 3019−3049.

(13) Heppeler, A.; Froidevaux, S.; Maecke, H. R.; Jermann, E.; Béhé, M.; Powell, P.; Hening, M. *Chem.—Eur. J.* **1999**, *5*, 1974−1981.

(14) Pool, S. E.; Krenning, E. P.; Koning, G. A.; van Eijck, C. H. J.; Teunissen, J. J. M.; Kam, B.; Valkema, R.; Kwekkeboom, D. J.; de Jong, M. *Semin. Nucl. Med.* **2010**, *40*, 209−218.

(15) Correia, J. G. G.; Paulo, A.; Raposinho, P. D.; Santos, I. *Dalton Trans.* **2011**, *40*, 6144−6167.

(16) Bandoli, G.; Dolmella, A.; Tisato, F.; Porchia, M.; Refosco, F. *Coord. Chem. Rev.* **2009**, *253*, 56−77.

(17) Cola, N. A.; Rarig, R. S. Jr.; Ouellette, W.; Doyle, R. P. *Polyhedron* **2006**, *25*, 3457−3462.

(18) (a) Craig, A. S.; Parker, D.; Adams, H.; Bailey, N. A. *J. Chem. Soc., Chem. Commun.* **1989**, 1793−1794. (b) Broan, C.; Cox, J. P.; Craig, A. S.; Kataky, R.; Parker, D.; Harrison, A.; Randall, A. M.; Ferguson, G. J. *J. Chem. Soc., Perkin Trans. 2* **1991**, 87−99.

(19) Jyo, A.; Kohno, T.; Terazono, Y.; Kawano, S. *Anal. Sci.* **1990**, *6*, 323−324.

(20) André, J. P.; Maecke, H. R.; Zehnder, M.; Macko, L.; Akyeld, K. G. *Chem. Commun.* **1998**, 1301−1302.

(21) Eisenwiener, K.-P.; Prata, M. I. M.; Buschmann, I.; Zhang, H.-W.; Santos, A. C.; Wenger, S.; Reubi, J. C.; Mäcke, H. R. *Bioconjugate Chem.* **2002**, *13*, 530−541.

(22) (a) Riss, P. J.; Kroll, C.; Nagel, V.; Rösch, F. *Bioorg. Med. Chem. Lett.* **2008**, *18*, 5364−5367. (b) McMurry, T. J.; Brechbiel, M. W.; Wu, C.; Gansow, O. A. *Bioconjugate Chem.* **1993**, *4*, 236−245. (c) Brechbiel, M. W.; McMurry, T. J.; Gansow, O. A. *Tetrahedron Lett.* **1993**, *34*, 3691−3694.

(23) Fellner, M.; Riss, P.; Loktionova, N.; Zhernosekov, K.; Thews, O.; Geraldes, C. F. G. C.; Kovács, Z.; Lukeš, I.; Rösch, F. *Radiochim. Acta* **2011**, *99*, 43−51.

(24) de Sá, A.; Prata, M. I. M.; Geraldes, C. F. G. C.; André, J. P. *J. Inorg. Biochem.* **2010**, *104*, 1051−1062.

(25) (a) Shetty, D.; Choi, S. Y.; Jeong, J. M.; Hoigebazar, L.; Lee, Y.-S.; Lee, D. S.; Chung, J.-K.; Lee, M. C.; Chung, Y. K. *Eur. J. Inorg. Chem.* **2010**, 5432−5438. (b) Shetty, D.; Jeong, J. M.; Ju, C. H.; Kim, Y. J.; Lee, J.-Y.; Lee, Y.-S.; Lee, D. S.; Chung, J.-K.; Lee, M. C. *Bioorg. Med. Chem.* **2010**, *18*, 7338−7347.

(26) Lukeš, I.; Kotek, J.; Vojtíšek, P.; Hermann, P. *Coord. Chem. Rev.* **2001**, *216*−*217*, 287−312.

(27) (a) Cole, E.; Copley, R. C. B.; Howard, J. A. K.; Parker, D.; Ferguson, G.; Gallagher, J. F.; Kaitner, B.; Harrison, A.; Royle, L. *J. Chem. Soc., Dalton Trans.* **1994**, 1619−1629. (b) Cole, E.; Parker, D.; Ferguson, G.; Gallagher, J. F.; Kaitner, B. *Chem. Commun.* **1991**, 1473−1475.

(28) Notni, J.; Hermann, P.; Havlíčková, J.; Kotek, J.; Kubíček, V.; Plutnar, J.; Loktionova, N.; Riss, P. J.; Rösch, F.; Lukeš, I. *Chem.—Eur. J.* **2010**, *16*, 7174−7185.

(29) Anderegg, G.; Arnaud-Neu, F.; Delgado, R.; Felcmann, J.; Popov, K. *Pure Appl. Chem.* **2005**, *77*, 1445−1495.

(30) Bevilacqua, A.; Galb, R. I.; Hebard, R. I.; Zompa, L. J. *Inorg. Chem.* **1987**, *26*, 2699−2706.

(31) Moedritzer, K.; Irani, R. R. *J. Org. Chem.* **1966**, *31*, 1603−1607.

(32) Remore, D. *J. Org. Chem.* **1978**, *43*, 992−996.

(33) Lázár, I.; Sherry, A. D. *Synthesis* **1995**, 453−457.

(34) Drahoš, B.; Pniok, M.; Havlíčková, J.; Kotek, J.; Císařová, I.; Hermann, P.; Lukeš, I.; Tóth, É. *Dalton Trans.* **2011**, *40*, 10131−10146.

(35) Bazakas, K.; Lukeš, I. *J. Chem. Soc., Dalton Trans.* **1995**, 1133−1137.

(36) Geraldes, C. F. G. C.; Marques, M. P. M.; Sherry, A. D. *Inorg. Chim. Acta* **1998**, *273*, 288−298.

(37) Lubal, P.; Kývala, M.; Hermann, P.; Holubová, J.; Rohovec, J.; Havel, J.; Lukeš, I. *Polyhedron* **2001**, *20*, 47−55.

(38) Kotková, Z.; Pereira, G. A.; Djanashvili, K.; Kotek, J.; Rudovský, J.; Hermann, P.; Elst, L. V.; Muller, R. N.; Geraldes, C. F. G. C.; Lukeš, I.; Peters, J. A. *Eur. J. Inorg. Chem.* **2009**, 119−136.

(39) Clegg, W.; Iveson, P. B.; Lockhart, J. C. *J. Chem. Soc., Dalton Trans.* **1992**, 3291−3298.

(40) Geraldes, C. F. G. C.; Sherry, A. D.; Marques, M. P. M; Alpoim, M. C.; Cortes, S. *J. Chem. Soc., Perkin Trans. 2* **1991**, 137−146.

(41) Lázár, I.; Ramasamy, R.; Brücher, E.; Geraldes, C. F. G. C.; Sherry, A. D. *Inorg. Chim. Acta* **1992**, *195*, 89−93.

(42) Geraldes, C. F. G. C.; Sherry, A. D.; Cacheris, W. P. *Inorg. Chem.* **1989**, *28*, 3336−3341.

(43) Drahoš, B.; Kubíček, V.; Bonnet, C. S.; Hermann, P.; Lukeš, I.; Tóth, É. *Dalton Trans.* **2011**, *40*, 1945−1951.

(44) O'Brien, P.; Salacinski, H.; Motevalli, M. *J. Am. Chem. Soc.* **1997**, *119*, 12695−12696.

(45) Hegetschweiler, K.; Ghisletta, M.; Fässler, T. F.; Nesper, R.; Schmalle, H. W.; Rihs, G. *Inorg. Chem.* **1993**, *32*, 2032−2041.

(46) (a) Kotek, J.; Lubal, P.; Hermann, P.; Císařová, I.; Lukeš, I.; Godula, T.; Svobodová, I.; Táborský, P.; Havel, J. *Chem.—Eur. J.* **2003**, *9*, 233−248. (b) Táborský, P.; Lubal, P.; Havel, J.; Kotek, J.; Hermann, P.; Lukeš, I. *Collect. Czech. Chem. Commun.* **2005**, *70*, 1909−1942.

(47) Cacheris, W. P.; Nickle, S. K.; Sherry, A. D. *Inorg. Chem.* **1987**, *26*, 958−861.

(48) Prata, M. I. M.; Santos, A. C.; Geraldes, C. F. G. C.; de Lima, J. J. P. *J. Inorg. Biochem.* **2000**, *79*, 359−363.
(49) Klamt, A.; Eckert, F.; Diedenhofen, M.; Beck, M. E. *J. Phys. Chem. A* **2003**, *107*, 9380−9386.
(50) Rong, M.; Welch, M. J.; Reibenspies, J.; Martell, A. E. *Inorg. Chim. Acta* **1995**, *236*, 75−82.
(51) Hermann, P.; Kotek, J.; Kubíček, V.; Lukeš, I. *Dalton Trans.* **2008**, 3027−3047.
(52) Geraldes, C. F. G. C.; Alpoim, M. C.; Marques, M. P. M.; Sherry, A. D.; Singh, M. *Inorg. Chem.* **1985**, *24*, 3876−3881.
(53) Morfin, J.-F.; Tóth, É. *Inorg. Chem.* **2011**, *50*, 10371−10378.
(54) Notni, J.; Šimeček, J.; Hermann, P.; Wester, H.-J. *Chem.—Eur. J.* **2011**, *17*, 14718−14722.
(55) Notni, J.; Pohle, K.; Peters, J. A.; Görls, H.; Platas-Iglesias, C. *Inorg. Chem.* **2009**, *48*, 3257−3267.
(56) Richman, J. E.; Atkins, T. J. *J. Am. Chem. Soc.* **1974**, *96*, 2268−2270.
(57) Försterová, M.; Svobodová, I.; Lubal, P.; Táborský, P.; Kotek, J.; Hermann, P.; Lukeš, I. *Dalton Trans.* **2007**, 535−549.
(58) (a) Kývala, M.; Lukeš, I. *International Conference Chemometrics '95*, Pardubice, Czech Republic, 1995, p 63. (b) Kývala, M.; Lubal, P.; Lukeš, I. IX. Spanish-Italian and Mediterranean Congress on Thermodynamics of Metal Complexes (SIMEC 98), Girona, Spain, 1998. The full version of OPIUM is available (free of charge) at http://www.natur.cuni.cz/_kyvala/opium.html.
(59) (a) Martell, A. E.; Smith, R. M. *Critical Stability Constants*; Plenum Press: New York, 1974−1989, Vols. *1*−*6*. (b) *NIST Standard Reference Database 46 (Critically Selected Stability Constants of Metal Complexes)*, version 7.0; National Institute of Standards and Technology: Gaithersburg, MD, 2003. (c) Baes, C. F., Jr.; Mesmer, R. E. *The Hydrolysis of Cations*; Wiley: New York, 1976.
(60) Frisch, M. J.; Trucks, G. W.; Schlegel, H. B.; Scuseria, G. E.; Robb, M. A.; Cheeseman, J. R.; Montgomery, J. J. A.; Vreven, T.; Kudin, K. N.; Burant, J. C.; Millam, J. M.; Iyengar, S. S.; Tomasi, J.; Barone, V.; Mennucci, B.; Cossi, M.; Scalmani, G.; Rega, N.; Petersson, G. A.; Nakatsuji, H.; Hada, M.; Ehara, M.; Toyota, K.; Fukuda, R.; Hasegawa, J.; Ishida, M.; Nakajima, T.; Honda, Y.; Kitao, O.; Nakai, H.; Klene, M.; Li, X.; Knox, J. E.; Hratchian, H. P.; Cross, J. B.; Bakken, V.; Adamo, C.; Jaramillo, J.; Gomperts, R.; Stratmann, R. E.; Yazyev, O.; Austin, A. J.; Cammi, R.; Pomelli, C.; Ochterski, J. W.; Ayala, P. Y.; Morokuma, K.; Voth, G. A.; Salvador, P.; Dannenberg, J. J.; Zakrzewski, V. G.; Dapprich, S.; Daniels, A. D.; Strain, M. C.; Farkas, O.; Malick, V.; Rabuck, A. D.; Raghavachari, K.; Foresman, J. B.; Ortiz, J. V.; Cui, Q.; Baboul, A. G.; Clifford, S.; Cioslowski, J.; Stefanov, B. B.; Liu, G.; Liashenko, A.; Piskorz, P.; Komaromi, I.; Martin, R. L.; Fox, D. J.; Keith, T.; Al-Laham, M. A.; Peng, C. Y.; Nanayakkara, A.; Challacombe, M.; Gill, M. W.; Johnson, B.; Chen, W.; Wong, M. W.; Gonzalez, C.; Pople, J. A. *Gaussian 03*, revision D.01; Gaussian Inc.: Wallingford, CT, 2004.
(61) Becke, A. D. *Phys. Rev. A* **1988**, *38*, 3098−3100.
(62) Perdew, J. P. *Phys. Rev. B* **1986**, *33*, 8822−8824.
(63) Schaefer, A.; Huber, C.; Ahlrichs, R. *J. Chem. Phys.* **1994**, *100*, 5829−5835.
(64) Barone, V.; Cossi, M. *J. Phys. Chem. A* **1998**, *102*, 1995−2001.
(65) Cossi, M.; Rega, N.; Scalmani, G.; Barone, V. *J. Comput. Chem.* **2003**, *24*, 669−681.
(66) Csaszar, P.; Pulay, P. *THEOCHEM* **1984**, *114*, 31−34.
(67) Farkas, Ö. Ph.D. Thesis, Eötvös Loránd University and Hungarian Academy of Sciences, Budapest, 1995.
(68) Farkas, Ö.; Schlegel, H. B. *J. Chem. Phys.* **1999**, *111*, 10806−10814.
(69) Frisch, M. J.; Trucks, G. W.; Schlegel, H. B.; Scuseria, G. E.; Robb, M. A.; Cheeseman, J. R.; Scalmani, G.; Barone, V.; Mennucci, B.; Petersson, G. A.; Nakatsuji, H.; Caricato, M.; Li, X.; Hratchian, H. P.; Izmaylov, A. F.; Bloino, J.; Zheng, G.; Sonnenberg, J. L.; Hada, M.; Ehara, M.; Toyota, K.; Fukuda, R.; Hasegawa, J.; Ishida, M.; Nakajima, T.; Honda, Y.; Kitao, O.; Nakai, H.; Vreven, T.; Montgomery, J. A., Jr.; Peralta, J. E.; Ogliaro, F.; Bearpark, M.; Heyd, J. J.; Brothers, E.; Kudin, K. N.; Staroverov, V. N.; Kobayashi, R.; Normand, J.; Raghavachari, K.; Rendell, A.; Burant, J. C.; Iyengar, S. S.; Tomasi, J.; Cossi, M.; Rega, N.; Millam, J. M.; Klene, M.; Knox, J. E.; Cross, J. B.; Bakken, V.; Adamo, C.; Jaramillo, J.; Gomperts, R.; Stratmann, R. E.; Yazyev, O.; Austin, A. J.; Cammi, R.; Pomelli, C.; Ochterski, J. W.; Martin, R. L.; Morokuma, K.; Zakrzewski, V. G.; Voth, G. A.; Salvador, P.; Dannenberg, J. J.; Dapprich, S.; Daniels, A. D.; Farkas, O.; Foresman, J. B.; Ortiz, J. V.; Cioslowski, J.; Fox, D. J. *Gaussian 09*, revision A.02; Gaussian, Inc.: Wallingford, CT, 2009.
(70) Zhao, Y.; Truhlar, D. G. *Theor. Chem. Acc.* **2008**, *120*, 215−241.
(71) Weigend, F.; Ahlrichs, R. *Phys. Chem. Chem. Phys.* **2005**, *7*, 3297−3305.
(72) Basis sets were obtained from the Extensible Computational Chemistry Environment Basis Set Database, version 02/02/06, as developed and distributed by the Molecular Science Computing Facility, Environmental and Molecular Sciences Laboratory, which is part of the Pacific Northwest National Laboratory (Richland, WA) and funded by the U.S. Department of Energy. The Pacific Northwest National Laboratory is a multiprogram laboratory operated by Battelle Memorial Institute for the U.S. Department of Energy under Contract DE-AC06-76RLO 1830. Contact Karen Schuchardt for further information.

APPENDIX 2

CHEMISTRY
A EUROPEAN JOURNAL

DOI: 10.1002/chem.201103503

TRAP, a Powerful and Versatile Framework for Gallium-68 Radiopharmaceuticals**

Johannes Notni,*[a] Jakub Šimeček,[a, b] Petr Hermann,[b] and Hans-Jürgen Wester[a]

Dedicated to Prof. em. Dr. rer. nat. habil. Ernst Anders on the occasion of his 70th birthday

The remarkable success of ^{68}Ga-labeled peptides in neuroendocrine tumor diagnostics gave a major boost to the development of ^{68}Ga-labeled tracers for positron emission tomography (PET).[1a] In contrast to common PET isotopes, ^{68}Ga ($t_{1/2}$ = 68 min; $E_{\beta+,max}$ = 1.89 MeV) is not produced by on-site cyclotrons but, similarly to ^{99m}Tc production for scintigraphy, is obtained from ^{68}Ge/^{68}Ga radioisotope generators ($t_{1/2}$(^{68}Ge) = 270.8 days). Conjugation of biologically active molecules to bifunctional chelate ligands and subsequent $^{68}Ga^{3+}$ complexation delivers radiopharmaceuticals that bind to pathologically overexpressed target structures with high affinity and thus allow for non-invasive molecular imaging in patients.

Until now, the design of ^{68}Ga tracers mainly relied on DOTA[1] (Scheme 1), which is ideally suited for larger metal ions (particularly lanthanides) but less so for the smaller Ga^{3+} ion. However, the utility of the smaller NOTA[2a] system (Scheme 1) for Ga^{3+} complexation has been shown two decades ago.[2] As it has been found that it forms Ga^{III} complexes with higher kinetic stability and allows higher ^{68}Ga labeling yields, conjugates of some of its bifunctional derivatives (mainly NODAGA,[2b] Scheme 1) are increasingly utilized in the development of ^{68}Ga radiopharmaceuticals in recent times. Inspired by these results, we report here the synthesis, properties, and preclinical evaluation of ^{68}Ga radiopharmaceuticals derived from NOTA-analogous *Tri*-*A*zacyclononane-*P*hosphinic acids[3] (abbreviated TRAP, see Scheme 1 and Table 1) and reveals their enormous utility for nuclear medicine and molecular imaging.

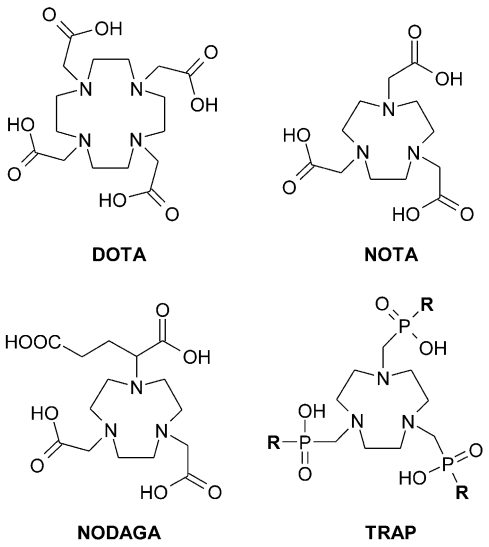

Scheme 1. Macrocyclic chelators discussed in the text (see also Table 1).

Table 1. TRAP ligands used in this study.

Identifier	Substituent R (Scheme 1)	Ref.
TRAP-H	H	[3a]
TRAP-Ph	Ph	[3b,c]
TRAP-OH	CH_2–OH	[4]
TRAP-Pr	CH_2–CH_2–COOH	[5]

The $^{68}Ga^{3+}$ complexation behavior was compared for TRAP ligands (Table 1), DOTA, and NOTA. Figure 1 shows that TRAP ligands are able to incorporate ^{68}Ga nearly quantitatively (>95%) at much lower ligand concentrations (c_L) and, due to the low pK_a of phosphinic acid moieties (ca. 0.7–1.5[4,5]), also in strongly acidic media; in the case of TRAP-OH[4] and TRAP-Pr[5] even at a pH as low as 0.5. As this allows ^{68}Ga labeling by directly using the neat eluate (0.1 M HCl) of the very popular Obninsk generator, greatly facilitated kit production of ^{68}Ga tracers could be achieved. Figure 2 illustrates that particularly TRAP-Pr rapidly incorporates ^{68}Ga at 25 °C and c_L = 3 μM, whereas neither DOTA nor NOTA can be labeled under these conditions. However, in line with previous reports[2c] we found that unlike DOTA, NOTA can be readily labeled at room temperature when using a fairly high ligand concentration of c_L = 100 μM (see the Supporting Information for details).

[a] Dr. J. Notni, J. Šimeček, Prof. Dr. H.-J. Wester
Lehrstuhl für Pharmazeutische Radiochemie
Technische Universität München
Walther-Meissner-Strasse 3, 85748 Garching (Germany)
and
Klinik für Nuklearmedizin
Technische Universität München
Ismaninger Strasse 22, 81675 München (Germany)
E-mail: johannes.notni@tum.de

[b] J. Šimeček, Prof. Dr. P. Hermann
Department of Inorganic Chemistry, Faculty of Science
Charles University in Prague (Czech Republic)

[**] TRAP = *Tria*zacyclononane-*p*hosphinic acid.

Supporting information for this article is available on the WWW under http://dx.doi.org/10.1002/chem.201103503.

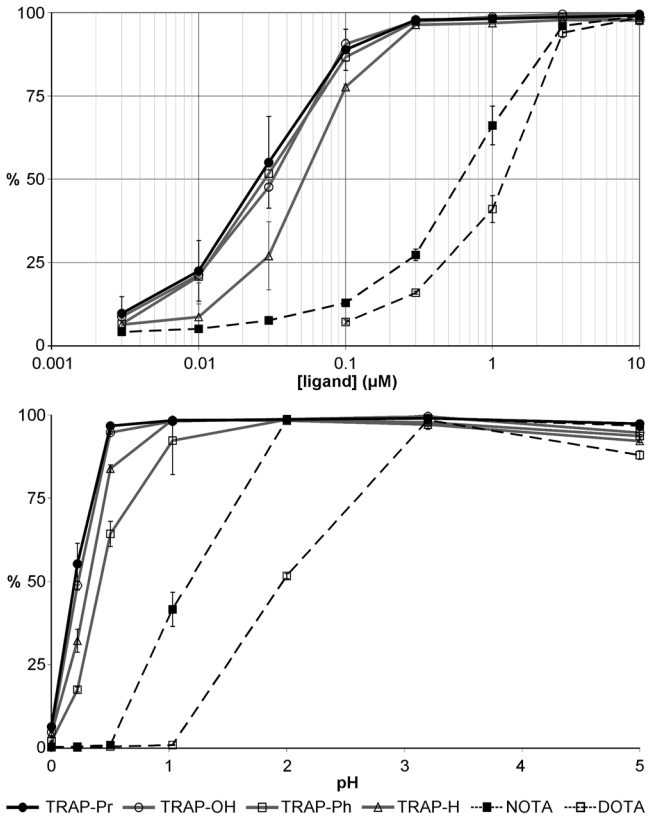

Figure 1. ^{68}Ga incorporation (%) by DOTA, NOTA, and TRAP ligands (20–30 MBq $\hat{=}$0.2–0.3 pmol of ^{68}Ga at 95 °C, 5 min) as functions of c_L (top, pH 3.3) and pH (bottom, c_L=10 μM $\hat{=}$ n_L=1 nmol).

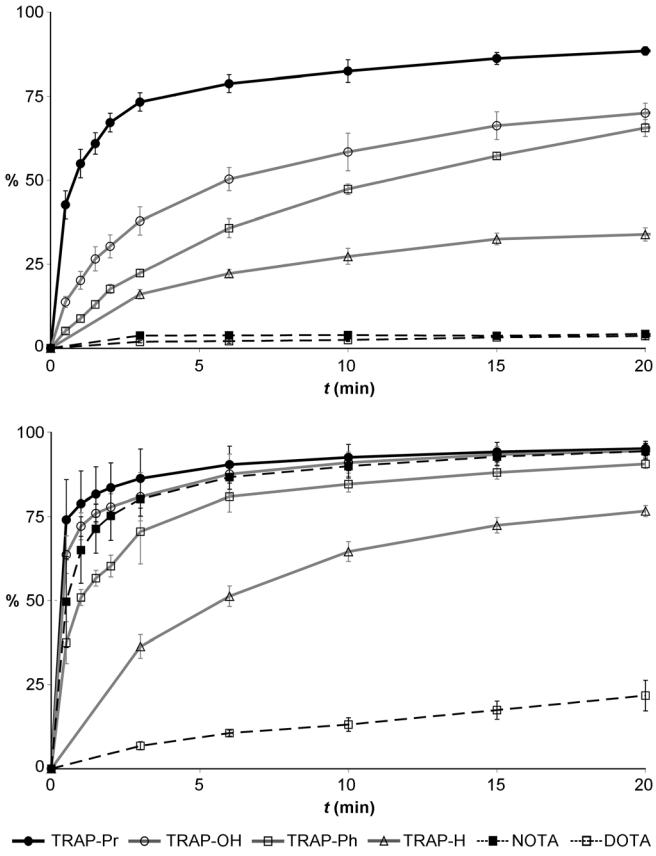

Figure 2. ^{68}Ga incorporation (%) by DOTA, NOTA, and TRAP ligands as functions of time (20–30 MBq $\hat{=}$0.2–0.3 pmol of ^{68}Ga at 25 °C, pH 3.3), top: c_L=3 μM $\hat{=}$ n_L=300 pmol, bottom: c_L=100 μM $\hat{=}$ n_L=10 nmol.

In addition to its remarkable labeling properties, TRAP-Pr is particularly suitable for innovative tracer design since it can be derivatized easily by amide formation without affecting the integrity of the complexation site.[5] Integrins, heterodimeric transmembrane adhesion receptors, are currently of particular interest for molecular imaging since they are involved in fundamental biological processes such as cell adhesion, migration, and proliferation. Cyclic pentapeptides of the cyclo(RGDfK) type possess a high integrin affinity and have been widely employed in clinical studies addressing $\alpha_v\beta_3$ integrin status in angiogenic, oncological, and cardiological evaluations.[6] Furthermore, multiple conjugates (multimers) of RGD peptides exhibited enhanced affinities due to the avidity effect, and thus appear better suited for in vivo imaging of integrin expression.[7]

TRAP(RGD)$_3$ (Scheme 2) combines multimericity with the exceptional $^{68}Ga^{3+}$ complexation performance of TRAP

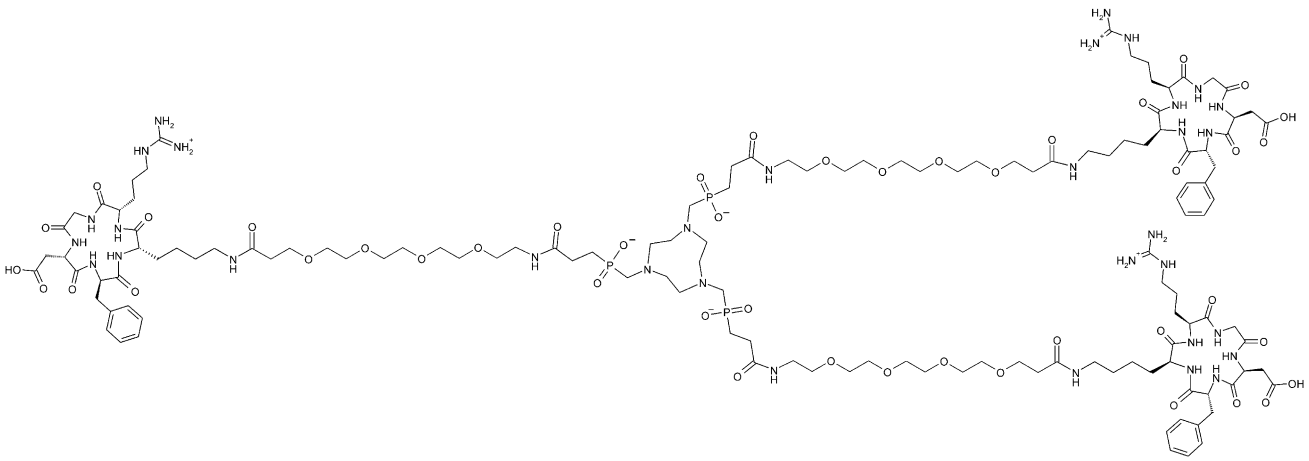

Scheme 2. TRAP(RGD)$_3$, a TRAP-based cyclo(RGDfK) trimer.

ligands. According to current GMP standards for clinical routine production, ^{68}Ga labeling of TRAP(RGD)$_3$ was done on a fully automated system (see the Supporting Information). Without the necessity of pre-purification or concentration of the generator eluate prior to labeling, ^{68}Ga-TRAP(RGD)$_3$ was produced in high yields and with extremely high specific activity (SA) exceeding 4 TBq μmol^{-1} (Table 2), thus enabling production of high specific activity

Table 2. Radiochemical yields for automated ^{68}Ga-TRAP-(RGD)$_3$ production and specific activities at injection time (i.e., decay corrected to 30 min after start of synthesis). Synthesis on GallElut$^+$ module using a SnO_2-based ^{68}Ge/^{68}Ga generator (iThembaLABS) eluted with 1.0 M HCl; eluate fraction of 1.25 mL (ca. 1 GBq ~10 pmol of ^{68}Ga) with 270 mg HEPES and 220 μL water, pH 2, reaction at 95–100 °C for 5 min (see the Supporting Information for details); radiochemical purity was always >99.0 % by radio-TLC and >99.8 % by radio-HPLC.

TRAP(RGD)$_3$ [nmol]	Radiochemical yield [%]	MBq	Specific activity GBq μmol^{-1}
1.00	95.2 ± 1.7	701 ± 12	701 ± 12
0.33	90.0 ± 2.7	663 ± 20	2009 ± 61
0.10	65.8 ± 5.6	485 ± 41	4848 ± 414

^{68}Ga tracers also using low ^{68}Ga activities for synthesis. As higher specific activity is tantamount to smaller absolute amounts of substance administered, TRAP radiopharmaceuticals are now coming much closer to the 'ideal tracer' concept: allowing the monitoring of biochemistry in vivo without disturbing the underlying biological processes and equilibria. Furthermore, the probability of undesired pharmacological effects occuring in human application is greatly reduced. Another advantage for modern preclinical small-animal imaging is the virtual elimination of disturbing saturation effects, which are frequently occuring and caused by too low specific activity,[8] such as competition of the unlabeled compound on receptors.

Comparison of ^{68}Ga-TRAP-(RGD)$_3$ with the clinically tested ^{18}F-Galacto-RGD[9] (monomer; structure given in the Supporting Information) in biodistribution studies using athymic nude mice bearing M21 ($\alpha_v\beta_3$-positive) and M21L (very low $\alpha_v\beta_3$-expressing) human melanoma xenografts on right and left shoulders and competition assays on M21 cells revealed a 7.3-fold higher $\alpha_v\beta_3$-integrin affinity and 3.9-fold higher tumor uptake of ^{68}Ga-TRAP(RGD)$_3$ (Table 3). PET imaging (Figure 3) shows a markedly increased uptake of the trimer in other organs such as thyroid or intestine; however, this uptake was proven to be highly specific, as virtually complete blocking was observed upon co-injection of 5 mg of unlabeled precursor per kg body weight.

Table 3. Octanol–water partition coefficients, IC_{50}, tumor uptake (% injected dose per g tumor), uptake ratios tumor/blood and tumor/muscle 90 min after injection of RGD radiotracers. IC_{50} values were determined by using non-active reference compounds (^{nat}Ga/^{19}F-labeled) in competition assays on M21 cells against ^{125}I-Echistatin.

Tracer	logP_{ow}	IC_{50} [nM]	ID/g [%] (M21)	M21/ blood	M21/ muscle
^{68}Ga-TRAP(RGD)$_3$	−3.9 ± 0.1	44[a]	5.33 ± 1.26	25.3 ± 7.2	6.7 ± 0.7
^{18}F-Galacto-RGD	−3.2[9b]	319	1.35 ± 0.53	6.1 ± 3.3	7.6 ± 1.7

[a] IC_{50} of the Ga-free compound is 43 nM.

After functionalization of TRAP-Pr with propargylamine, the synthetic performance of click chemistry (CuAAC) can be utilized for the bioconjugation to the TRAP ligand, which has been illustrated by the synthesis of an RGD-′click′-trimer (Scheme 3, see the Supporting Information for details). Further examples for the versatility of the TRAP ligand are a TRAP-biotin trimer to be used in avidin-biotin targeting systems and a TRAP(RGD)$_2$(rhodamine) heteromultimer, which emphasizes the facile accessibility of

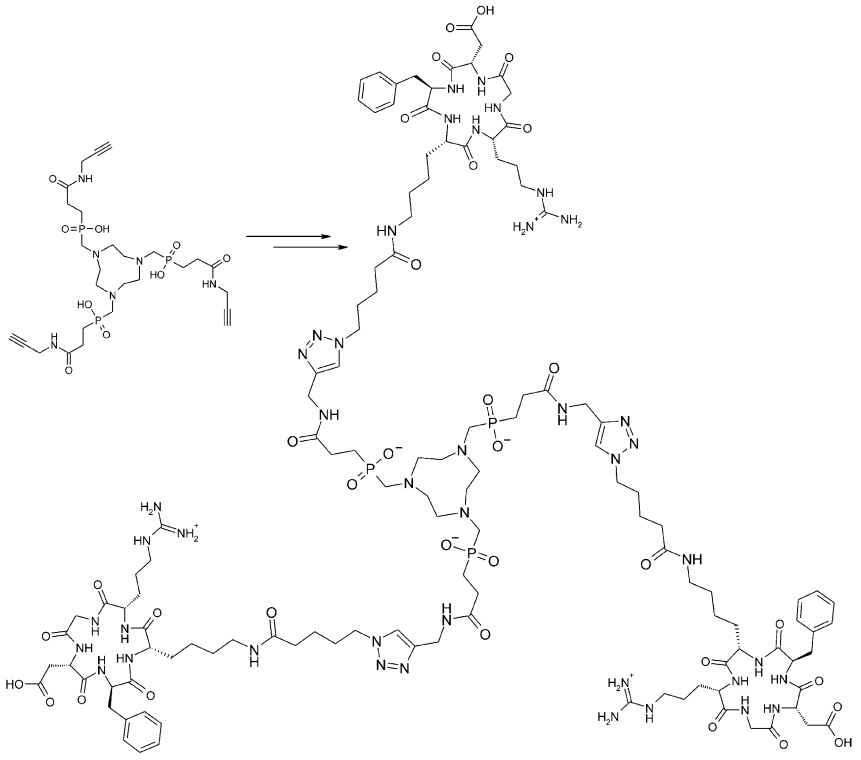

Scheme 3. Synthesis of a TRAP-based RGD trimer employing Cu^{II}-catalyzed alkyne–azide cycloaddition (CuAAC).

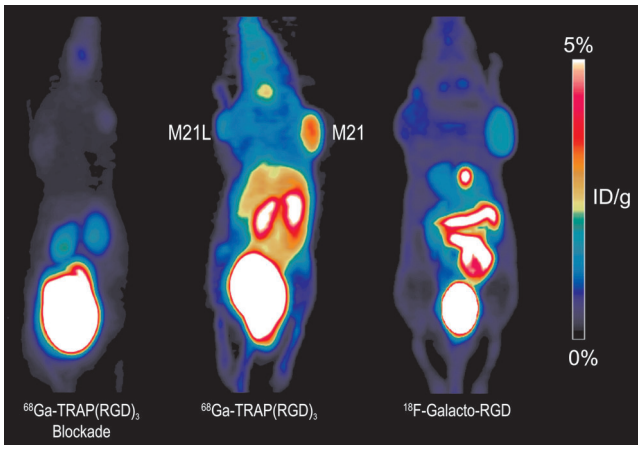

Figure 3. microPET scans (MIP, 75 min p. i.) of nude mouse bearing tumor xenografts on both shoulders (left: M21L, right: M21).

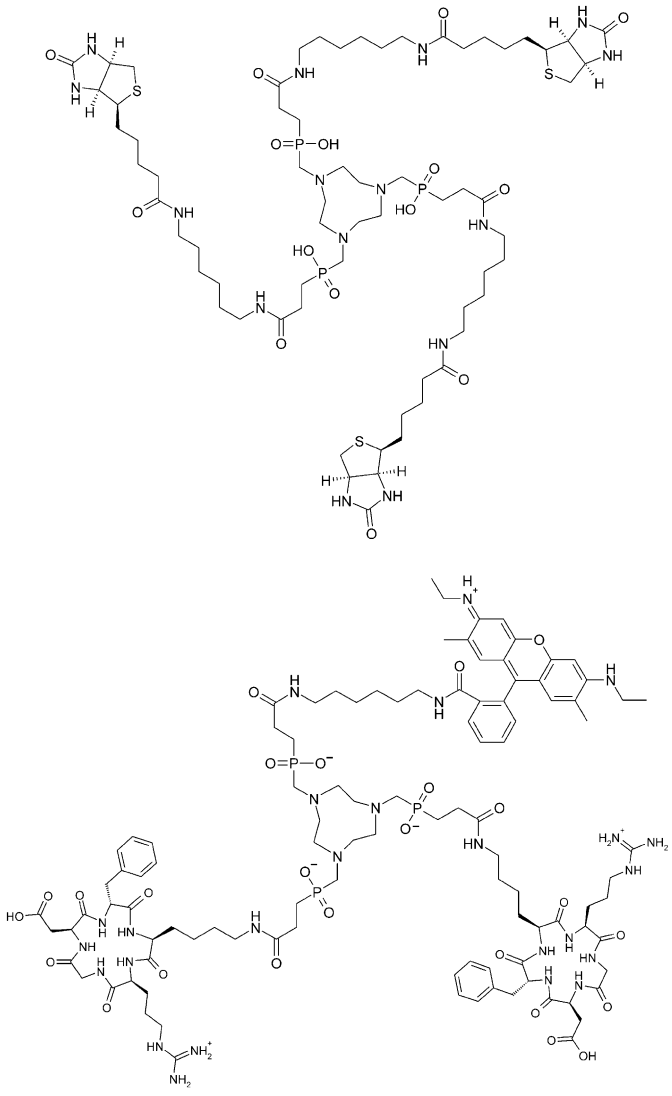

Scheme 4. TRAP(biotin)$_3$ trimer (top) and TRAP(RGD)$_2$(rhodamine-6G), aRGD dimer with additional rhodamine 6G fluorophor (bottom).

TRAP-based tracers for the increasingly important field of multimodal imaging (Scheme 4). These conjugates incorporated ^{68}Ga with similar efficiency as TRAP(RGD)$_3$.

We conclude that TRAP ligands are exceptionally well suited for the development of ^{68}Ga tracers for in vivo molecular imaging with PET, as they allow highly efficient $^{68}Ga^{3+}$ complexation in a wide pH range (0.5–5) and at 10–30-fold lower concentrations than NOTA and DOTA, the currently most frequently used ^{68}Ga chelator systems. For the example of the TRAP-based cyclo(RGDfK) trimer ^{68}Ga-TRAP-(RGD)$_3$ it was shown that multimeric TRAP tracers are easily accessible and can be ^{68}Ga-labeled in full automation, thereby reaching hitherto unparalleled specific activities of several TBq μmol^{-1} without separation from excess precursor. Utility of the resulting radiotracer was proven in a preclinical imaging study. Further examples demonstrated the versatility of the TRAP system in tailoring molecular imaging agents and multimodal probes, all of which is justifying high expectations for future applications of TRAP.

Acknowledgements

Financial support by GACR (No. 203/09/1056), MSMT CR (No. MSM0021620857), GAUK (No. 19310), EU COST Actions D38 and PhoSciNet, and by the German Research Foundation (DFG SFB 824/Z1) is gratefully acknowledged. We thank K. Pohle for determining the integrin affinities, and Dr. J. Plutnar and O. Zemek, Prague, for acquisition of the NMR spectra.

Keywords: gallium-68 · macrocyclic ligands · molecular imaging · positron emission tomography · radiopharmaceuticals

[1] a) W. A. P. Breeman, E. de Blois, H. S. Chan, M. Konijnenberg, D. J. Kwekkeboom, E. P. Krenning, *Semin. Nucl. Med.* **2011**, *41*, 314–321; b) H. Stetter, W. Frank, *Angew. Chem.* **1976**, *88*, 760; *Angew. Chem. Int. Ed. Engl.* **1976**, *15*, 686.

[2] a) K. Wieghardt, U. Bossek, P. Chaudhuri, W. Herrmann, B. C. Menke, J. Weiss, *Inorg. Chem.* **1982**, *21*, 4308–4314; b) K.-P. Eisenwiener, M. I. M. Prata, I. Buschmann, H.-W. Zhang, A. C. Santos, S. Wenger, J. C. Reubi, H. R. Mäcke, *Bioconjugate Chem.* **2002**, *13*, 530–541; c) I. Velikyan, H. Maecke, B. Langstrom, *Bioconjugate Chem.* **2008**, *19*, 569–573; d) A. S. Craig, D. Parker, H. Adams, N. A. Bailey, *J. Chem. Soc. Chem. Commun.* **1989**, 1793; e) C. J. Broan, J. P. L. Cox, A. S. Craig, R. Kataky, D. Parker, A. Harrison, A. M. Randall, G. Ferguson, *J. Chem. Soc. Perkin Trans. 2* **1991**, 87–99; f) T. J. Norman, F. C. Smith, D. Parker, A. Harrison, L. Royle, C. A. Walker, *Supramol. Chem.* **1995**, *4*, 305–308; g) A. Harrison, C. A. Walker, K. A. Pereira, D. Parker, L. Royle, R. C. Matthews, A. S. Craig, *Nucl. Med. Commun.* **1992**, *13*, 667–672; h) S. K. Rhind (Celltech Ltd.), WO 89/01475; i) D. Parker, N. R. A. Beeley, T. A. Millican (Celltech Ltd.), WO/1990/009379; j) D. Parker, M. A. W. Eaton (Celltech Ltd.), WO/1991/000285; k) D. Parker, N. R. A. Beeley, T. A. Millican (Celltech Ltd.), WO/1991/016078.

[3] a) K. Bazakas, I. Lukeš, *J. Chem. Soc. Dalton Trans.* **1995**, 1133–1137; b) E. Cole, D. Parker, G. Ferguson, J. F. Gallagher, B. Kaitner, *J. Chem. Soc. Chem. Commun.* **1991**, 1473–1475; c) C. J. Broan, E. Cole, K. J. Jankowski, D. Parker, K. Pulukkody, B. A. Boyce, N. R. A. Beeley, K. Millar, A. T. Millican, *Synthesis* **1992**, 63–68; d) C. J. Broan, K. J. Jankowski, R. Kataky, D. Parker, *J. Chem. Soc. Chem.*

Commun. **1990**, 1738–1739; e) E. Cole, R. C. B. Copley, J. A. K. Howard, D. Parker, G. Ferguson, J. F. Gallagher, B. Kaitner A. Harrison, L. Royle, *J. Chem. Soc. Dalton Trans.* **1994**, 1619–1625; f) M. I. M. Prata, A. C. Santos, C. F. G. C. Geraldes, J. J. P. de Lima, *Nucl. Med. Biol.* **1999**, *26*, 707–710.

[4] J. Šimeček, M. Schulz, J. Notni, J. Plutnar, V. Kubíček, J. Havlíčková, P. Hermann, *Inorg. Chem.* **2011**, DOI: 10.1021/ic202103v.

[5] J. Notni, P. Hermann, J. Havlíčková, J. Kotek, V. Kubíček, J. Plutnar, N. Loktionova, P. J. Riss, F. Rösch, I. Lukeš, *Chem. Eur. J.* **2010**, *16*, 7174–7185.

[6] a) E. Lohof, E. Planker, C. Mang, F. Burkhart, M. A. Dechantsreiter, R. Haubner, H. J. Wester, M. Schwaiger, G. Hölzemann, S. L. Goodman, H. Kessler, *Angew. Chem.* **2000**, *112*, 2868–2871; *Angew. Chem. Int. Ed.* **2000**, *39*, 2761–2764; b) M. Schottelius, B. Laufer, H. Kessler, H. J. Wester, *Acc. Chem. Res.* **2009**, *42*, 969–980.

[7] a) H. J. Wester, H. Kessler, *J. Nucl. Med.* **2005**, *46*, 1940–1945; b) T. Poethko, M. Schottelius, G. Thumshirn, M. Herz, R. Haubner, G. Henriksen, H. Kessler, M. Schwaiger, H. J. Wester, *Radiochim. Acta* **2004**, *92*, 317–328; c) G. Thumshirn, U. Hersel, S. L. Goodman, H. Kessler, *Chem. Eur. J.* **2003**, *9*, 2717–2725; d) C. Wängler, S. Maschauer, O. Prante, M. Schäfer, R. Schirrmacher, P. Bartenstein, M. Eisenhut, B. Wängler, *ChemBioChem* **2010**, *11*, 1–15.

[8] S. Froidevaux, M. Calame-Christe, J. Schuhmacher, H. Tanner, R. Saffrich, M. Henze, A. N. Eberle, *J. Nucl. Med.* **2004**, *45*, 116–123.

[9] a) R. Haubner, H. J. Wester, W. A. Weber, C. Mang, S. I. Ziegler, S. L. Goodman, R. Senekowitsch-Schmidtke, H. Kessler, M. Schwaiger, *Cancer Res.* **2001**, *61*, 1781–1785; b) R. Haubner, B. Kuhnast, C. Mang, W. A. Weber, H. Kessler, H. J. Wester, M. Schwaiger, *Bioconjugate Chem.* **2004**, *15*, 61–69; c) R. Haubner, W. A. Weber, A. J. Beer, E. Vabuliene, D. Reim, M. Sarbia, K. F. Becker, M. Goebel, R. Hein, H. J. Wester, H. Kessler, M. Schwaiger, *PLoS Med.* **2005**, *2*, e70.

Received: November 7, 2011
Published online: December 6, 2011

APPENDIX 3

DOI: 10.1002/cmdc.201200261

A Monoreactive Bifunctional Triazacyclononane Phosphinate Chelator with High Selectivity for Gallium-68

Jakub Šimeček,[a, b] Ondřej Zemek,[b] Petr Hermann,[b] Hans-Jürgen Wester,[a] and Johannes Notni*[a]

In recent years, the significance of the radioisotope ^{68}Ga ($t_{1/2}$ = 68 min; $E_{\beta^+,max}$ = 1.89 MeV) for positron emission tomography (PET) has been widely recognized,[1] particularly in light of the success of ^{68}Ga-labeled somatostatin analogues, such as ^{68}Ga-DOTATOC, in neuroendocrine tumor imaging.[2] The main advantages of ^{68}Ga are easy handling, quick and uncomplicated labeling procedures, and cyclotron-independent on-site production in radioisotope generators. In such devices, ^{68}Ga is constantly generated by the decay of ^{68}Ge ($t_{1/2}$ = 270.8 days, EC), similar to ^{99m}Tc production in ^{99}Mo/^{99m}Tc generators. This facilitates the implementation of global coverage of PET, an imaging modality which, in view of its high sensitivity and spatial resolution relative to scintigraphy, is considered an extremely valuable tool in functional molecular imaging and personalized healthcare.

Targeted ^{68}Ga radiopharmaceuticals, e.g., for peptide receptor imaging, are usually bioconjugates that consist of one or more bioactive vectors and a chelating unit for $^{68}Ga^{3+}$ binding. As the inherent complexation properties of the chelator readily determine the labeling efficiency and thus the specific activity of the tracers, chelator optimization is a pivotal issue in tracer improvement.[3]

About two decades ago, 1,4,7-triazacyclononanes with phosphinic acid side chains were found to be good chelators for various metal ions, including Ga^{3+}.[4] More recently, our research groups reported a novel bifunctional triazacyclononane triphosphinic acid chelator (TRAP), which complexes $^{68}Ga^{3+}$ much more efficiently than the established bifunctional chelator NODAGA and also constitutes an ideal framework for the preparation of trimeric bioconjugates.[5–8] Pursuing this approach, we devised the related structure NOPO (see Scheme 1), which possesses only one site for bioconjugation. It is therefore ideally suited for synthetic tasks in which strictly monoconjugation is desired, such as for conjugates of somatostatin receptor agonists which internalize into cells after binding. NOPO therefore perfectly complements the portfolio of TRAP-like chelators in terms of synthetic strategy.

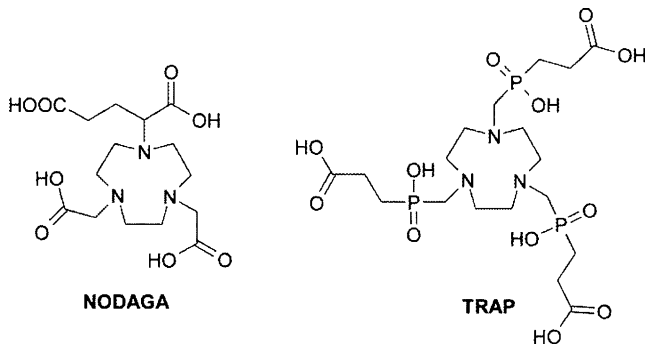

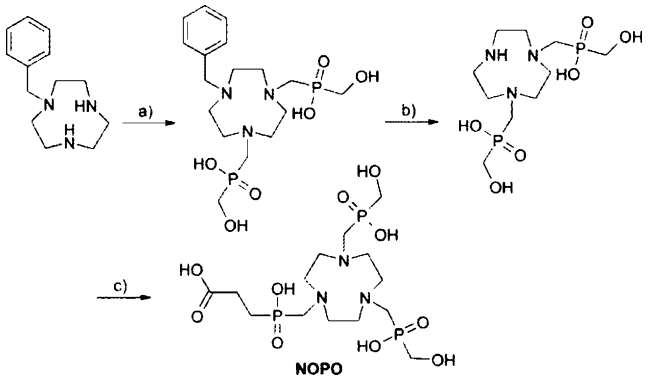

Scheme 1. Synthesis of the NOPO chelator. *Reagents and conditions:* a) H_3PO_2, H_2C=O, 6 M HCl, RT, 24 h; b) Pd/C in H_2O, H_2, RT, 12 h; c) (2-carboxyethyl)phosphinic acid, H_2C=O, 6 M HCl, 70 °C, 24 h. Overall yield: 18–30%.

NOPO was synthesized by a multistep Moedritzer–Irani reaction,[9] as shown in Scheme 1 (see the Supporting Information for details). As expected, owing to the lower basicity of phosphinate-containing ligands relative to those featuring carboxylates, the stability constant of the $[Ga(NOPO)]^-$ complex ($\log K$ = 25.01, determined by potentiometry) is lower than that of [Ga(NOTA)] ($\log K$ = 29.60),[7] but similar to that of $[Ga(TRAP)]^{3-}$ ($\log K$ = 26.24).[6] Nevertheless, the $[Ga(NOPO)]^-$ complex was found to possess pronounced kinetic inertness against acid-promoted decomplexation. No disintegration of the complex was observed in 6 M $HClO_4$ over a period of three months at room temperature.

For proof-of-concept studies, two well-investigated peptidic receptor ligands, cyclo(RGDfK) ("RGDfK", targeting of $\alpha_v\beta_3$ integrins)[10] and Nal-octreotide ("NOC", targeting of somatostatin receptor subtypes 2 and 5),[11] were conjugated to the carboxylic acid moiety of NOPO by amide formation (see also Supporting Information). Because chelator conjugates of these targeting groups are very well investigated, their choice allows comparison with a sound basis of prior data. Conjugation of NOPO is particularly convenient, as no protection of the phosphinate moieties is required during the reaction.

[a] J. Šimeček, Prof. Dr. H.-J. Wester, Dr. J. Notni
Pharmazeutische Radiochemie, Technische Universität München
Walther-Meißner-Str. 3, 85748 Garching (Germany)
E-mail: johannes.notni@tum.de
Homepage: http://www.prc.ch.tum.de

[b] J. Šimeček, O. Zemek, Prof. Dr. P. Hermann
Department of Inorganic Chemistry
Faculty of Science, Charles University in Prague
Hlavova 2030, 12840 Prague 2 (Czech Republic)

Supporting information for this article is available on the WWW under http://dx.doi.org/10.1002/cmdc.201200261.

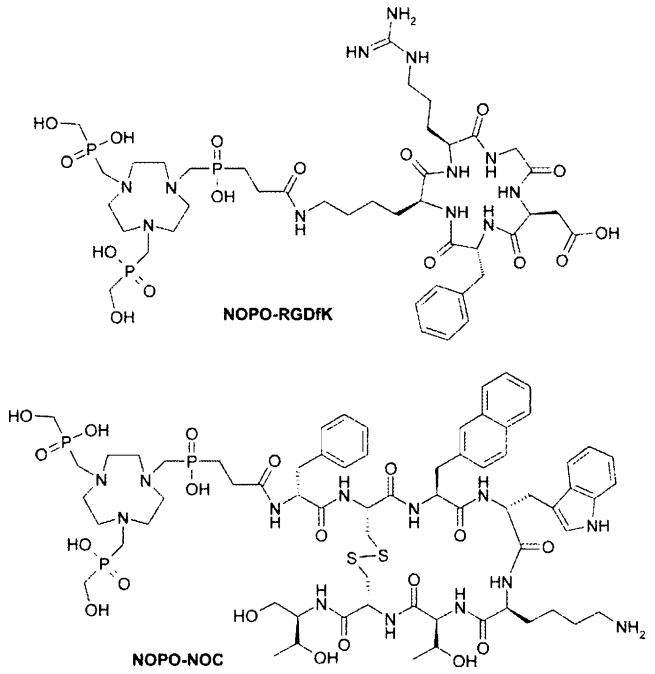

In line with previous studies that outlined the superior ^{68}Ga labeling efficiency of 1,4,7-triazacyclononane phosphinate ligands relative to their carboxylate analogues,[5,6] NOPO was shown to incorporate ^{68}Ga at very low ligand concentrations, which is typical for TRAP-type chelators. Moreover, bioconjugation does not significantly change ^{68}Ga labeling performance; Figure 1 shows that the radioactivity incorporation into NOPO and NOPO–RGDfK is essentially identical within the margins of error. For both compounds, near-quantitative (>95%) labeling can be achieved at chelator concentrations as low as 0.1 μM. ^{68}Ga-NOPO–RGDfK showed no loss of activity, neither over a period of 3 h in PBS or 0.25 M EDTA at 37 °C, nor in vivo.

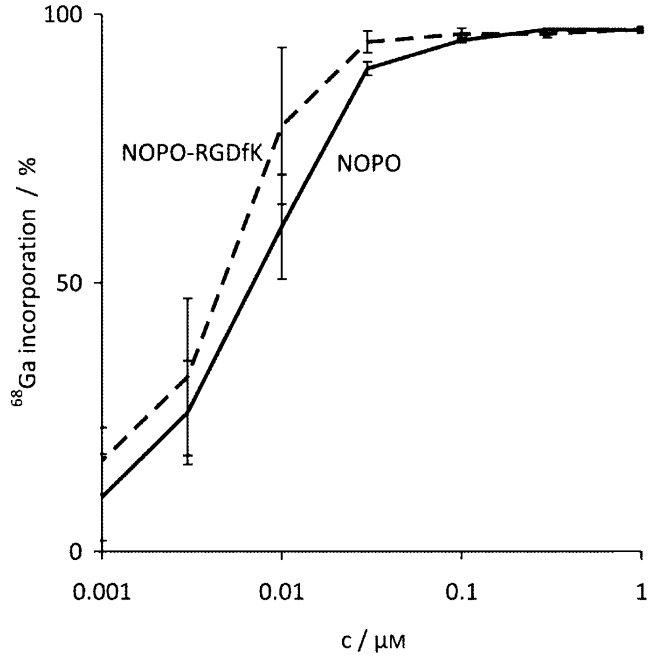

Figure 1. Radioactivity incorporation (%) by NOPO and NOPO–RGDfK as functions of precursor concentration (T = 95 °C, t = 5 min, pH 2.8).

Due to competition with $^{68}Ga^{3+}$ for the chelator, contamination of ^{68}Ge/^{68}Ga generator eluates with various metal ions originating from the column matrix or the eluents was recognized earlier as being responsible for considerably decreased radiochemical yields during ^{68}Ga labeling. In view of the very similar coordination behavior of Ga^{3+} and Fe^{3+}, the latter ion is considered particularly problematic. Moreover, the presence of Zn^{2+} in the eluate cannot be circumvented, as ^{68}Zn is constantly formed as a stable daughter of ^{68}Ga. To avoid potential problems caused by these metal ion contaminants during subsequent complexation, various strategies for eluate purification, i.e., removal of non-Ga^{3+} cations, have been developed.[12–14] However, Figure 2 shows a pronounced selectivity

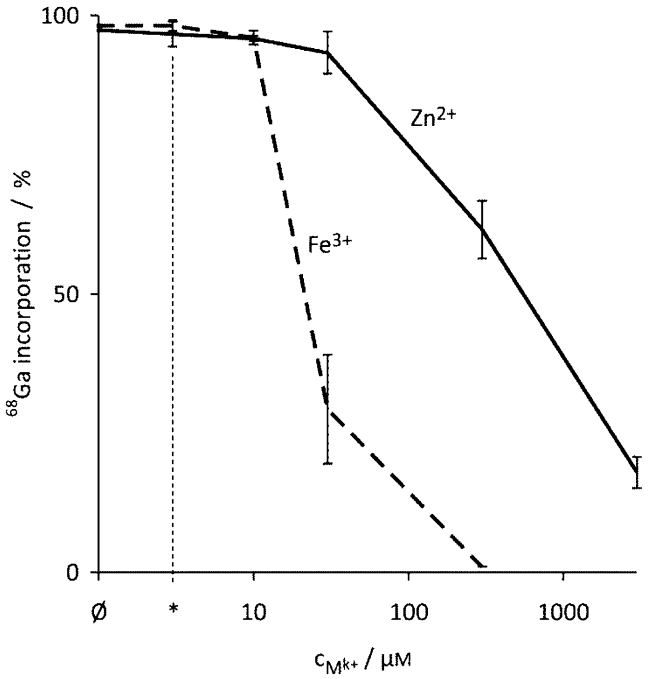

Figure 2. Radioactivity incorporation (%) by NOPO as a function of concentration of added metal ions (c_{NOPO} = 3 μM, T = 95 °C, t = 5 min, pH 3.3); Ø: none added; *: [NOPO]/[M^{k+}] = 1 (3 μM).

of NOPO for Ga^{3+}. Almost quantitative ^{68}Ga binding is observed even in the presence of 30 μM Zn^{2+} or 10 μM Fe^{3+} (i.e., 10 and 3.3 equiv of NOPO, respectively), which exceeds by far the single-digit ppm concentration range in which these ions are maximally present in generator eluates.[15–17] For NOPO, the usual contents of Fe^{3+} and particularly Zn^{2+} in eluates can therefore be considered irrelevant, rendering the removal of these ions unnecessary.

GMP-compliant production of radiopharmaceutical formulations of ^{68}Ga-NOPO–peptides was performed in a fully automated process as described before.[5,18] Exceptionally high specific activities can be achieved reproducibly; for example, labeling reactions with 100 pmol NOPO–RGDfK and 970±60 MBq ^{68}Ga (≈10 pmol) yielded formulations of ^{68}Ga-NOPO–RGDfK

with radiochemical yields of 77.2 ± 2.1 % (decay-corrected), while specific activities (calculated for $t = 30$ min after the start of synthesis)[19] reached 5600 ± 500 GBq μmol^{-1}. For a typical dose used in small-animal imaging, such as 15 MBq, this results in a total injected amount of both labeled and unlabeled NOPO–RGDfK of ~2.7 pmol or 3.1 ng, which is impressively low. Accordingly, a hypothetical patient dose of 185 MBq (5 mCi) would contain only ~33 pmol or 38 ng of RGDfK conjugates. ^{68}Ga-NOPO–peptides can therefore be considered ideal radiotracers and even meet concentration requirements far below the microdosing approach. Due to their extremely high specific activity without the need for a purification step, NOPO–peptide conjugates allow convenient adjustment to an ideal specific activity by the addition of cold reference and thus are very useful for studies of the influence of the specific activity of ^{68}Ga-labeled peptides on specific tracer uptake in vivo.

The suitability of ^{68}Ga-NOPO–peptides for molecular imaging was proven in preliminary PET studies. ^{68}Ga-NOPO–RGDfK was used for mapping of $\alpha_v\beta_3$ integrin expression in a nude mouse bearing human melanoma xenografts M21 (high $\alpha_v\beta_3$ expression) and M21L (low $\alpha_v\beta_3$ expression) on the right and left shoulders, respectively. Figure 3 (left) shows that M21 is clearly delineated in the PET image. In accordance with previous studies, we also observed considerable uptake in the abdominal region.[5,18,20] However, all of this uptake was shown to be integrin-specific, as nearly complete blocking was achieved by co-injection of excess NOPO–RGDfK (5 mg kg^{-1}; see Supporting Information figure S5). PET imaging of an AR42J-xenografted mouse using ^{68}Ga-NOPO–NOC (Figure 3, right) shows low background and high tracer uptake in the tumor, while only insignificant amounts of activity remain in the kidneys. Again, specificity of binding was proven by complete extinction of tumor uptake by administration of a blocking dose of 5 mg kg^{-1} NOPO–NOC (see Supporting Information figure S6).

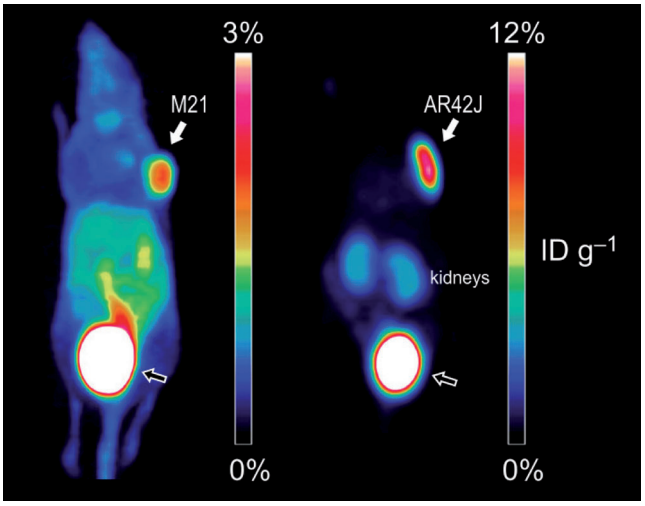

Figure 3. PET images (MIP, 75 min p.i.) of nude mouse tumor xenografts. Left: ^{68}Ga-NOPO–RGDfK (M21 human melanoma); right: ^{68}Ga-NOPO–NOC (AR42J rat pancreas carcinoma). Accumulation of activity is observed in the urinary bladder (indicated by outline arrows) due to renal excretion.

We conclude that our novel chelator NOPO is highly appropriate for the preparation of ^{68}Ga PET radiopharmaceuticals. Its radiochemical properties, namely excellent efficiency and selectivity in $^{68}Ga^{3+}$ complexation, are of outstanding value for clinical daily practice. In addition, due to the eradication of undesired pharmacological or saturation effects, the high specific activity achievable for NOPO peptides is of high importance for preclinical studies in rodents. In view of the convincing results of the proof-of-concept PET study, we assume that NOPO has a bright future in the design of next-generation monomeric ^{68}Ga PET tracers.

Acknowledgements

Financial support by the Grant Agency of Charles University (Grant No. 19310), the Ministry of Education of the Czech Republic (Grant No. MSM0021620857), the Deutsche Forschungsgemeinschaft (SFB 824, Project Z1), and EU COST Actions CM0802 and TD1004, is gratefully acknowledged. The Authors thank Jana Havlíčková and Jan Plutnar (Charles University) for potentiometry measurements and recording of NMR spectra, respectively.

Keywords: bioconjugates · gallium-68 · macrocyclic ligands · phosphinic acid · positron emission tomography

[1] a) C. Decristoforo, R. D. Pickett, A. Verbruggen, *Eur. J. Nucl. Med. Mol. Imaging* **2012**, *39*, S31 – S40; b) I. Velikyan, *Med. Chem.* **2011**, *7*, 338 – 372.
[2] a) W. A. P. Breeman, E. de Blois, H. S. Chan, M. Konijnenberg, D. J. Kwekkeboom, E. P. Krenning, *Semin. Nucl. Med.* **2011**, *41*, 314 – 321; b) M. Fani, J. P. André, H. R. Mäcke, *Contrast Media Mol. Imaging* **2008**, *3*, 67 – 77.
[3] J. Notni, *Nachr. Chem.* **2012**, *6*, 645 – 649.
[4] a) K. Bazakas, I. Lukeš, *J. Chem. Soc. Dalton Trans.* **1995**, 1133 – 1137; b) E. Cole, D. Parker, G. Ferguson, J. F. Gallagher, B. Kaitner, *J. Chem. Soc. Chem. Commun.* **1991**, 1473 – 1475; c) C. J. Broan, E. Cole, K. J. Jankowski, D. Parker, K. Pulukkody, B. A. Boyce, N. R. A. Beeley, K. Millar, A. T. Millican, *Synthesis* **1992**, 63 – 68; d) C. J. Broan, K. J. Jankowski, R. Kataky, D. Parker, *J. Chem. Soc. Chem. Commun.* **1990**, 1738 – 1739; e) E. Cole, R. C. B. Copley, J. A. K. Howard, D. Parker, G. Ferguson, J. F. Gallagher, B. Kaitner, A. Harrison, L. Royle, *J. Chem. Soc. Dalton Trans.* **1994**, 1619 – 1625; f) M. I. M. Prata, A. C. Santos, C. F. G. C. Geraldes, J. J. P. de Lima, *Nucl. Med. Biol.* **1999**, *26*, 707 – 710.
[5] J. Notni, J. Šimeček, P. Hermann, H. J. Wester, *Chem. Eur. J.* **2011**, *17*, 14718 – 14722.
[6] J. Notni, P. Hermann, J. Havlíčková, J. Kotek, V. Kubíček, J. Plutnar, N. Loktionova, P. J. Riss, F. Rösch, I. Lukeš, *Chem. Eur. J.* **2010**, *16*, 7174 – 7185.
[7] J. Šimeček, M. Schulz, J. Notni, J. Plutnar, V. Kubíček, J. Havlíčková, P. Hermann, *Inorg. Chem.* **2012**, *51*, 577 – 590.
[8] J. Notni, J. Plutnar, H. J. Wester, *EJNMMI Res.* **2012**, *2*, 13.
[9] K. Moedritzer, R. R. Irani, *J. Org. Chem.* **1966**, *31*, 1603 – 1607.
[10] M. Schottelius, B. Laufer, H. Kessler, H. J. Wester, *Acc. Chem. Res.* **2009**, *42*, 969 – 980.
[11] D. Wild, J. S. Schmitt, M. Ginj, H. R. Mäcke, B. F. Bernard, E. Krenning, M. de Jong, S. Wenger, J. C. Reubi, *Eur. J. Nucl. Med. Mol. Imaging* **2003**, *30*, 1338 – 1347.
[12] K. P. Zhernosekov, D. V. Filosofov, R. P. Baum, P. Aschoff, H. J. Adrian, H. Bihl, A. A. Razbash, M. Jahn, M. Jennewein, F. Rösch, *J. Nucl. Med.* **2007**, *48*, 1741 – 1748.

[13] G. J. Meyer, H. R. Mäcke, J. Schuhmacher, W. H. Knapp, M. Hofmann, *Eur. J. Nucl. Med. Mol. Imaging* **2004**, *31*, 1097 – 1104.
[14] N. S. Loktionova, A. N. Belozub, D. V. Filosofov, K. P. Zhernosekov, T. Wagner, A. Türler, F. Rösch, *Appl. Radiat. Isot.* **2011**, *69*, 942 – 946.
[15] E. de Blois, H. S. Chan, C. Naidoo, D. Prince, E. P. Krenning, W. A. P. Breeman, *Appl. Radiat. Isot.* **2011**, *69*, 308 – 315.
[16] W. A. P. Breeman, M. de Jong, E. de Blois, B. F. Bernard, M. Konjinenberg, E. P. Krenning, *Eur. J. Nucl. Med. Mol. Imaging* **2005**, *32*, 478 – 485.
[17] D. D. Rossouw, W. A. P. Breeman, *Appl. Radiat. Isot.* **2012**, *70*, 171 – 175.
[18] K. Pohle, J. Notni, J. Bussemer, H. Kessler, M. Schwaiger, A. J. Beer, *Nucl. Med. Biol.* **2012**, DOI: 10.1016/j.nucmedbio.2012.02.006.
[19] Specific activities were calculated from molar amounts of precursor and product activity, as described previously.[5,18] As our ^{68}Ga tracer production logistics commonly allow tracer administration 30 min after the start of synthesis, specific activities are given for that time point to provide realistic data.
[20] R. A. Dumont, F. Deininger, R. Haubner, H. R. Maecke, W. A. Weber, M. Fani, *J. Nucl. Med.* **2011**, *52*, 1276 – 1284.

Received: May 21, 2012
Published online on June 12, 2012

CHEMMEDCHEM
Chemistry & Drug Discovery

Supporting Information

A Monoreactive Bifunctional Triazacyclononane Phosphinate Chelator with High Selectivity for Gallium-68

Jakub Šimeček,[a, b] Ondřej Zemek,[b] Petr Hermann,[b] Hans-Jürgen Wester,[a] and Johannes Notni*[a]

cmdc_201200261_sm_miscellaneous_information.pdf

Table of Contents

1. Materials & Methods

Instrumentation: NMR spectra were recorded using Varian Unity Inova (400 MHz), VNMRS (300 MHz) or Bruker Avance-III (600 MHz) NMR systems. ^{1}H and ^{13}C NMR shifts are referenced to *tert*-butanol signal (internal standard; 1.25 and 30.29 ppm, respectively), ^{31}P NMR shifts are referenced relative to 85 % aq. H_3PO_4 solution as external standard (0.0 ppm) and ^{71}Ga NMR shifts are referenced to 0.2 M aq. $[Ga(OH)_4]^-$ (222 ppm) or $[Ga(H_2O)_6]^{3+}$ (0 ppm) solutions as external standards. ESI-MS spectra in positive and/or negative modes were measured on Bruker Esquire 3000 or Varian Ion-trap 500 spectrometers. Ultrafiltration was performed using an Amicon (Millipore) apparatus (50 mL stirred cell model 8050, CDS10 selector valve and RC800 mini-reservoir), in combination with cellulose acetate membranes (Ultracel, filter code YC05, cut-off 500 Da). Elemental analysis was performed using a Perkin Elmer CHN/S Elemental analyser 2400 II. The thermodynamic stability constant of the $[Ga(NOPO)]^-$ complex was determined by potentiometry as described before.[1]

Starting materials: The solvents and reagents used for syntheses were commercially available. 1-Benzyl-1,4,7-triazacyclononane was purchased from Chematech (Dijon, France). (2-carboxy-ethyl)phosphinic acid was prepared as described before.[2] Peptides were synthesized according to standard Fmoc protocol on solid phase support.

HPLC, TLC: Bioconjugates were purified using preparative HPLC, consisting of a Sykam system with two separate solvent pumps, on a YMC C18ec column (250 × 30 mm, 5 µm particle size) and UV detection (220 nm and 254 nm), flow rate 20 mL/min. Analytical HPLC was performed using a Sykam HPLC system with low-pressure gradient mixer, equipped with a Nucleosil C18-RP column (100 × 4.6 mm, 5 µm particle size) and UV detection (220 nm), flow rate 1 mL/min. Radio-HPLC was performed on a Sykam system using a Chromolith column (Merck, 100 × 4.6 mm) with radioactivity and UV detection (220 nm), flow rate 2 mL/min, eluents were water and acetonitrile, both containing 0.1 % TFA (isocratic elution with 3 % MeCN for 2 min followed by a gradient to 60 % MeCN in 6 min and isocratic elution with 95 % MeCN for 3 min). Radio-TLC was done on silica gel 60 with 0.1 M aqueous sodium citrate as mobile phase (TLC1) and on Varian silica impregnated chromatography paper with a 1:1 (v/v) mixture of 1 M aqueous NH_4OAc and MeOH as mobile phase (TLC2).

2. Synthesis of NOPO and its gallium(III) complex

1,4,7-triazacyclononane-1,4-bis[methylene(hydroxymethyl)phosphinic acid]-7-[methylene(2-carboxyethyl)phosphinic acid] (NOPO): 1-benzyl-1,4,7-triazacyclononane (1.28 g, 5.88 mmol) and paraformaldehyde (0.44 g, 14.7 mmol) were suspended in 50 % aq. H_3PO_2 (6.60 mL, 60.3 mmol) and water (5 mL). Reaction mixture was stirred for 12 h at ambient temperature and then purified on cationic exchanger (Dowex 50 in H^+ cycle). The column was washed with water and the triazacyclononane-containing compounds were eluted with a 1:1 (v/v) mixture of 6 M aq. HCl and EtOH. The eluate was evaporated and crude product was dissolved in 6 M aq. HCl (20 mL), paraformaldehyde (0.73 g, 24.3 mmol) was added and solution was refluxed for 5 h. Then the solvent was evaporated and the residue was purified on silicagel with a 3:1:2 mixture (by volumes) of MeCN, MeOH, and NH_4OH as mobile phase. Fractions containing pure product (as monitored by ^{31}P NMR spectroscopy) were collected and the eluent evaporated in vacuo to give 1.20 g of a dark-yellow solid. This was dissolved in water (5 mL), 10 % Pd/C (0.10 g) was added and the mixture was stirred under H_2 atmosphere at ambient temperature for 12 h. ^{31}P NMR reaction monitoring showed that after this time, deprotection was quantitative. The catalyst was filtered off with a fine glass frit, and the solvent evaporated in vacuo, resulting in 0.90 g of crude intermediate. This was dissolved in 6 M aq. HCl, 2-(carboxyethyl)phosphinic acid (0.53 g, 3.80 mmol) was added, and the mixture heated to 75 °C. Paraformadehyde (0.35 g, 11.7 mmol) was added in small portions during 24 h. Then, the solvent was removed in vacuo, the residue repeatedly co-evaporated with water in order to remove HCl, and loaded on cation exchange resin (Dowex 50 in H^+ cycle). The resin was eluted with water and the fractions containing the product were identified by ^{31}P NMR. These were collected, the eluent removed in vacuo, the residue dissolved again in water and lyophilized, yielding 0.53 g (18 %) of a microcrystalline, pale yellow solid (NOPO·0.6 H_2O).

^1H NMR (600 MHz, D_2O), δ/ppm: 3.58 (s, ring C$\underline{H}_2$, 4H), 3.61 (s, ring C$\underline{H}_2$, 2H), 3.495 (d, $^2J_{PH}$ = 6.4 Hz, N–C$\underline{H}_2$–P, 2H), 3.83 (d, $^2J_{PH}$ = 5.8 Hz, P–C$\underline{H}_2$–OH, 4H), 3.50 (d, $^2J_{PH}$ = 5.5 Hz, N–C$\underline{H}_2$–P, 4H), 2.09 (m, P–C$\underline{H}_2$–CH_2, 2H), 2.69 (m, P–CH_2–C$\underline{H}_2$, 2H); $^{13}C\{^1H\}$ NMR (150 MHz, D_2O), δ/ppm: 52.29 (s, ring $\underline{C}H_2$, 2C), 52.39 (s, ring $\underline{C}H_2$, 4C), 53.82 (d, $^1J^{PC}$ = 86.6 Hz, N–$\underline{C}H_2$–P, 2C), 60.20 (d, $^1J_{PC}$ = 112.9 Hz, P–$\underline{C}H_2$–OH, 2C), 55.38 (d, $^1J_{PC}$ = 90.4 Hz, N–$\underline{C}H_2$–P, 1C), 25.51 (d, $^1J_{PC}$ = 94.7 Hz, P–$\underline{C}H_2$–CH_2, 1C), 27.52 (d, $^1J_{PC}$ = 3.5 Hz, P–CH_2–$\underline{C}H_2$, 1C), 177.91 (d, $^3J_{PC}$ = 12.6 Hz, C=O, 1C); $^{31}P\{^1H\}$ NMR (121 MHz, D_2O), δ/ppm: 34.7 (s, 2P), 40.3 (s, 1P). ESI-MS(+): *m/z* = 496 $(M+H^+)^+$. Elemental analysis calculated (%) for $C_{14}H_{32}N_3O_{10}P_3$·0.6 H_2O: C 33.22, H 6.61, N 8.30; found C 32.31, H 6.67, N 8.22.

$[Ga(NOPO)]^-$ solution for NMR: Solutions of NOPO and $Ga(NO)_3$ (2 mL of 2 mM of each) were mixed in NMR tube. $^{31}P\{^1H\}$ NMR (121.4 MHz, D_2O), δ/ppm: 37.3 (s, $\underline{P}$–CH_2–OH, 2P), 41.6 (s, $\underline{P}$–

$(CH_2)_2CO_2H$, 1P). ^{71}Ga NMR (122 MHz, D_2O), δ/ppm: 136 (s). ESI-MS(–): *m/z* = 560 $(M–H^+)^–$, 596 $(M+K^+–2H^+)^–$. ESI-MS(+): *m/z* = 562 $(M+H^+)^+$, 584 $(M+Na^+)^+$, 600 $(M+K^+)^+$.

3. Synthesis of the NOPO peptide conjugates

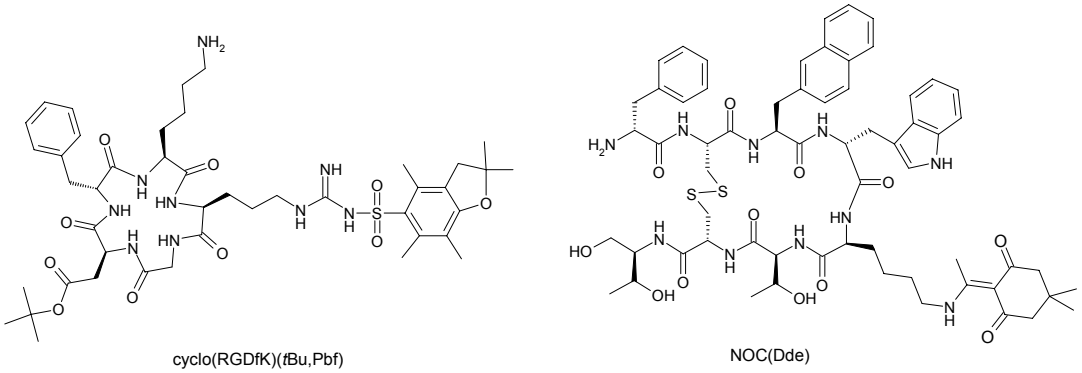

Figure S1: Structures of the protected peptides used as starting compounds for synthesis of conjugates.

NOPO-RGDfK: NOPO·0.6 H_2O (24.8 mg, 49 µmol) and cyclo(RGDfK)(Pbf,*t*Bu) (50.0 mg, unknown TFA content, ca. 50 µmol) were dissolved in dry DMSO (0.5 mL), and DIPEA (86.0 µL, 63.8 mg, 494 µmol) was added. Then HATU (57.2 mg, 150 µmol) was added and the solution was stirred for 10 min at ambient temperature. The precipitate obtained by addition of the reaction mixture to sat. aq. NaCl solution was separated by centrifugation, the solid was dissolved in water and subjectied to diafiltration with water (ca. 200 mL). The retentate was lyophilized, and TFA (80 %, 1 mL) was added for removal of acid-sensititive protecting groups Pbf and *t*Bu. The product was precipitated by addition into diethyl ether (10 mL), the precipitate centrifuged off and purified by preparative HPLC (gradient: 27 % to 37 % MeCN in water, both containing 0.1 % TFA, in 30 min). Fractions containing the product were collected, the organic solvent evaporated in vacuo and the remaining aqueous solution lyophilized to give 21 mg (40 %) of NOPO-RGDfK.

Analytical HPLC: gradient 20 % to 80 % MeCN in water, both containing 0.1 % TFA, in 24 min. t_R = 6.5 min. ESI-MS(+): *m/z* =1081 $(M+H^+)^+$, ESI-MS(–): *m/z* = 1079 $(M–H^+)^–$.

[Ga(NOPO-RGDfK)] solution: Solutions of $Ga(NO_3)_3$ and NOPO-RGDfK (0.1 mL of 2 mM of each) were mixed. The complex was identified by ESI-MS(+): *m/z* = 1147 $(M+H^+)$.

NOPO-NOC: This compound was prepared as described for NOPO-RGDfK, starting out from NOC(Dde) (10.0 mg, unknown TFA content, ca 7.5 µmol), NOPO (5.5 mg, 11.1 µmol) and using DMSO (0.5 mL), DIPEA (14.3 mg, 19.3 µL, 111 µmol) and HATU (21.1 mg, 55.5 µmol). Deprotection (removal of Dde) was done with 2 % hydrazine in DMF. Purification was done by preparative HPLC (gradient 25 % to 45 % MeCN in water, both containing 0.1 % TFA, in 60 min), yield 5.9 mg (51 %).

Analytical HPLC: gradient 20 % to 60 % MeCN in water, both containing 0.1 % TFA, in 16 min. t_R = 8.5 min. ESI-MS(+): *m/z* = 1528 $(M–H_2O+H^+)^+$, 774 $(M–H_2O+2H^+)^{2+}$

[Ga(NOPO-NOC)] solution: Solutions of $Ga(NO_3)_3$ and NOPO-NOC (0.1 mL of 2 mM of each) were mixed. ESI-MS(+): *m/z* = 1612 $(M+H^+)^+$, 806 $(M+2H^+)^{2+}$.

4. Automated ^{68}Ga labeling

^{68}Ga-labeling was performed using a synthesis module (GallElut$^+$ by Scintomics, Fürstenfeldbruck, Germany) as described before, the synthetic procedures being carried out in full automation, controlled by a computer program. Briefly, ^{68}Ga was obtained from a generator with SnO_2 matrix (IThemba LABS, South Africa, distributed by IDB Holland) which was eluted with 1 M aq. HCl. NOPO-RGDfK or NOPO-NOC (0.1–1 nmol) and HEPES (0.4 mL of solution resulting from mixing 7.2 g of HEPES with 6 mL of water) were placed in a 5 mL conical reaction vial (AllTech). For labeling, a 1.25 mL fraction of the generator eluate, containing the highest activity (between 900 and 1000 MBq) was added, resulting in pH of 1.8. The vial was heated to 100 °C for 5 min. Then, the reaction mixture was passed through an SPE cartridge (Waters SepPak C18 classic), the cartridge was purged with 10 mL of water in order to remove non-complexed $^{68}Ga^{3+}$, other ions, and HEPES, and purged with air. The product was eluted with ethanol (1 mL) into a 10 mL flask. In order to obtain a formulation suitable for animal experiments, water (2 mL) and PBS (1 mL) were added and the solution concentrated in vacuo until a final volume of 1 mL was reached, the solution thus possessing suitable pH and osmolality for injection. Product purity was determined by radio-TLC and radio-HPLC.

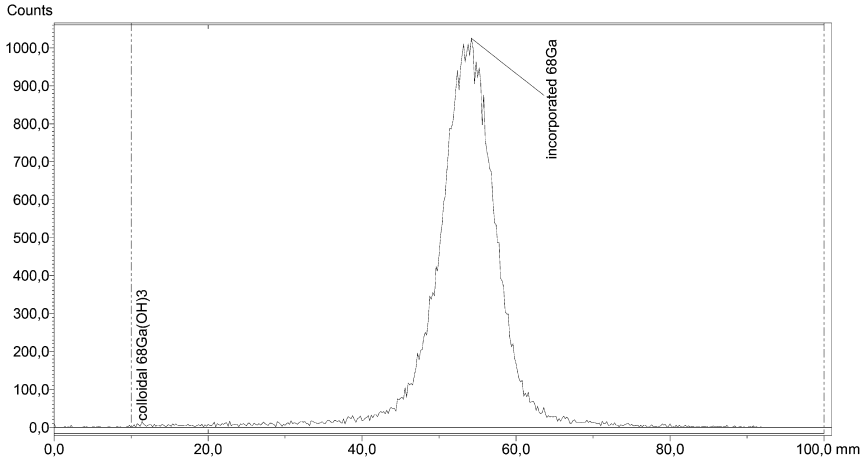

Regions: TLC

Name	Start (mm)	End (mm)	Retention (RF)	Height (Counts)	Area (Counts)	%ROI (%)	%Total (%)
colloidal 68Ga(OH)3	0,0	20,0	0,0	14,0	314,0	0,70	0,70
incorporated 68Ga	20,0	100,0	0,5	1025,0	44260,0	99,30	99,30
2 Peaks					44574,0	100,00	100,00

Figure S2: Radio-TLC of ^{68}Ga-NOPO-RGDfK (TLC1).

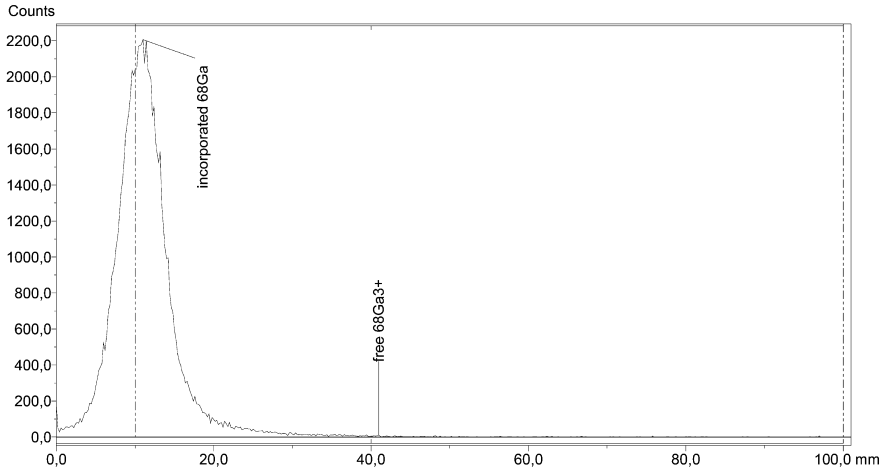

Regions: TLC

Name	Start (mm)	End (mm)	Retention (RF)	Height (Counts)	Area (Counts)	%ROI (%)	%Total (%)
incorporated 68Ga	0,0	40,0	0,0	2206,0	78886,0	99,55	99,55
free 68Ga3+	40,0	100,0	0,3	11,0	359,0	0,45	0,45
2 Peaks					79245,0	100,00	100,00

Figure S3: Radio-TLC of ^{68}Ga-NOPO-RGDfK (TLC2).

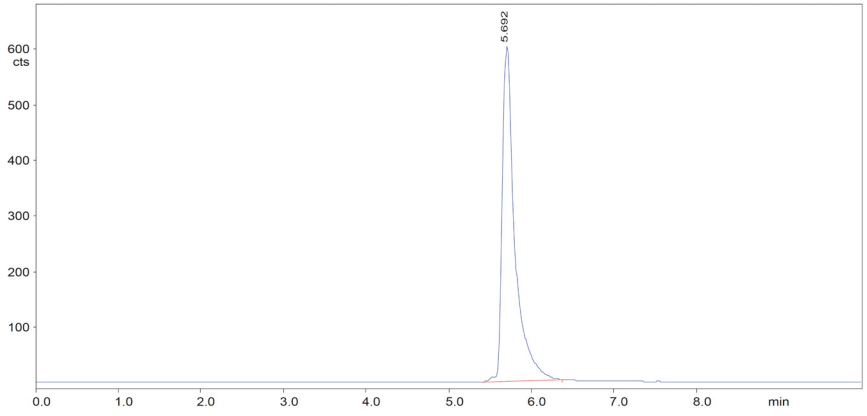

Figure S4: Radio-HPLC of ^{68}Ga-NOPO-RGDfK.

5. Manual radiolabeling and radiolabeling in the presence of Zn^{2+} and Fe^{3+}

A 1.25 mL fraction of the ^{68}Ga eluate was mixed with 800 µL of HEPES solution (7.2 g of HEPES dissolved in 6 mL of water) resulting in pH 2.8. 90 µL of that solution was added to 10 µL of NOPO or NOPO-RGDfK (0.01–10 µM stock solutions), which resulted in total labeling volume of 0.1 mL (0.001–1 µM solutions containing 100 pm–0.1 nmol of a ligand). Such solution was heated to 95 °C for 5 min and then cooled down in a water bath. $^{68}Ga^{3+}$ incorporation was evaluated by radio-TLC.

Labeling in the presence of Fe^{3+} or Zn^{2+} was done at a constant ligand concentration of 3 µM and pH 3.3. Stock solutions of $ZnCl_2$ (3.63 mM) or $FeCl_3$ (72.7 mM) were prepared in 1 M aq. HCl in order to prevent formation of colloidal hydroxides, keeping the pH constant after mixing with the generator eluate. A fraction of the eluate was "contaminated" with these solutions, resulting in a total volume of 1.25 mL. Then, 930 µL of standard HEPES solution (see above) was added. The labeling procedure and analysis were identical as described above. For example, labeling in the presence of Fe^{3+} in concentration of 30 µM was done as following: $FeCl_3$ stock solution (10 µL) was mixed with 1 M aq. HCl (990 µL). 100 µL of that solution was mixed with generator eluate (1.15 mL) and HEPES solution (930 µL). 90 µL of that solution was added to a 30 µM solution of NOPO (10 µL) (resulting in $c_{NOPO} = 3$ µM and $c_{Fe^{3+}} = 30$ µM). This mixture was heated to 95 °C for 5 min, the reaction stopped by cooling in a water bath, and the radioactivity incorporation assessed by radio-TLC.

6. Stability studies

Stability studies in vitro were done with approximately 10 MBq of ^{68}Ga-NOPO-RGDfK solution formulated for injection into the animals (see below). A sample was mixed with PBS or 0.25 M aq. disodium EDTA (0.5 mL) and incubated at 37 °C for 3 h. Radio-HPLC was done at 0.5, 1, 2, and 3 h after mixing. For in vivo experiments, nude mice (see below) were administered approximately 30 MBq of ^{68}Ga-NOPO-RGDfK or ^{68}Ga-NOPO-NOC and sacrificed after 30 min. Dissected organs were frozen in liquid nitrogen, homogenized using a ball mill, and suspended PBS (0.5 mL) containing 10 µg of the precursor. The solid and liquid phases were separated by centrifugation at 1500 rpm for 5 min. The suspension was washed with PBS and subjected to ultrafiltration (30 kDa MWCO). Both pellet and supernatant were measured in a γ-counter (1480 WIZARD™, PerkinElmer Wallac) in order to determine the extraction efficiency. The extracts of liver, kidney, tumour, blood and the urine sample were chromatographed on silica-impregnated chromatography paper (Varian) using 1 M aq. ammonium acetate as mobile phase. Chromatograms were analyzed by autoradiography (using BAS-IP MS 2025 Imaging Plates by Fujifilm, a Dürr Medical CR35BIO for readout and Aida image analyser v 4.24 program for data analysis). No decomposition of the tracer was observed in any of the experiments.

7. Animal models and PET imaging

All animal experiments were performed in accordance with general animal welfare regulations in Germany, and necessary permissions were obtained from the responsible authorities (approval #55.2-1-54-2531-35-06). CD-1 nude mice (Charles River, Germany) were injected subcutaneously with M21 and M21L cells (human melanoma) to the right and to the left shoulder, respectively, as the tumor xenograft models for evaluation of NOPO-RGDfK. For evaluation of NOPO-NOC, the animals were injected with AR42J cells (rat pancreatic carcinoma) to the right shoulder. The animals were anaesthetized with isoflurane, and ~15 MBq of ^{68}Ga-NOPO-RGDfK or ^{68}Ga-NOPO-NOC (prepared as described above) were injected into the tail vein. Anaesthesia was interrupted between injection and imaging. PET scans were recorded 75 min p.i. for 15 min. For blockade, 100 µg of the respective unlabeled compounds in 100 µL PBS were injected 10 min prior to tracer administration. The images were reconstructed using a 3D ordered subsets expectation maximum (OSEM3D) algorithm without scanner and attenuation correction.

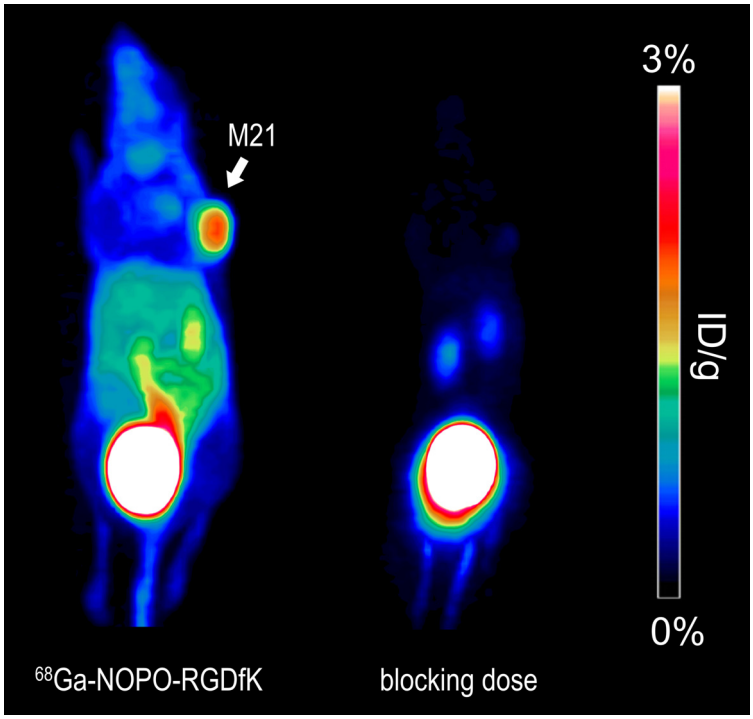

Figure S5: PET images (maximum intensity projections, 75 min p.i.) of nude mouse tumor xenografts (M21 human melanoma) using ^{68}Ga-NOPO-RGDfK (left) and with a blocking dose of excess unlabeled (5 mg per kg body weight) (right).

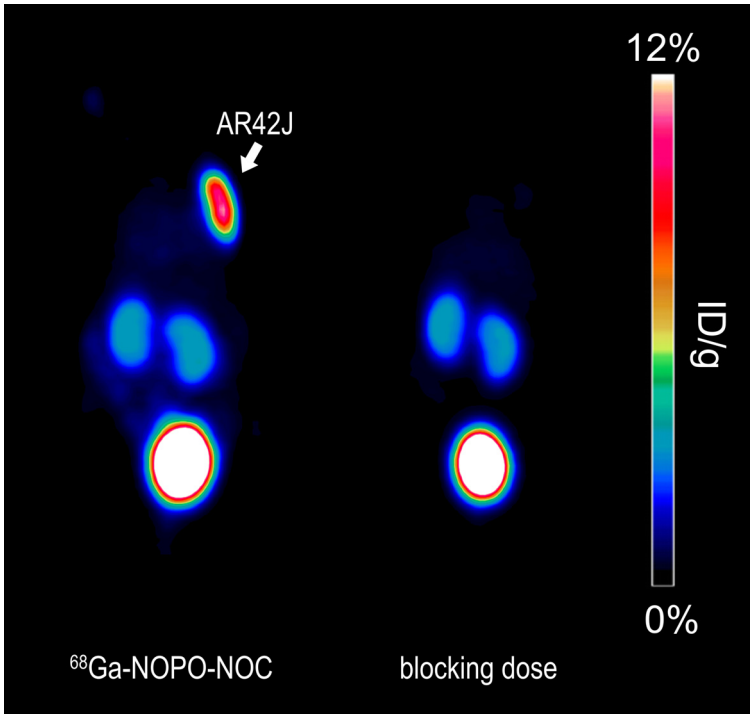

Figure S6: PET images (maximum intensity projections, 75 min p.i.) of nude mouse tumor xenografts (AR42J rat pancreas tumor) using ^{68}Ga-NOPO-NOC (left) and with a blocking dose of excess unlabeled (5 mg per kg body weight) (right).

References

[1] Notni, J.; Hermann, P.; Havlíčková, J.; Kotek, J.; Kubíček, V.; Plutnar, J.; Loktionova, N.; Riss, P. J.; Rösch, F.; Lukeš, I. *Chem. Eur. J.* **2010**, 16, 7174–7185.

[2] Řezanka, P.; Kubíček, V.; Hermann, P.; Lukeš, I. *Synthesis* **2008**, 9, 1431–1435.

Appendix: Spectra and Chromatograms

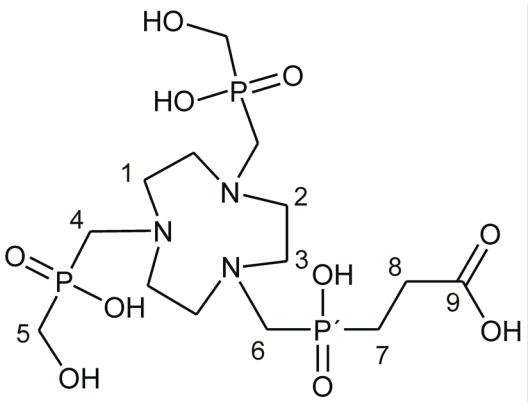

Figure S7: Structure of NOPO with atom labelling scheme used in assignment of NMR spectra.

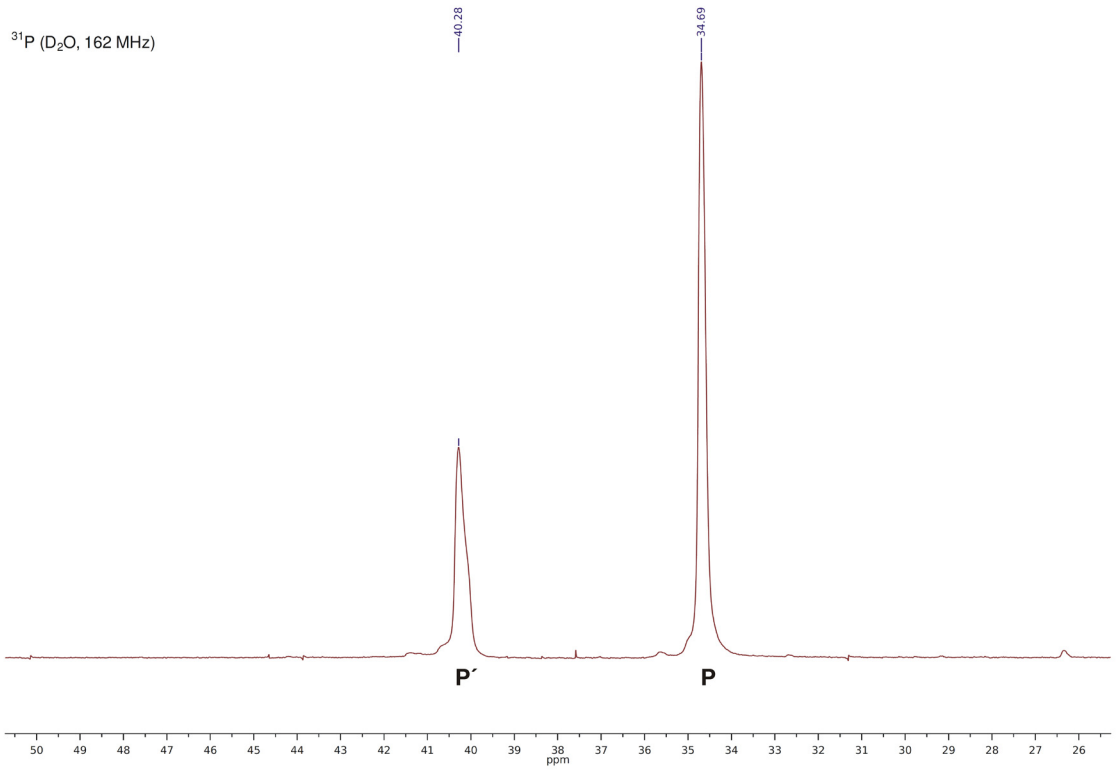

Figure S8: $^{31}P\{^{1}H\}$ NMR spectra of NOPO.

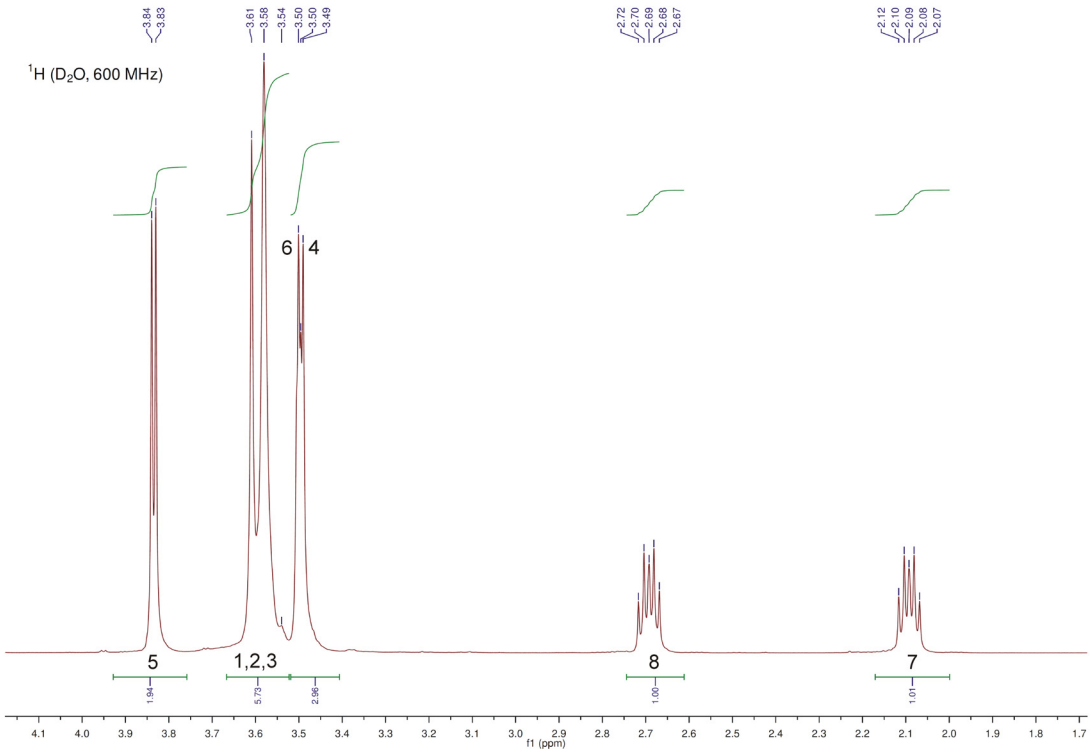

Figure S9: ^{1}H NMR spectra of NOPO.

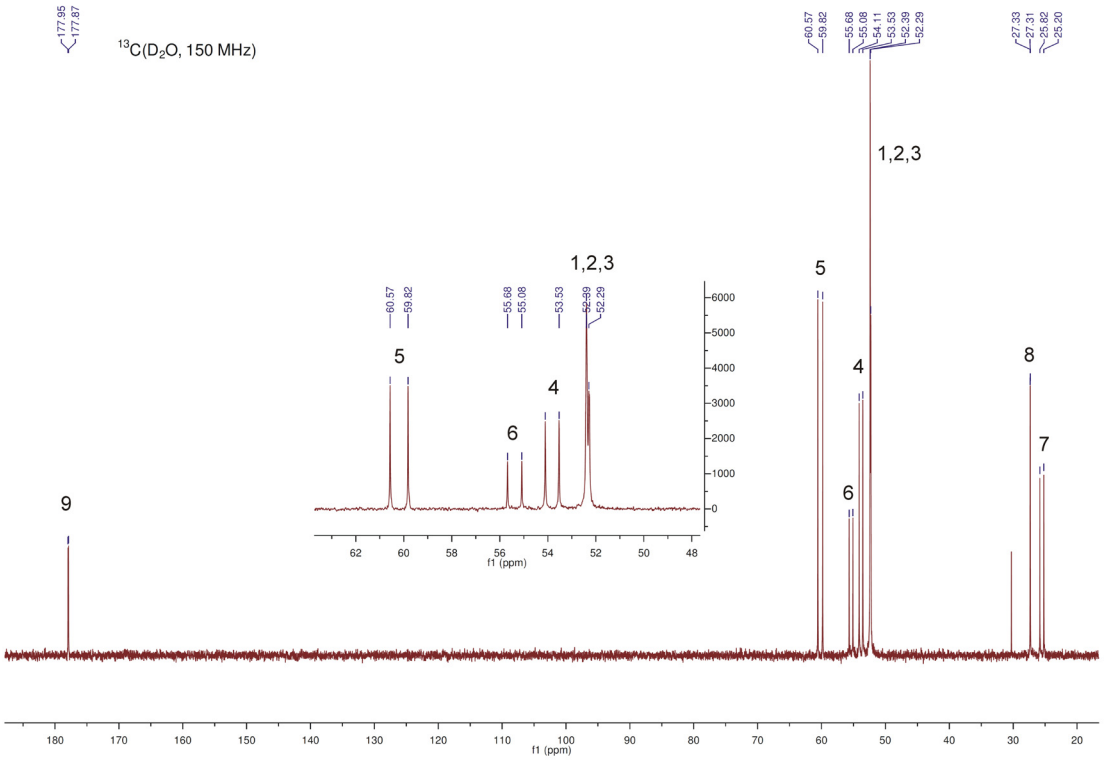

Figure S10: ^{13}C{^{1}H} NMR spectra of NOPO.

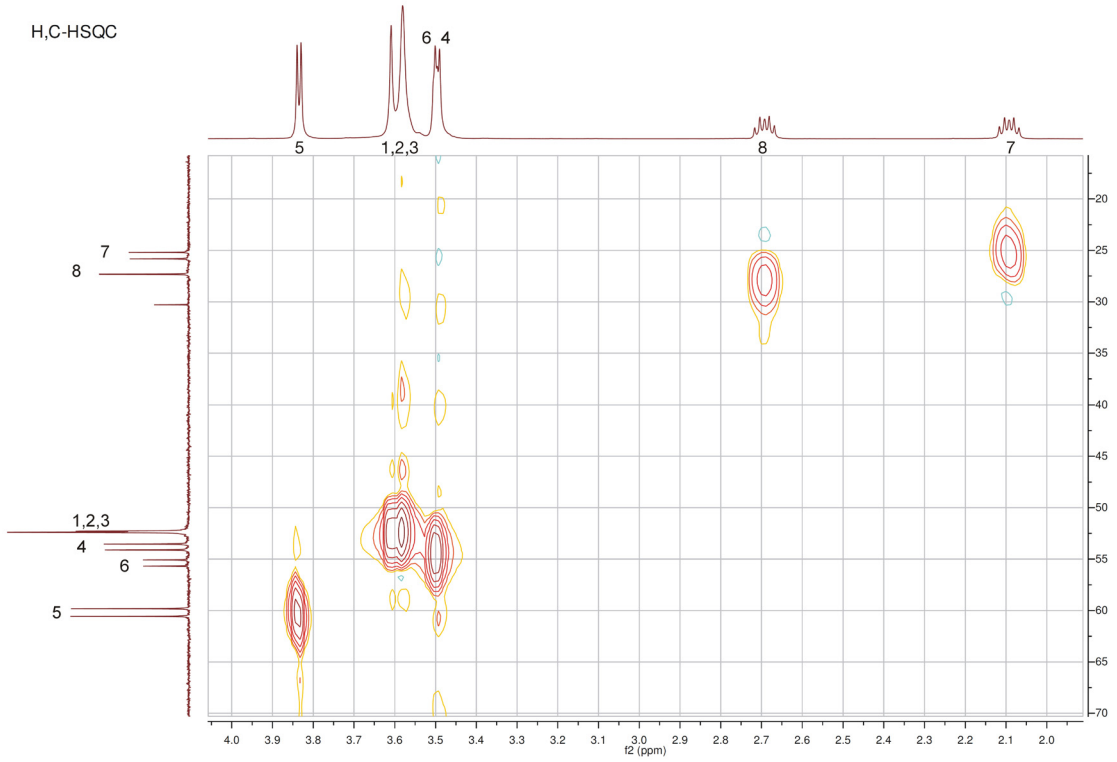

Figure S11: ^{1}H-^{13}C HSQC NMR spectra of NOPO.

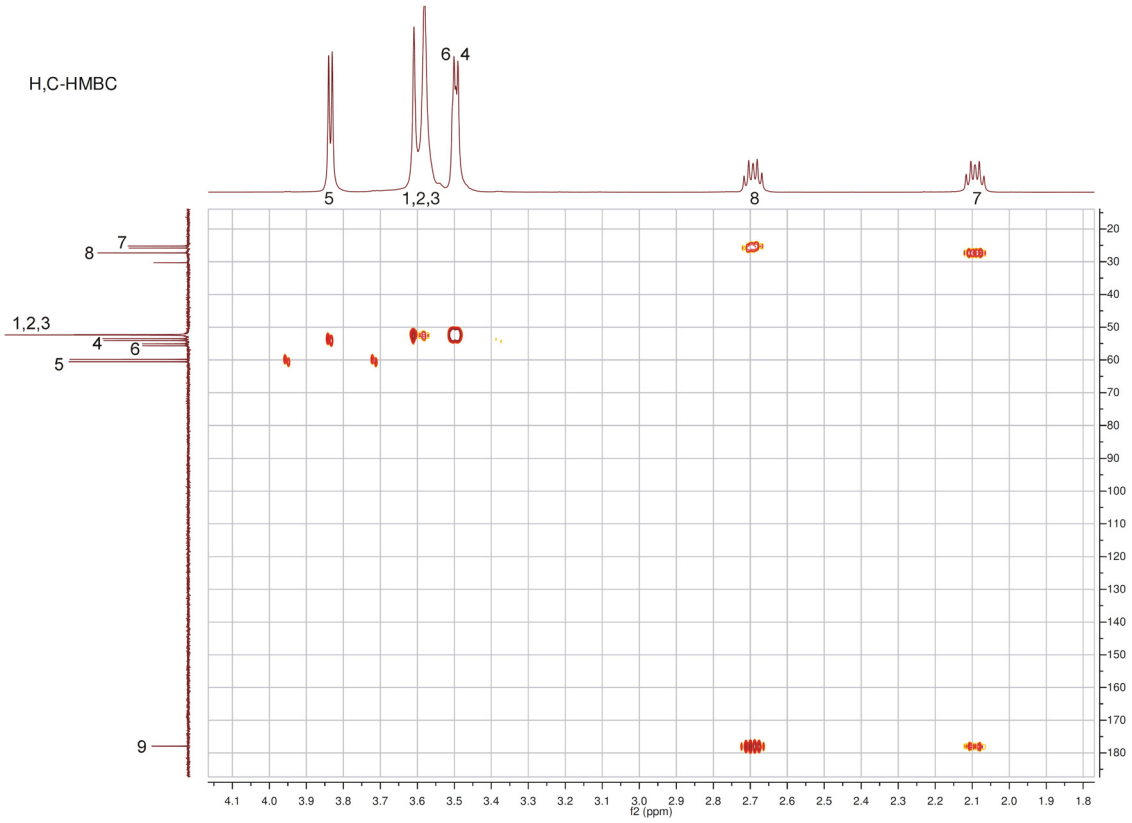

Figure S12: ^{1}H-^{13}C HMBC NMR spectra of NOPO.

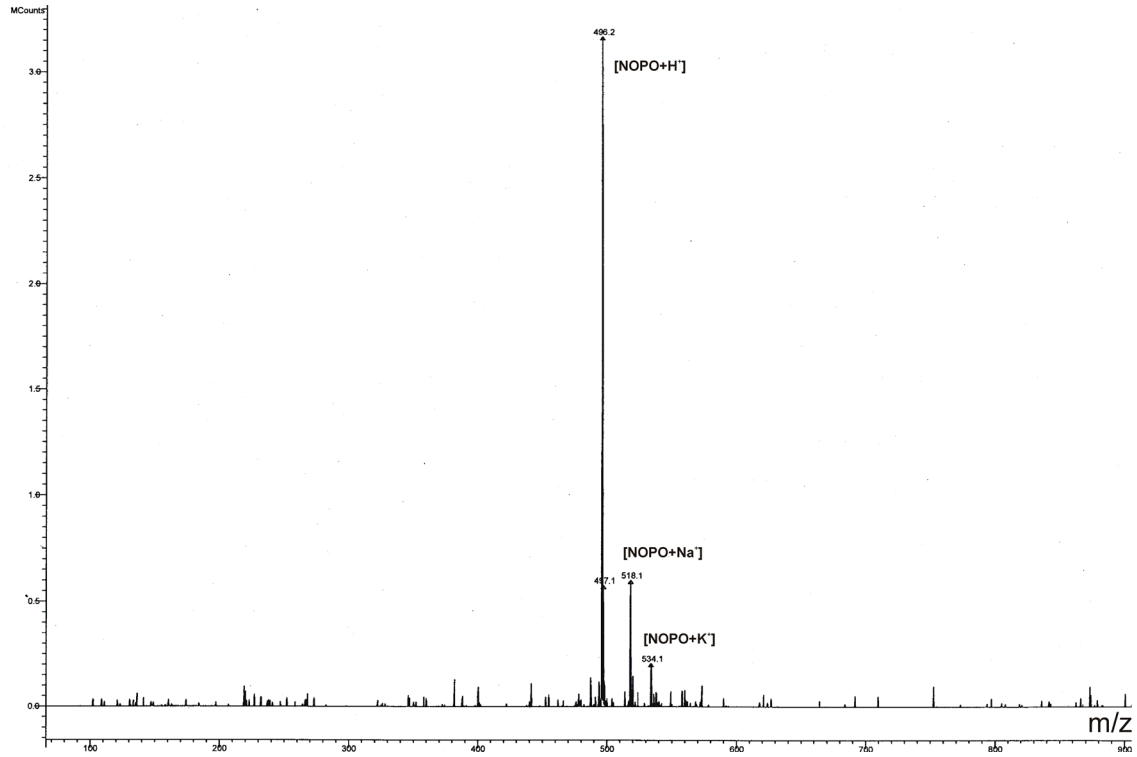

Figure S13: ESI-MS(+) spectra of NOPO.

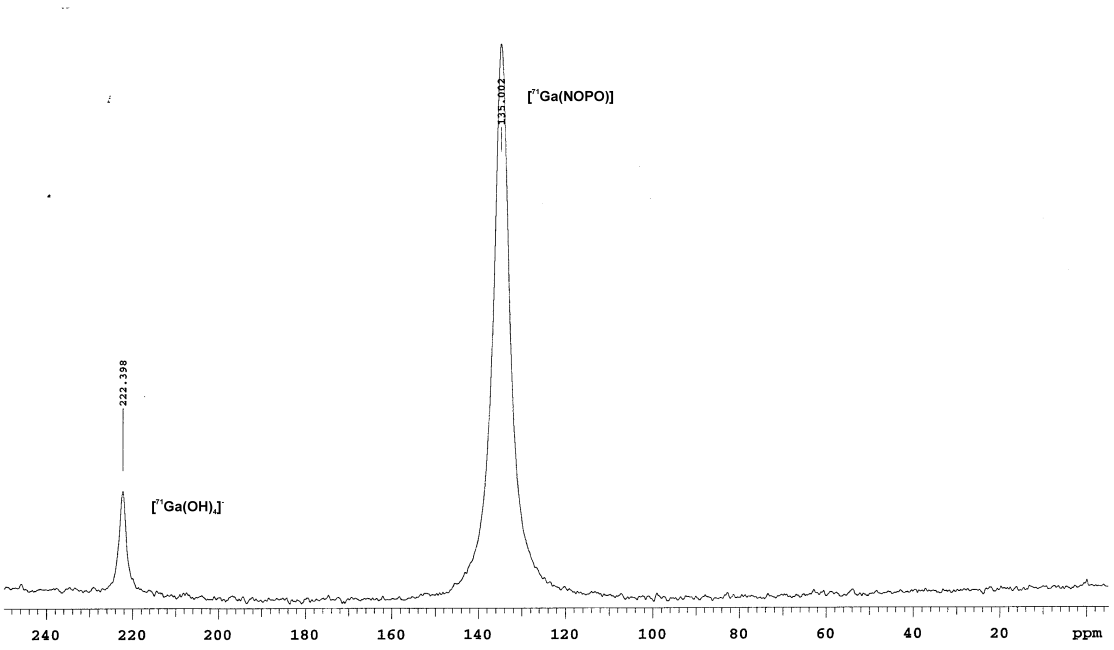

Figure S14: ^{71}Ga NMR spectra of the $[Ga(NOPO)]^{-}$ complex.

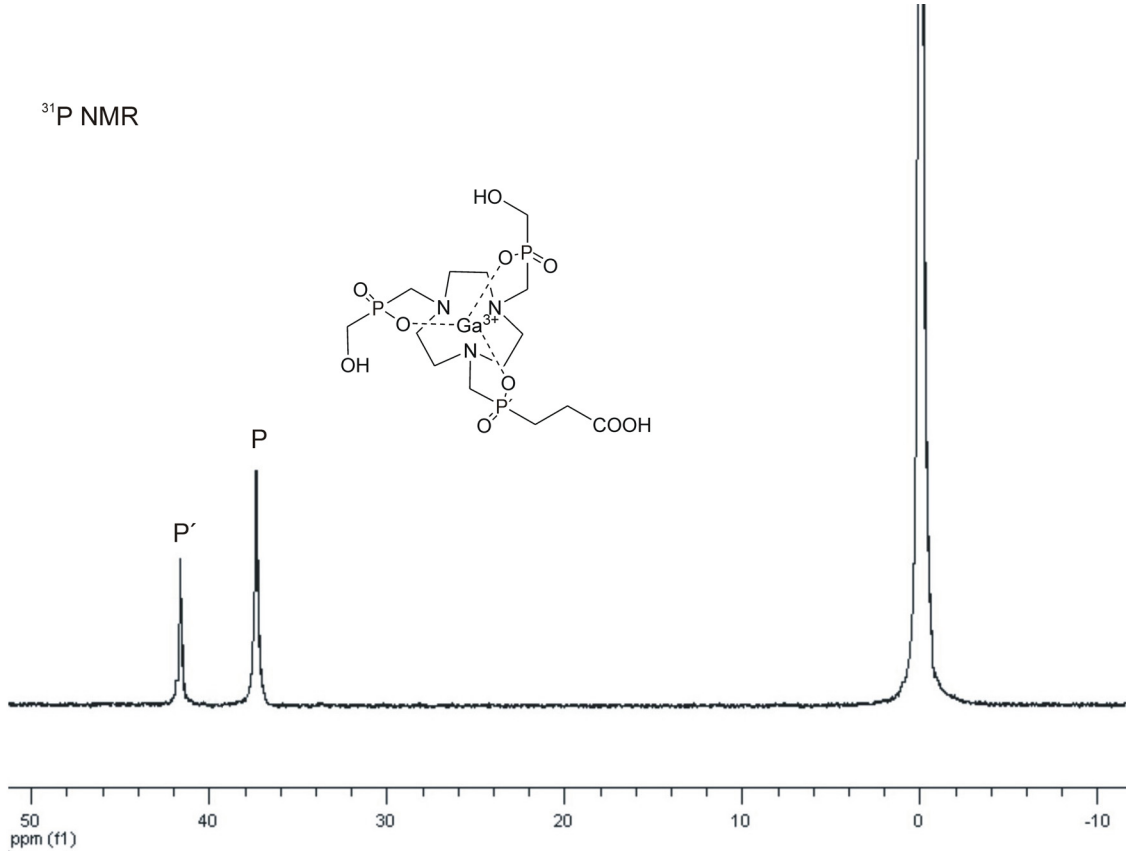

Figure S15: $^{31}P\{^{1}H\}$ NMR spectra of the $[Ga(NOPO)]^{-}$ complex (0 ppm: reference signal, insert tube).

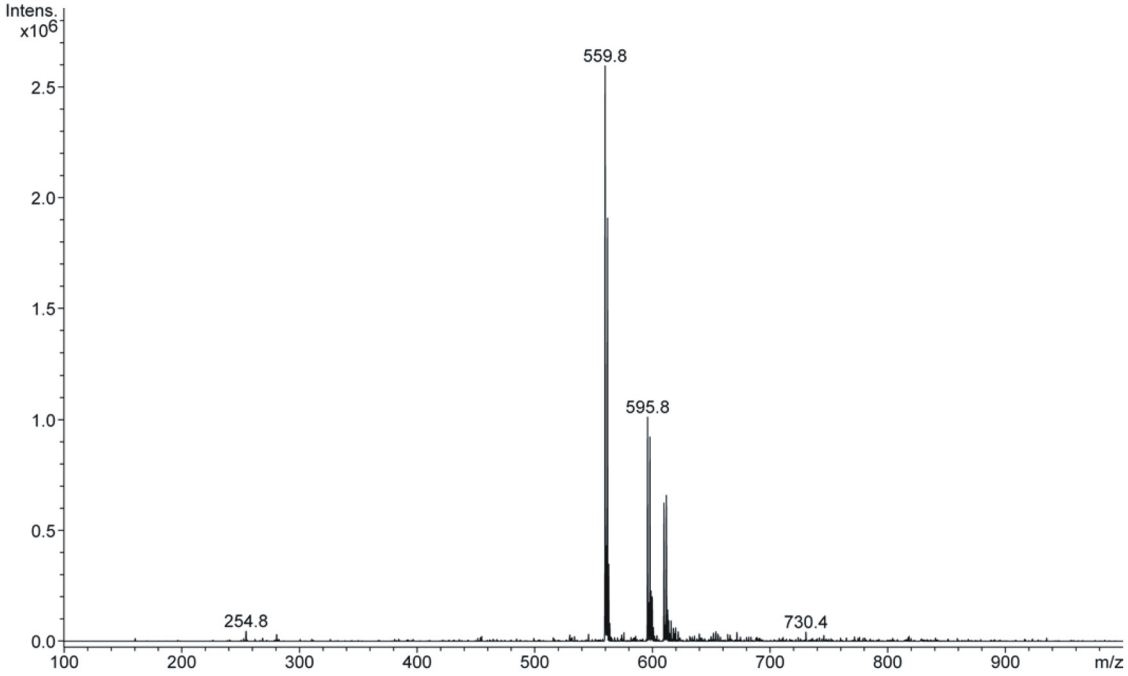

Figure S16: ESI-MS(–) spectra of the $[Ga(NOPO)]^{-}$ complex.

APPENDIX 4

DOI: 10.1002/cmdc.201200471

How is ^{68}Ga Labeling of Macrocyclic Chelators Influenced by Metal Ion Contaminants in ^{68}Ge/^{68}Ga Generator Eluates?

Jakub Šimeček,[a] Petr Hermann,[b] Hans-Jürgen Wester,[a] and Johannes Notni*[a]

To assess the influence of Zn^{2+}, Cu^{2+}, Fe^{3+}, Al^{3+}, Ti^{IV}, and Sn^{IV} on incorporation of $^{68}Ga^{3+}$ into pendant-arm macrocyclic chelators, the ^{68}Ga labeling of 1,4,7-triazacyclononane-1,4,7-triacetic acid (NOTA), 1,4,7,10-tetraazacyclododecane-1,4,7,10-tetraacetic acid (DOTA), 1,4,7-triazacyclononane-1,4,7-tris[methyl(2-carboxyethyl)phosphinic acid]) (TRAP), and 1,4,7-triazacyclononane-1-[methyl(2-carboxyethyl)phosphinic acid]-4,7-bis-[methyl(2-hydroxymethyl)phosphinic acid] (NOPO), as well as their peptide conjugates, was investigated in the presence of varying concentrations of these metal ions. The ^{68}Ga labeling yield for carboxylate-type chelators NOTA and DOTA is decreased at lower metal ion contaminant concentrations compared with phosphinate-type chelators TRAP and NOPO. The latter are able to rapidly exchange coordinated Zn^{II} with $^{68}Ga^{3+}$, as confirmed by mass spectrometry and ^{31}P NMR spectroscopy. ^{68}Ga labeling of Zn^{II} complexes of TRAP and NOPO proceeds as efficient as labeling of neat NOTA; this applies also to the corresponding peptide conjugates of these chelators. This behavior results in substantially improved selectivity for Ga^{3+} and, therefore, in more robust and reliable ^{68}Ga labeling procedures. In addition, none of the investigated chelators binds ^{68}Ge, rendering post-labeling purification protocols, for example, solid-phase extraction, a reliable means of removal of ^{68}Ge contamination from ^{68}Ga radiopharmaceuticals.

Introduction

^{68}Ge/^{68}Ga generators have attracted high interest during the last decade as they allow for the quick, simple and comparably inexpensive preparation of ^{68}Ga radiopharmaceuticals for positron emission tomography (PET).[1] Commercially available ^{68}Ge/^{68}Ga generators are portable, lead-shielded chromatographic separation columns. Typically, such columns contain ^{68}Ge adsorbed onto a matrix of TiO_2, SnO_2, or a suitable organic polymer, from which $^{68}Ga^{3+}$ (for radiolabeling purposes) is eluted with hydrochloric acid of varying concentration (0.05–1 M).[2] In contrast to the more frequently used PET nuclides ^{18}F or ^{11}C, there is no need for an on-site cyclotron. At the same time, more detailed good manufacturing practice (GMP) standards for production of radiopharmaceuticals in Europe call for robust and reproducible production routines for ^{68}Ga radiopharmaceuticals.[3]

In clinical nuclear medicine, interest in ^{68}Ga mainly arose due to the remarkable success of ^{68}Ga-labeled peptides, namely ^{68}Ga-DOTATOC, ^{68}Ga-DOTATATE, and ^{68}Ga-DOTANOC, in PET imaging of neuroendocrine tumors.[4] Precursors used for ^{68}Ga labeling are usually bioconjugates, consisting of a biomolecule (e.g., a peptide) as the targeting group and a chelator responsible for strong and irreversible binding of ^{68}Ga.[5] Labeling is done conveniently by chelation of $^{68}Ga^{3+}$ by the labeling precursor or, more precisely, the chelator contained therein. Hence, radiochemical yields are determined by the inherent ability of the chelator to complex Ga^{3+} from highly diluted solutions. Currently, 1,4,7,10-tetraazacyclododecane-1,4,7,10-tetraacetic acid (DOTA)[6] and 1,4,7-triazacyclononane-1,4-bis(acetic acid)-7-(2-glutaric acid) (NODAGA),[7] a bifunctional derivative of 1,4,7-triazacyclononane-1,4,7-triacetic acid (NOTA), are the most frequently utilized chelators in ^{68}Ga radiopharmaceuticals (Figure 1). Recently, our groups have shown that the chelators 1,4,7-triazacyclononane-1,4,7-tris[methyl(2-carboxyethyl)phosphinic acid]) (TRAP-Pr)[8–10] and 1,4,7-triazacyclononane-1-[methyl(2-carboxyethyl)phosphinic acid]-4,7-bis[methyl(2-hydroxymethyl)phosphinic acid] (NOPO)[11] possess markedly improved affinity to $^{68}Ga^{3+}$ and, therefore, higher ^{68}Ga-labeling efficiency. Compared to DOTA and NOTA, quantitative transformation of $^{68}Ga^{3+}$ into $^{68}Ga^{III}$ chelates requires a much smaller concentration of these chelators, which is why TRAP and NOPO-based radiopharmaceuticals can be prepared with extremely high specific activities.[11,12] Furthermore, ^{68}Ga labeling of triazacyclononane-triphosphinates can be performed at lower temperatures and over a broad pH range (0.5–5), which is why meticulous adjustment of labeling pH is far less important.

Apart from the ^{68}Ga-binding efficiency of the chelator, there are other factors influencing the performance of ^{68}Ga-labeling reactions. One of them is the presence of other metal ions in

[a] J. Šimeček, Prof. Dr. H.-J. Wester, Dr. J. Notni
Pharmaceutical Radiochemistry, Technische Universität München
Walther-Meißner-Strasse 3, 85748 Garching (Germany)
E-mail: johannes.notni@tum.de
Homepage: http://www.prc.ch.tum.de

[b] Prof. Dr. P. Hermann
Department of Inorganic Chemistry
Faculty of Science, Charles University in Prague
Hlavova 2030, 12840 Prague 2 (Czech Republic)

Supporting information for this article is available on the WWW under http://dx.doi.org/10.1002/cmdc.201200471.

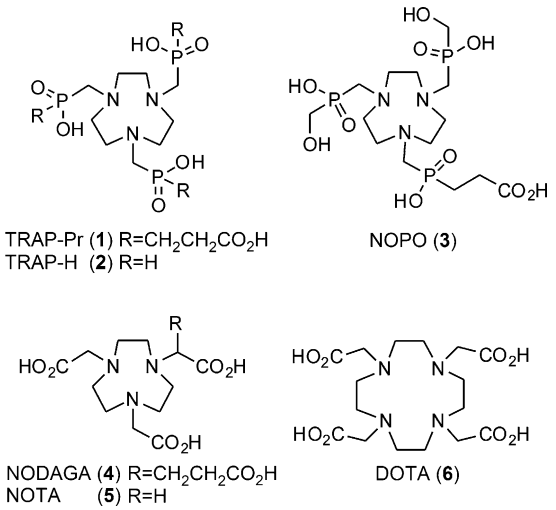

Figure 1. Polyazacycloalkane-based chelators used for trivalent gallium. Abbreviations: 1,4,7,10-tetraazacyclododecane-1,4,7,10-tetraacetic acid (DOTA); 1,4,7-triazacyclononane-1-[methyl(2-carboxyethyl)phosphinic acid]-4,7-bis-[methyl(2-hydroxymethyl)phosphinic acid] (NOPO); 1,4,7-triazacyclononane-1,4,7-triacetic acid (NOTA); 1,4,7-triazacyclononane-1,4,7-tris[methyl(2-carboxyethyl)phosphinic acid]) (TRAP); (1,4,7-triazacyclononane-1,4-bis(acetic acid)-7-(2-glutaric acid) (NODAGA).

the $^{68}Ge/^{68}Ga$ generator eluate. These can compete with $^{68}Ga^{3+}$ for the chelator and thus diminish the labeling yield, which is particularly problematic in view of the low concentration of the carrier-free ^{68}Ga in the eluate. For example, using a typical generator containing 1.85 GBq ^{68}Ge in equilibrium with ^{68}Ga, approximately 1 GBq of $^{68}Ga^{3+}$ can be collected in a fraction of 1 mL eluate, which is equivalent to an absolute amount of 10 pmol of $^{68}Ga^{3+}$ and hence a concentration of 10 nM. However, the eluate inevitably also contains Zn^{2+} formed by ^{68}Ga decay, as well as other metal cations that originate from the matrix material, or are present in the eluent hydrochloric acid in the first place. For example, the total amount of metal contaminants (Ga, Ge, Zn, Ti, Sn, Fe, Al and Cu) in the eluate of a SnO_2-based generator was reported to be <10 ppm (<3 ppm Zn^{2+}; <1 ppm for each of the other ions).[13] In fractionated eluate from a generator with a TiO_2 matrix, concentrations of $Fe^{2+/3+}$ and Zn^{2+} up to 50 nM were found.[14]

The influence of metal ions in $^{68}Ge/^{68}Ga$ generator eluates on ^{68}Ga labeling has always been contemplated, and considerable efforts have been made to remove these contaminants, together with the long-lived, and thus problematic, radiochemical impurity ^{68}Ge ($t_{1/2}=270$ days). A simple yet quite effective method is fractionation, which involves the separation of an eluate fraction (typically 1–2 mL) that contains the highest activity concentration and 70–80% of the total activity.[13,14] This procedure maximizes the $^{68}Ga/^{68}Ge$ ratio, although at the cost of losing some ^{68}Ga, and according to our experience, is suitable for reduction of ^{68}Ge contamination to an acceptable level. Furthermore, several purification strategies have been developed and are still being improved. One approach uses strong anionic exchange (SAX) resin.[15] Addition of concentrated hydrochloric acid to the generator eluate results in formation of $[GaCl_4]^-$, which is trapped on a SAX solid-phase extraction (SPE) cartridge. After purging off all liquid with a stream of air, $^{68}Ga^{3+}$ can be eluted with a small amount of water. A well-established method for removal of ^{68}Ge and other contaminants consists of trapping all cations on strong cation exchange (SCX) resin, where after $^{68}Ga^{3+}$ is separated from metal ion contaminants by fractionated elution with an acetone/HCl mixture.[16] However, not all non-Ga^{3+} ions, particularly Fe^{3+}, are removed completely hereby,[17] and the presence of acetone during ^{68}Ga labeling was recently shown to result in ^{68}Ga peptide radiopharmaceuticals containing considerable amounts of radiochemical impurities.[18] To produce $^{68}Ga^{3+}$ solutions that do not contain reagents with regulatory concern, and thus are suitable for kit labeling, a very elegant modification of the cation exchanger purification was recently reported by Mueller et al., who employed slightly acidic aqueous sodium chloride to liberate the $^{68}Ga^{3+}$ from the SCX cartridge.[18] However, this method mainly aims at removing ^{68}Ge; other metal cations remain in the solution.

Curiously, although being the subject of various concerns, to the best of our knowledge, the influence of metal ion contaminants on ^{68}Ga labeling has never been assessed systematically, apart from a study by Velikyan et al. who investigated how $^{68}Ga^{3+}$ incorporation by DOTATOC is affected by the presence of Fe^{3+}, Al^{3+} and In^{3+}.[19] Hence, in order to provide sound data for quantitative assessment, we decided to study the influence of the most relevant metal ions contained in generator eluates on the $^{68}Ga^{3+}$ incorporation into important macrocyclic chelators **1**–**6** (Figure 1). In addition, we expanded these investigations to some chelator–peptide conjugates (NODAGA-RGD, NOPO-RGD,[11] and TRAP(RGD)$_3$,[10a,20] see Figure 2) in order to obtain data of clinical relevance.

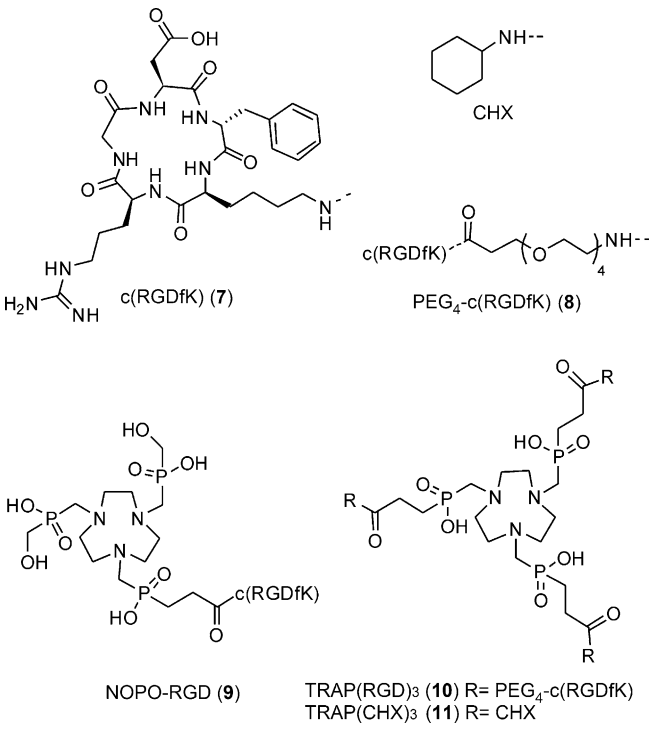

Figure 2. Structures of functionalized chelators (conjugates) studied. Abbreviations: cyclo(Arg–Gly–Asp–D-Phe–Lys) [c(RGDfK)]; poly(ethylene glycol) (PEG).

Results and Discussion

As it is not of importance for interpretation of the data and increases readability, pH-dependent protonation states and resulting variable charges of complexes are not indicated in formulae. For example, [Zn(DOTA)] stands for any of the species $[Zn(H_2DOTA)]$, $[Zn(HDOTA)]^-$ or $[Zn(DOTA)]^{2-}$; hence describes what is commonly referred to as a "zinc(II)–DOTA complex". Notation of formal charges on simple ions refers to their aqua complexes in aqueous solution (e.g., Zn^{2+} abbreviates $[Zn(H_2O)_6]^{2+}$). When referring to metal ions in other complexes, including poorly defined species contained in solutions, the oxidation state is indicated in roman numerals according to International Union of Pure and Applied Chemistry (IUPAC) nomenclature (e.g., Sn^{IV}).

Figure 3 shows the dependency of $^{68}Ga^{3+}$ incorporation on the concentration of Zn^{2+}, Cu^{2+}, Fe^{3+}, Al^{3+}, Sn^{IV}, and Ti^{IV} for various macrocyclic chelators. These metal ions were chosen as they are commonly reported as prevailing contaminants found in the eluates of $^{68}Ge/^{68}Ga$ generators.[13,14] A chelator concentration of 3 μM in the labeling solution (in our experimental setup, 0.3 nmol in 100 μL) was chosen as optimal for these experiments with respect to the influence of added metallic impurities, because we previously found that, for TRAP, NOTA, and DOTA, nearly quantitative labeling is reached at this concentration, at 95 °C and at a pH of ≈3, in case no prior purification or concentration of the eluate is done.[10a] Ascending concentrations of respective metal ions (0.3 μM to 30 mM) were achieved by addition of suitable stock solutions of metal salts in 1 M aqueous hydrochloric acid to the pH-adjusted labeling solutions, resulting in lowered ^{68}Ga-labeling yields, depending on the chelator and contaminant. In agreement with our previously published results,[10a] $^{68}Ga^{3+}$ incorporation in the absence of any contaminant (Ø in Figure 3) was found to be near quantitative for all chelators under the chosen conditions. For comparison, in the eluates we used, the actual amounts of contaminants found (≤0.5 ppm for Al^{3+}; low ppb for Zn^{2+}, Fe^{3+}, Sn^{IV}, Ti^{IV}, and Cu^{2+}; inductively coupled plasma optical emission spectrometry (ICP-OES) analysis data are available in the Supporting Information) correspond to concentrations of ≤10 μM for Al^{3+}, and less than 1 μM for the other cations.

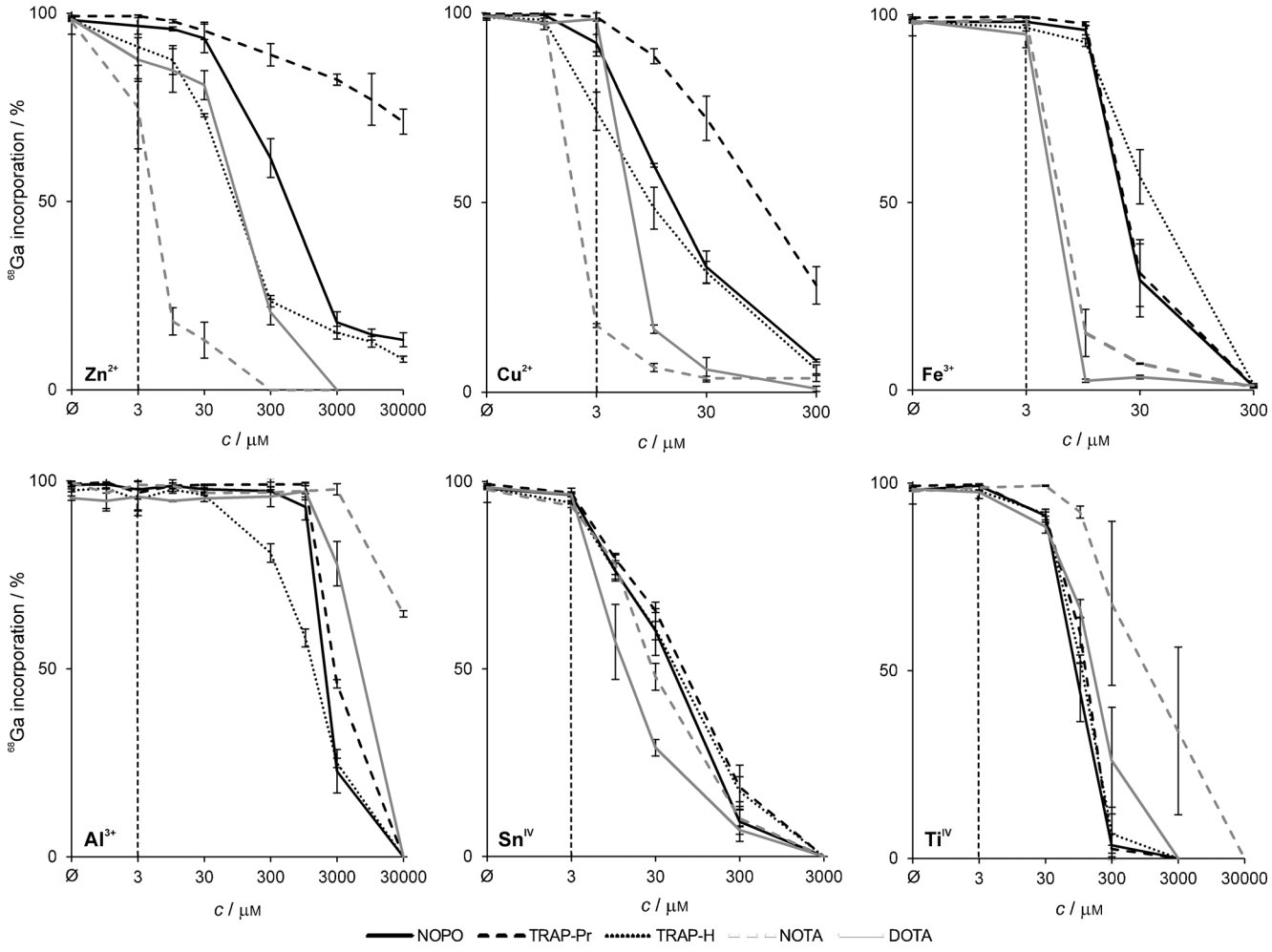

Figure 3. Incorporation of $^{68}Ga^{3+}$ (10–20 MBq ≈ 0.1–0.2 pmol; concentration: ~1–2 nM, 95 °C, pH 3) by NOPO, TRAP-Pr, TRAP-H, NOTA, and DOTA as functions of increasing concentrations of metal ions (Zn^{2+}, Cu^{2+}, Fe^{3+}, Al^{3+}, Sn^{IV}, and Ti^{IV}). Ø = no metal added. Vertical dashed lines indicate equal concentrations of chelator and contaminant (3 μM). Hypothetical contents of contaminants of 1 ppm (by mass) in the generator eluate are equivalent to the following concentrations in the reaction mixture: 8.7 μM (Zn^{2+}), 9.0 μM (Cu^{2+}), 10.2 μM (Fe^{3+}), 21.2 μM (Al^{3+}), 4.8 μM (Sn^{IV}), 11.9 μM (Ti^{IV}).

Zinc

Generally, high ^{68}Ga-labeling yields are observed even in cases where the molar amount of added Zn^{2+} is equal to the molar amount of chelator ($c = 3\ \mu M$). However, even though the NOTA–Ga^{III} complex exhibits a much higher thermodynamic stability than the corresponding Zn^{II} complex ($\log K_{[Ga(NOTA)]} - \log K_{[Zn(NOTA)]} = 8$),[9] ^{68}Ga labeling of NOTA is most affected among all chelators investigated. DOTA and TRAP-H were less influenced by the presence of Zn^{2+}; still, $^{68}Ga^{3+}$ incorporation is considerably decreased when the concentration of Zn^{2+} is more than ten-times higher than that of the chelator.

Surprisingly, in contrast to carboxylate-based chelators NOTA and DOTA, incorporation of $^{68}Ga^{3+}$ by the phosphinate chelators TRAP-H, NOPO, and TRAP-Pr is never entirely inhibited by the presence of Zn^{2+}, not even at concentrations of 30 mM (Figure 3). In this respect, the performance of TRAP-Pr is most impressive as it can still be labeled with a radiochemical yield of approximately 70% under these conditions. This is particularly remarkable in view of the actual concentration of $^{68}Ga^{3+}$, which, in our experiments, was in the range of 1–2 nM (10–20 MBq in 100 μL), and therefore was exceeded by the concentration of Zn^{2+} by a factor of around 10^7.

As TRAP-type chelators have been shown to quickly form fairly thermodynamically stable complexes with Zn^{2+} ($\log K_{[Zn(TRAP)]} = 13$–17; see Table S2 in the Supporting Information), we concluded that at high Zn^{2+} concentrations, $^{68}Ga^{3+}$ incorporation can only occur by transmetallation of Zn^{II} complexes. This hypothesis was proven by means of ^{71}Ga and ^{31}P NMR spectroscopy, using the simple TRAP-triamide TRAP-$(CHX)_3$[8a] (**11**) as a model compound. The chemical shifts in the ^{31}P NMR spectrum of TRAP$(CHX)_3$ change due to the formation of [Zn(TRAP$(CHX)_3$)] after addition of one equivalent of Zn^{2+} in the form of an aqueous solution of zinc(II) chloride (spectra A to B, Figure 4). Addition of 0.5 equivalents of Ga^{3+} in the form of an aqueous solution gallium(III) nitrate results in the presence of equimolar amounts of [Zn(TRAP$(CHX)_3$)] and [Ga(TRAP-$(CHX)_3$)] (spectrum C, Figure 4), and the signal of the Zn^{II} complex disappears completely upon addition of a total of one equivalent of Ga^{3+} (spectrum D, Figure 4).

The ^{71}Ga NMR chemical shift (δ) at $\approx$135 ppm found for the [Ga(TRAP$(CHX)_3$)] complex (Figure S6 in the Supporting Information) strongly suggests the presence of an in-cage structure, with N_3O_3-coordinated Ga^{III}. The same set of experiments was repeated with NOPO and TRAP-Pr (Figures S3 and S4 in the Supporting Information), yielding comparable results. However, after addition of aqueous gallium(III) nitrate to a solution of [Zn(NOTA)] followed by heating to 95 °C for a few seconds, formation of [Ga(NOTA)] could also be observed by mass spectrometry (see the Supporting Information), suggesting that ^{68}Ga labeling of [Zn(NOTA)] complexes by transmetallation should, in principle, also be possible. Therefore, the ^{68}Ga-labeling properties of Zn^{II} complexes of NOPO, TRAP-Pr, NOTA, as well as their corresponding RGD conjugates, were compared in detail.

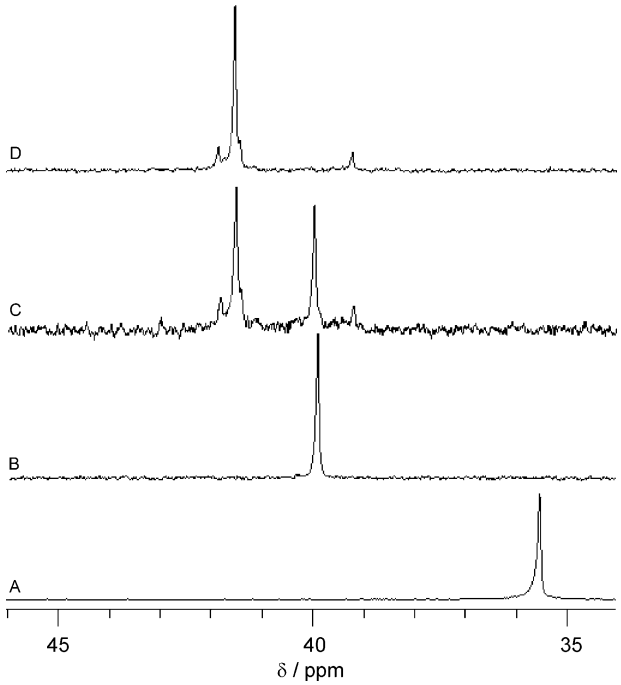

Figure 4. $^{31}P\{^1H\}$ NMR spectra showing transmetallation of [Zn(TRAP$(CHX)_3$)] with Ga^{3+} to form [Ga(TRAP$(CHX)_3$)] at room temperature, pH 3. A) TRAP-$(CHX)_3$; B) [Zn(TRAP$(CHX)_3$)]; C) [Zn(TRAP$(CHX)_3$)] + 0.5 equiv of Ga^{3+}; D) [Zn-(TRAP$(CHX)_3$)] + 1 equiv of Ga^{3+}, resulting in complete transmetallation to [Ga(TRAP$(CHX)_3$)]. For spectra with the full ppm range, see Figure S5 in the Supporting Information.

Zn^{II} complexes of NOPO and TRAP-Pr were shown to be ^{68}Ga-labeled at 95 °C with similar efficiency (Figure 5 A). A radioactivity incorporation of greater than 95% was reached at precursor concentrations of 0.3 μM. Upon further increase, a decreasing labeling efficiency can be observed, which we currently cannot explain satisfactorily. In contrast, [Zn(NOTA)] incorporated only up to 50% of $^{68}Ga^{3+}$ while requiring a concentration of at least 10 μM, and ^{68}Ga labeling of this complex could not be substantially improved by further enhancing its concentration in the labeling solution.

In order to further assess the practical usability of ^{68}Ga labeling of zinc(II) chelates, we investigated $^{68}Ga^{3+}$ incorporation by chelator-conjugated peptides, as well as their corresponding Zn^{II} complexes, at 25 °C. To achieve 90% $^{68}Ga^{3+}$ incorporation, approximately a ten-times greater concentration of [Zn(NOPO-RGD)] than NOPO-RGD is required (Figure 5 B). By further increasing the amount of [Zn(NOPO-RGD)], labeling efficiency could be improved to reach near-quantitative yield at 100 μM. A comparable situation was observed for TRAP$(RGD)_3$ and its Zn^{II} complex. Interestingly, the size of the substituents on the phosphorus atoms of TRAP-type chelators appears to have a marked influence on the transmetallation reaction. While [Zn-(TRAP$(CHX)_3$] incorporates ^{68}Ga just slightly less efficiently than [Zn(NOPO-RGD)], ^{68}Ga labeling of [Zn(TRAP$(RGD)_3$] is already substantially hampered. However, the latter is still much more capable of binding ^{68}Ga than the Zn^{II} complex of NODAGA-RGD. In good agreement with the slower metal exchange kinetics observed for the NOTA system, [Zn(NODAGA-RGD)] did

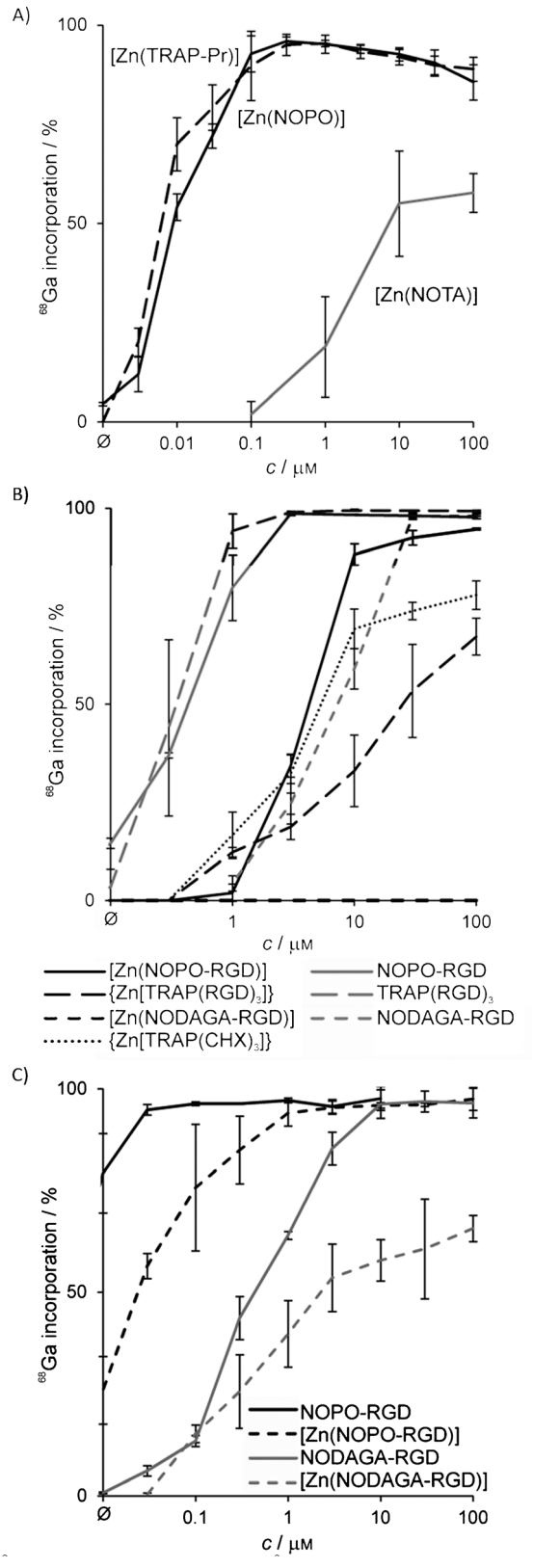

Figure 5. Incorporation of $^{68}Ga^{3+}$ (10–20 MBq ≈ 0.1–0.2 pmol, pH 3, $n = 3$) as functions of compound concentrations. A) [Zn(NOTA)], [Zn(NOPO)], and [Zn(TRAP-Pr)] (95 °C); B) NOPO-, TRAP-, and NODAGA-conjugates and their Zn^{II} complexes (25 °C); C) NOPO-RGD and NODAGA-RGD and the respective Zn^{II} complexes (95 °C).

not show any signs of replacement of Zn^{2+} by $^{68}Ga^{3+}$; similarly, no labeling of [Zn(NOTA)] could be observed at room temperature (data not shown).

Most notably, the ^{68}Ga-labeling efficiency of NODAGA-RGD is easily met even by the [Zn(NOPO-RGD)] complex, and by far exceeded by NOPO-RGD itself (Figure 5B). This was further confirmed when the same experiment was conducted at 95 °C (Figure 5C). Here, both NOPO-RGD and its Zn^{II} complex are outperforming neat NODAGA-RGD. These results clearly illustrate the significant ^{68}Ga-labeling performance of NOPO and further emphasize the potential of triazacyclononane-phosphinates for ^{68}Ga tracer development.

Finally, in order to assess the usability of Zn^{II} complexes of chelator–peptide conjugates as precursors for production of ^{68}Ga radiopharmaceuticals, fully automated ^{68}Ga labeling of selected compounds was performed using 1 nmol of precursor ($c \approx 0.5$ μM in the reaction vial). As expected, lower radiochemical yields are observed throughout for the Zn^{II} complexes (Table 1). However, both [Zn(NOPO-RGD)] and [Zn(TRAP(RGD)$_3$)] could be produced with radiochemical yields comparable to that of neat NODAGA-RGD.

Table 1. Automated ^{68}Ga labeling of selected conjugates and their zinc(II) complexes at 95 °C, pH 3.[a]

Ligand	Radiochemical yield [%]	
	free ligand	Zn^{II} complex
NOPO-RGD	96.4 ± 0.2	76.7 ± 3.6
TRAP(RGD)$_3$	95.2 ± 1.7[12]	65.3 ± 12.7
NODAGA-RGD	74.1 ± 15.2[30]	42.6 ± 3.6

[a] Ligand concentration used: 1 nmol. Data represents the mean ± SD, $n = 3$.

Copper

Judging from the shape of the curves in Figure 3, the influence of Cu^{2+} on ^{68}Ga labeling of individual chelators appears to be quite similar to that of Zn^{2+}. This is not surprising as both cations possess quite similar physical properties (size, charge, and surface charge density). Nevertheless, Cu^{2+} exerts its effect on $^{68}Ga^{3+}$ incorporation at concentrations approximately ten-times lower than that of Zn^{2+}, which is why Cu^{2+} deserves more attention than Zn^{2+} when considering the chemical purity of generator eluates. As for Zn^{2+}, the labeling performance of NOPO and TRAP chelators is less influenced by Cu^{2+} than those of DOTA and NOTA. Particularly, an equimolar concentration of Cu^{2+} and NOTA causes $^{68}Ga^{3+}$ incorporation by this chelator to decrease to 18%. This illustrates the high affinity of NOTA for Cu^{2+}, and these observations are in accordance with recent studies pointing out the suitability of NOTA and its bifunctional derivatives, such as NODAGA, for ^{64}Cu labeling.[21] Inhibition of $^{68}Ga^{3+}$ incorporation was observed to a comparable extent for DOTA, albeit at an approximately three-times higher Cu^{2+} concentration. An explanation can be found in the fact that Cu^{II} has a higher affinity for nitrogen donors, that is, the chelator cage, due to its softer character; likewise, the

hard phosphinate donors are less appropriate for Cu^{II} than carboxylates (see also the comments on iron below).

Iron

The presence of iron in the eluate appears to be inevitable, as even very pure hydrochloric acid (e.g., Merck Ultrapur) contains small amounts of Fe^{3+}, leading to a measurable iron content in the dilute hydrochloric acid we used for elution (27.5 ± 0.8 ppb in the 1 M aq HCl). In addition, Fe^{III} can be regarded as a particularly problematic contaminant because, due to its physical properties (charge +3, ionic radius 65 pm, c.f. 62 pm for Ga^{3+}),[22] its complexation behavior is very similar to that of Ga^{III}. Seemingly contradictory, we found that although NOPO and TRAP chelators possess higher affinity for $^{68}Ga^{3+}$ (that is, they incorporate $^{68}Ga^{3+}$ at a much lower ligand concentration than NOTA and DOTA),[10,12] the presence of 10 μM of Fe^{3+} had little effect on the ^{68}Ga-labeling yield for phosphinates (> 90%), whereas that of the carboxylates was decreased almost to a negligible level. A rationale for this observation is that, according to Pearson's hard–soft acid–base (HSAB) concept, Ga^{III} can be considered harder than Fe^{III}; likewise, phosphinates are harder donors than carboxylates, and thus prefer Ga^{III} over Fe^{III}. Although we have previously pointed out that the hard donor properties of phosphinates are likely to be the main reason for the high ^{68}Ga-labeling efficiency of NOPO and TRAP chelators,[9] this has not been demonstrated with such consummate clarity by any previous experiment.

Aluminum

Although Al^{3+} is a hard, trivalent metal ion and, due to the proximity of Al to Ga in the periodic table, it can be considered a smaller analogue of Ga^{3+}, the presence of Al^{3+} had no influence on labeling of all investigated chelators at concentrations below 30 μM. Since such high Al^{3+} concentrations are very unlikely to ever occur in generator eluates, Al^{3+} contamination can be considered irrelevant. Nevertheless, at higher Al^{3+} concentrations, ^{68}Ga incorporation by TRAP-H decreases, followed by the other chelators at Al^{3+} concentrations greater than 1 mM, while NOTA labeling is influenced to the least extent. The very hard Al^{3+} cation has a smaller radius (53 pm)[22] compared with Ga^{3+}, and thus is least fitting the NOTA or even larger DOTA cavity, resulting in only moderate thermodynamic complex stabilities ($\log K_{ML} = 17.5$ and 18.0, respectively).[23] However, the low influence on ^{68}Ga labeling could also be caused by precipitation of Al^{III} in the form of aluminum(III) hydroxide or slow kinetics of the exchange of aquo ligands on $[Al(H_2O)_6]^{3+}$, which was reported previously.[24]

Tetravalent metal ions

The significance of Sn^{IV} and Ti^{IV} is somewhat obvious because, as explained above, these metals are the main constituents of the matrix materials commonly used in ^{68}Ge/^{68}Ga generators, namely TiO_2 and SnO_2. The main difficulty in determining the influence of Sn^{IV} and Ti^{IV} arises from their aqueous chemistry, which is quite different from that of the previously discussed metal ions. Unlike these, moderately acidic solutions of Sn^{IV} and Ti^{IV} do not contain only the aquo complexes, but rather mixtures of mono- and oligomeric entities, bearing oxo- and hydroxo ligands in terminal and bridging positions. Furthermore, the abundance of the different species is highly dependent on pH, ionic strength of solutions, the presence of additional coordinating entities, concentration, and temperature.[25] In particular, when the pH is substantially changed and/or solutions are heated, colloids can form and precipitation can occur, which markedly affects ^{68}Ga labeling.

In our experiments, stock solutions of tin(IV) chloride or titanium(IV) chloride in 1 M aqueous hydrochloric acid were mixed with the generator eluate (also 1 M aq HCl), the pH was adjusted with aqueous 4-(2-hydroxyethyl)-1-piperazineethanesulfonic acid (HEPES), and the solutions were heated during labeling. As such, labeling might be expected to be influenced far more by formation of colloidal species, involving co-precipitation of ^{68}Ga, than by actual complexation of Sn^{4+} or Ti^{4+} ions by the chelators. Eventually, we observed that the influence of tetravalent tin and titanium was comparable for all investigated ligands, albeit Ti^{IV} species influenced the labeling efficiency to a lesser extent than Sn^{IV}. Compared with other chelators, DOTA showed to be slightly more influenced by the presence of Sn^{IV}, whereas NOTA was less influenced by Ti^{IV}.

Ge and ^{68}Ge

Preparing a solution of Ge^{IV} proved not to be straightforward as addition of germanium tetrachloride (a fuming liquid) to 1 M aqueous hydrochloric acid only led to precipitation. Heating of such a mixture was not desirable since germanium tetrachloride is usually prepared by distillation from concentrated hydrochloric acid, which is why heating could result in partial evaporation of Ge and thus a change in its concentration.

However, the ability of the chelators to coordinate dissolved Ge was assessed using $^{68}Ge^{IV}$. Labeling experiments were performed using a solution containing ^{68}Ge (and, therefore, ^{68}Ga and ^{68}Zn) in 1 M hydrochloric acid at 95 °C, while pH was adjusted to 3.3 using HEPES, as for ^{68}Ga labeling. We found that under these conditions, none of the investigated chelators bind ^{68}Ge (see the TLC analyses in Figure S1 of the Supporting Information). Hence, we conclude that ^{68}Ge contamination of labeling solutions does not lead to ^{68}Ge-labeled species as contaminants of ^{68}Ga radiopharmaceuticals. Confirming extensive practical experience of many radiopharmaceutical laboratories, we conclude that ^{68}Ge contaminants can be removed safely and reliably from ^{68}Ga radiopharmaceuticals by post-labeling solid-phase extraction, for example, using reverse-phase SPE cartridges and subsequent elution.

Overall impact of contaminants on ^{68}Ga labeling

From the data presented in Figure 3, we learn that copper(II) is the most critical contaminant for all chelators, affecting labeling to a greater extent than zinc(II). This is important as Cu^{2+} contaminants have been occasionally observed in generator el-

uates.[13,26] Furthermore, although its influence on labeling is less pronounced, zinc(II) is nevertheless of significance. In the generator, it is accumulated in the course of ^{68}Ga decay, and a critical Zn^{2+} level will eventually be reached when no elution is performed. However, this effect should not be overestimated; after elution of any generator, it takes approximately one week to reach a Zn/Ga molar ratio of 100:1, and even after this time, not more than a total of 1 nmol of Zn^{2+} is formed in a 1 GBq generator (for plots illustrating the zinc formation, see Figures S8–S10 in the Supporting Information). To what extent the regeneration time affects ^{68}Ga incorporation depends very strongly on the amount of chelator used; at a concentration of 3 μM, as used in our experiments, a regeneration time in the range of a couple of hours does not have any effect.

Furthermore, while Al^{3+} seems not to be of practical relevance, the influence of Fe^{3+} has to be considered mainly in the context of differences between phosphinate and carboxylate chelators. As stated above, Fe^{3+} contamination markedly impacts the ^{68}Ga labeling of DOTA and NOTA, but affects phosphinate chelators to a lesser extent. Neglecting smaller irregularities, this situation appears to be archetypical for all the critical ions; the ^{68}Ga-labeling performance of carboxylate-type chelators is generally more influenced by the presence of Zn^{2+}, Cu^{2+}, and Fe^{3+}, than that of phosphinate-type ligands (see Figure 3 and also Figure S2 in the Supporting Information).

In order to assess the overall suitability of a chelator for ^{68}Ga, the fact that the impact of all individual contaminants is cumulative should be kept in mind. While the presence of a single ion might be tolerated up to a certain level (concentration), the presence of several types of ions, each in subcritical amount, might nevertheless have a strong influence on the ^{68}Ga incorporation yield. According to our results, NOTA is the most delicate system, as it is particularly susceptible to either Zn^{2+}, Cu^{2+}, and Fe^{3+} (Figure 3). This observation is perfectly in line with previous work. When using small amounts of NODAGA-RGD in order to produce ^{68}Ga-NODAGA-RGD with high specific activity, a pre-elution of the generator, resulting in a low concentration of contaminants in the next eluate used for labeling, has been found essential for good radiochemical yields.[30] In our experience, the effect of such pre-elution is far less pronounced for DOTA peptides.

Phosphinate chelators TRAP and NOPO are particularly tolerant towards metal ion contaminants. As explained above, the presence of Zn^{2+} does not have a significant impact, due to efficient ^{68}Ga labeling of even their Zn^{II} complexes, and consequently Zn^{2+} does not contribute to the cumulative contamination effect. Therefore, a considerably larger amount of other contaminants, namely Cu^{2+} and Fe^{3+}, can be tolerated; moreover, as stated above, susceptibility of $^{68}Ga^{3+}$ complexation to these ions is much lower. As a result, ^{68}Ga labeling of triazacyclononane-triphosphinic acid chelators is exceptionally robust. Even when using very small precursor amounts, radiochemical yields are high and reproducibility of syntheses is excellent, which allows for the reliable production of ^{68}Ga-labeled TRAP and NOPO peptides with extremely high specific activities.[11,12] In particular, with respect to novel eluate purification methods that remove only ^{68}Ge but, in exchange, do not require reagents of regulatory concern (see above),[18] a pronounced tolerance of metal ion contaminants is of high practical value and might trigger a considerable step forward in development and implementation of ^{68}Ga labeling kits.

Conclusions

While studying the influence of Zn^{2+}, Cu^{2+}, Fe^{3+}, Al^{3+}, Ti^{IV}, and Sn^{IV} on ^{68}Ga labeling of various chelate ligands and corresponding peptide conjugates, we found that labeling efficiency of polyazacycloalkane chelators with *N*-acetic acid substituents (NOTA, DOTA) is generally more susceptible to the presence of the aforementioned contaminants than to that of analogous chelators bearing *N*-methylenephosphinic acid side arms (TRAP, NOPO). The pronounced $^{68}Ga^{3+}$ selectivity of the latter is rooted in a combination of several chemical aspects and mechanisms, the most remarkable of which is the ability of the phosphinate-type chelators to swiftly exchange coordinated Zn^{II} with Ga^{III}. This process runs so smoothly that incorporation of $^{68}Ga^{3+}$ by zinc(II) complexes of phosphinate ligands occurs at least equally as efficient as ^{68}Ga labeling of neat carboxylate-type chelators.

This finding is particularly remarkable in view of the popular notion that de- or transmetallation is easily performed with metal complexes of open-chain ligands, whereas complexes of pendant-arm azamacrocycles are often kinetically inert. This is due to the fact that the latter features two-step complexation and decomplexation mechanisms[27] with a substantial energy barrier, resulting in higher activation enthalpies and therefore slower rates of formation as well as of decomplexation, namely dissociation or transmetallation. In the context of radiolabeling, these aspects play a decisive role, because the extremely low concentrations of short-lived radionuclides generally entail dramatically decreased reaction rates, while at the same time, decay is limiting the timespan available for syntheses. Accordingly, the possibility of ^{68}Ga radiolabeling by transmetallation has never been seriously considered, and metal ion contaminants were thought to merely consume the labeling precursor by competitive complex formation. In this respect, the facile transmetallation of zinc(II) complexes of 1,4,7-triazacyclononane-1,4,7-tris(phosphinates) with Ga^{3+} ion is a unique and highly interesting feature of this ligand type, particularly since the resulting Ga^{III} complexes are, in turn, kinetically inert.[8a,9,10a,11] Furthermore, we are now able to provide a rationale for the observation that ^{68}Ga labeling of TRAP peptides is highly reproducible,[12] whereas, for example, reproducibility is lower for NODAGA peptides,[12,30] as they are markedly susceptible to the presence of certain contaminants.

We conclude that an additional benefit of using triazacyclononane-triphosphinate chelators in ^{68}Ga radiopharmaceutical development lies in more robust and reliable ^{68}Ga-labeling processes. High and fluctuating concentrations of metal ion contaminations in the eluate, caused by varying regeneration times of the ^{68}Ge/^{68}Ga generator or originating from other sources, impact their ^{68}Ga-incorporation performance to a lesser extent. In combination with their overall much higher ^{68}Ga-labeling efficiency and the high in vivo stability of their

Ga^{III} complexes,[10a,11,12] the bifunctional triazacyclononane-triphosphinates TRAP and NOPO thus appear to be truly unique Ga^{3+} chelators with ideal properties for development of ^{68}Ga PET imaging agents.

Experimental Section

General

The ligands and conjugates NOTA,[28] DOTA,[29] TRAP-Pr,[8a] TRAP-H,[9] NOPO,[11] $TRAP(CHX)_3$,[8a] NOPO-RGD,[11] and $TRAP(RGD)_3$[10a] were synthesized as described previously. NODAGA-RGD was purchased from ABX GmbH (Radeberg, Germany). Metal chlorides were purchased from Sigma–Aldrich or Merck, and were of at least 99.99% purity. Mass spectrometry (MS) spectra were recorded on a Varian Ion-trap 500 with electrospray ionization (ESI) in the positive or negative mode. NMR spectra were recorded using a Varian Unity Inova (400 MHz) or a Varian VNMRS (300 MHz) system. NMR chemical shifts are referenced relative to 85% aq H_3PO_4 (^{31}P) or 0.2 M aq $Ga(NO_3)_3$ (^{71}Ga) as external standards solutions in insert tubes. Automated ^{68}Ga labeling of NOPO-RGD, NODAGA-RGD, and their Zn^{II} complexes was done as described previously.[10a,11,30a]

Manual ^{68}Ga labeling

Labeling was done using eluate from a SnO_2-based $^{68}Ge/^{68}Ga$ generator (iTHEMBA Labs, Cape Town, South Africa), eluted with 1 M aq HCl (for details, see the Supporting Information). A 1250 μL fraction containing the highest activity was adjusted to pH 3.3 by addition of 4-(2-hydroxyethyl)-1-piperazineethanesulfonic acid (HEPES) in aqueous solution (930 μL), prepared by dissolving HEPES (7.2 g, 30 mmol) in Merck Ultrapur water (6 mL). Aliquots of this $^{68}Ga^{3+}$ solution (90 μL, 10–20 MBq, equivalent to ~0.1–0.2 pmol $^{68}Ga^{3+}$) were added to solutions of the respective ligand (30 μM, 10 μL), resulting in a ligand concentration of 3 μM (0.3 nmol in total). This mixture was heated to 95 °C for 5 min, then rapidly cooled to RT in a water bath, and evaluated by thin-layer chromatography (TLC) (silica-impregnated chromatography paper, Varian; mobile phase: 1 M aq NH_4OAc/MeOH, 1:1). For labeling in the presence of metal ion contaminants, the appropriate amount of a stock solution of the respective metal chloride in 1 M aq HCl (corresponding to pH of the eluate and preventing hydroxide formation) necessary to obtain the desired contaminant concentration was added to a fraction of the eluate, reaching a final volume of 1250 μL. Labeling and evaluation was performed in the same way.

^{68}Ga Labeling of zinc(II) complexes

Zn^{II} complexes of NOTA, TRAP-Pr, NOPO, NODAGA-RGD, $TRAP(RGD)_3$, NOPO-RGD and $TRAP(CHX)_3$ were prepared by mixing equimolar amounts of chelator and $ZnCl_2$ in water. Quantitative formation of Zn^{II} complexes was confirmed by MS (i.e., complete exchange of $[M+H]$ peaks with $[M+Zn]$ signals). For the free chelators, ^{68}Ga labeling and TLC of complexes was done as described above. For conjugates, ^{68}Ga labeling was performed at 22–25 °C and evaluated by TLC as described above, with the exception of ^{68}Ga–$TRAP(RGD)_3$, for which TLC was run on silica gel plates (Merck silica gel 60, 0.2 mm, on aluminum foil) with 0.1 M aq $Na_3C_6H_5O_7$ as the mobile phase.

^{68}Ge Labeling

^{68}Ge was obtained by collecting the eluate from a three-year-old SnO_2-based $^{68}Ge/^{68}Ga$ generator, which showed significant ^{68}Ge breakthrough due to not being eluted for several months. Two fractions of 1250 μL (1 M aq HCl) with activities of 316 and 153 kBq were processed in parallel, each mixed with aq HEPES (930 μL, prepared as described above for standard ^{68}Ga labeling). An aliquot of this solution (90 μL) was mixed with selected ligands in water (1 mM, 100 nmol per vial), and the solutions were heated to 95 °C for 5 min, then cooled and evaluated by TLC (stationary and mobile phases similar to those described above for the ^{68}Ga labeling experiments). $^{68}Ge/^{68}Ga$ labeling solution alone was run as a control. Developed TLC plates were dried and subjected to autoradiography for 1 h using BAS-IP MS 2025 imaging plates (Fujifilm, Japan). Readout was done on a Dürr Medical CR35BIO reader, and images were evaluated using Aida Image Analyzer software (version 4.24). The readout procedure was repeated after three days. For TLC autoradiograms and additional comments, see the Supporting Information.

Acknowledgements

Financial support by the Deutsche Forschungsgemeinschaft (DFG) (SFB 824, Projects B5 and Z1), and by the Ministry of Education of the Czech Republic (No. MSM0021620857), is gratefully acknowledged. The authors would like to thank Ondřej Zemek (Charles University, Prague) for NMR measurements.

Keywords: gallium-68 · germanium-68 · macrocyclic ligands · phosphinates · radiopharmaceuticals

[1] a) C. Decristoforo, R. D. Pickett, A. Verbruggen, *Eur. J. Nucl. Med. Mol. Imaging* **2012**, *39*, 31–40; b) J. Notni, *Nachr. Chem.* **2012**, *60*, 645–649.
[2] a) M. W. Greene, W. D. Tucker, *Int. J. Appl. Radiat. Isot.* **1961**, *12*, 62–63; b) C. Loc'h, B. Mazière, D. Comar, *J. Nucl. Med.* **1980**, *21*, 171–173; c) J. Schuhmacher, W. Maier-Borst, *Int. J. Appl. Rad. Isot.* **1981**, *32*, 31–26; d) Abstract from the *Annual Congress of the Annual Congress of the European Association of Nuclear Medicine 2010* (October 9–13, 2010), Vienna, Austria: K. Zhernosekov, M. Harfensteller, J. Moreno, O. Leib, O. Buck, A. Tuerler, R. Henkelmann, T. Nikula, *Eur. J. Nucl. Med. Mol. Imaging* **2010**, *37 (Suppl. 2)*, S251.
[3] H. J. Wester, *Nuklearmedizin* **2012**, *51*, N1–N4.
[4] a) M. Hofmann, H. Maecke, A. R. Börner, E. Weckesser, P. Schöffski, M. L. Oei, J. Schumacher, M. Henze, A. Heppeler, G. Meyer, W. H. Knapp, *Eur. J. Nucl. Med.* **2001**, *28*, 1751–1757; b) M. Fani, J. P. André, H. R. Maecke, *Contrast Media Mol. Imaging* **2008**, *3*, 67–77; c) W. A. Breeman, E. de Blois, H. Sze Chan, M. Konijnenberg, D. J. Kwekkeboom, E. P. Krenning, *Semin. Nucl. Med.* **2011**, *41*, 314–321.
[5] a) T. Wadas, E. H. Wong, G. R. Weisman, C. J. Anderson, *Chem. Rev.* **2010**, *110*, 2858–2902; b) B. M. Zeglis, J. S. Lewis, *Dalton Trans.* **2011**, *40*, 6168–6195; c) I. Velikyan, *Med. Chem.* **2011**, *7*, 338–372; d) J. Notni, K. Pohle, J. A. Peters, H. Görls, C. Platas-Iglesias, *Inorg. Chem.* **2009**, *48*, 3257–3267.
[6] N. Viola-Villegas, R. P. Doyle, *Coord. Chem. Rev.* **2009**, *253*, 1906–1925.
[7] K. P. Eisenwiener, M. I. M. Prata, I. Buschmann, H. W. Zhang, A. C. Santos, S. Wenger, J. C. Reubi, H. R. Mäcke, *Bioconjugate Chem.* **2002**, *13*, 530–541.
[8] a) J. Notni, P. Hermann, J. Havlíčková, J. Kotek, V. Kubíček, J. Plutnar, N. Loktionova, P. J. Riss, F. Rösch, I. Lukeš, *Chem. Eur. J.* **2010**, *16*, 7174–7185; b) J. Šimeček, J. Notni, V. Kubíček, P. Hermann, *Nucl. Med. Biol.* **2010**, *37*, 679.
[9] a) J. Šimeček, M. Schulz, J. Notni, J. Plutnar, V. Kubíček, J. Havlíčková, P. Hermann, *Inorg. Chem.* **2012**, *51*, 577–590.

[10] a) J. Notni, J. Šimeček, P. Hermann, H. J. Wester, *Chem. Eur. J.* **2011**, *17*, 14718 – 14722; b) Poster presented at the *19th International Symposium on Radiopharmaceutical Sciences* (Aug 28 – Sept 2, 2011), Amsterdam, The Netherlands: J. Notni, J. Šimeček, P. Hermann, H. J. Wester, *J. Labelled Compd. Radiopharm.* **2011**, *54*, S407; c) J. Šimeček, H. J. Wester, J. Notni, *Dalton Trans.* **2012**, *41*, 13803 – 13806.
[11] J. Šimeček, O. Zemek, P. Hermann, H. J. Wester, J. Notni, *ChemMedChem* **2012**, *7*, 1375 – 1378.
[12] J. Notni, K. Pohle, H. J. Wester, *EJNMMI Res.* **2012**, *2*, 28.
[13] E. de Blois, H. S. Chan, C. Naidoo, D. Prince, E. P. Krenning, W. A. P. Breeman, *Appl. Radiat. Isot.* **2011**, *69*, 308 – 315.
[14] W. A. P. Breeman, M. de Jong, E. de Blois, B. F. Bernard, M. Konijnenberg, E. P. Krenning, *Eur. J. Nucl. Med. Mol. Imaging* **2005**, *32*, 478 – 485.
[15] G.-J. Meyer, H. Mäcke, J. Schuhmacher, W. H. Knapp, M. Hofmann, *Eur. J. Nucl. Med. Mol. Imaging* **2004**, *31*, 1097 – 1104.
[16] a) K. P. Zhernosekov, D. V. Filosofov, R. P. Baum, P. Aschoff, H. Bihl, A. A. Razbash, M. Jahn, M. Jennewein, F. Rösch, *J. Nucl. Med.* **2007**, *48*, 1741 – 1748; b) F. Zoller, P. J. Riss, F. P. Montforts, F. Rösch, *Radiochim. Acta* **2010**, *98*, 157 – 160; c) N. S. Loktionova, A. N. Belozub, D. V. Filosofov, K. P. Zhernosekov, T. Wagner, A. Tuerler, F. Rösch, *Appl. Radiat. Isot.* **2011**, *69*, 942 – 946.
[17] Abstract from the *44th Annual Meeting of the German Society of Nuclear Medicine* (April 5 – 8, 2006), Berlin, Germany: D. Müller, I. Klette, R. Wortmann, R. P. Baum, *Nuklearmedizin* **2006**, *45*, A88 – A89.
[18] a) D. Mueller, I. Klette, R. P. Baum, M. Gottschaldt, M. K. Schultz, W. A. P. Breeman, *Bioconjugate Chem.* **2012**, *23*, 1712 – 1717; b) M. K. Schultz, D. Mueller, R. P. Baum, G. L. Watkins, W. A. P. Breeman, *Appl. Radiat. Isot.* **2012**, DOI: 10.1016/j.apradiso.2012.08.011.
[19] I. Velikyan, G. J. Beyer, E. Bergström-Pettermann, P. Johannsen, M. Bergstöm, B. Långström, *Nucl. Med. Biol.* **2008**, *35*, 529 – 536.
[20] J. Notni, K. Pohle, H. J. Wester, *Nucl. Med. Biol.* **2012**, DOI: 10.1016/j.nucmedbio.2012.08.006.
[21] S. Ait-Mohand, P. Fournier, V. Dumulon-Perreault, G. E. Kiefer, P. Jurek, C. L. Ferriera, F. Benard, B. Guerin, *Bioconjugate Chem.* **2011**, *22*, 1729 – 1735.
[22] R. D. Shannon, *Acta Crystallogr. Sect. A* **1976**, *32*, 751 – 767.
[23] a) J. P. André, H. Maecke, A. Kaspar, B. Kuennecke, M. Zehnder, L. Macko, *J. Inorg. Biochem.* **2002**, *88*, 1 – 6; b) M. Kodama, E. Kimura, *Bull. Chem. Soc. Jpn.* **1995**, *68*, 852 – 857.
[24] J. P. Nordin, D. J. Sullivan, B. L. Phillips, W. H. Casey, *Inorg. Chem.* **1998**, *37*, 4760 – 4763.
[25] a) C. H. Brubaker, *J. Am. Chem. Soc.* **1955**, *77*, 5265 – 5268; b) J. S. Johnson, K. A. Kraus, *J. Phys. Chem.* **1959**, *63*, 440 – 441.
[26] a) M. Asti, G. D. Pietri, A. Fraternali, E. Grassi, R. Sghedoni, F. Fioroni, F. Roesch, A. Versari, D. Salvo, *Nucl. Med. Biol.* **2008**, *35*, 721 – 724; b) I. Velikyan, G. J. Beyer, B. Långström, *Bioconjugate Chem.* **2004**, *15*, 554 – 560.
[27] a) C. A. Chang, Y. L. Liu, C. Y. Chen, X. M. Chou, *Inorg. Chem.* **2001**, *40*, 3448 – 3455; b) J. Moreau, E. Guillon, J. C. Pierrard, J. Rimbault, M. Port, M. Aplincourt, *Chem. Eur. J.* **2004**, *10*, 5218 – 5232.
[28] S. Größ, H. Elias, *Inorg. Chim. Acta* **1996**, *251*, 347 – 354.
[29] J. F. Desreux, *Inorg. Chem.* **1980**, *19*, 1319 – 1324.
[30] a) K. Pohle, J. Notni, J. Bussemer, H. Kessler, M. Schwaiger, A. J. Beer, *Nucl. Med. Biol.* **2012**, *39*, 777 – 784; b) Poster presented at the *19th International Symposium on Radiopharmaceutical Sciences* (Aug 28 – Sept 2, 2011), Amsterdam, The Netherlands: K. Pohle, J. Notni, J. Bussemer, H. Kessler, M. Schwaiger, A. J. Beer, *J. Labelled Compd. Radiopharm.* **2011**, *54*, S229.

Received: October 15, 2012
Published online on November 7, 2012

APPENDIX 5

Dalton Transactions

Dynamic Article Links

Cite this: *Dalton Trans.*, 2012, **41**, 13803

www.rsc.org/dalton

COMMUNICATION

Copper-64 labelling of triazacyclononane-triphosphinate chelators†

Jakub Šimeček, Hans-Jürgen Wester and Johannes Notni*

Received 16th August 2012, Accepted 27th September 2012
DOI: 10.1039/c2dt31880f

The 1,4,7-triazacyclononane-1,4,7-tris(methylenephosphinic acid) chelators TRAP and NOPO are complexing copper-64 with similar efficiency as 1,4,7-triazacyclononane-triacetic acid (NOTA). The kinetic stability of Cu-64-labelled TRAP-peptides is sufficient for PET imaging at early time points (1–2 h post injection). For labelling of TRAP conjugates, Cu-64 can be recommended as an alternative to Ga-68 to achieve higher resolution of PET images.

Positron emission tomography (PET) is a valuable molecular imaging modality for diagnosis of a variety of diseases and radiotherapy control. Contrary to the recently very popular PET nuclide ^{68}Ga ($E_{\beta+,max}$ = 1.89 MeV, $t_{1/2}$ = 68 min),[1] ^{64}Cu has a low β^+ energy ($E_{\beta+,max}$ = 656 keV) which is comparable to that of the gold standard, ^{18}F ($E_{\beta+,max}$ = 633 keV), and ensures imaging with high resolution.[2] In addition, its half-life of 12.7 h is compatible with the slow pharmacokinetics of proteins, such as antibodies or their fragments.[3] For binding the radiometal and to prevent subsequent loss of activity from the tracer, ^{64}Cu(II) has to be bound to a thermodynamically stable and kinetically inert complex, which requires tracer molecules to be equipped with a suitable chelating moiety. Many structures have been proposed for use with ^{64}Cu,[4] for example the cyclam derivatives TETA,[5] TE2A,[6] and CB-TE2A,[7] as well as bicyclic hexaamines, mainly derivatives of AmSar[8], see Chart 1. Due to its popularity, DOTA has been used as a bifunctional chelator for ^{64}Cu but reportedly shows considerable loss of ^{64}Cu from the chelate, caused by enzymatic activity in the liver.[9,10] More recently, the NOTA system, which is frequently used for the PET nuclide ^{68}Ga, has been found to form ^{64}Cu complexes with high stability *in vivo*, and corresponding bioconjugates have been used successfully in ^{64}Cu-PET imaging.[10] Recently, we found that the triazacyclononane-triphosphinate chelators TRAP[11] and NOPO,[12] as well as their bioconjugates, possess superior ^{68}Ga labelling properties in comparison to DOTA and NOTA.[13,14] Consequently, we were interested whether this holds true also for ^{64}Cu, since the latter is a desirable complementary label for ^{68}Ga, and compatibility with ^{64}Cu is thus of high significance for the application scope of triazacyclononane-triphosphinates in PET imaging.

Pharmazeutische Radiochemie, Technische Universität München, Walther-Meißner-Str. 3, D-85748 Garching, Germany. E-mail: johannes.notni@tum.de

†Electronic supplementary information (ESI) available. See DOI: 10.1039/c2dt31880f

A representative selection of chelators (DOTA, NOTA, TRAP-H, TRAP-Pr, NOPO) as well as chelator-conjugates of the cyclic pentapeptides c(RGDfK) (NOPO-RGD,[12] NODA-GA-RGD[15] and TRAP(RGD)$_3$,[16] for structures see ESI, Fig. S1†) were labelled using a solution of ^{64}Cu^{2+} with a pH value of 3 (obtained by dilution of ^{64}Cu in 0.1 M HCl with water, 1 : 100 by volume), since such a pH was found to be optimal for ^{68}Ga labelling of both NOTA and TRAP chelators.[13] Labelling was done at 25 °C for 5 min. Contrary to DOTA, triazacyclononane (TACN) based ligands were fully labelled already at 1 μM concentration (see Fig. 1 and ESI, Fig. S2†). However, at ligand concentrations of 0.3 μM, labelling yields were poorly reproducible, particularly using different ^{64}Cu production batches. This can be attributed to varying amounts of impurities. According to the ^{64}Cu manufacturer's data sheet, the maximum cumulative content of non-Cu^{2+} metal cations was ≈20 pmol of Pb^{2+}, Zn^{2+}, Ni^{2+}, and Fe^{3+}, competing with ≈0.2–0.3 pmol of ^{64}Cu^{2+} per labelling. At a concentration of 0.3 μM (30 pmol in total), all possibly contained metal ions and the chelators are present in approximately equimolar ratios, causing diminished and highly variable labelling yields. Furthermore, at concentrations of 0.3 and 1 μM, the level of incorporated ^{64}Cu remained stable after 0.5 min, showing that no free chelator was available after that time.

Since the half-life of ≈13 h is compatible with the often quite slow pharmacokinetics of large biomolecules, *e.g.* antibodies, the feasibility of ^{64}Cu-labelling under mild conditions adequate for such targeting vectors was also examined, using the above-mentioned RGD peptide conjugates as model compounds. In acetate- and HEPES-buffered solutions (5 min reaction at pH 5.6, 25 °C, and pH 5.7, 37 °C, respectively), 1 nmol of conjugates could be labelled with 3–4 MBq of ^{64}Cu in excellent yields (99% and >95%, respectively; for details see ESI†).

Kinetic stabilities of ^{64}Cu-labelled acyclic and cyclic chelators were assessed in a transchelation challenge under pseudo-first-order reaction conditions (Fig. 2). In 0.1 M EDTA, ^{64}Cu was quantitatively released from the open-chain ligand DEDPA[17] after 1 h, which corroborates recent work of Boros *et al.*[18] and confirms that DEDPA is not a suitable chelator for ^{64}Cu. As expected, all ^{64}Cu-labelled macrocycles show little to no loss of ^{64}Cu after 1 h. However, after 12 h considerable differences become apparent, as up to 50% of transmetallation is observed. Interestingly, the substituent on the phosphinate moieties of TRAP has a marked influence on transchelation rate, as the fraction of the intact complex after 12 h varies from 83% for ^{64}Cu-TRAP-OH to 49% for ^{64}Cu-TRAP-Pr.

Fig. 3 illustrates that compared to the respective unsubstituted chelators, the ^{64}Cu-labelled conjugates are generally more stable

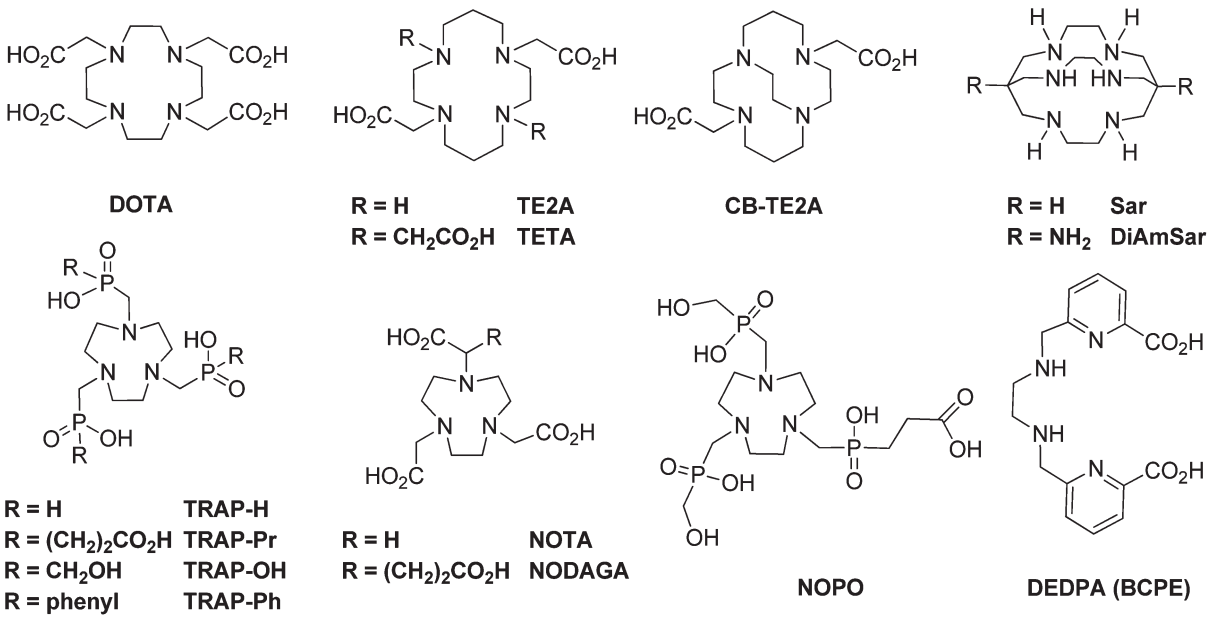

Chart 1

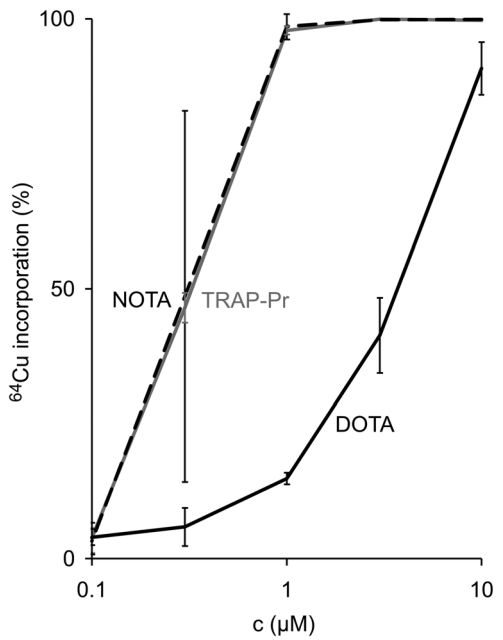

Fig. 1 ^{64}Cu incorporation as a function of chelator concentration. 1.9–2.5 MBq of ^{64}Cu in 1 mM HCl (0.1 mL, pH 3), 25 °C, 5 min, $n = 3$.

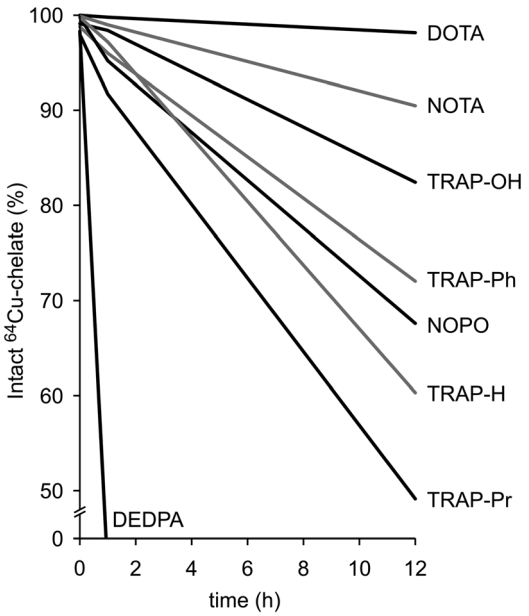

Fig. 2 Stability of ^{64}Cu complexes with selected chelators in 0.1 M EDTA. Error bars are omitted for clarity. Percentages of intact ^{64}Cu chelates were determined after 1, 2 and 12 h.

in EDTA. Moreover, all conjugates were almost fully stable in plasma over 12 h. A particularly pronounced gain of stability is observed for ^{64}Cu-TRAP(RGD)$_3$ in comparison to ^{64}Cu-TRAP-Pr; conjugation of the three RGD peptide units considerably increases kinetic inertness here. However, of the TACN-based chelators investigated, the NOTA motif appears to be the best choice for ^{64}Cu, judging from labelling and stability data; ^{64}Cu-NODAGA-RGD is the only compound which is fully stable over a period of 12 h, both in EDTA and plasma.

Table 1 shows that ^{64}Cu-labelled TRAP and NOPO conjugates possess considerably lower hydrophilicity in comparison to their ^{68}Ga-labelled analogues. A similar trend was reported before for ^{64}Cu- and ^{68}Ga-NODAGA-RGD,[9c] and can be explained, in terms of Pearson's HSAB concept, with a higher polarization effect of the hard Ga^{3+} cation compared to the considerably softer (borderline) Cu^{2+}. Changing the metal label therefore cannot be considered innocent, and polarity-related alterations of biodistribution and excretion pathways should be taken into account when switching between ^{68}Ga and ^{64}Cu.

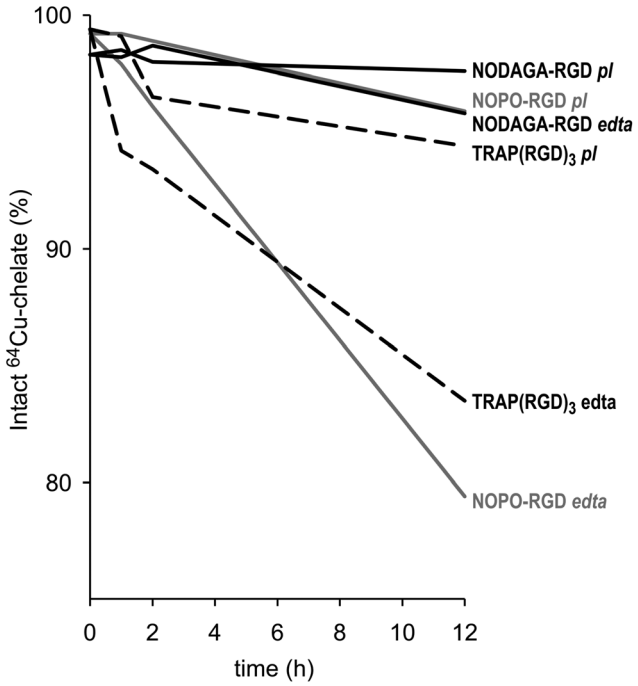

Fig. 3 Stability of ^{64}Cu-labelled conjugates in 0.1 M EDTA (edta) and human plasma (pl). Error bars are omitted for clarity. Percentages of intact ^{64}Cu chelates were determined after 1, 2 and 12 h.

Table 1 Octanol–water partition coefficients (log *P*) of ^{64}Cu- and ^{68}Ga-labelled c(RGDfK) conjugates

Conjugate	^{64}Cu(II)	^{68}Ga(III)
NOPO-RGD	−2.18 ± 0.05	−4.64 ± 0.12[12]
TRAP(RGD)$_3$	−2.40 ± 0.02	−3.90 ± 0.10[13]
NODAGA-RGD[9c]	−2.76 ± 0.08	−3.27 ± 0.01

Proof-of-principle micro-PET imaging was done using a nude mouse with an $\alpha_v\beta_3$ integrin-overexpressing tumour. Fig. 4 shows that 75 min post injection, quite similar results are obtained for the non-internalising peptides ^{68}Ga- and ^{64}Cu-labelled TRAP(RGD)$_3$, thus demonstrating feasibility of label exchange for this compound at early time points. Localization of the tumour was still possible after 18 h, albeit uptake was reduced. Based on preceding literature, we interpret the observed activity uptake in the liver and intestines as being caused by slow demetallation of ^{64}Cu-TRAP(RGD)$_3$, followed by specific uptake of ^{64}Cu by copper-binding proteins and sequestration in the liver.[9,10]

We conclude that although ^{68}Ga incorporation of triazacyclononane-triphosphinates TRAP and NOPO is much more efficient compared to NOTA,[13] a similar enhancement is not observed for ^{64}Cu, which is bound by these chelators with comparable efficiency. In addition, despite the fact that ^{64}Cu-labelled TRAP peptides are slightly less stable than their NODAGA counterparts, they are nevertheless well suited for PET acquisition up to 1–2 h post injection, which is compatible with the pharmacokinetics of most peptide receptor ligands. ^{64}Cu can therefore be recommended as a complementary label for ^{68}Ga-TRAP-peptides in cases where higher resolution of PET images is desired.

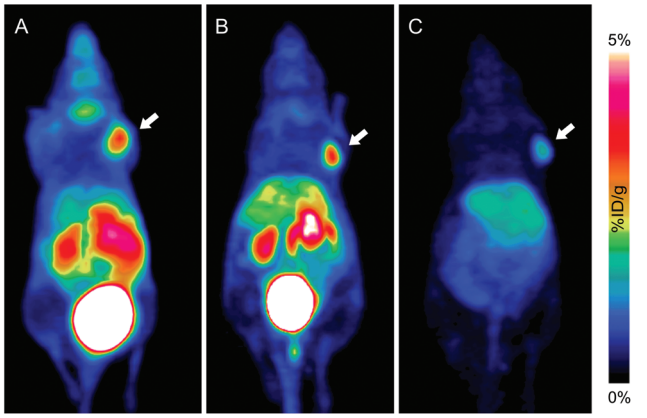

Fig. 4 PET imaging of CD-1 nude mice, bearing M21 human melanoma xenografts (high $\alpha_v\beta_3$ integrin expressing tumours, indicated by arrows). (A) ^{68}Ga-TRAP(RGD)$_3$, 12 MBq, 75 min p.i.; (B) ^{64}Cu-TRAP(RGD)$_3$, 30 MBq, 75 min p.i.; (C) same animal as (B), 18 h p.i.

Acknowledgements

Financial support by the Deutsche Forschungsgemeinschaft (SFB 824, Projects B5 and Z1) is gratefully acknowledged. The authors thank Karolin Pohle (Radiopharmaceutical Chemistry, TUM) for help with determination of log *P* values, and Carlos Platas Iglesias (Universidade da Coruña, Spain) for providing a sample of DEDPA.

References

1 (*a*) C. Decristoforo, R. D. Pickett and A. Verbruggen, *Eur. J. Nucl. Med. Mol. Imaging*, 2012, **39**, S31–S40; (*b*) J. Notni, *Nachr. Chem.*, 2012, **60**, 645–649.
2 H. A. Williams, S. Robinson, P. Julyan, J. Zweit and D. Hastings, *Eur. J. Nucl. Med. Mol. Imaging*, 2005, **32**, 1473–1480.
3 B. M. Zeglis and J. S. Lewis, *Dalton Trans.*, 2011, **40**, 6168–6195.
4 T. J. Wadas, E. H. Wong, G. R. Weisman and C. J. Anderson, *Chem. Rev.*, 2010, **110**, 2858–2902.
5 R. Delgado and J. J. R. Frausto da Silva, *Talanta*, 1982, **29**, 815–822.
6 (*a*) I. M. Helps, D. Parker, J. Chapman and G. Ferguson, *J. Chem. Soc., Chem. Commun.*, 1988, 1094–1095; (*b*) D. N. Pandya, J. Y. Kim, J. C. Park, H. Lee, P. B. Phapale, W. Kwak, H. Choi, G. J. Cheon, Y. R. Yoon and J. Yoo, *Chem. Commun.*, 2010, **46**, 3517–3519.
7 E. H. Wong, G. R. Weisman, D. C. Hill, D. P. Reed, M. E. Rogers, J. P. Condon, M. A. Fagan, J. C. Calabrese, K. C. Lam, I. A. Guzei and A. L. Rheingold, *J. Am. Chem. Soc.*, 2000, **122**, 10561.
8 G. A. Bottomley, I. J. Clark, I. I. Creaser, L. M. Engelhardt, R. J. Geue, K. S. Hagen, J. M. Harrowfield, G. A. Lawrance, P. A. Lay, A. M. Sargeson, A. J. See, B. W. Skelton, A. H. White and F. R. Wilner, *Aust. J. Chem.*, 1994, **47**, 143–179.
9 (*a*) C. A. Boswell, X. Sun, W. Niu, G. R. Weisman, E. H. Wong, A. L. Rheingold and C. J. Anderson, *J. Med. Chem.*, 2004, **47**, 1465–1474; (*b*) T. J. Wadas, E. H. Wong, G. R. Weisman and C. J. Anderson, *Curr. Pharm. Des.*, 2007, **13**, 3–16; (*c*) R. A. Dumont, F. Deininger, R. Haubner, H. R. Maecke, W. A. Weber and M. Fani, *J. Nucl. Med.*, 2011, **52**, 1276–1284.
10 S. Ait-Mohand, P. Fournier, V. Dumulon-Perreault, G. E. Kiefer, P. Jurek, C. L. Ferreira, F. Benard and B. Guerin, *Bioconjugate Chem.*, 2011, **22**, 1729–1735.
11 (*a*) J. Notni, P. Hermann, J. Havlíčková, J. Kotek, V. Kubíček, J. Plutnar, N. Loktionova, P. J. Riss, F. Rösch and I. Lukeš, *Chem.–Eur. J.*, 2010,

16, 7174–7185; (*b*) J. Šimeček, M. Schulz, J. Notni, J. Plutnar, V. Kubíček, J. Havlíčková and P. Hermann, *Inorg. Chem.*, 2012, **51**, 577–590; (*c*) ; (c) J. Šimeček, J. Notni, V. Kubiček and P. Hermann, *Nucl. Med. Biol.*, 2010, **37**, 679.
12 J. Šimeček, O. Zemek, P. Hermann, H. J. Wester and J. Notni, *ChemMedChem*, 2012, **7**, 1375–1378.
13 (*a*) J. Notni, J. Šimeček, P. Hermann and H. J. Wester, *Chem.–Eur. J.*, 2011, **17**, 14718–14722; (*b*) J. Notni, J. Šimeček, P. Hermann and H. J. Wester, *J. Label. Compd. Radiopharm.*, 2011, **17**, S407.
14 J. Notni, K. Pohle and H. J. Wester, *EJNMMI Res.*, 2012, **2**, 28.
15 K. Pohle, J. Notni, J. Bussemer, H. Kessler, M. Schwaiger and A. J. Beer, *Nucl. Med. Biol.*, 2012, **39**, 777–784.
16 J. Notni, K. Pohle and H. J. Wester, *Nucl. Med. Biol.*, 2012, DOI: 10.1016/j.nucmedbio.2012.08.006.
17 (*a*) R. Ferreirós-Martínez, D. Esteban-Gómez, C. Platas-Iglesias, A. de Blas and T. Rodríguez-Blas, *Dalton Trans.*, 2008, 5754–5765; (*b*) E. Boros, C. L. Ferreira, J. F. Cawthray, E. W. Price, B. O. Patrick, D. W. Wester, M. J. Adam and C. Orvig, *J. Am. Chem. Soc.*, 2010, **132**, 15726–15733.
18 E. Boros, J. F. Cawthray, C. L. Ferreira, B. O. Patrick, M. J. Adam and C. Orvig, *Inorg. Chem.*, 2012, **51**, 6279–6284.

Electronic Supplementary Material (ESI) for Dalton Transactions

Supporting Information

Copper-64 labelling of triazacyclononane-triphosphinate chelators

Jakub Šimeček, Hans-Jürgen Wester and Johannes Notni

Pharmazeutische Radiochemie, Technische Universität München, Walther-Meißner-Str. 3, D-85748 Garching, Germany, email:johannes.notni@tum.de

1. Materials and reagents

^{64}Cu was obtained from ACOM (Montecosaro Scalo, Italy) in 0.1 M HCl. Content of non-^{64}Cu metals according to the manufacturer: Pb ≤ 0.129 µg/mL, Ni ≤ 0.394 µg/ml, Cu ≤ 0.165 µg/mL, Zn ≤ 0.338 µg/mL, Fe ≤ 0.465 µg/mL. NODAGA-RGD was purchased from ABX (Radeberg, Germany), NOTA[1], DOTA[2], TRAP-H[3], TRAP-Pr[4], NOPO[5], TRAP(RGD)$_3$[6] and NOPO-RGD[5] were prepared as described in the literature. A sample of DEDPA was kindly provided by Carlos Platas Iglesias, Universidade da Coruña, Spain. Buffers (HEPES, sodium acetate) and water (Ultrapur) were purchased from Merck (Darmstadt, Germany).

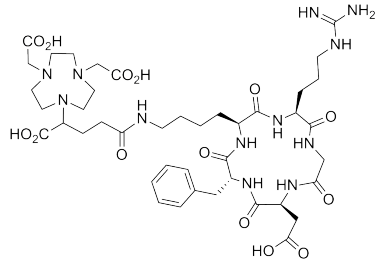

NODAGA-RGD

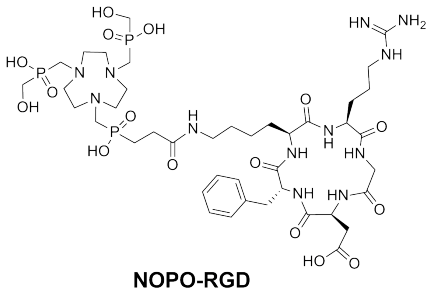

NOPO-RGD

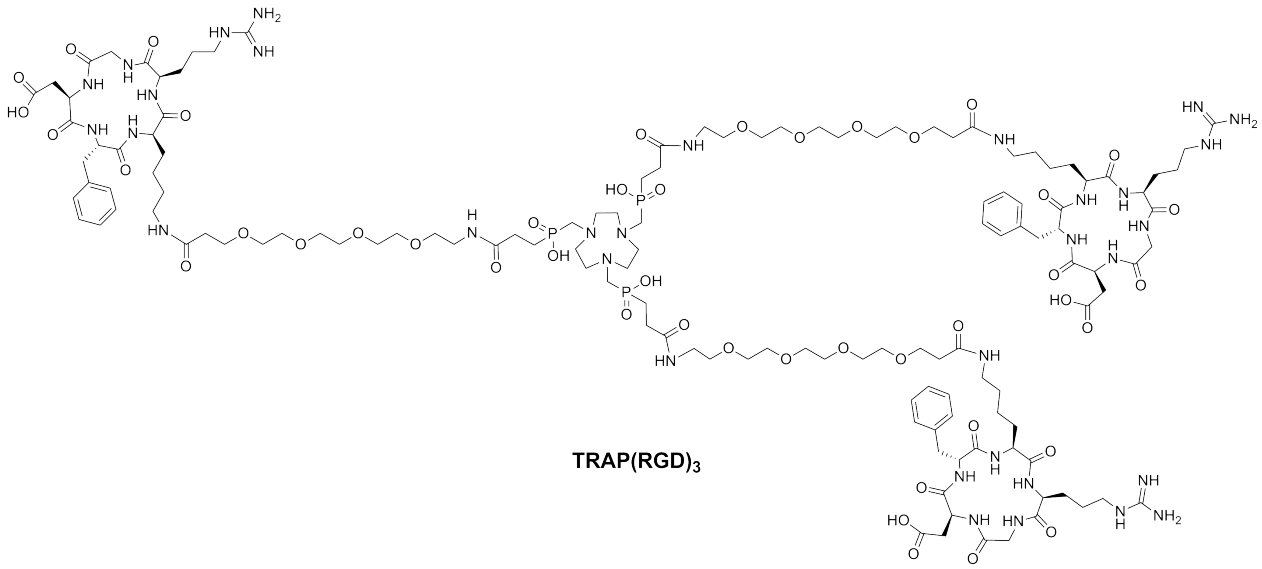

TRAP(RGD)$_3$

Figure S1: Structures of RGD peptide conjugates.

2. ^{64}Cu-labelling

Non-buffered solutions: For experiments at pH 3, 100 µL of ^{64}Cu in 0.1 M HCl was mixed with 9.9 mL of water. 90 µL of that solution was mixed with 10 µL of ligand solution, resulting in ligand concentrations of 0.1, 0.3, 1, 3 and 10 µM. Activity of added ^{64}Cu was in the range of 1.9–2.5 MBq (0.2–0.3 pmol). Labelling was done for 5 min at 25 °C, whereafter ^{64}Cu incorporation was determined by radio-TLC (see below).

Labelling in NaOAc buffer: Mixing 10 µL of 100 µM solution (1 nmol of ligand in total) of TRAP(RGD)$_3$, NOPO-RGD and NODAGA-RGD with 5 µL of 1 M aq. NaOAc and additon of 7 µL of ^{64}Cu in 0.1 M HCl (~ 3 MBq) resulted in pH 5.6. The mixtures was left standing for 5 min at 25 °C and then evaluated by radio-TLC (see below).

Labelling in HEPES buffer: TRAP(RGD)$_3$, NOPO-RGD and NODAGA-RGD (10 µL of 100 µM solution, 1 nmol) were mixed with 80 µL of aq. HEPES solution (7.2 g of HEPES + 6 mL water) and 10 µL of ^{64}Cu (~ 4 MBq) in 0.1 M HCl was added, which resulted in pH 5.7. The mixtures were incubated for 5 min at 37 °C and evaluated by radio-TLC (see below).

Preparation of the tracer for in vivo injection: TRAP(RGD)$_3$ (5 nmol) in water (50 µL) was mixed with 5 µL of aq. HEPES solution and 0.1 M NaOH (40 µL). ^{64}Cu in 0.1 M HCl (50 µL, 120 MBq, 13.2 pmol) was added (final pH ~ 4.4) and the solution was heated for 30 min to 95 °C. ^{64}Cu-labelled tracer was purified by solid phase extraction, using a C8 light cartridge (Waters), preconditioned with 10 mL of ethanol and 10 mL of water. The reaction mixture was passed over the cartridge, purged with 1 mL of water in order to remove free ^{64}Cu, and the product eluted with 1 mL of ethanol. After addition of water (1 mL) and PBS (1 mL), the ethanol was evaporated in vacuo and the solution simultaneously concentrated to 1 mL. Before injection, the formulation was filtered over a 0.22 µM sterile filter.

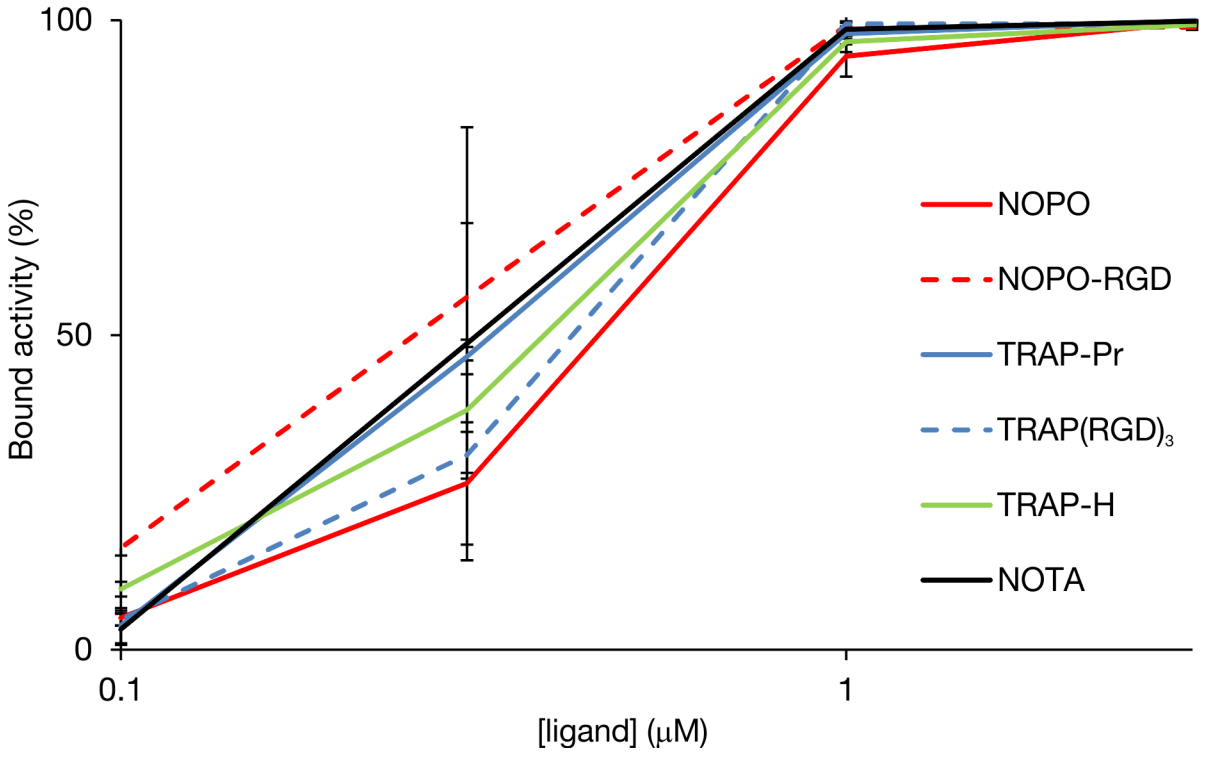

Figure S2: ^{64}Cu incorporation as function of chelator concentration.

2.1. Comment on metal-to-ligand ratio and incorporation efficiency

Even though the labelling with low activity of ^{64}Cu showed to be highly efficient using low chelator amount, e.g. 0.1–1 nmol (Figure 1), the labelling efficiency showed to be highly dependent on the metal-to-ligand (M:L) ratio. Labelling with higher activity of ^{64}Cu and similar ligand concentration did not lead to comparable activity incorporation. Therefore, for preparation of higher doses, e.g. for injection purposes, the strategy similar to that for routine labelling with ^{177}Lu is of choice, i.e., calculation of a well-defined, known optimal excess of chelator. On the contrary, when labelling of e.g. 1 nmol of TRAP chelators with ^{68}Ga, quantitative activity incorporation independent on the absolute activity is observed.

For example, labelling of 0.1 nmol (c = 1 μM) of precursors with ~ 2.2 MBq of ^{64}Cu (~ 0.24 pmol, M:L ratio 1:417) resulted in quantitative ^{64}Cu incorporation at r.t. Contrary, labelling of a ten times higher concentration of TRAP(RGD)$_3$ (c = 10 μM, 1 nmol) with ^{64}Cu (120 MBq, 13.2 pmol, pH 3.1 adjusted with aq. HEPES) resulted in a M:L ratio of 1:75, which was too low to yield labelled product, even at 95 °C. However, a radiochemical yield of > 95 % was reached by labelling 5 nmol of the precursor (M:L ratio is then 1:378). In further experiments, adjusting the pH to 4.4 helped to reduce the reaction time to 20 min at 95 °C. Specific activities were typically ranging around 20 GBq/μmol.

3. Analysis

^{64}Cu incorporation by chelators was evaluated by TLC (silica 60 coated alumina sheets, Merck), using 0.1 M aq. EDTA as mobile phase. Labelled chelators/conjugates stay at the origin (R_f = 0), whereas unbound ^{64}Cu is complexed by EDTA and moves with the front (R_f = 0.9–1.0).

4. EDTA challenge and stability in human plasma

The chelators (1–2 nmol of each) were labelled with ~ 12 MBq of ^{64}Cu, using a mixture of ^{64}Cu in 0.1 M HCl (7 μL) and 1 M NaOAc (5 μL), pH 5.7, 5 min reaction at 95 °C. Full labelling was confirmed by TLC. Then, each sample was diluted with PBS to reach a volume of 50 μL. 20 μL of the solutions were added to 100 μL of 0.1 M EDTA and left standing at room temperature. Samples for TLC analysis were withdrawn after 1, 2 and 12 h.

The stability of ^{64}Cu-labelled NOPO-RGD, TRAP(RGD)$_3$ and NODAGA-RGD was tested also in human plasma, for which purpose 20 μL of the solutions containing labelled conjugate (prepared as described before) were transferred to 100 μL of plasma, and incubated at room temperature. Samples for TLC analysis were taken after 1, 2 and 12 h of incubation.

5. log*P* determination

50 μL (~ 0.5 MBq) of PBS solution of a purified tracer was mixed with 450 μL of PBS and 500 μL of n-octanol. After 1 min of vigorous shaking, the phases were separated by centrifugation and the activity contained in 100 μL aliquots of both water and n-octanol phases were measured in a γ-counter (1480 WIZARD^{TM}, PerkinElmer Wallac). Experiments were repeated 8 times.

6. Small animal PET imaging

The animal model for $\alpha_v\beta_3$ integrin expression was described before in detail.[6] Briefly, CD-1 athymic nude mice were used, bearing tumor xenografts (M21 human melanoma with high $\alpha_v\beta_3$ integrin expression) on the right shoulder.

MicroPET imaging was performed using small animal PET/CT scanner (Siemens Inveon). ^{68}Ga-TRAP(RGD)$_3$ (12 MBq, prepared as described[6]) or ^{64}Cu- TRAP(RGD)$_3$ in PBS (30 MBq) was injected to the tail vain of a mouse anaesthetised with isoflurane. PET data was recorded for 15 min, 75 min p.i. (^{68}Ga- and ^{64}Cu-TRAP(RGD)$_3$) and 18 h p.i. (^{64}Cu-TRAP(RGD)$_3$ only). Images were reconstructed using Inveon Research Workplace software; 3D ordered-subsets expectation maximum (OSEM3D) algorithm without scanner and attenuation correction. All animal experiments were performed in accordance with general animal welfare regulations in Germany.

References

1 S. Grös, H. Elias, *Inorg. Chim. Acta* **1996**, *251*, 347–354.

2 J. F. Desreux, *Inorg. Chem.* **1980**, *19*, 1319–1324.

3 J. Šimeček, M. Schulz, J. Notni, J. Plutnar, V. Kubíček, J. Havlíčková, P. Hermann, *Inorg. Chem.* **2012**, *51*, 577– 590.

4 J. Notni, P. Hermann, J. Havlíčková, J. Kotek, V. Kubíček, J. Plutnar, N. Loktionova, P. J. Riss, F. Rösch, I. Lukeš, *Chem. Eur. J.* **2010**, *16*, 7174–7185.

5 J.Šimeček, O. Zemek, P. Hermann, H.-J. Wester, J. Notni, *ChemMedChem* **2012**, *7*, 1375–1378.

6 J. Notni, J. Šimeček, P. Hermann, H. J. Wester, *Chem. Eur. J.* **2011**, *17*, 14718–14722.